[redacted]

DOWNGRADED AT 3 YEAR INTERVALS:
DECLASSIFIED AFTER 12 YEARS
DOD DIR 5200.10

CLASSIFICATION CHANGE
To UNCLASSIFIED
By authority of Gil - Ed Mar
Changed by L. Shirley Date 12/5/72
Classified Document Master Control Station, NASA
Scientific and Technical Information Facility

MASSACHUSETTS INSTITUTE OF TECHNOLOGY

APOLLO
GUIDANCE AND NAVIGATION

Approved Milton B. Trageser Date 6/1/64
MILTON B. TRAGESER, ASSOCIATE DIRECTOR
APOLLO GUIDANCE AND NAVIGATION PROGRAM

Approved Roger B. Woodbury Date 3/21/64
ROGER B. WOODBURY, DEPUTY DIRECTOR
INSTRUMENTATION LABORATORY

[redacted]

(Unclassified Title)

REPORT E-1573

QUARTERLY TECHNICAL PROGRESS REPORT

PROJECT APOLLO GUIDANCE

AND

NAVIGATION PROGRAM

Period ended March 1964

[redacted]

INSTRUMENTATION LABORATORY

CAMBRIDGE 39, MASSACHUSETTS

COPY # 143 OF 205 COPIES
THIS DOCUMENT CONTAINS 318 PAGES

[redacted]

ACKNOWLEDGEMENT

This report was prepared under the auspices of DSR Project 55-191, sponsored by the Manned Spacecraft Center of the National Aeronautics and Space Administration through Contract NAS9-153.

PREFACE

This report consists of two principal parts. Part I consists of progress summaries of the various phases of the Apollo Program at MIT/IL. Part II consists of technical sections that are primarily the presentations made at a Design Review Meeting at MIT/IL on 25 and 26 March 1964.

The report also includes a list of all meetings attended by MIT/IL Apollo personnel as well as the Bibliography of all reports on the Apollo Program published by MIT Instrumentation Laboratory.

TABLE OF CONTENTS

PART I

PROGRESS SUMMARIES

PART I

PROGRESS SUMMARIES

The delivery schedule for command module Guidance and Navigation (G&N) Systems is shown in Fig. I-1.

Failure Effects Analysis: MIT/IL requested Raytheon Manufacturing Co. to provide support and assistance to MIT/IL for Failure Effects Analysis of Command Module Guidance and Navigation Equipment. Operating modes will be identified with mission phases, times, and environments. Within each operating mode and mission phase, failure modes of assemblies, subassemblies, and significant parts will be identified and associated with the effects on system performance and mission success. Relative criticalities based on severity of effect, probability of occurrence and availability of indication, maintenance, or alternate mode operation shall be assigned. (Reference TD R-137, 18 March 1964.)

Block I Drawings: MIT/IL authorized AC Spark Plug (ACSP), Raytheon, and Kollsman Instrument Corp. to assume responsibility for the maintenance and preparation of Command Module Block I flight hardware and Ground Support Equipment (GSE) design drawings. Technical responsibility for design will remain with MIT/IL. (Reference TD's A-219, R-150, and K-124, 5 March 1964.)

Test Data Reduction and Analysis Planning: AC Spark Plug is to develop under MIT/IL direction (through in-house effort) an integrated plan for the reduction and analysis of both Command Module (C/M) and Lunar Excursion Module (LEM) G&N test data and to establish the associated test data and instrumentation requirements in order to implement the objectives and concepts of the C/M and LEM G&N Test Plans and provide a basis for modification of these plans. The task includes all flight data and reliability data and further includes integration of the ground test data plan being prepared by Raytheon under TD R-145. (Reference TD A-193, 23 March 1964.)

AGE-4 has been assembled in a system harness and operated in all system modes, both manually and with AGC-4. ATP procedures proofing using AGE-4 and the GSE is continuing. The AGE-4 schedule is shown in Fig. I-2.

The AGE-5 schedule is shown in Fig. I-3. AGE-5 Inertial Subsystem has been assembled and preliminary alignment and calibration performed. ISS assembly and test procedures are continuing.

APOLLO MILESTONE CHART FOR C/M G&N SYSTEM DELIVERY

Fig. I-I

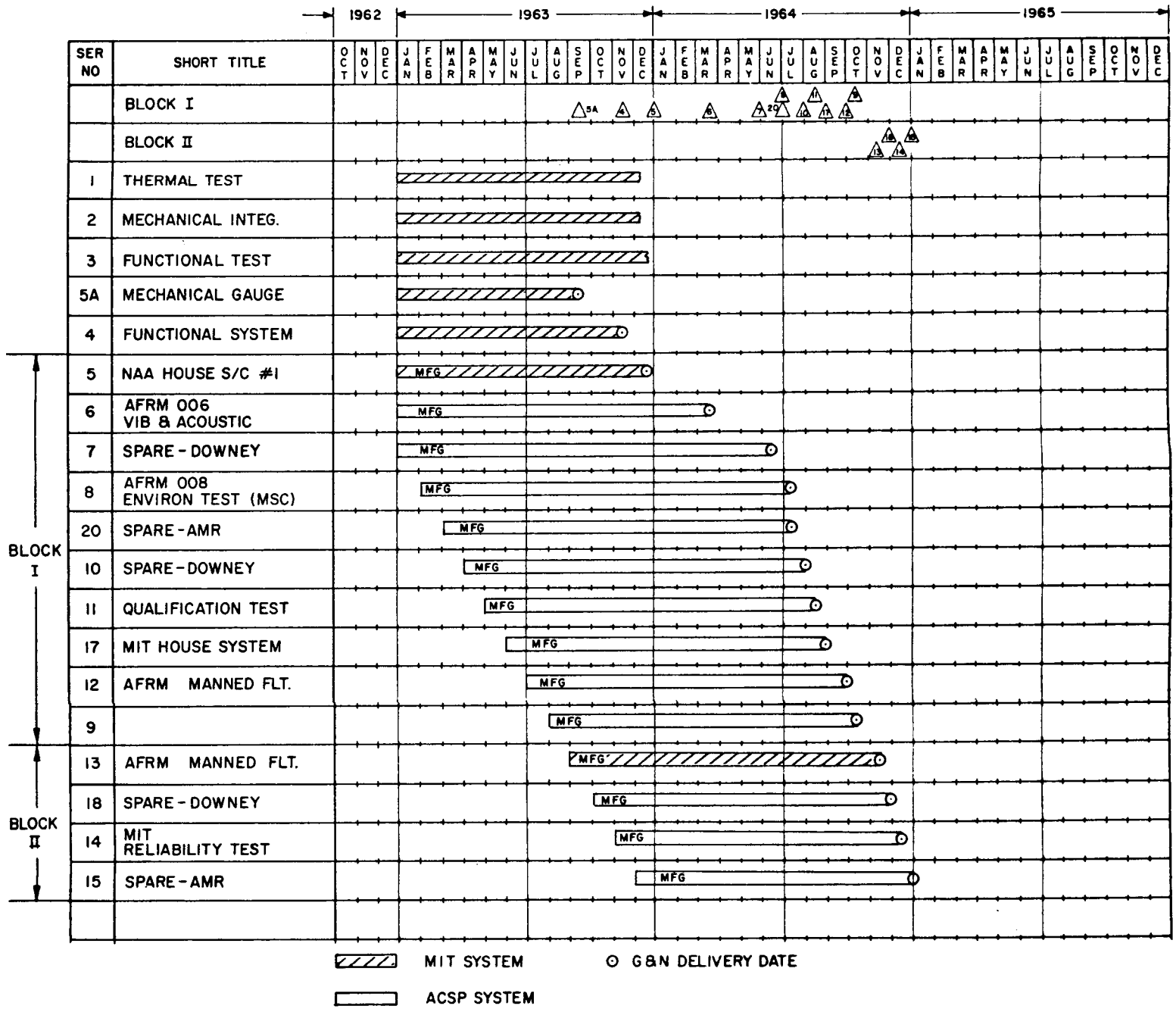

APOLLO MILESTONE CHART FOR AGE 4

Fig 1-2

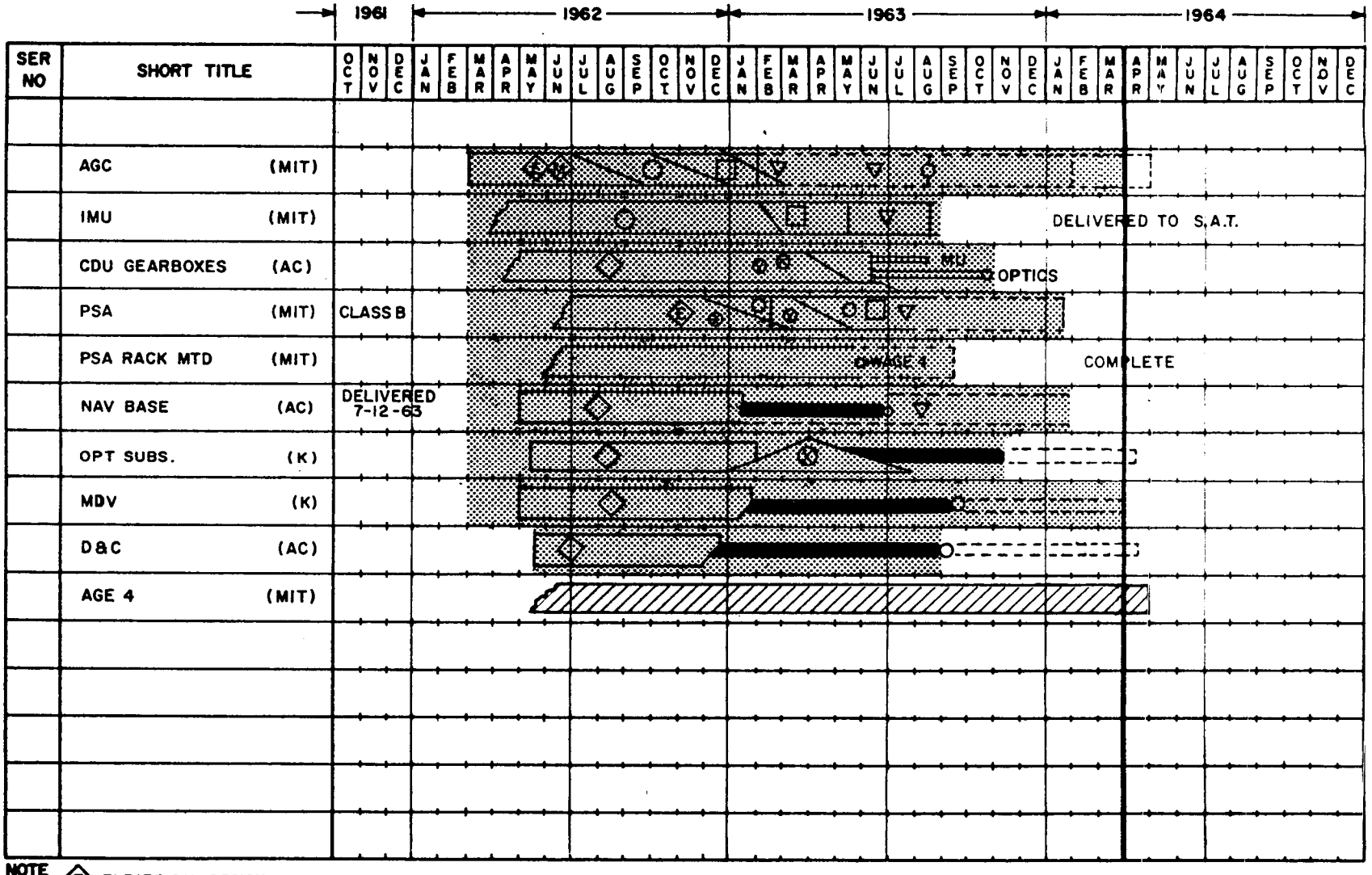

APOLLO MILESTONE CHART FOR AGE 5

Fig I-3

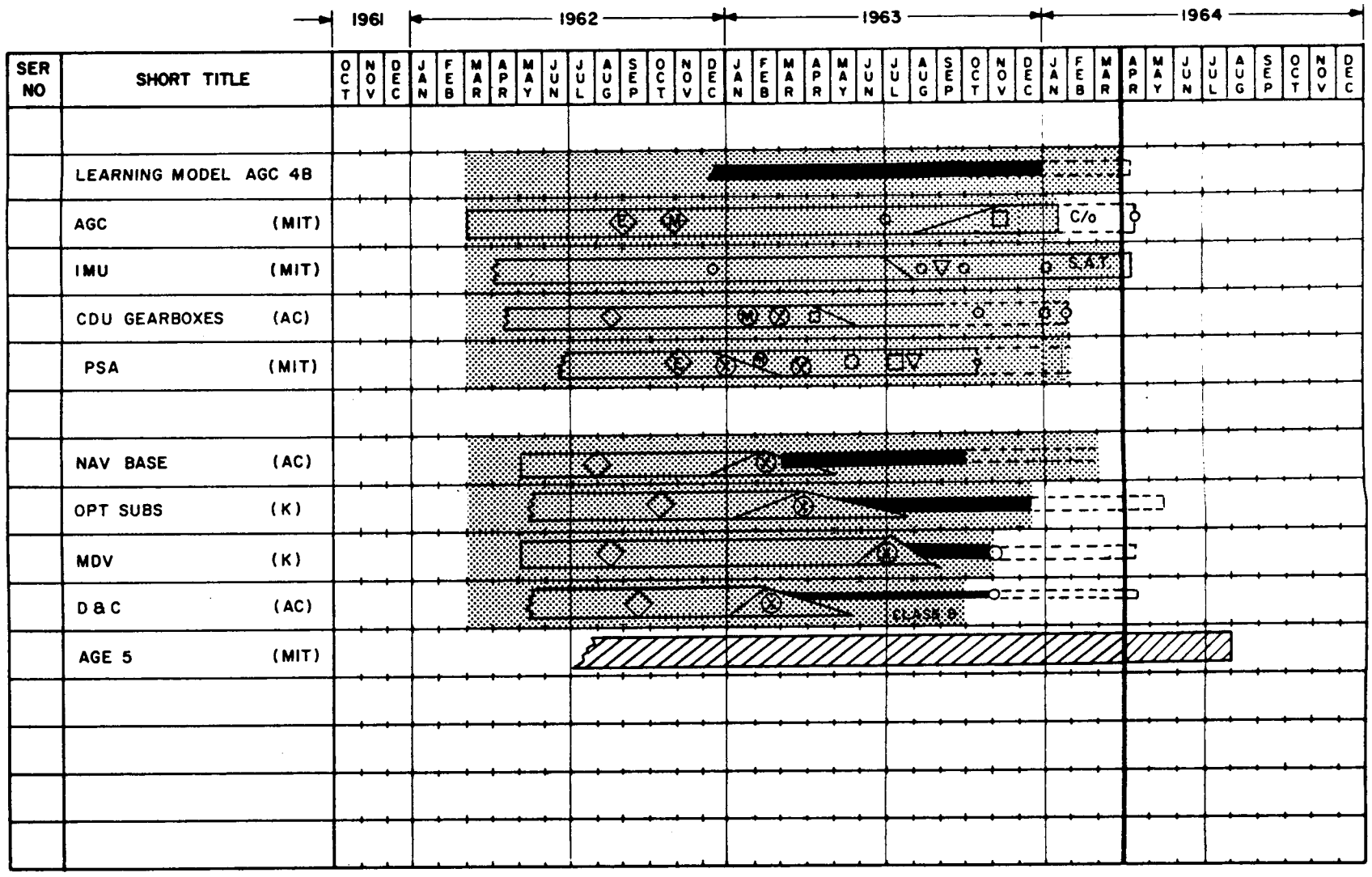

The computer delivery schedule is shown in Fig. I-4.

AGC-4B: Raytheon reports all items for use on AGC-4B have been completed with the exception of the cover plate assembly and rope sticks which will be delivered as required.

AGC-5: Raytheon reports subassemblies for AGC-5 are now expected to be completed during April.

Block I AGC Core Ropes: MIT/IL directed Raytheon to wire sense lines for the following eight modules as specified by Computer Program Assembly NASA Drawing #1021100, Program Artemis.

Quantity	Module	Assembly No.
2	B-21	1021100-4
2	B-22	1021100-4
2	B-23	1021100-4
2	B-24	1021100-4

Raytheon will retain the completed ropes for factory test. (Reference MIT/IL Letter AG 258-64, 13 March 1964.)

MIT/IL directed Raytheon to wire sense lines for three modules as specified by Computer Program Assembly Drawing #1021101 (Moon Glow):

Module	Assembly No.
B-21	1021101-1
B-28	1021101-1
B-29	1021101-1

(Reference MIT/IL Letter AG 276-64, 18 March 1964.)

AGC-4B Core Ropes: MIT/IL directed Raytheon to wire sense lines for one complete set, six modules, Assembly Numbers 1021100-4 as specified by computer assembly NASA Drawing #1021100, Program Artemis. The ropes will be retained at Raytheon for factory test. (Reference MIT/IL Letter AG 259-64, 13 March 1964.)

Subassembly Reliability and Qualification Test: MIT/IL requested Raytheon to plan and conduct a parts qualification test program as described in MIT/IL Report R-389, and prepare and submit test plans to MIT/IL 30 days prior to the start of testing. Testing shall be accomplished in accordance with the requirements of qualification specifications ND 1002037 and ND 1002044 through ND 1002058 as applicable, depending upon system usage of the particular part. Overstress testing will be performed as necessary to establish adequate safety margins under the more critical stress developed for the particular component. Parts involved in this program must be procured in accordance with Class A documents and subjected to all required acceptance tests, inspection and burn-in. (Reference TD R-125, 18 March 1964.)

Fig I-4

APOLLO MILESTONE CHART FOR APOLLO GUIDANCE COMPUTER (AGC)

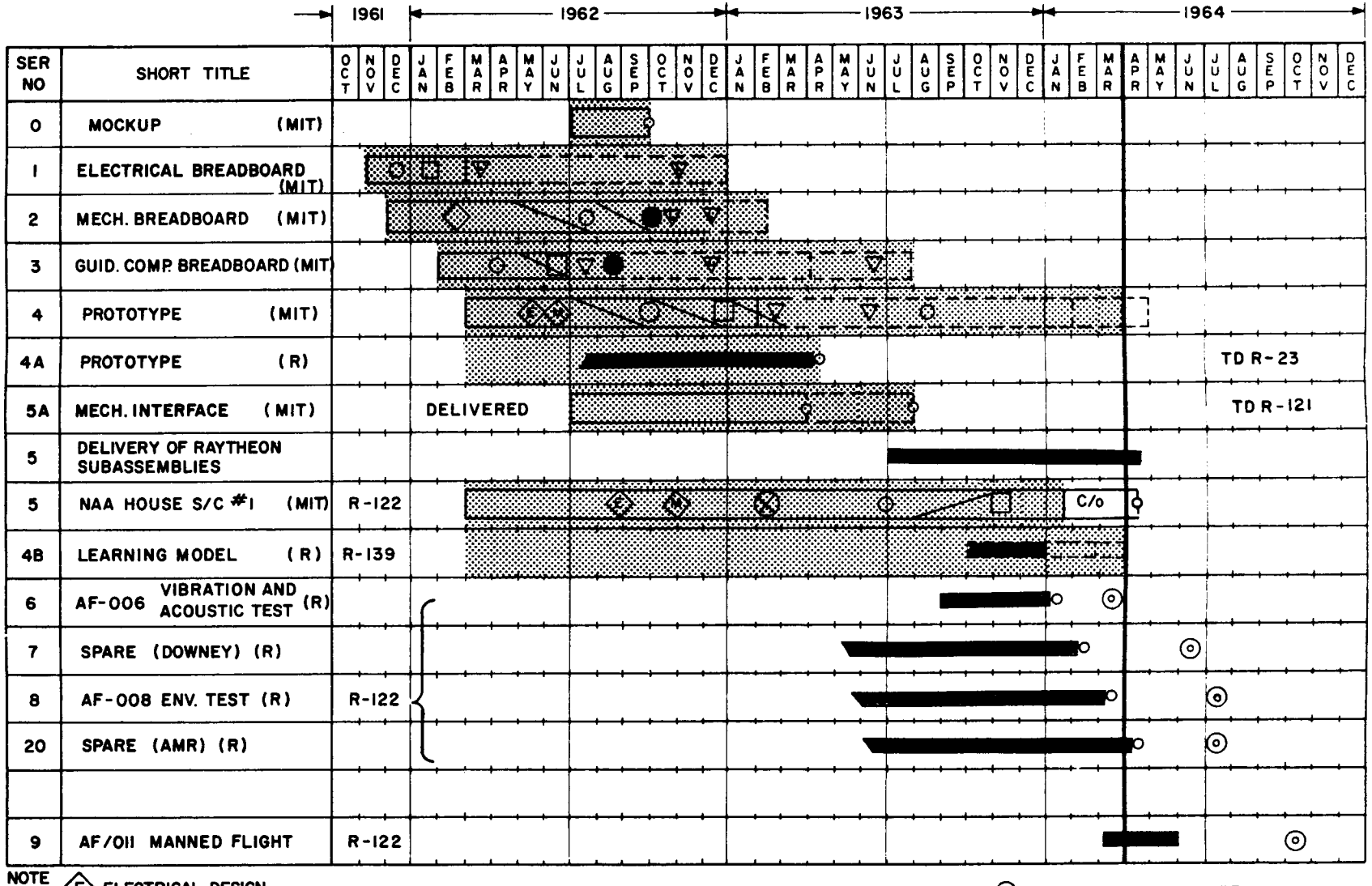

APOLLO MILESTONE CHART FOR APOLLO GUIDANCE COMPUTER (cont.)

Fig. I-4 (cont)

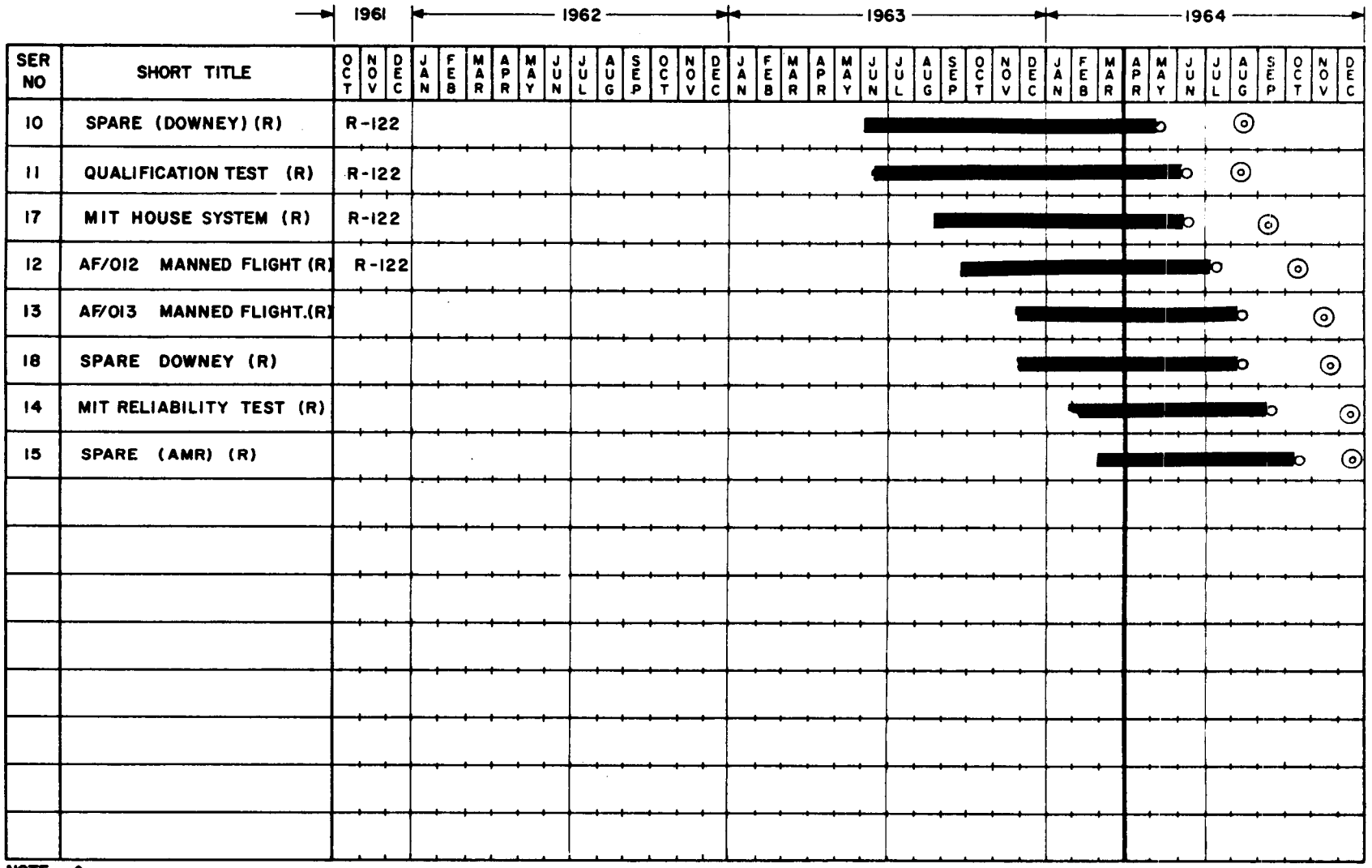

Figure I-5 shows the Apollo Guidance Computer Programming which is a continuing program.

The Inertial Measurement Unit (IMU) delivery schedule is shown in Fig. I-6. IMU-1, 2, and 3 are development models remaining in test at MIT/IL. IMU-4 is undergoing system tests as part of AGE-4. IMU-5 is undergoing inertial subsystem tests in the IMU Lab.

Figure I-7 shows the Power & Servo Assembly (PSA) schedule.

PSA Packaging Engineering: MIT/IL issued amendment number 2 to TD A-118 deleting six PSA tray harness drawings (numbers 1015743 through 1015748) which were to be prepared by ACSP. Ten additional drawings (numbered 1015764 through 1015773) were added to the list of tray harness drawings to be prepared by ACSP from MIT/IL wiring diagrams. (Reference MIT/IL Letter AG 239-64, 9 March 1964.)

Block I Harness and PSA End Connector Assembly: MIT/IL authorized ACSP to conduct environmental tests and perform an engineering evaluation of the Block I G&N Harness and PSA End Connector Assembly, P/N 1014606. AC Spark Plug will prepare environmental test plans and procedures for MIT/IL approval in accordance with MIT/IL Report R-389; design and fabricate test fixtures and tooling; and conduct the environmental tests. (Reference TD A-223, 25 March 1964.)

The Coupling & Display Unit (CDU) delivery schedule is shown in Fig. I-8.

Environmental Tests: MIT/IL authorized ACSP to prepare environmental test plans and procedures in accordance with MIT/IL Report R-389. Plans and procedures shall be submitted to MIT/IL for approval. AC Spark Plug will design and fabricate test fixtures and tooling to implement test plans after MIT/IL approval of the test plans. AC Spark Plug will conduct and evaluate the environmental tests and submit reports to MIT/IL within one month after completion of the tests. Two of the CDU's to be delivered under TD A-147 will be selected by MIT/IL for environmental testing. (Reference TD A-208, 16 March 1964.)

The Navigation Base delivery schedule is shown in Fig. I-9.

Retrofit Isolators for AGE-4: MIT/IL directed ACSP to redesign the resiliant mounts for cast aluminum instead of stainless steel. Retrofit isolators for AGE-4 shall consist of the following:

Quantity		P/N
1	Mount, Resiliant, Rear	1899969
2	Mount, Resiliant, Front	1899970

The AGE-4 isolators are to be shipped to ACSP, Milwaukee, for use in Phase II engineering evaluation testing. (Reference MIT/IL Letter AG 206-64, 25 February 1964.)

APOLLO GUIDANCE COMPUTER PROGRAMMING SCHEDULE

Fig. I-5

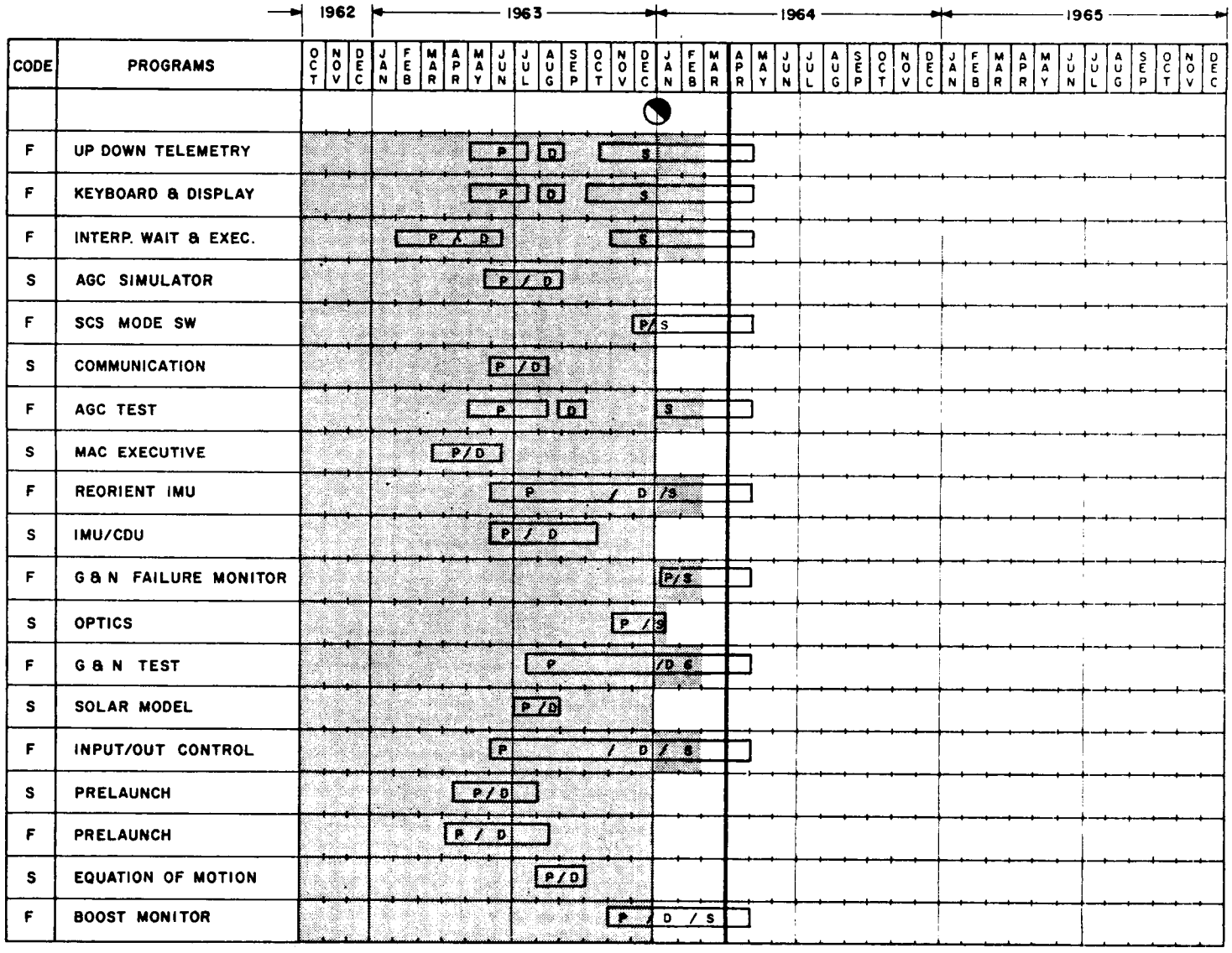

F = FLIGHT
S = SIMULATION
P = PROGRAM FOR AGC
D = PERFORM DUMMY TEST
S = TEST ON APOLLO SIMULATOR
◔ = NASA MISSION INFO REQD

Fig. I-5 (cont)

APOLLO GUIDANCE COMPUTER PROGRAMMING SCHEDULE (cont.)

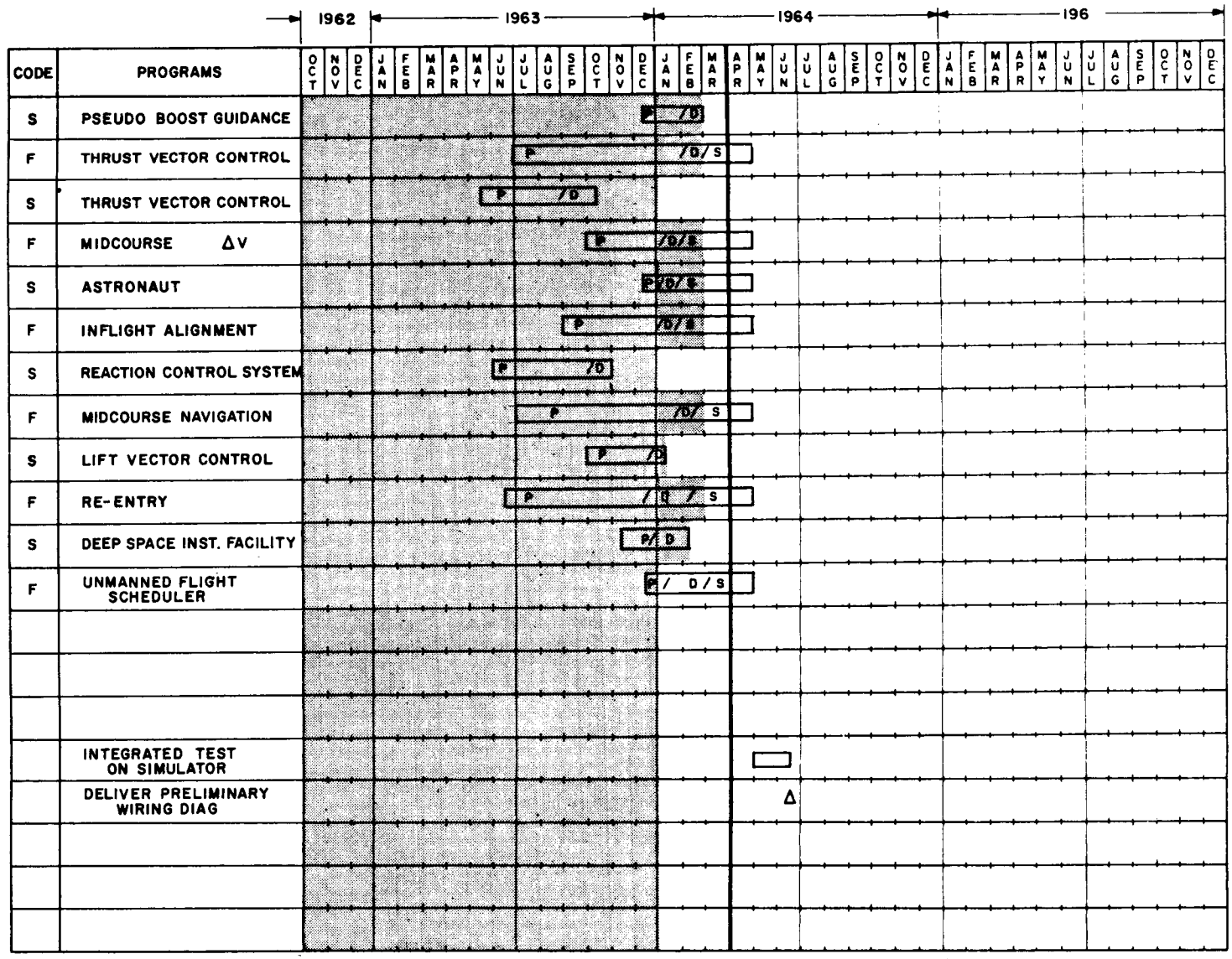

APOLLO MILESTONE CHART FOR IMU DEVELOPMENT PLAN

Fig. I-6

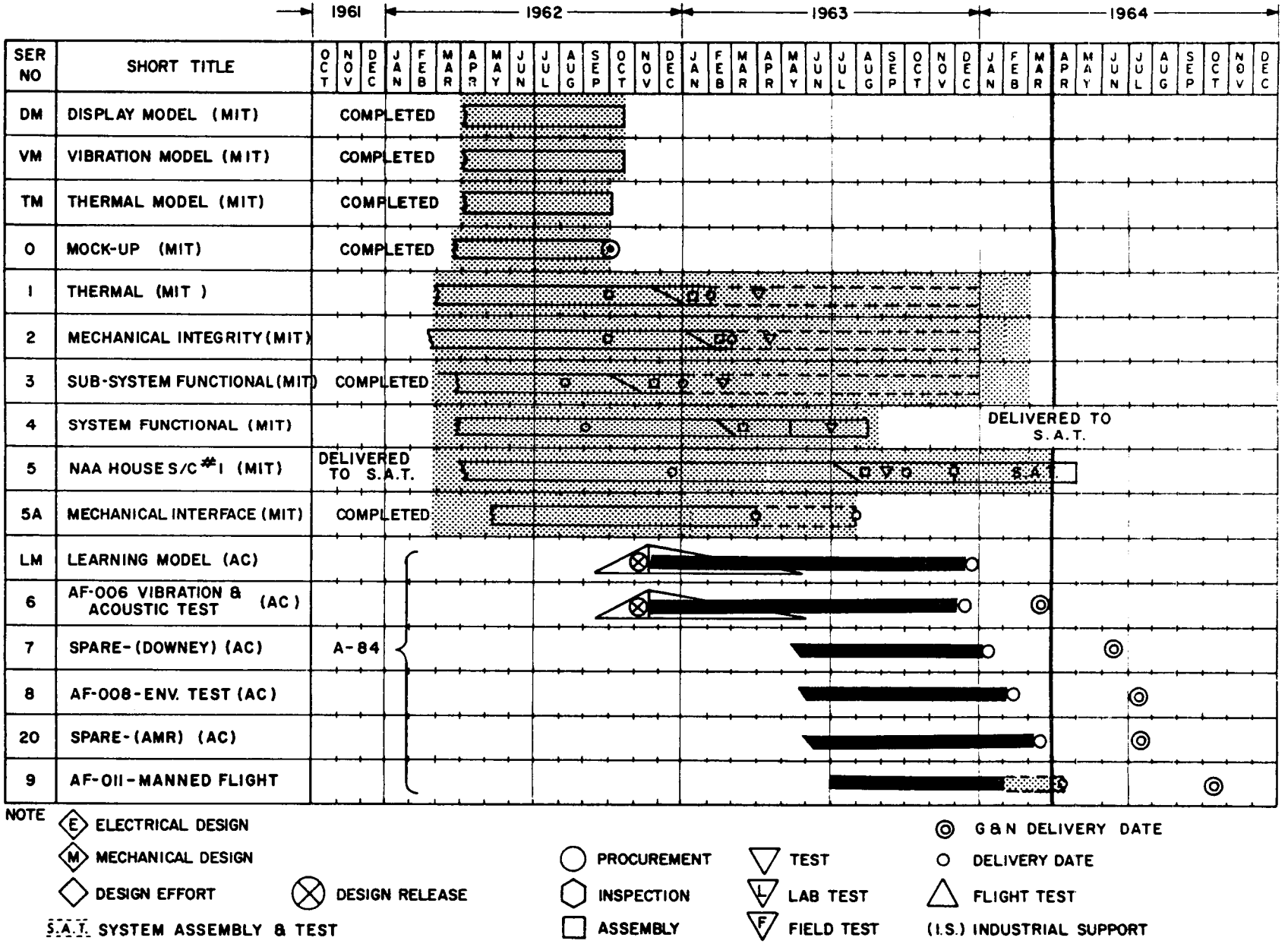

APOLLO MILESTONE CHART FOR IMU DEVELOPMENT PLAN (cont.)

Fig. I-6 (cont)

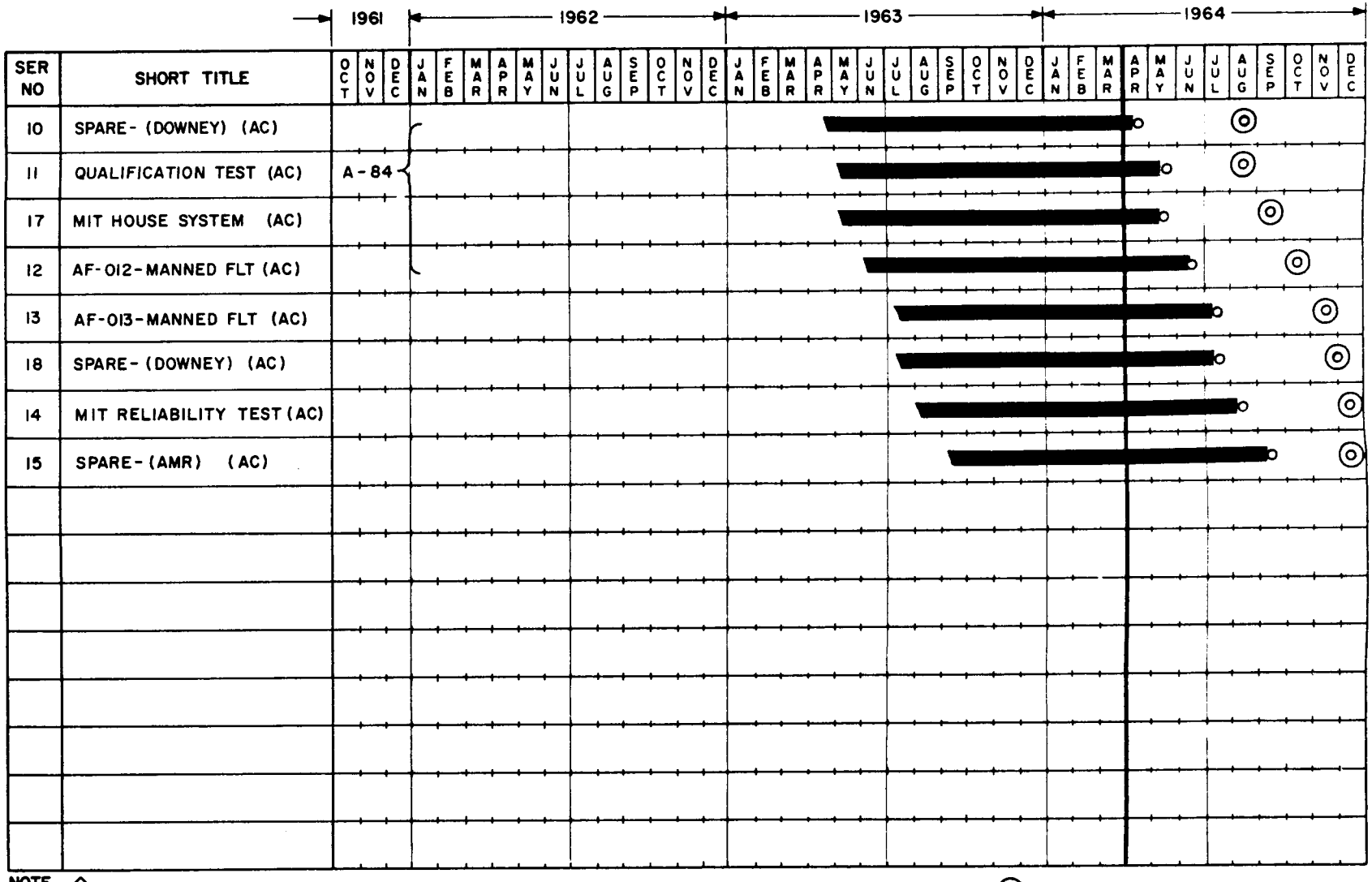

APOLLO MILESTONE CHART FOR POWER AND SERVO ASSEMBLY (PSA)

Fig. I-7

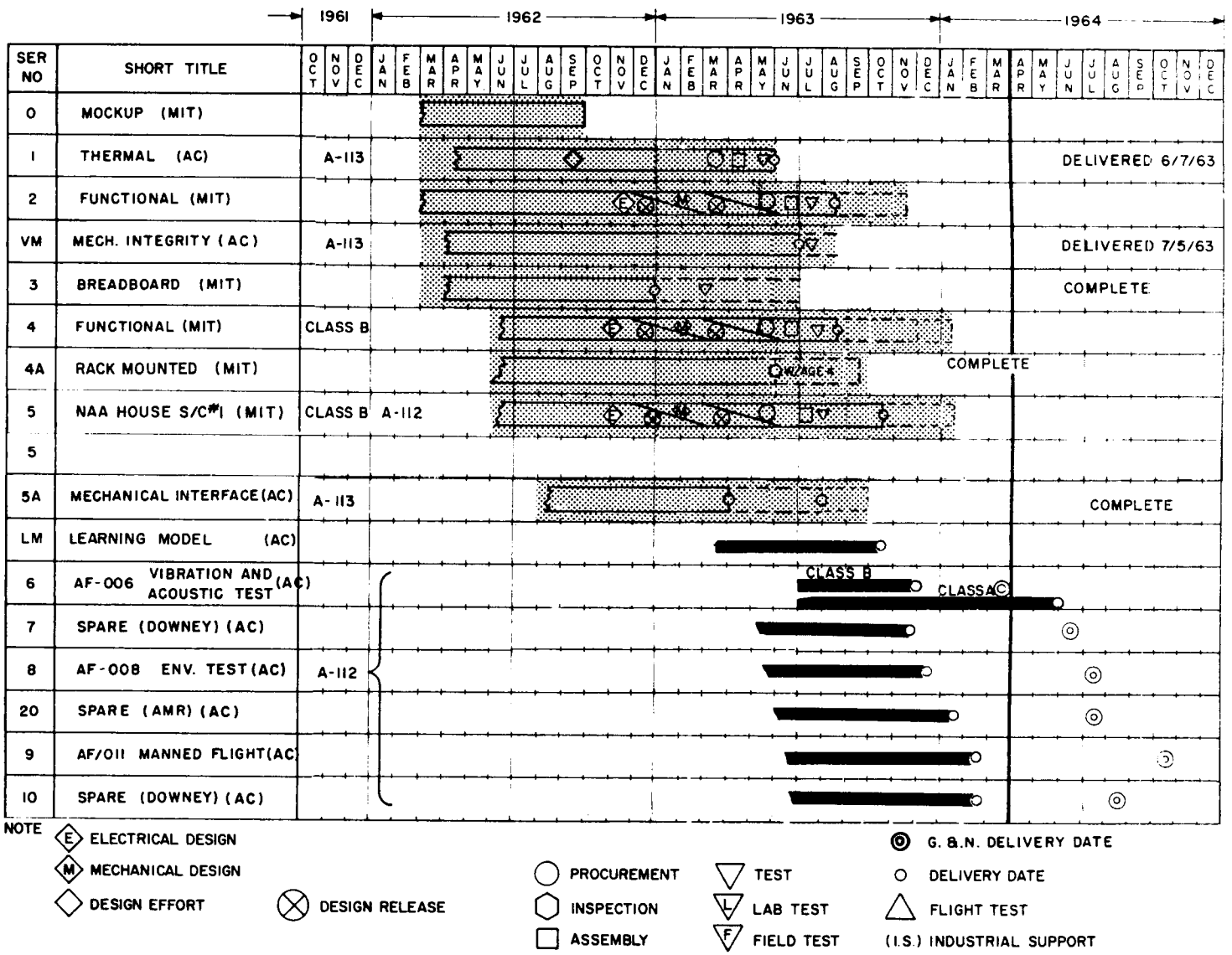

APOLLO MILESTONE CHART FOR POWER AND SERVO ASSEMBLY cont.

Fig. I-7 (cont)

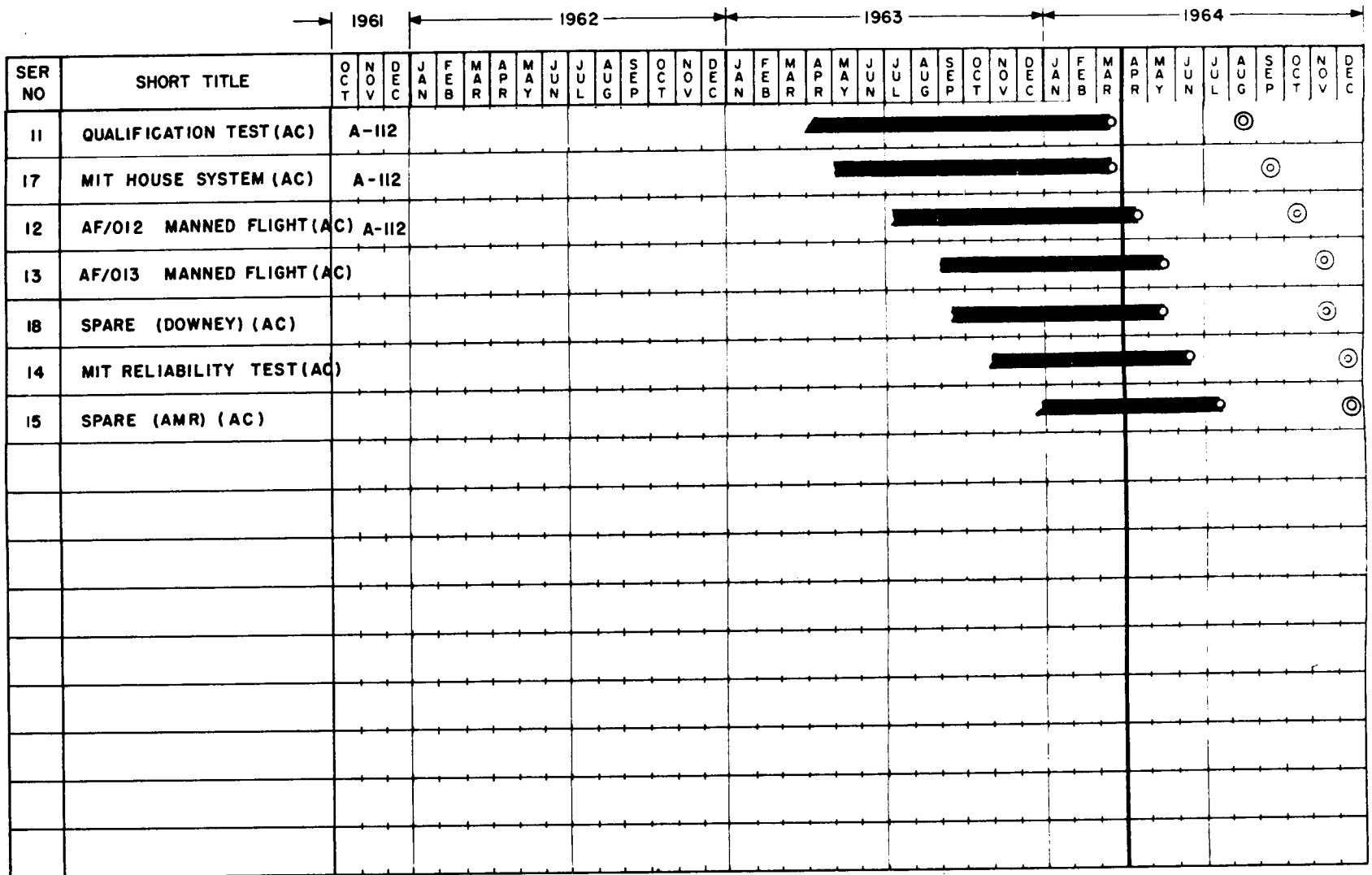

APOLLO MILESTONE CHART FOR CDU GEARBOXES

Fig. 8

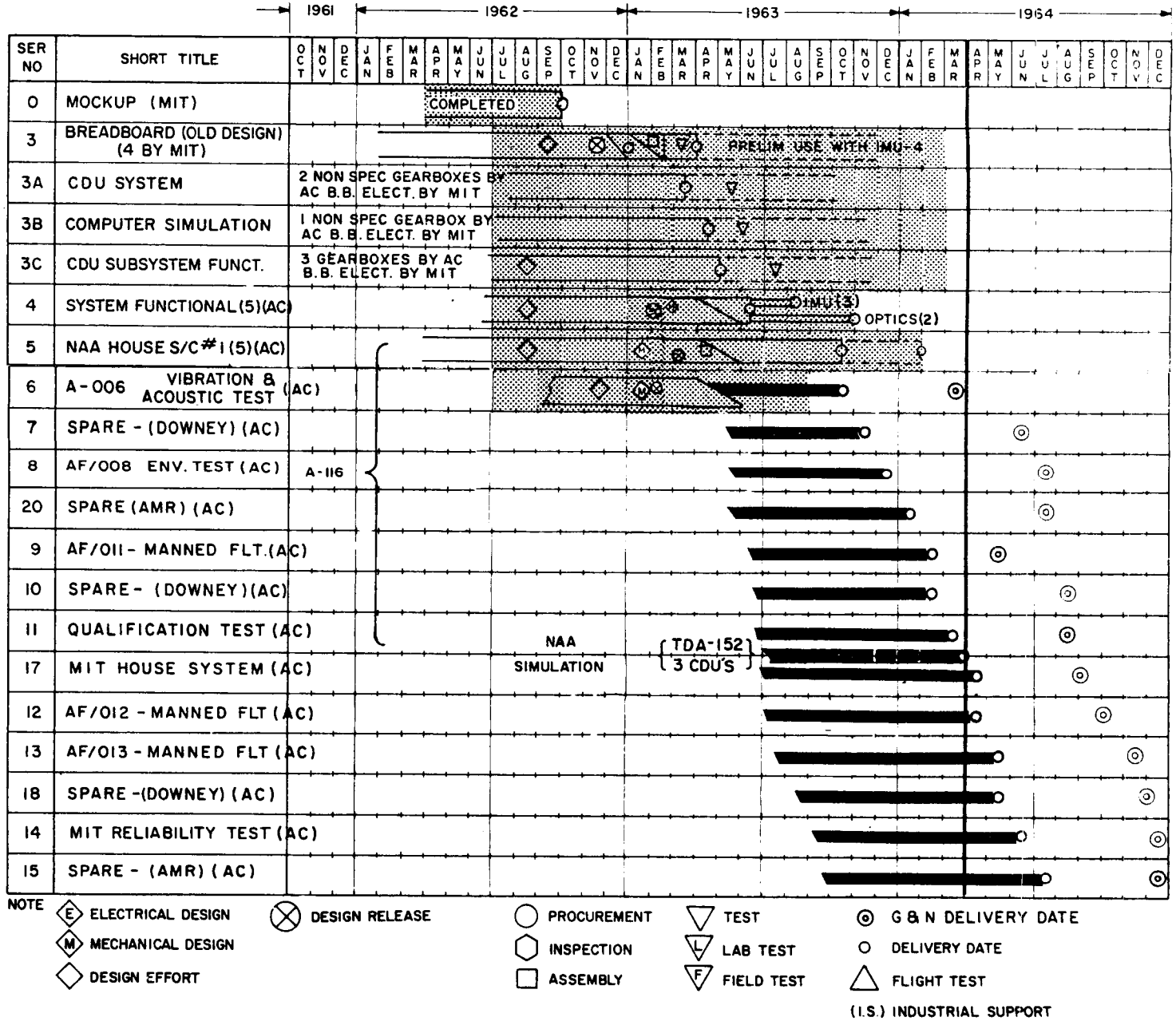

Fig I 9

APOLLO MILESTONE CHART FOR NAVIGATION BASE SUB-SYSTEM

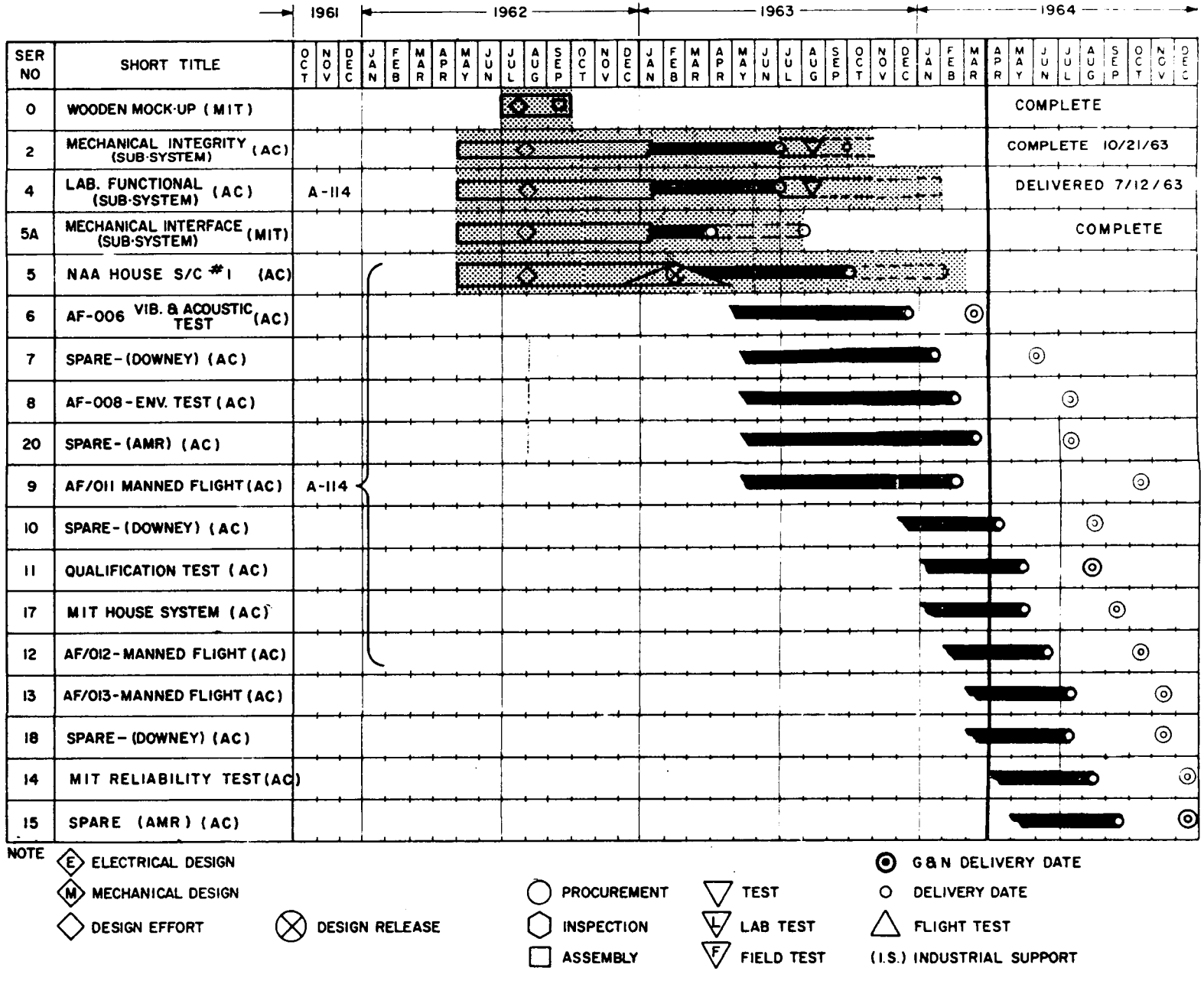

Figure I-10 shows the Display & Control (D&C) delivery schedule.

Control Electronics Assembly: MIT/IL requested ACSP to construct a mechanical gage of the Control Electronics Assembly, P/N 1015003. The gage shall become part of the D&C Group Hardware for the AGE-5A mechanical interface gage.

Vibration Test: MIT/IL authorized ACSP to conduct vibration tests on one fiberglass shroud and cover assembly, similar to P/N 1014502. The purpose of the tests is to determine the feasibility of using fiberglass as a replacement material for honey comb aluminum. It is felt that fiberglass will be lighter in weight, more economical, and will be less difficult to fabricate. If a fiberglass unit can successfully meet the vibrational requirements, serious consideration will be given toward incorporating the fiberglass material on Command Module hardware. (Reference MIT/IL Letter AG 237-64, 11 March 1964.)

Block I Harness and PSA End Connector Assembly: As noted in the PSA section, MIT/IL authorized ACSP to conduct environmental tests and perform an engineering evaluation of the Block I G&N Harness and PSA End Connector Assembly, P/N 1014606. AC Spark Plug will prepare environmental test plans and procedures for MIT/IL approval in accordance with MIT/IL Report R-389; design and fabricate test fixtures and tooling; and conduct the environmental tests. (Reference TD A-223, 25 March 1964.)

The Optics delivery schedule is shown in Fig. I-11.

Failure Analysis: MIT/IL authorized Kollsman to establish a program and facility to perform analyses of failed or defective parts and material occasioned during field, final test, or factory operations. Analyses shall be performed as deemed necessary by the Kollsman Corrective Action Board or as directed by MIT/IL or NASA. This effort shall include:

a) Disassembly of encapsulated assemblies to determine the cause of failure or rejection.

b) Disassembly of piece parts to determine the cause of failure or rejection.

c) Mechanical or metallurgical analysis of problems resulting from field operations.

The Map & Data Viewer delivery schedule is shown in Fig. I-12.

Condition Light Assemblies: MIT/IL requested Kollsman to supply a total of seventeen Condition Light Assemblies. These assemblies will be utilized as follows:

10	Assemblies for systems
3	Assemblies for breadboards
1	Assembly for Kollsman Learner Model
3	Assemblies for qualification testing at Kollsman.

(Reference MIT/IL Letter AG 168-64, 2 March 1964.)

Fig. I-10

APOLLO MILESTONE CHART FOR DISPLAY & CONTROL SUBSYSTEMS

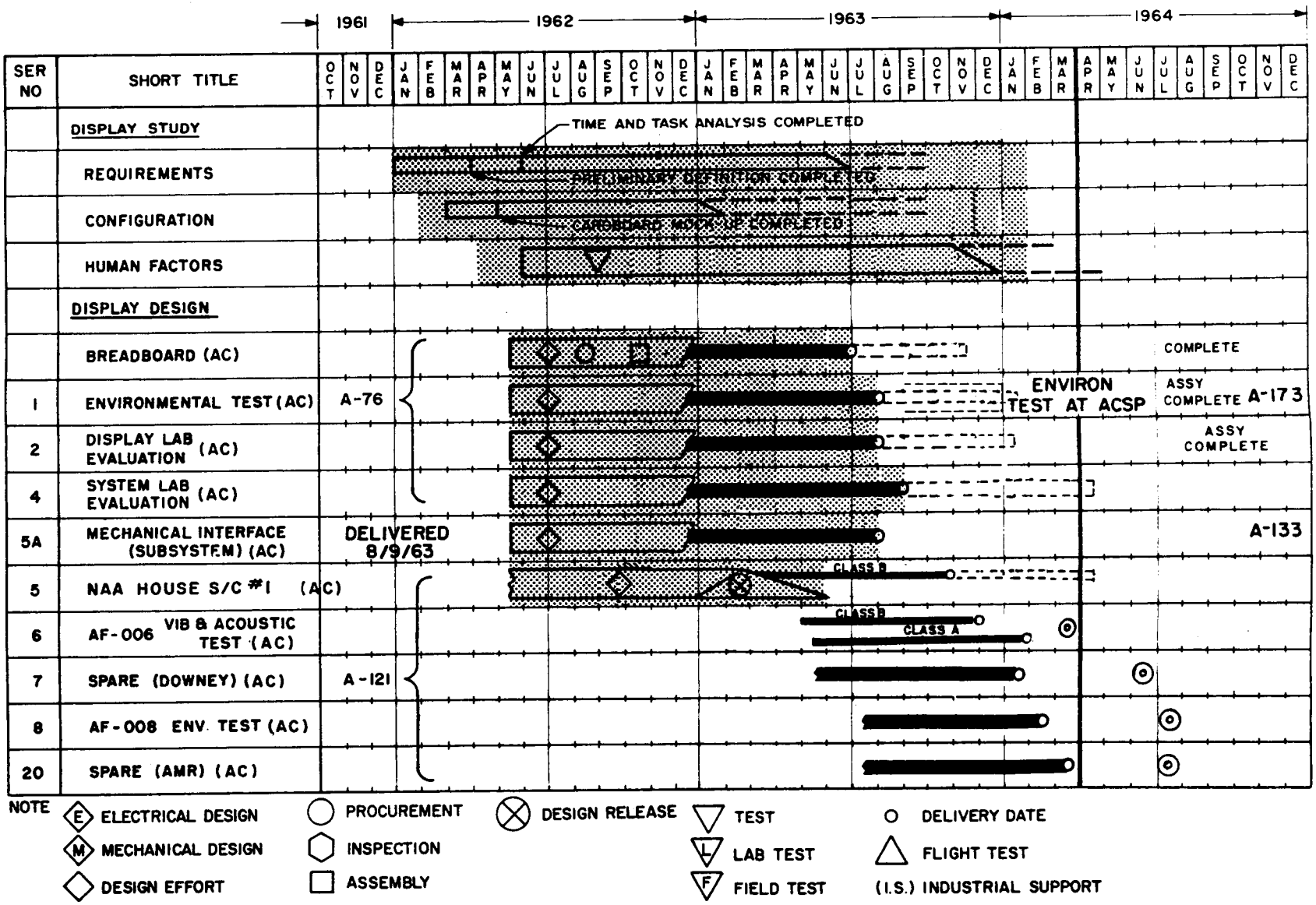

APOLLO MILESTONE CHART FOR DISPLAY AND CONTROL SUBSYSTEM

Fig I-10 (cont.)

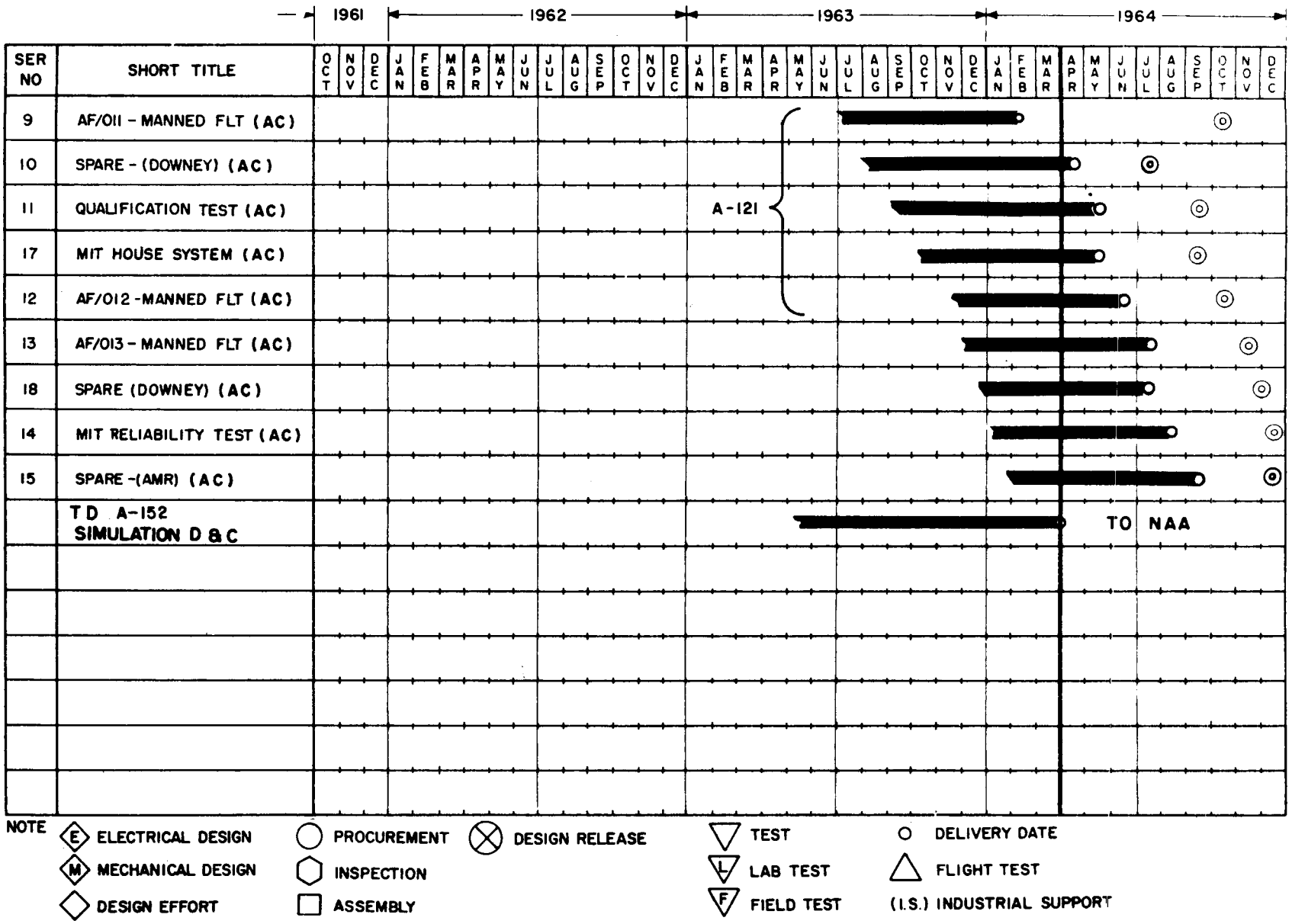

APOLLO MILESTONE CHART FOR OPTICAL SUBASSEMBLY

Fig. I-11

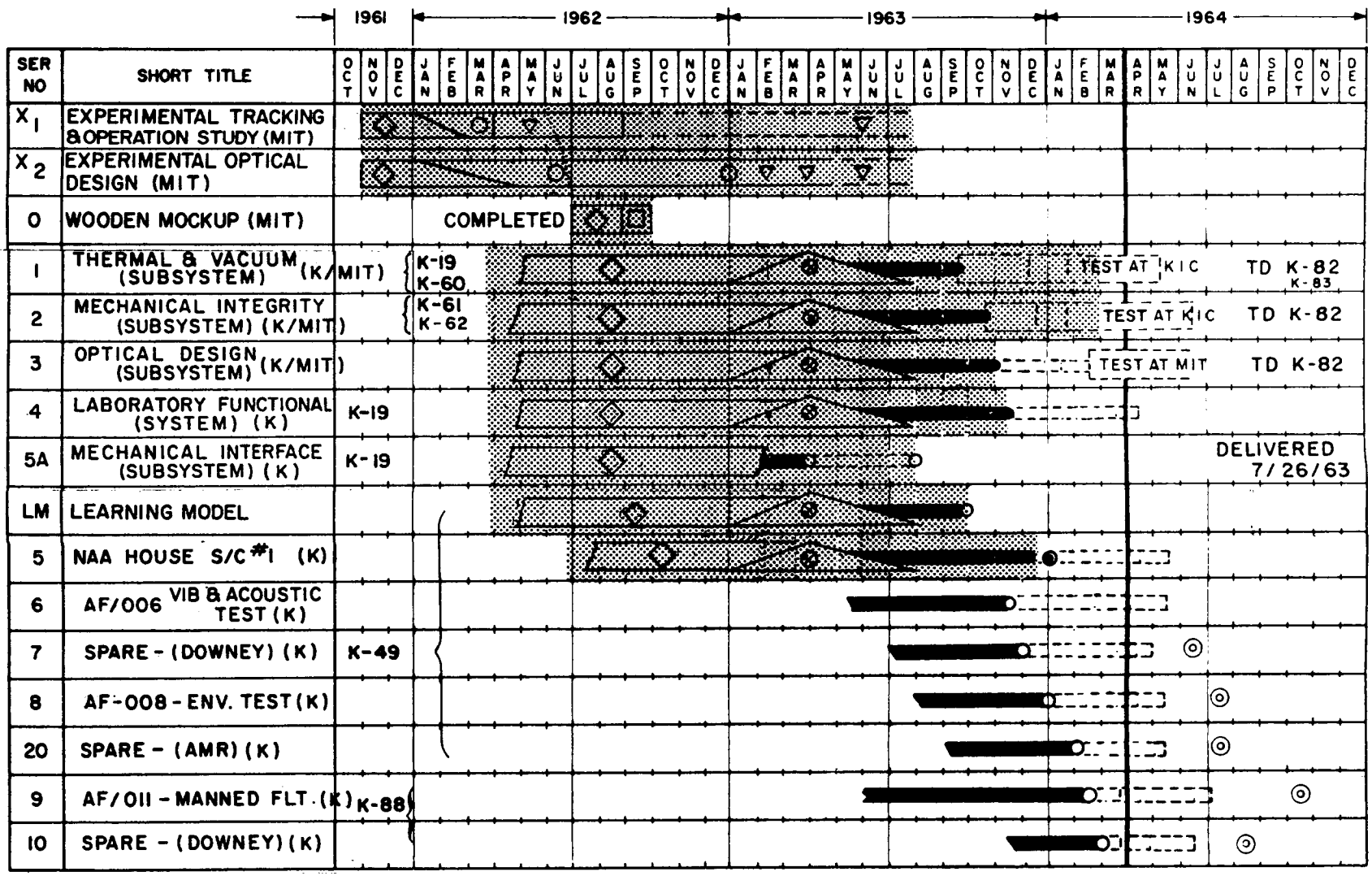

APOLLO MILESTONE CHART FOR OPTICAL SUBASSEMBLY (CON'T.)

Fig. I-11 (cont)

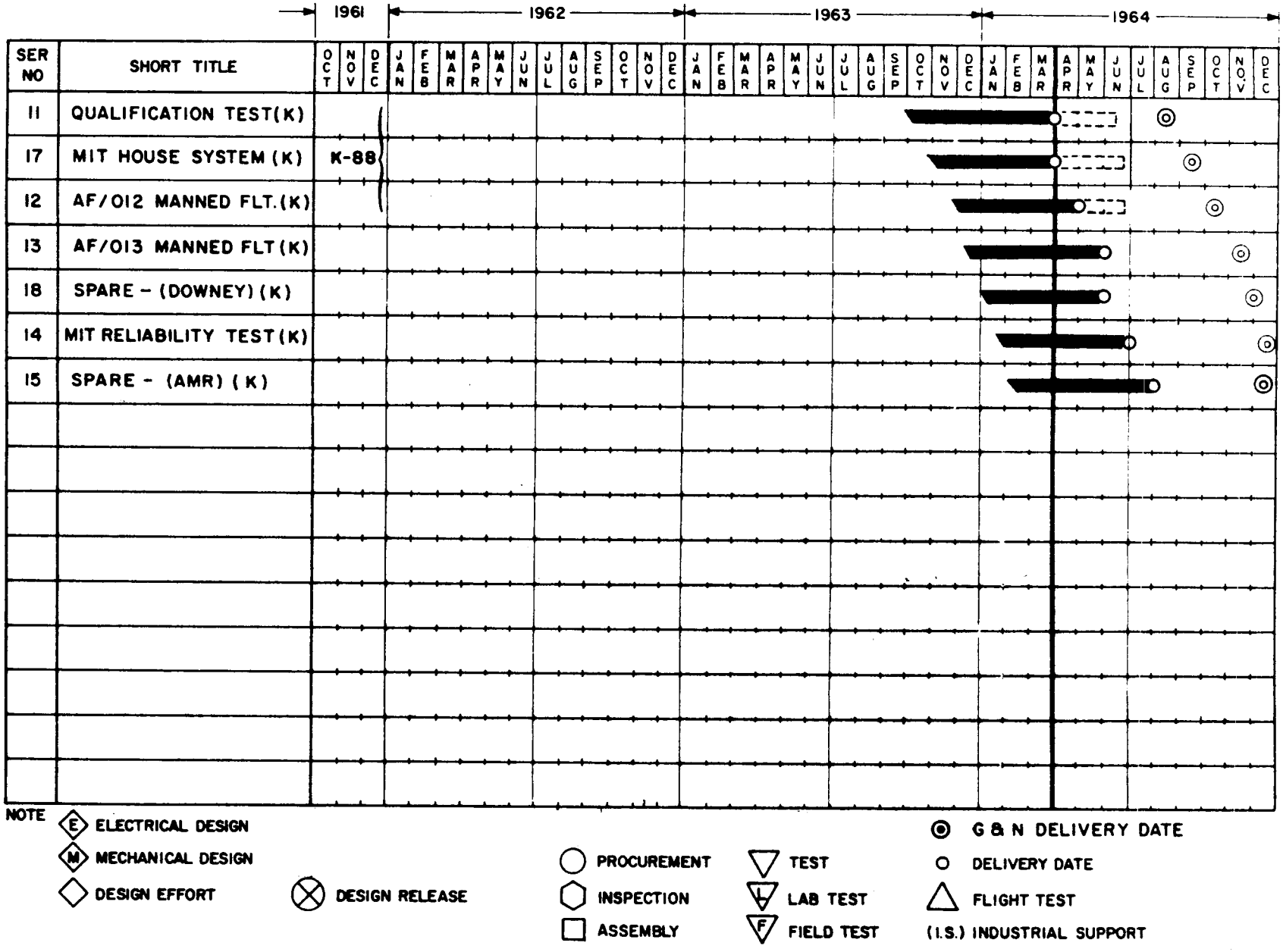

APOLLO MILESTONE CHART FOR MAP AND DATA VIEWER SYSTEM

Fig. 1-2

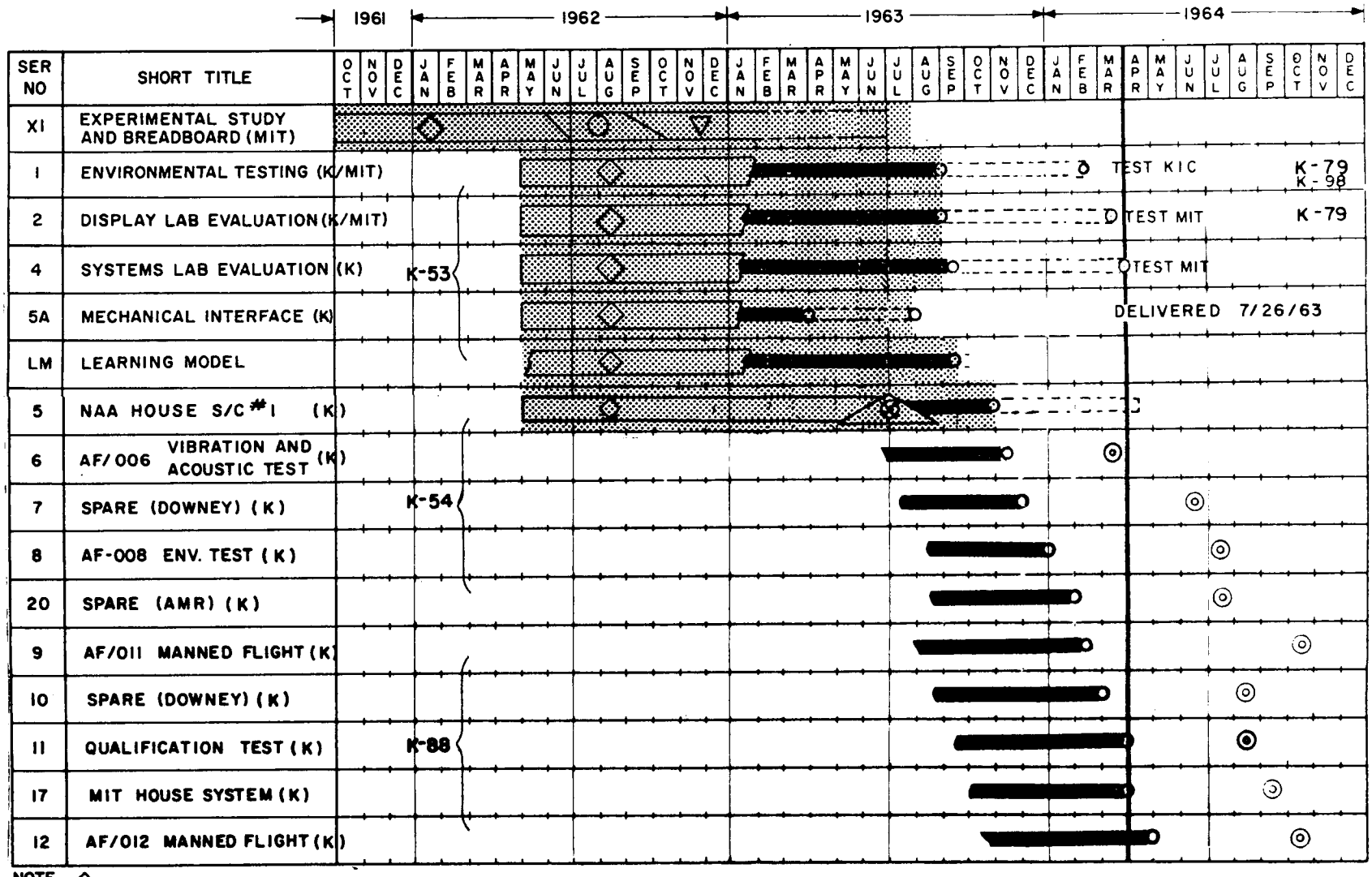

NOTE

- E ELECTRICAL DESIGN
- M MECHANICAL DESIGN
- DESIGN EFFORT
- DESIGN RELEASE
- PROCUREMENT
- INSPECTION
- ASSEMBLY
- TEST
- L LAB TEST
- F FIELD TEST
- G & N. DELIVERY DATE
- DELIVERY DATE
- FLIGHT TEST
- (I.S.) INDUSTRIAL SUPPORT

APOLLO MILESTONE CHART FOR MAP AND DATA VIEWER SYSTEM (cont.)

Fig 1 2 (cont)

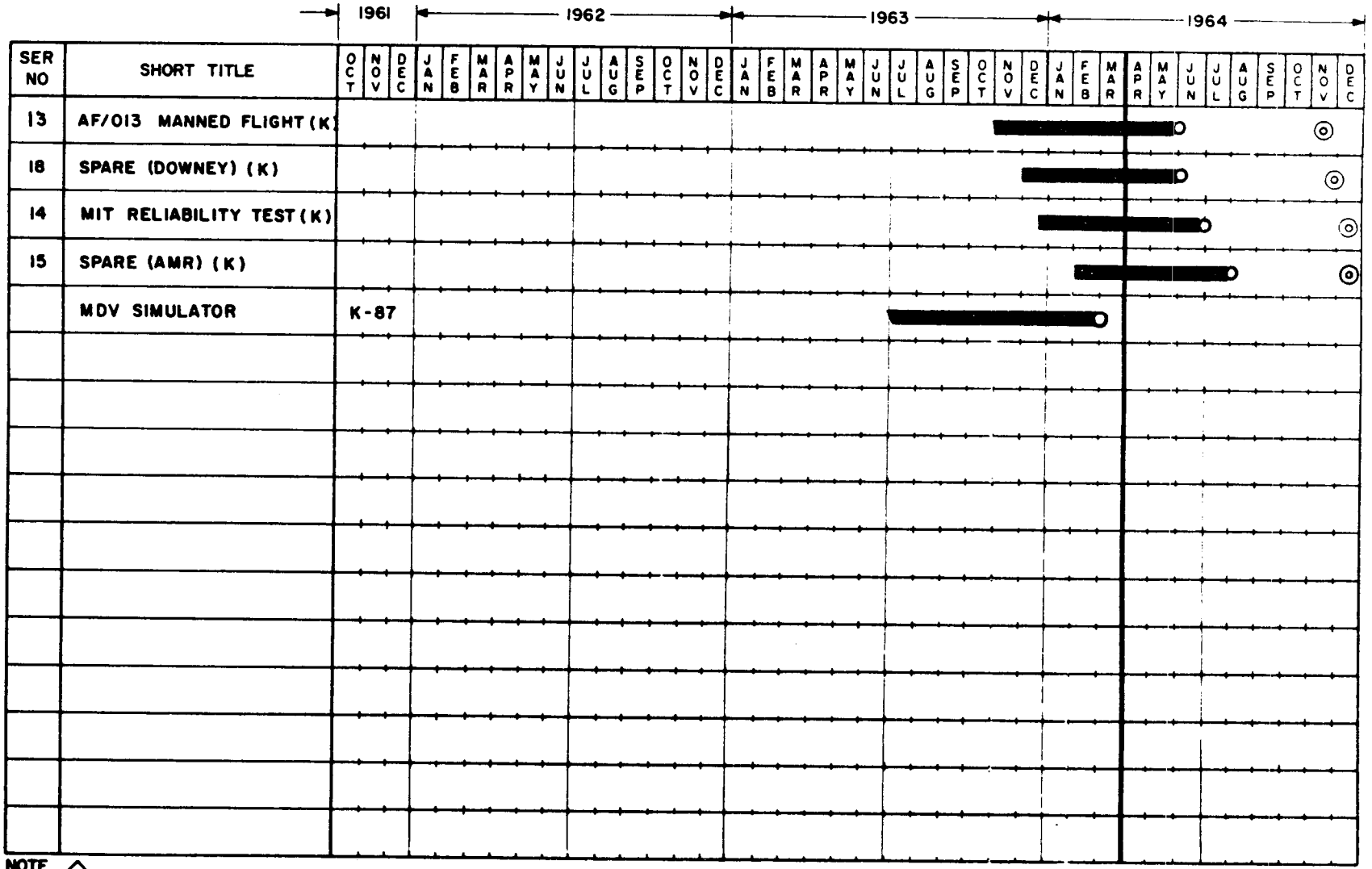

Figure I-13 is the Midcourse Guidance Study, which is a continuing effort.

Raytheon's GSE delivery schedule is shown in Fig. I-14.

Computer Test Set: The next delivery is Test Set Number 4, now expected to occur 2 April 1964.

Computer Simulators: Simulator Number 11 was delivered to ACSP 27 March 1964. This completes Raytheon's simulator deliveries.

AC Spark Plug's GSE delivery schedule is shown in Fig. I-15.

Breadboard GSE For Block II Inertial Subsystem Test: MIT/IL authorized ACSP to develop a breadboard GSE which will support testing of a Block II breadboard Inertial Subsystem at MIT/IL. AC Spark Plug will perform the following tasks:

1. Design and fabricate the following units which shall be functionally and mechanically consistent with MIT/IL drawings SK-C-734000, SK-C-734002, and SK-C-734004 supplied to ACSP.
    a. Test Control Panel
    b. Gyro Caging - Torquing Electronics Panel.
    c. Precision Set - Cardinal Point Test Electronics Panel.
2. Provide support engineering, detailed design and testing, and detailed documentation for the above breadboard units.
3. Deliver the breadboard units to MIT/IL completed and fully tested by 1 June 1964. (Reference TD A-220, 12 March 1964.)

Kollsman's GSE delivery schedule is shown in Fig. I-16.

Precision Test Fixture Stands: MIT/IL authorized Kollsman to include two stands for use with and as part of the Precision Test Fixture. Stand number 1 will be delivered to Kollsman and number 2 will be delivered to ACSP. Stand number 1 has already been delivered to Kollsman. Stand number 2 will be to the same design and configuration as stand number 1. (Reference MIT/IL Letter AG 211-64, 5 March 1964.)

GSE Certification Equipment: MIT/IL directed Kollsman to purchase and/or fabricate parts (with the exception of Tallyvel Levels) to manufacture the following additional GSE Certification Equipment and storage containers for supporting the below listed GSE equipment:

Quantity	Nomenclature
1	Precision Test Fixture
4	Alignment Mirror Assembly
3	Short Periscope

All parts shall conform to Class 3 quality assurance requirements per NASA Specification ND 1015404. This task shall be considered complete upon delivery and acceptance of the above equipment at sites to be designated by MIT/IL as the equipment is prepared for delivery. (Reference TD K-125, 20 March 1964.)

Fig. I-13

APOLLO SCHEDULE - MIDCOURSE GUIDANCE STUDY

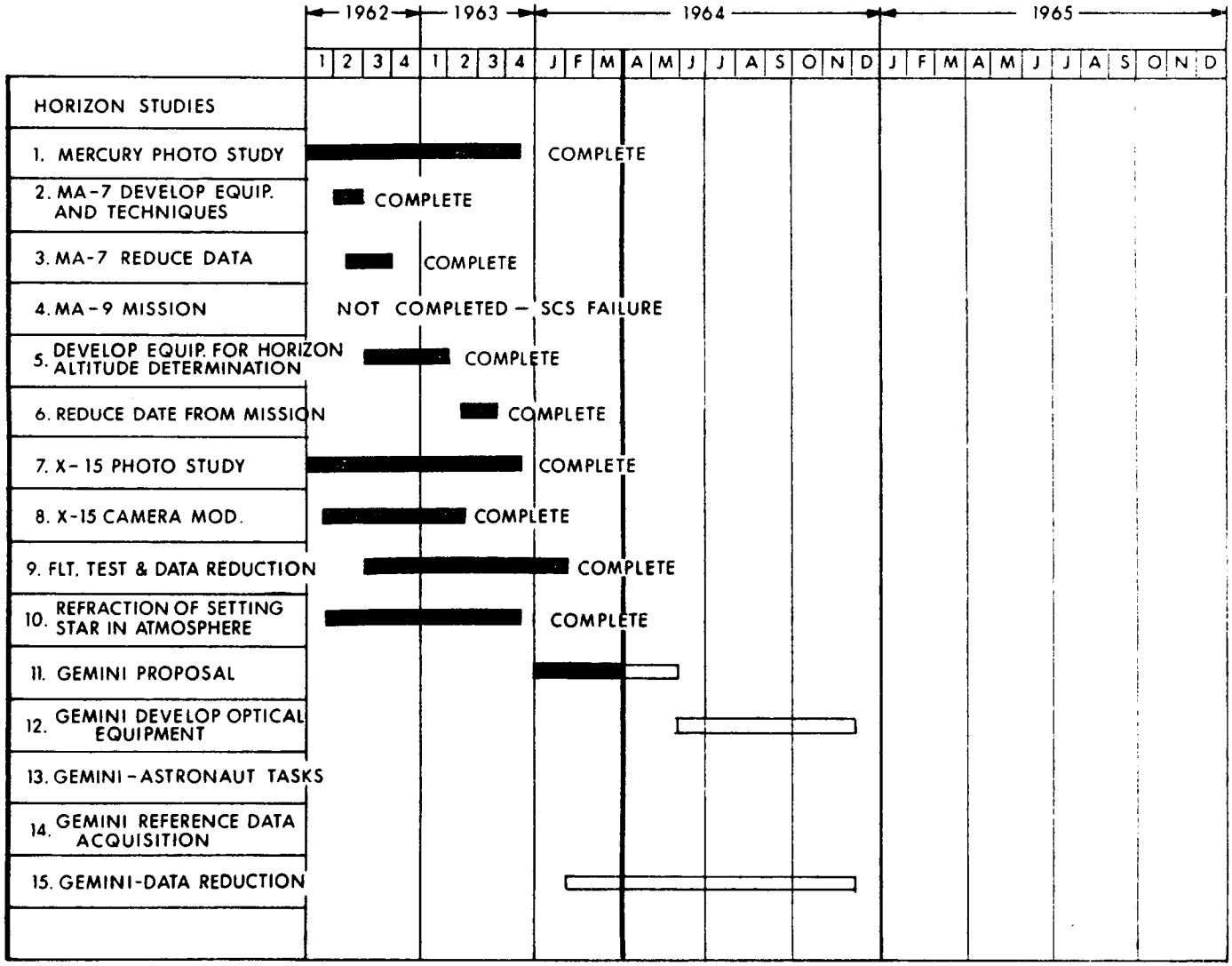

APOLLO SCHEDULE - MIDCOURSE GUIDANCE STUDY (cont.)

Fig. I-3 (cont)

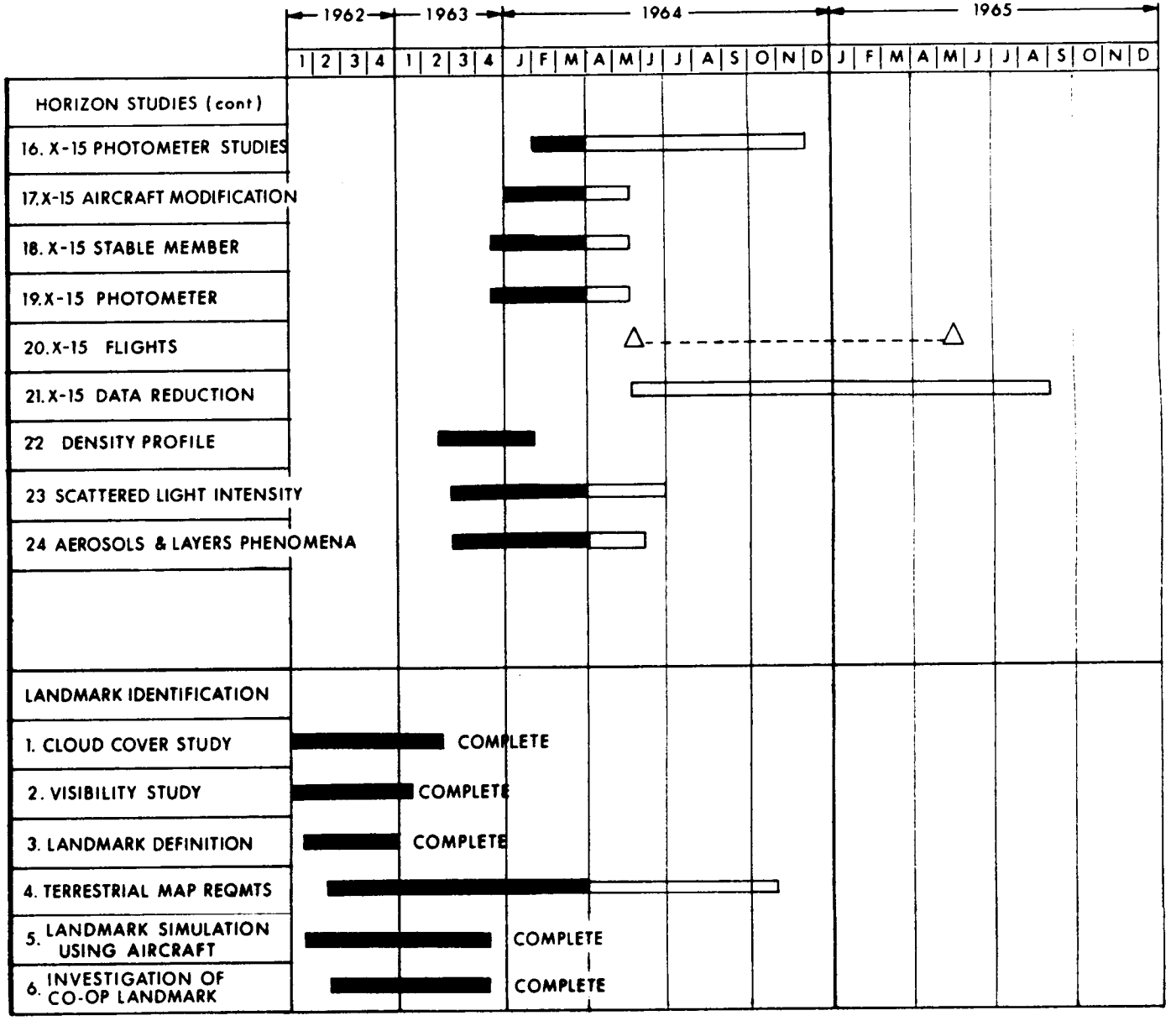

APOLLO SCHEDULE - MIDCOURSE GUIDANCE STUDY (cont.) Fig I-13 (cont)

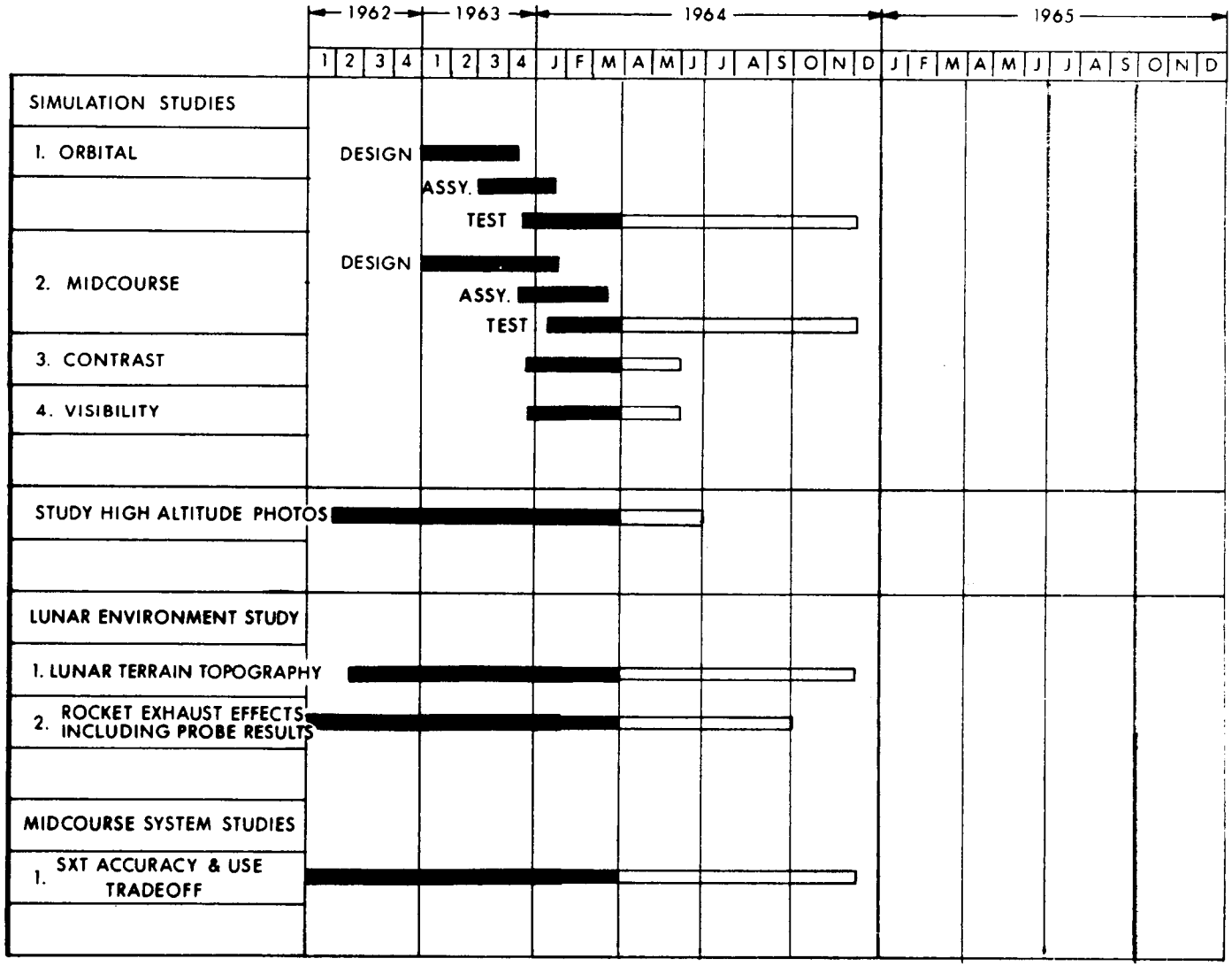

APOLLO SCHEDULE - MIDCOURSE GUIDANCE STUDY (cont.)

Fig. 1-13 (cont)

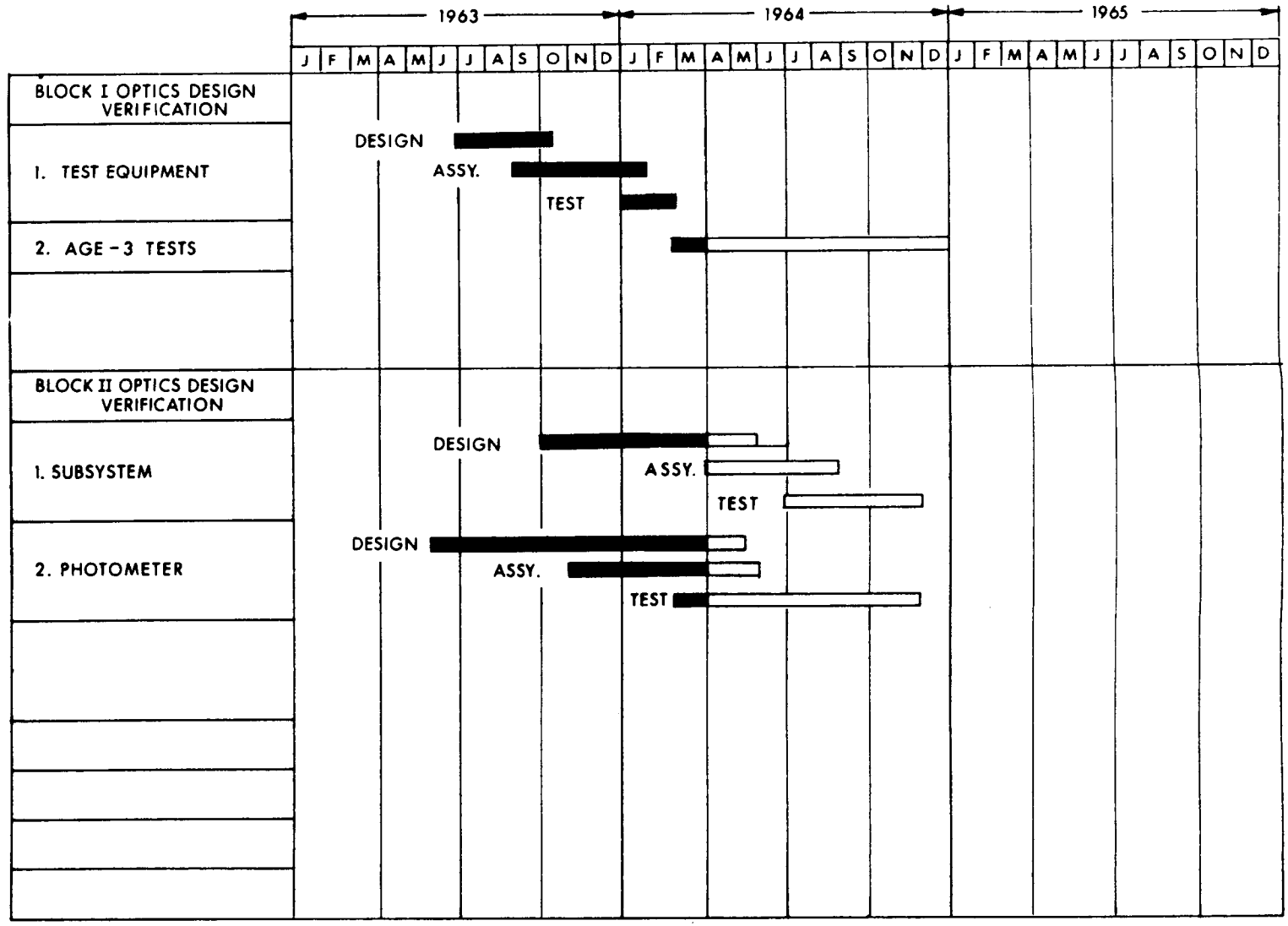

Fig. I-4

APOLLO - RAYTHEON GSE DELIVERY SCHEDULE

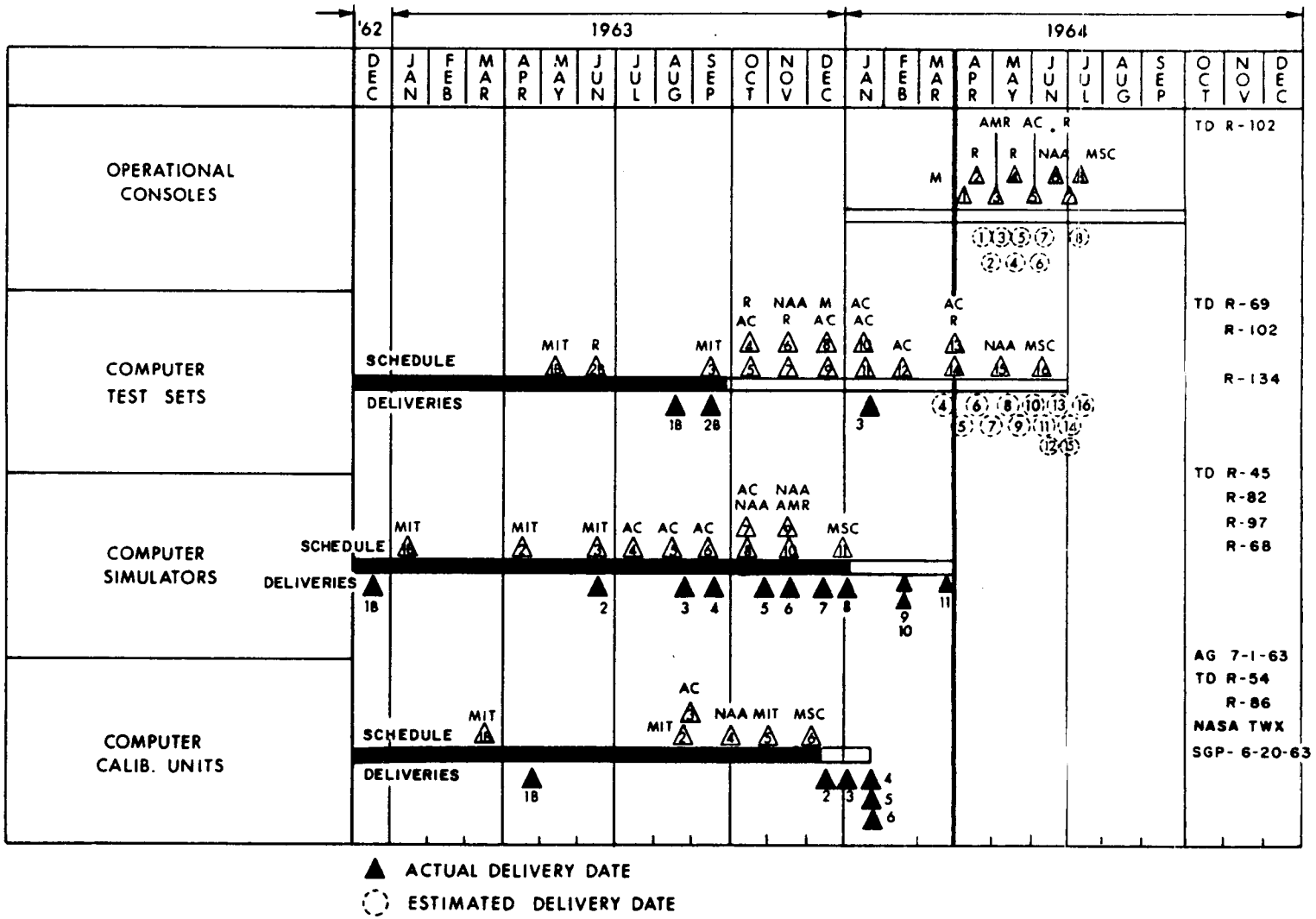

Fig I-5

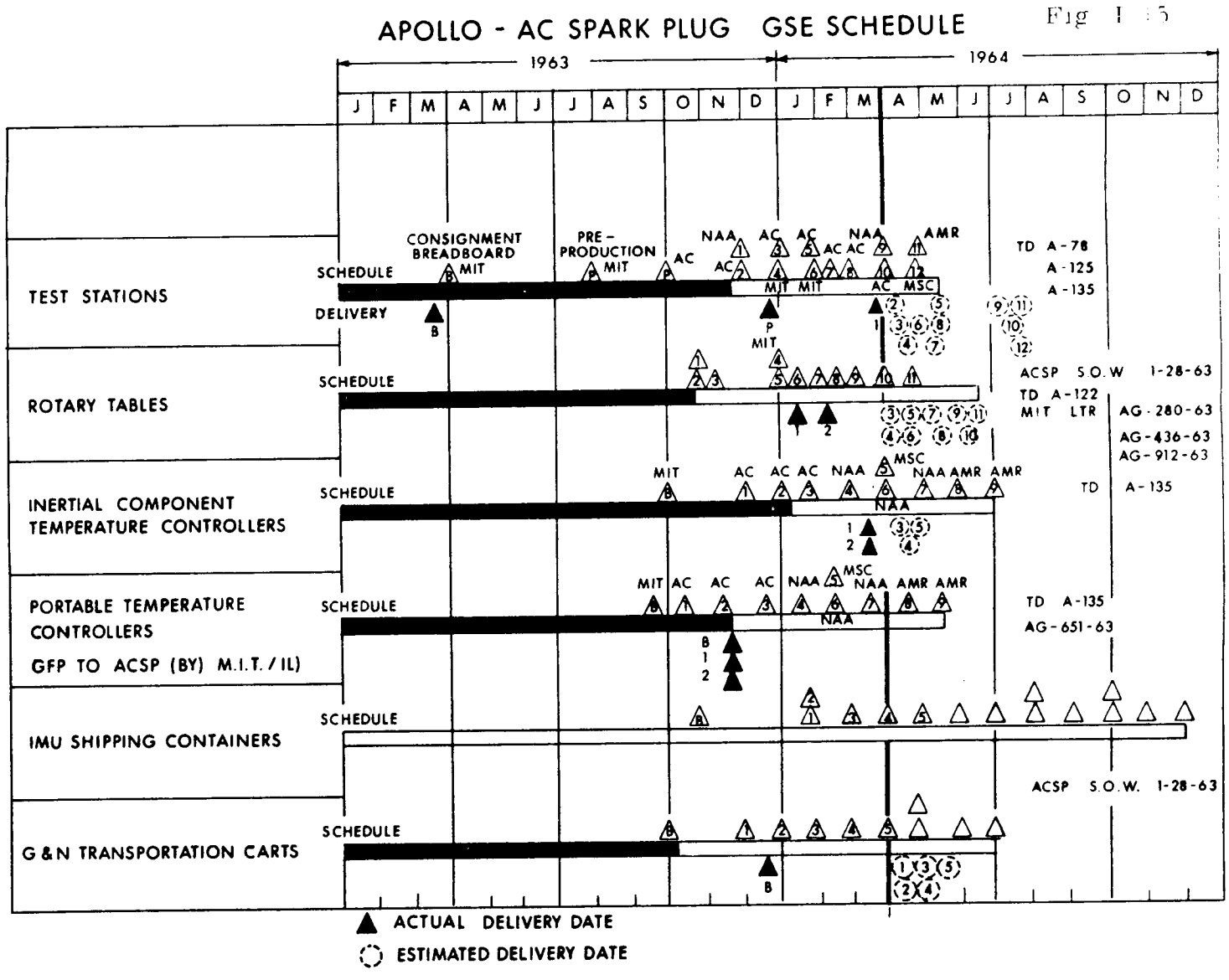
APOLLO - AC SPARK PLUG GSE SCHEDULE
1963
1964
J F M A M J J A S O N D J F M A M J J A S O N D
TEST STATIONS
ROTARY TABLES
INERTIAL COMPONENT TEMPERATURE CONTROLLERS
PORTABLE TEMPERATURE CONTROLLERS
GFP TO ACSP (BY) M.I.T. / IL)
IMU SHIPPING CONTAINERS
G & N TRANSPORTATION CARTS
SCHEDULE
DELIVERY
CONSIGNMENT BREADBOARD MIT
PRE - PRODUCTION MIT
TD A-78
A-125
A-135
ACSP S.O.W 1-28-63
TD A-122
MIT LTR
AG-280-63
AG-436-63
AG-912-63
TD A-135
TD A-135
AG-651-63
ACSP S.O.W. 1-28-63
ACTUAL DELIVERY DATE
ESTIMATED DELIVERY DATE

Fig 1

APOLLO MILESTONE CHART FOR KOLLSMAN GSE SCHEDULE

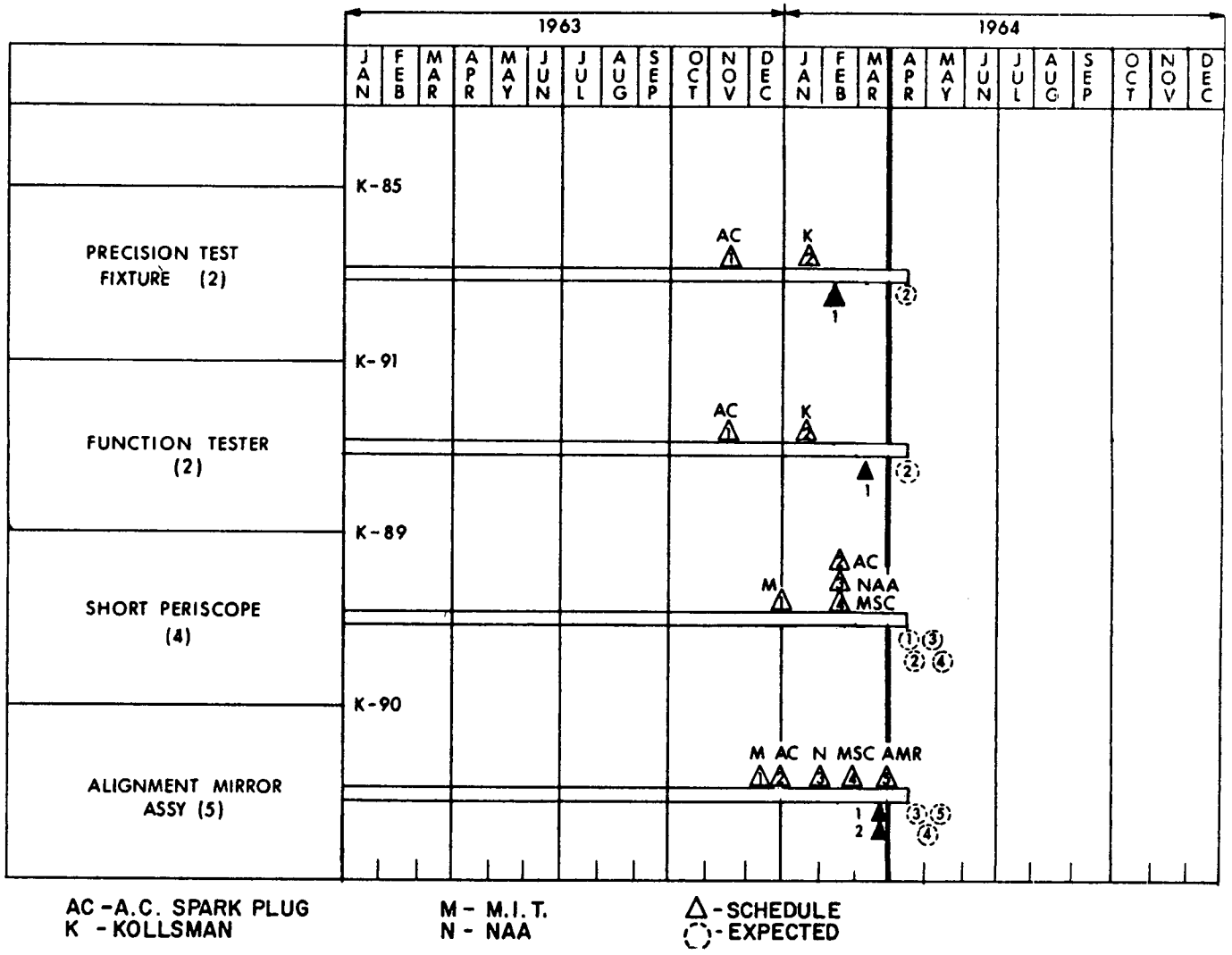

Fig I-16 (cont)

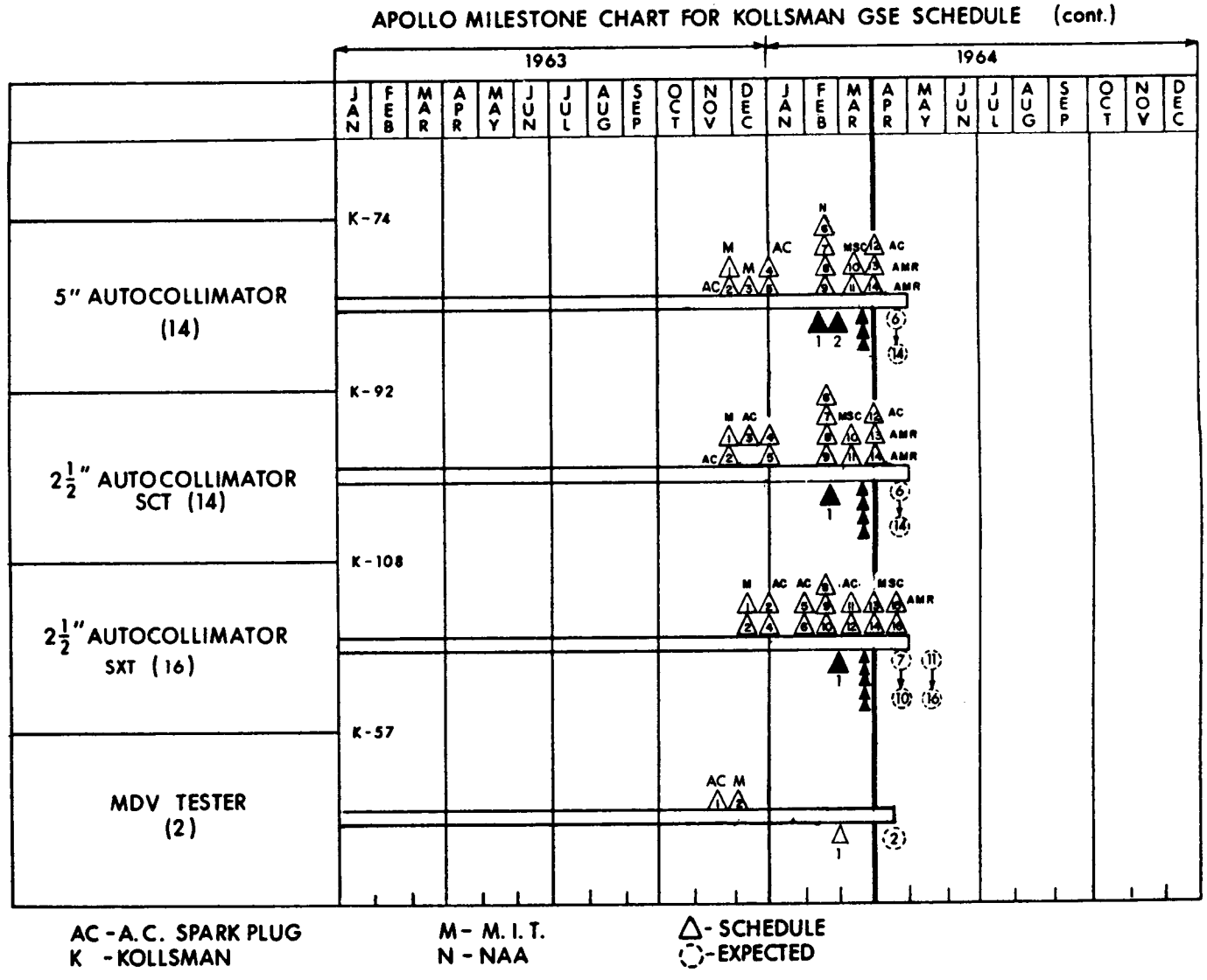
APOLLO MILESTONE CHART FOR KOLLSMAN GSE SCHEDULE (cont.)
1963
1964
JAN FEB MAR APR MAY JUN JUL AUG SEP OCT NOV DEC JAN FEB MAR APR MAY JUN JUL AUG SEP OCT NOV DEC
K-74
5" AUTOCOLLIMATOR (14)
K-92
2½" AUTOCOLLIMATOR SCT (14)
K-108
2½" AUTOCOLLIMATOR SXT (16)
K-57
MDV TESTER (2)
AC - A.C. SPARK PLUG
K - KOLLSMAN
M - M.I.T.
N - NAA
△ - SCHEDULE
◌ - EXPECTED

APOLLO MILESTONE CHART FOR KOLLSMAN GSE SCHEDULE (cont.)

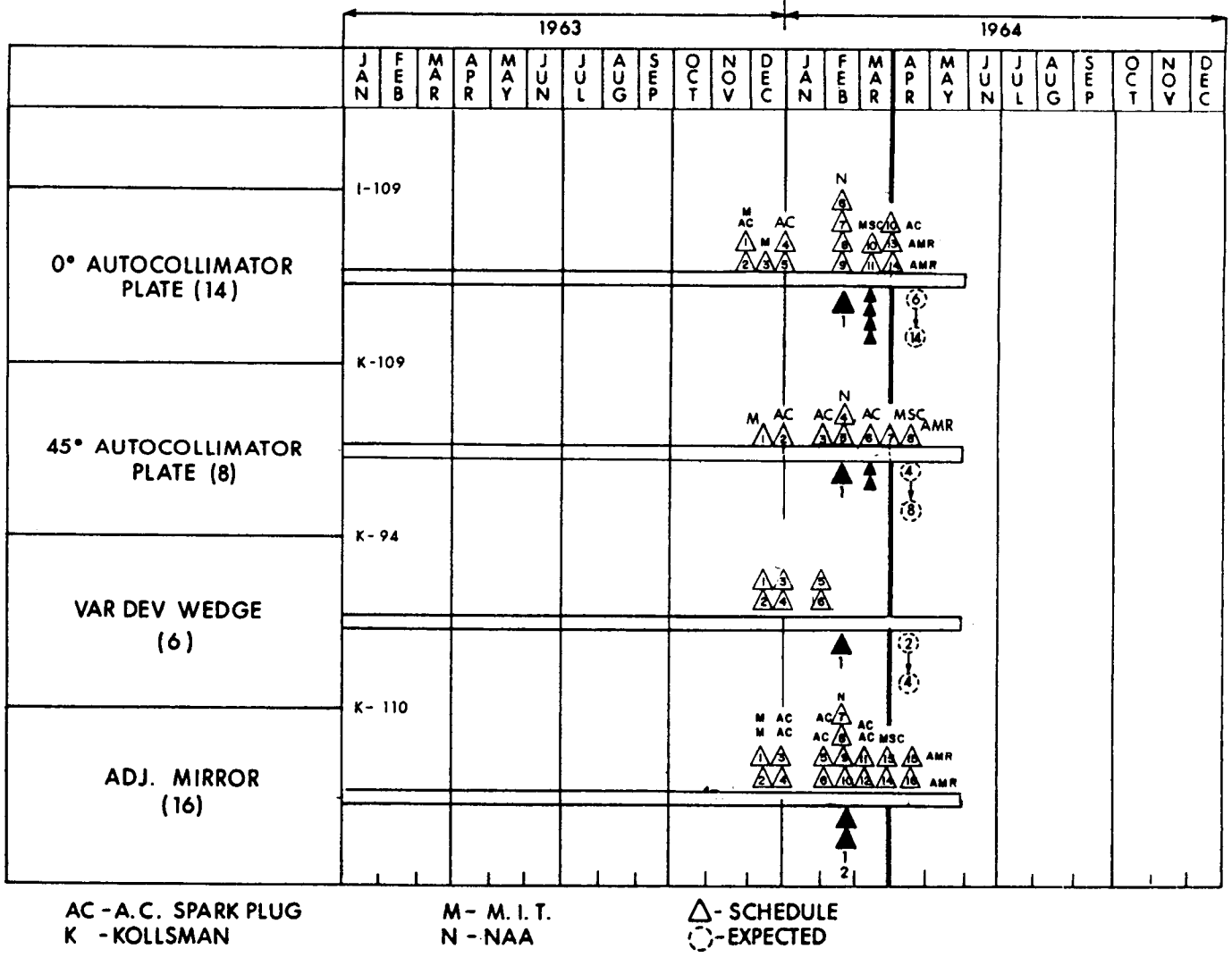

Fig. I-16 (cont.)

APOLLO - KOLLSMAN GSE SCHEDULE (cont.)

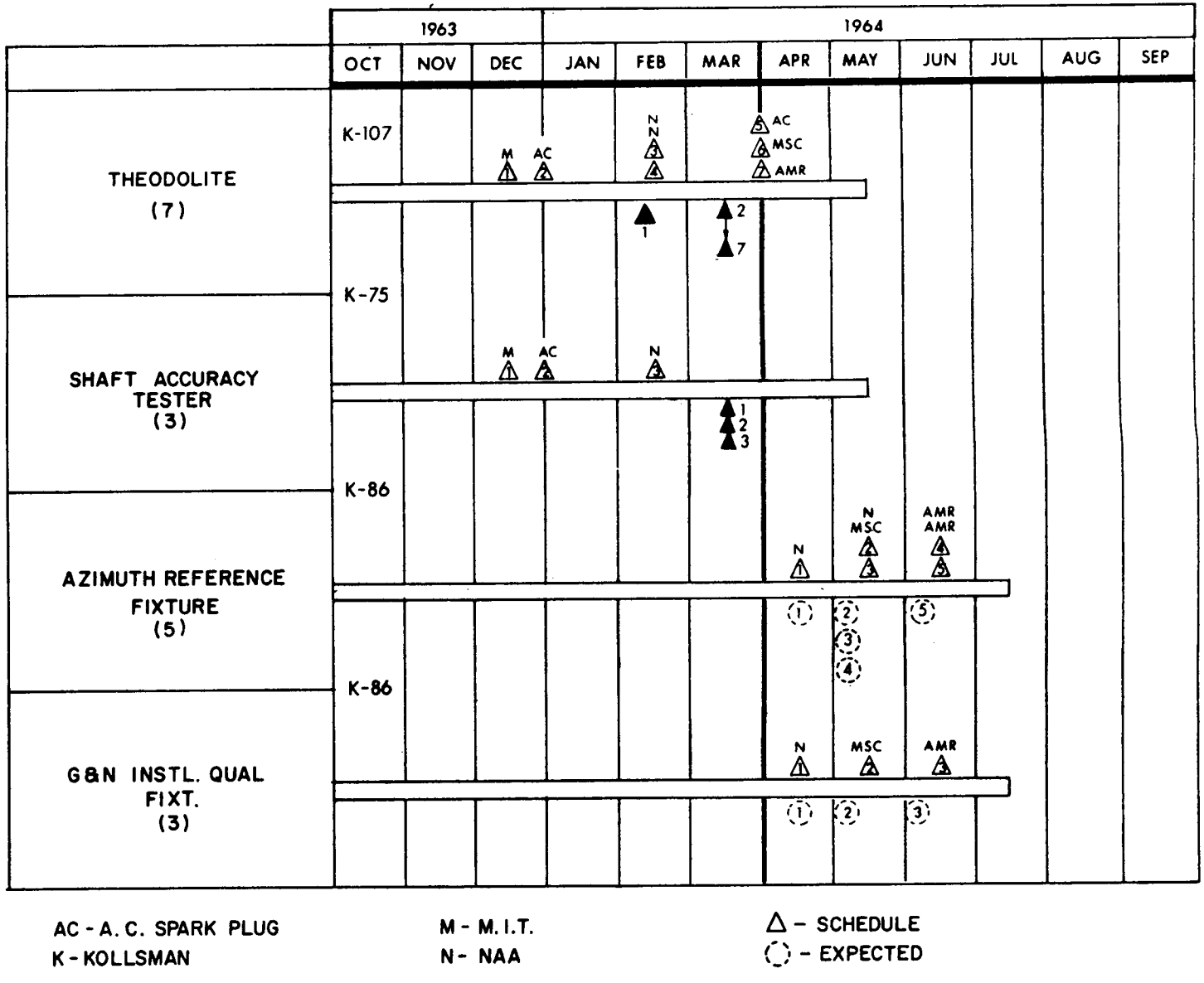

Deviation Variable Wedges: The number of wedges to be delivered by Kollsman has been reduced from sixteen to six. (Reference MIT/IL Letter AG 294-64, 25 March 1964.)

The PIP delivery schedule is shown in Fig. I-17.

The IRIG delivery schedule is shown in Fig. I-18.

Fig 1 17

APOLLO MILESTONE CHART FOR PIP REQUIREMENTS & DELIVERY SCHEDULES

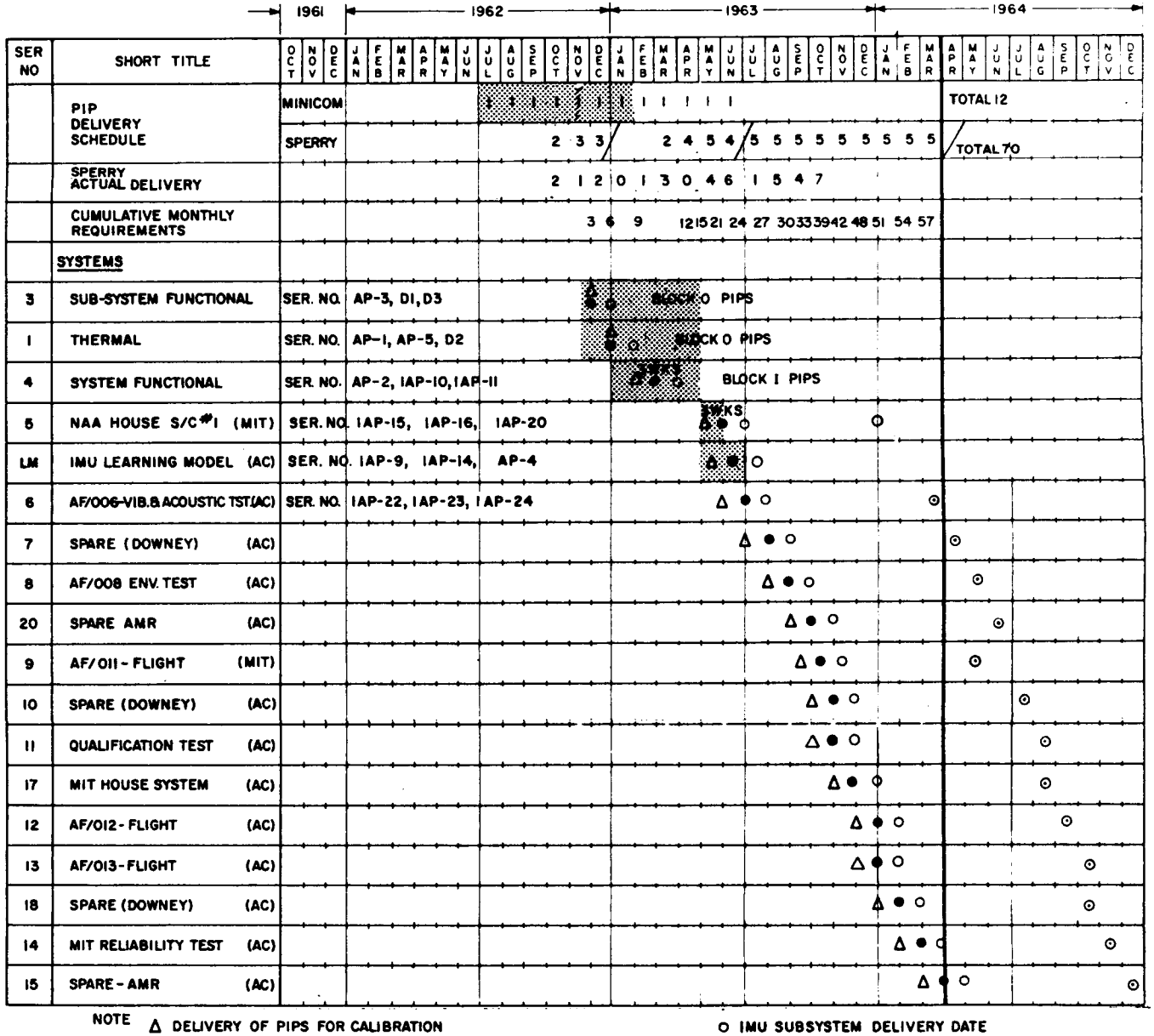

NOTE
Δ DELIVERY OF PIPS FOR CALIBRATION
● DELIVERY OF PIPS FOR INSTALLATION ASSY.
○ IMU SUBSYSTEM DELIVERY DATE
⊙ G&N DELIVERY DATE (READY TO INSTALL IN S/C)

PART II

TECHNICAL PRESENTATIONS

PART II

TECHNICAL PRESENTATIONS

Section 1

G&N FAMILIARIZATION PRESENTATION

D. G. Hoag

The guidance and navigation (G&N) equipment has three tasks to perform: first, the obvious one of keeping track at all times of position and velocity of the vehicle; second, to determine those major velocity changes necessary for going from one trajectory to another, as well as those minor corrections necessary to adjust the present trajectory to result in more accurate end conditions; and third, to measure and control these maneuvers in a steering mode.

To do this requires two types of operation: (1) guidance and (2) navigation. The guidance function relates to steering control and measurements under accelerated conditions. Sensing, in this case, is inertial only, except in the Lunar Excursion Module (LEM), when optical line-of-sight data and radar data are also used. The basic output is the control of the rockets, both in thrust magnitude and thrust direction. The navigation function occurs mostly during the free-fall stage, which is the majority of the mission time. Basic input to navigation is line-of-sight data to the near planets and stars, although communication from the ground can enhance the navigation function. Basic outputs of navigation are the position, the velocity, and any other trajectory parameters required. The navigation function also provides conditions for guidance. The velocity changes due to the thrust are measured by the guidance equipment to keep the navigation updated during the thrusting phases.

The phases in which guidance control will occur are shown by the heavier lines in Fig. 1-1. The operation with the Saturn, both the boost into orbit and the boost into the translunar phase, is under control of the Saturn guidance system, although there are some backup phases and monitoring phases associated with Apollo Guidance Equipment (AGE). Enroute to the moon small corrections are made to arrive at the correct perilune condition and to inject into lunar orbit. The LEM system is used for insertion into the letdown trajectory, landing phases, ascent phases, some midcourse corrections to achieve correct rendezvous conditons, and maneuver into the rendezvous. The AGE determines transearth injection and any transearth, midcourse corrections to achieve proper re-entry and the re-entry control. The accelerated phases, shown by the heavier lines in Fig. 1-1, are under inertial guidance control. They account for only 0.6 hour total time.

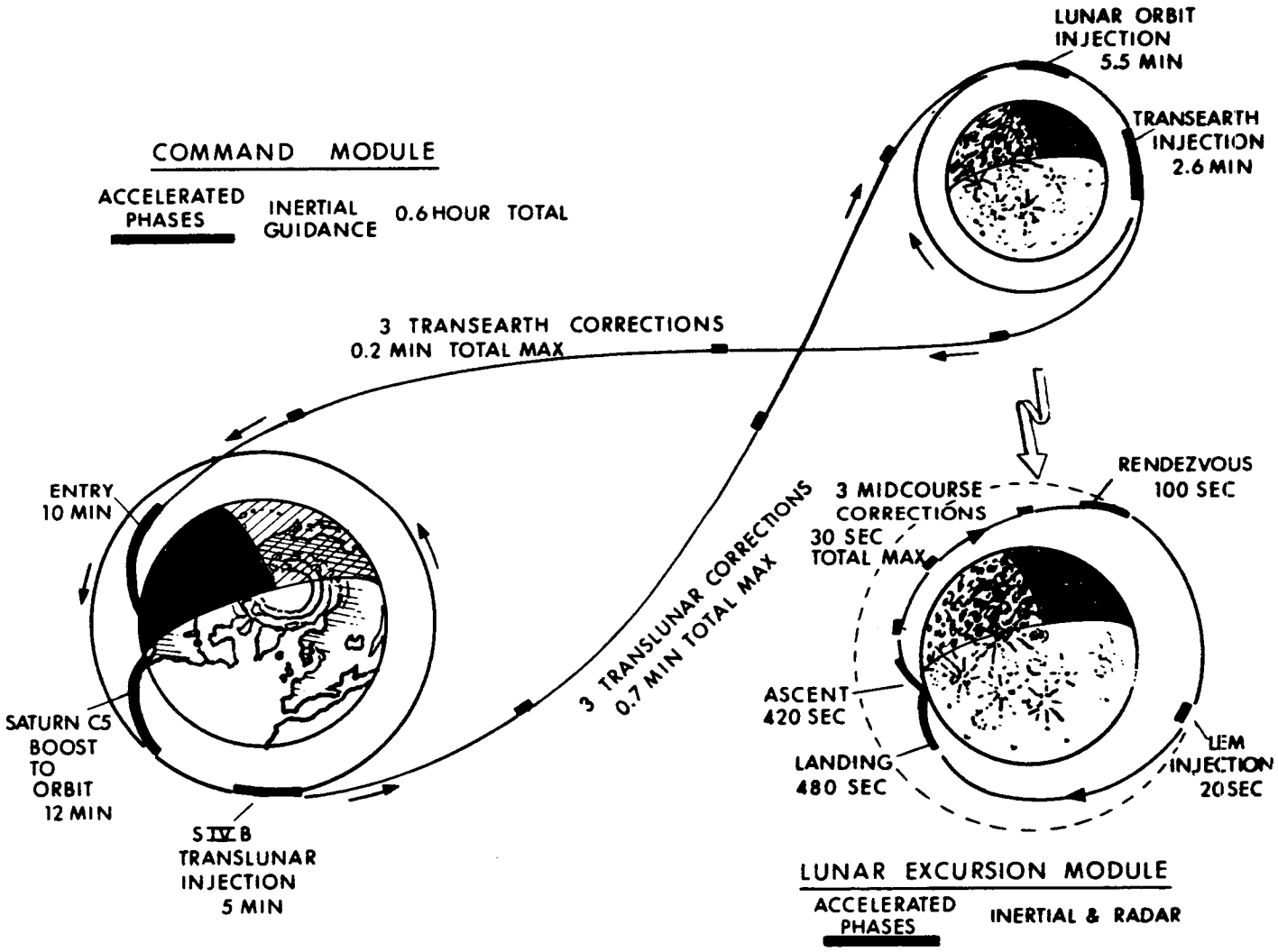

Fig. 1-1 Guidance mission phases.

More than 99 percent of this mission, as shown in Fig. 1-2, is under free-fall conditions with a navigation mode of operation. These free-fall phases are shown in the lighter lines on these charts. In low orbital phases, landmark tracking and horizon sensing are made for navigation. Up-telemetry from the ground may occur at any phase of the mission. Inertial Measurement Unit (IMU) alignments will be made at various times in preparation for measuring and controlling accelerating phases as they occur, but most of the time during free-fall the IMU is not operating. In midcourse, when well away from the earth or moon, the star-landmark angle measurements are made by the sextant.

In the LEM, the radar is involved in navigation as well as in guidance. Radar measurements between the spacecraft (S/C) and LEM are the basis upon which to make velocity corrections for rendezvous. The foregoing is the nucleus of the AGE operation.

Inertial control is synonymous with the guidance phase. The gyroscope in Fig. 1-3 is essentially the same gyro that was used in the Polaris. It is slightly modified, for the pulse torquing interface within the digital computer. The basic input, of course, is any angular deviation away from a reference about the input axis. The signal generator output is a measure of that rotation. The torquer provides for precession of the reference orientation. Acceleration measurements are made with the pulsed pendulum shown in Fig. 1-4, which is very much like the Mark 2 Polaris instrument.

Three of each of these two instruments are mounted on the stable member of the three-degree-of-freedom gimbal system shown in Fig. 1-5. The inner stabilized member is kept nonrotating by the signals from the gyros acting through servos to the gimbal axis servomotors. The three pendulums on the stable member with their associated circuitry measure the net velocity change of the spacecraft due to maneuver forces in the stable member coordinates. Their interface is with the computer which operates as it is needed during this phase.

In summary, the basic input to the inertial system is vehicle attitude and translational motions. The basic output is the translational motion signal which is processed in the computer. Attitude is also measured by the orientation given by IMU gimbal angle transducers.

Unique to Apollo is the fact that one's position in space is determined during these free-fall phases by observing the position of the earth and moon against the background stars. The heaven of stars gives excellent directional references. Where the earth and moon appear against that background is a measure of one's position. This is done by making angle measurements between specific stars and specific earth and moon landmarks or other distinct features of the two planets. Figure 1-6 represents a hypothetical situation showing the definition of conical loci of position defined by particular star-landmark measurements. The three cones intersect at the location of the spacecraft. At the moon, in this case, a point on the moon is not used; instead, the elevation of the star Antares

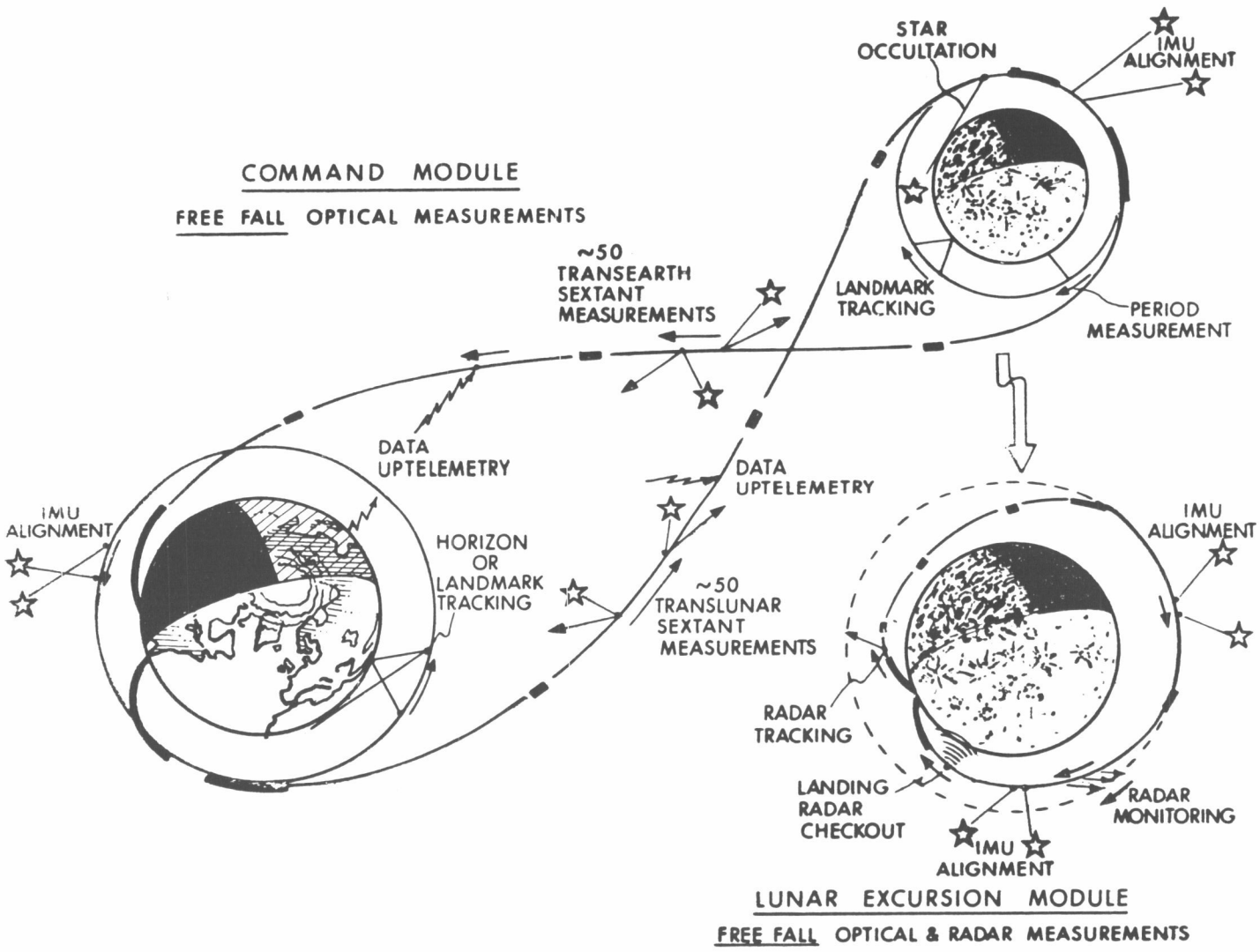

Fig. 1-2 Navigation mission phases.

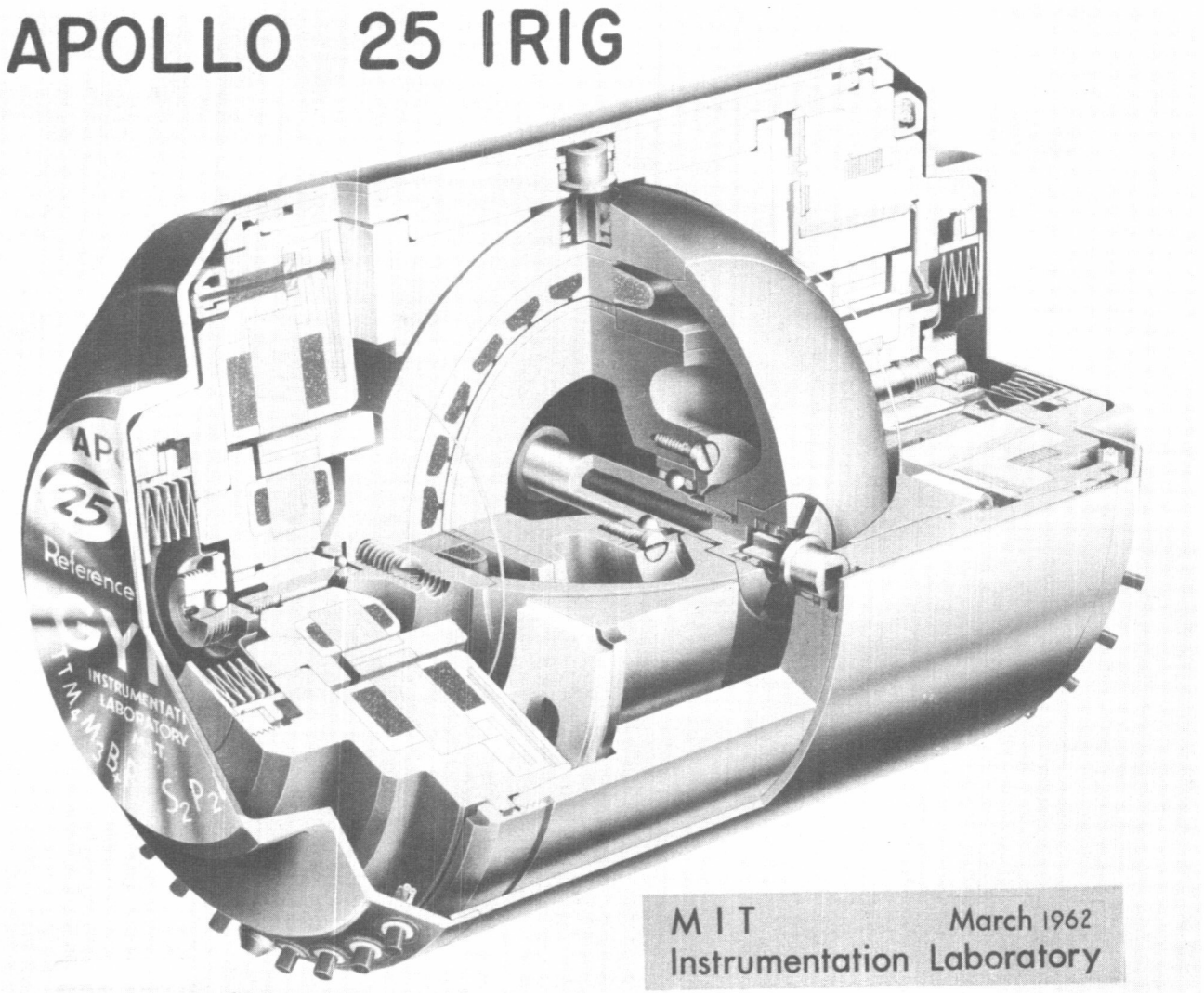

Fig. 1-3

CONFIDENTIAL

APOLLO

16 PULSED INTEGRATING PENDULUM · MOD D

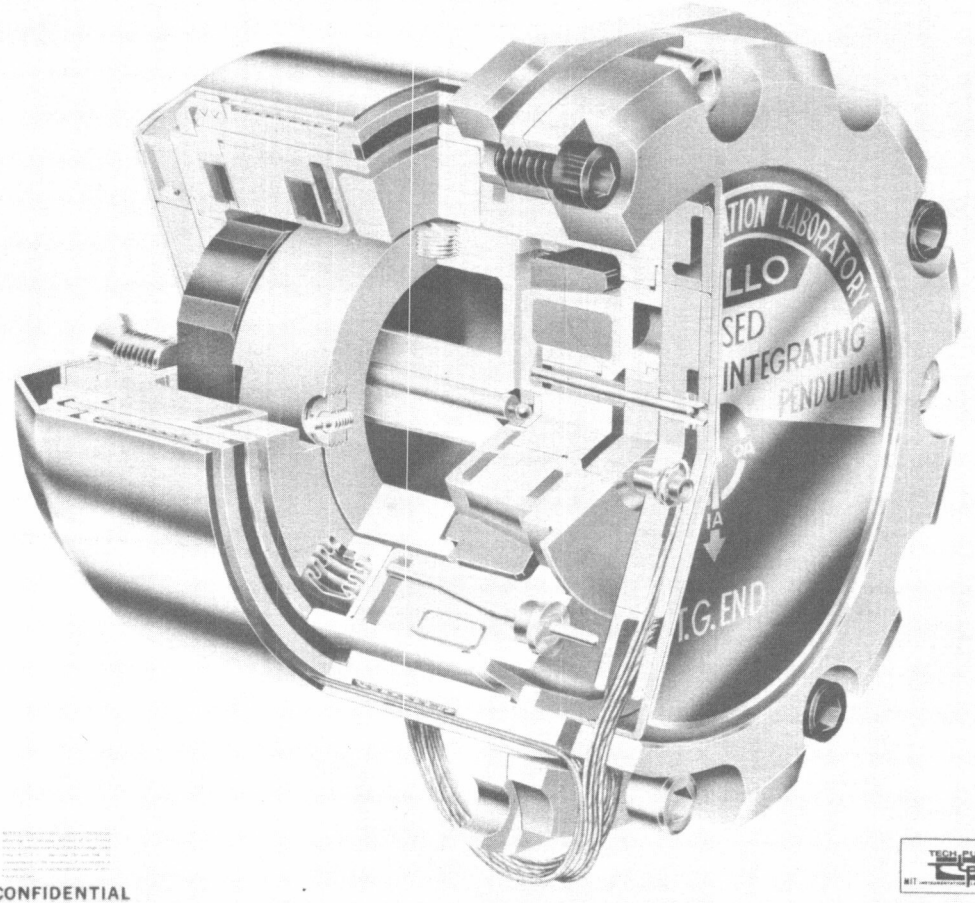

CONFIDENTIAL

MIT INSTRUMENTATION LABORATORY **NOV 1962**

Fig. 1-4

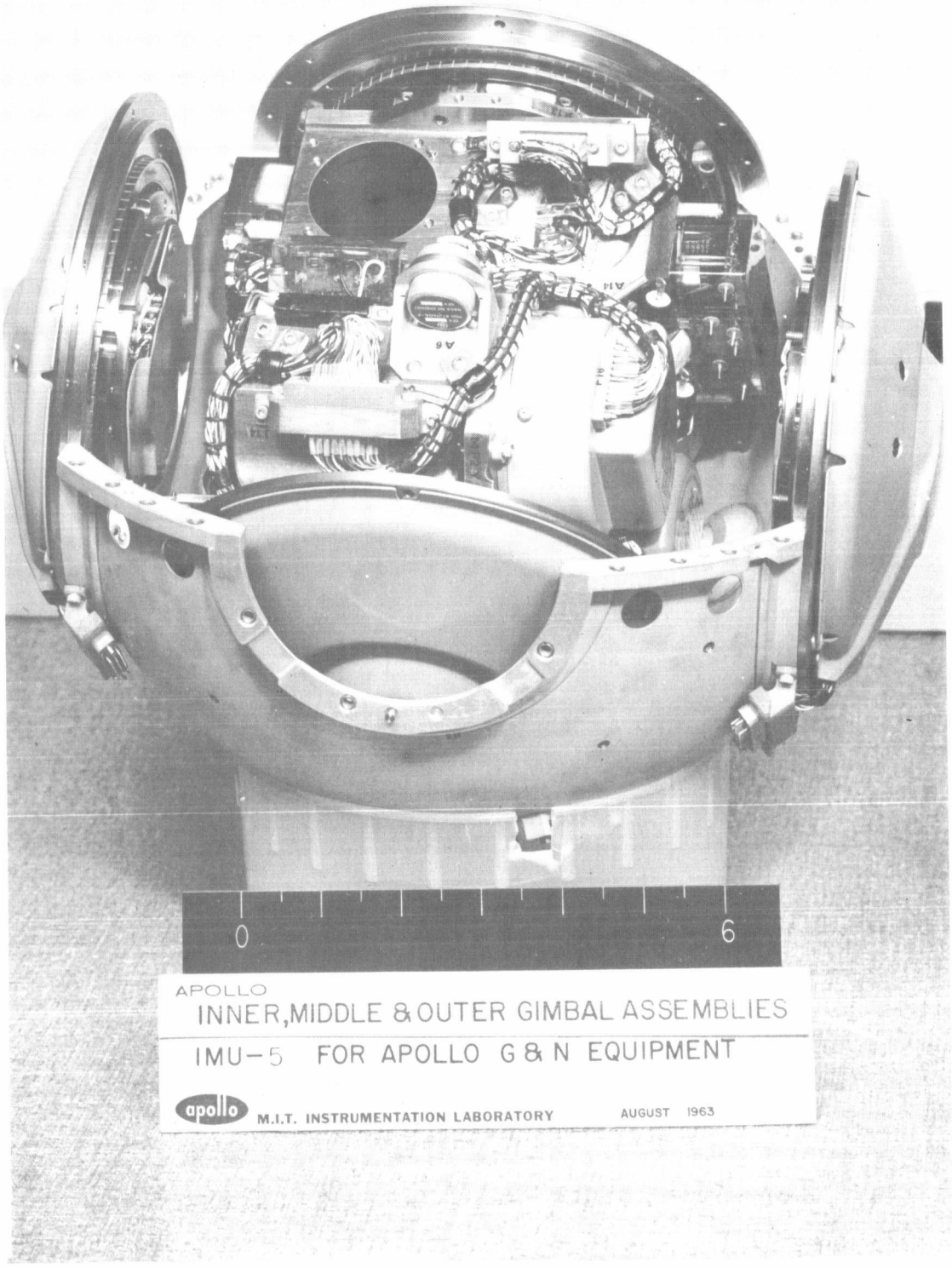
0
6
APOLLO
INNER, MIDDLE & OUTER GIMBAL ASSEMBLIES
IMU-5 FOR APOLLO G & N EQUIPMENT
apollo
M.I.T. INSTRUMENTATION LABORATORY
AUGUST 1963

Fig. 1-5 IMU 5.

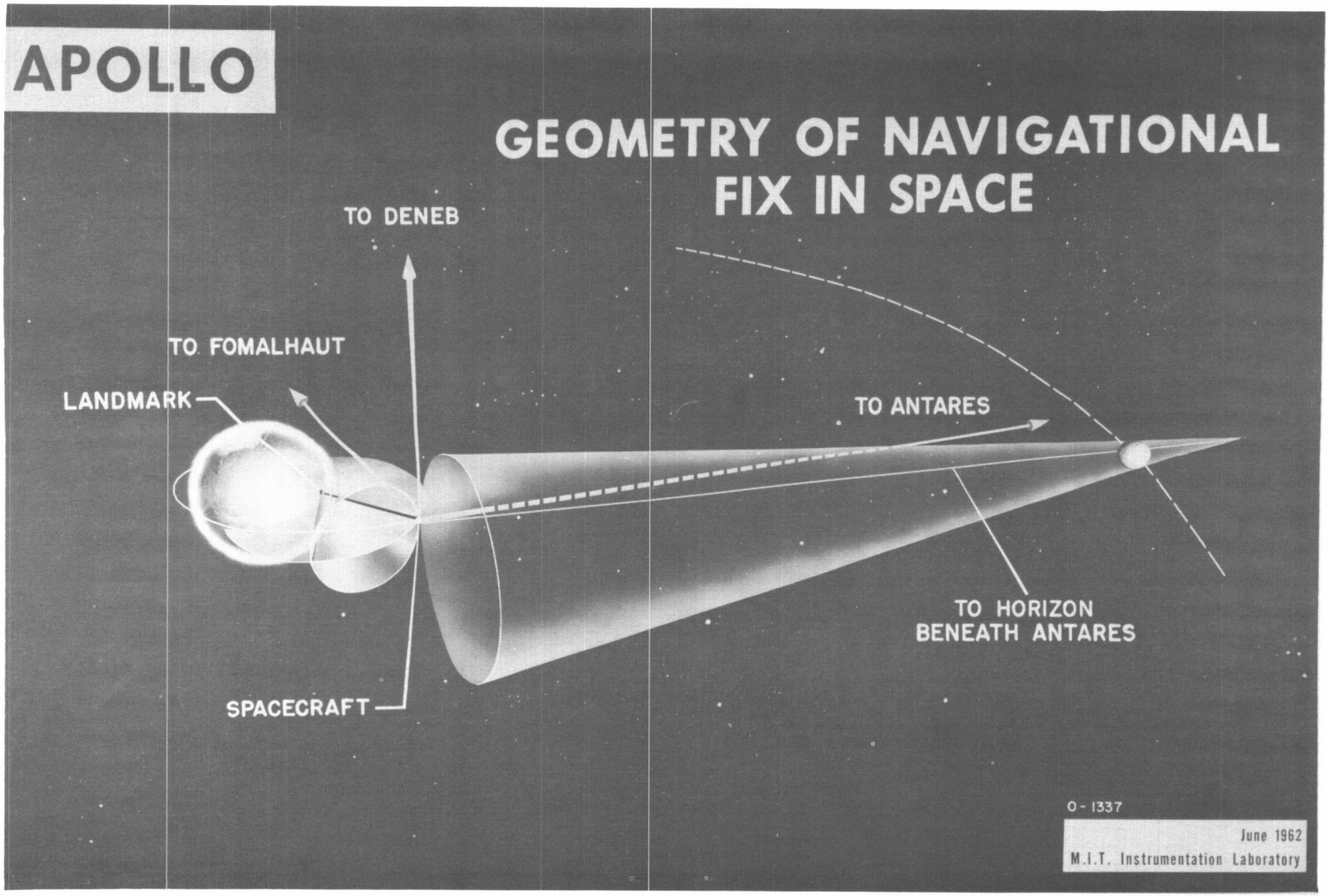
APOLLO
GEOMETRY OF NAVIGATIONAL FIX IN SPACE
TO DENEB
TO FOMALHAUT
LANDMARK
TO ANTARES
TO HORIZON BENEATH ANTARES
SPACECRAFT
O-1337
June 1962
M.I.T. Instrumentation Laboratory

Fig. 1-6

above the lunar horizon is the angle measured. The moon is an excellent target for navigation measurements, both optically and visually, because it has no atmosphere. Its features and horizon are very distinct; however, this is not true with the earth due to the atmospheric disturbances.

Looking at San Francisco Bay on a cloudless day through the sextant optical instrument, one might see something as shown in Fig. 1-7. Inside the instrument the star-landmark images are superimposed. By his control of the instrument, the navigator will superimpose the star image on an identifiable landmark and make the measurement by the necessary angle set into the sextant. However, San Francisco Bay may be covered up and since, in low orbit, one does not see much of the earth's surface, there may not be at some particular phase of the mission any suitable landmark targets visible. For this reason attention has been directed on the phenomenon of the illuminated horizon as a navigation measurement. As shown in Fig. 1-8 the actual sea level horizon is not visible from outer space due to the scattered sunlight in the dense atmosphere. At a 100,000-foot altitude the more tenuous atmosphere scatters back the same bright blue color seen from the ground looking up. This altitude is fortunately above disturbing clouds. The brightness of a local area here is essentially a fixed fraction of the peak brightness of blue light at lower altitudes. By means of photometer measurements the line of sight to some known altitude above the actual true sea level horizon can be found. Using the altitude thus determined with a star in our instrument, an angle measurement can be made to provide a basic navigation measurement.

There are two optical instruments in the Apollo system shown schematically in Fig. 1-9. On the left is a sextant instrument with two lines of sight, like a normal marine sextant. In this case the line of sight associated with the landmark passes straight through the instrument as it does in the marine sextant. The line of sight which is identified with the star can be articulated by rotation of the mirror about a so-called trunnion axis and the rotation of the whole instrument about the shaft which is parallel to the landmark line. The light from the star enters a beam splitter and is combined with the light from the landmark. The light from the landmark passes through a polarizer before it enters the beam splitter so that the landmark can be attenuated with respect to the star to get the visual constrast that is desirable to make the best measurement. Built into the sextant are the photometric instruments: a photometer and a star tracker. The photometer measures horizon brightness. The necessary star tracker uses the same articulated mirror as the visual part of the instrument but otherwise uses a separate set of optics. These components provide the automatic sensing which has been built into this instrument.

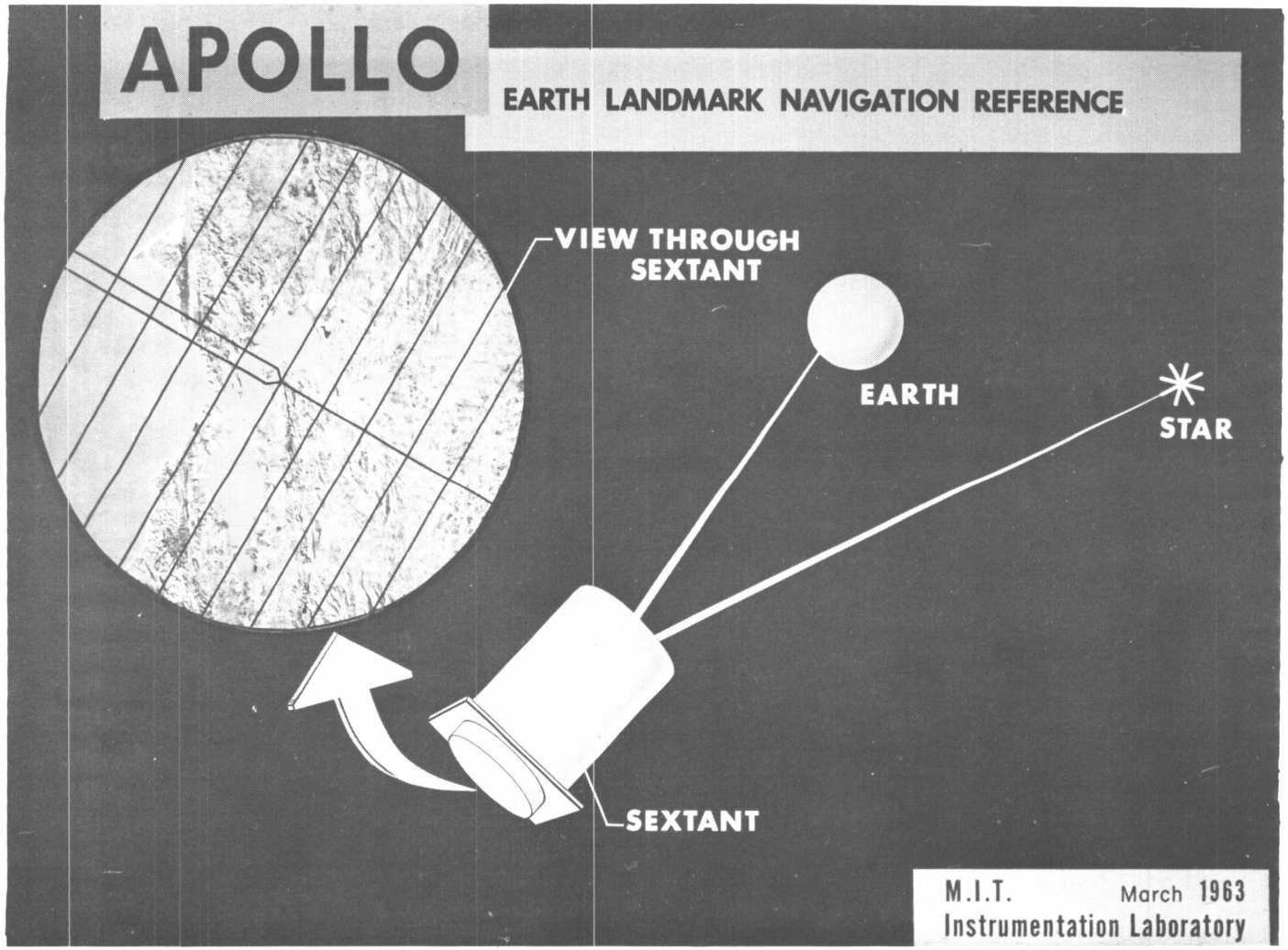
APOLLO
EARTH LANDMARK NAVIGATION REFERENCE
VIEW THROUGH SEXTANT
EARTH
STAR
SEXTANT
M.I.T.
March 1963
Instrumentation Laboratory

Fig. 1-7

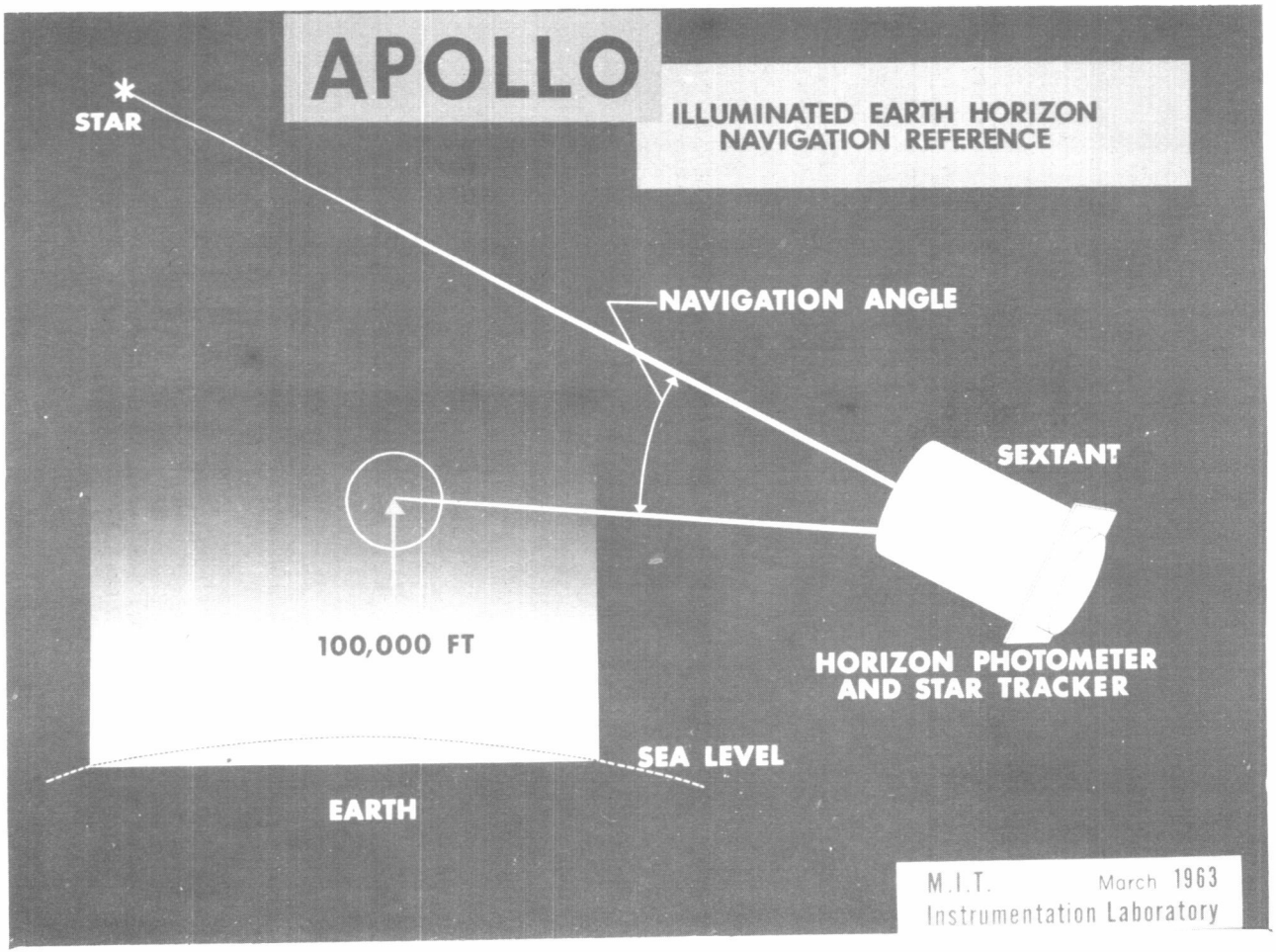
APOLLO
ILLUMINATED EARTH HORIZON
NAVIGATION REFERENCE
STAR
NAVIGATION ANGLE
SEXTANT
100,000 FT
HORIZON PHOTOMETER
AND STAR TRACKER
SEA LEVEL
EARTH
M.I.T. March 1963
Instrumentation Laboratory

Fig. 1-8

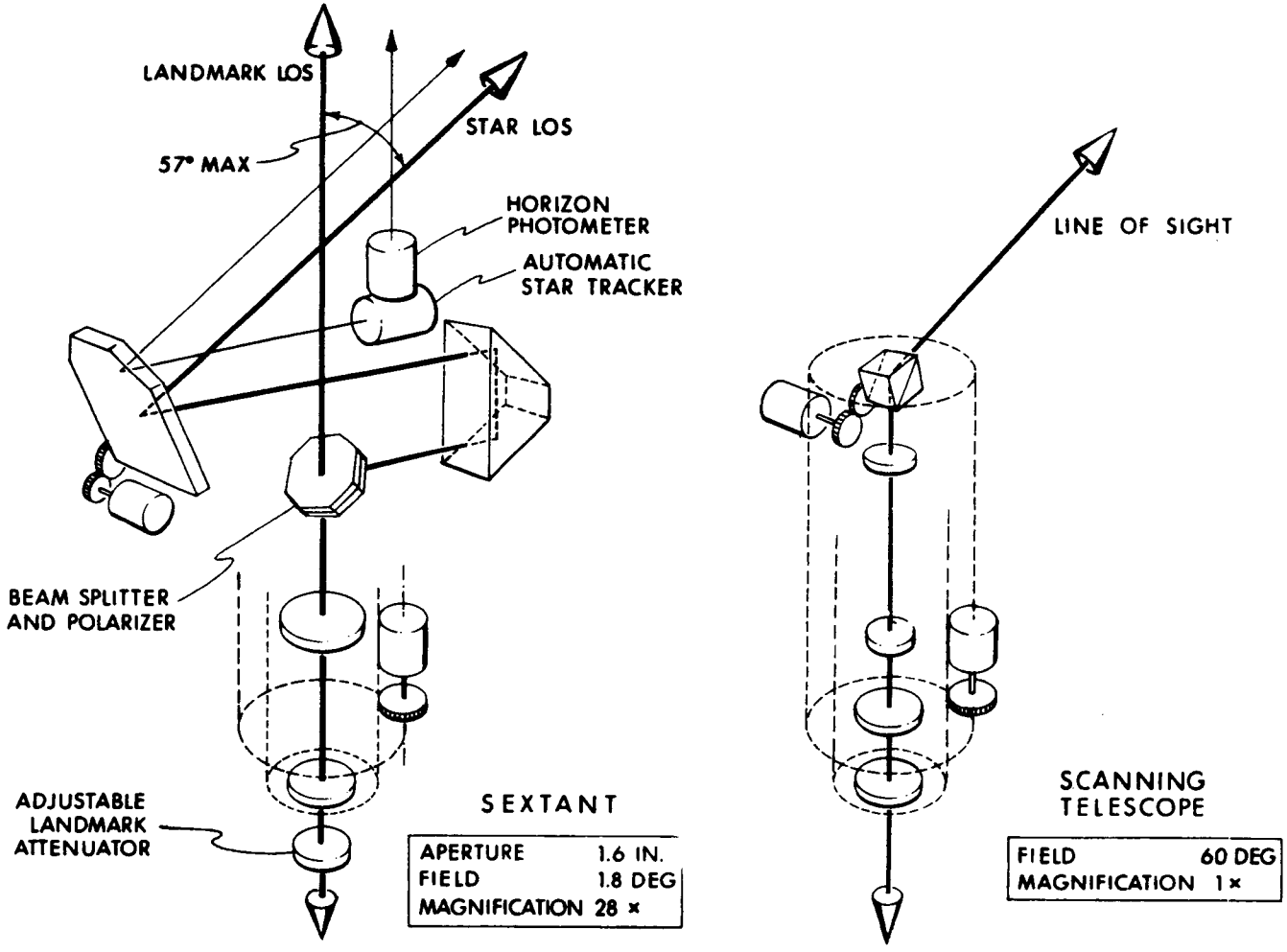

Fig. 1-9 Optical schematics.

The SXT is a high-powered instrument; at 28-power it gives good resolution but not very much field (1.8 degrees). For this reason a second instrument, the scanning telescope, having unity power and a 60-degree field, is used as an acquisition instrument and for general viewing. Its line of sight is articulated in the same directions possible by the sextant star line but uses a double-dove prism instead of a mirror.

Since the landmark line of the sextant passes straight through the instrument and is tied to the instrument (and therefore tied to the spacecraft), the landmark line must be aimed by rotating the spacecraft attitude as a whole. This is done so that the landmark comes into the 1.8^{o} field of view as shown in Fig. 1-10. Then, by modifying the shaft angle which defines the measurement plane and the trunnion angle which defines the desired angle, the astronaut makes his measurement by superimposing the star image onto the landmark. The acquisition of the star and landmark images in the sextant is done by using the scanning telescope. Figure 1-11 is one phase of the acquisition process which is a simulation of what the view might be some 70,000 miles away from the earth. (More detail of the acquisition process can be found in MIT/IL Report R-411.) This figure represents what might be seen through the wide-field-of-view telescope when the astronaut has reached a situation where he has acquired both the particular landmark and the star. He can then move his eye to the sextant and see the star superimposed on the background landmark, Fig. 1-12. Here the star appears near the Isle of Pines off Cuba. He can move the background field by changing the spacecraft attitude by application of few small attitude jet impulse commands. The only requirement is that he keeps the landmark target within the sextant 1.8^{o} field and preferably near the center where the resolution of the optics is better. His attention can be focused to control the movement of the star over on top of the landmark. When superposition is achieved he pushes a "mark" button which signals the computer to record both the angle in the sextant and the time of measurement.

During orbital conditions as represented in Fig. 1-13 the landmark features pass beneath at too high an angular velocity to use the two-line-of-sight instrument successfully. In this case, though, the error in direction to landmark is not so important as it is when the sextant is used farther away from the planet. Therefore, a single-line-of-sight instrument is used to visually track the apparent motion of the landmark as it passes beneath. Landmark direction is measured through the telescope angles with respect to the spacecraft and to the operating IMU to provide the measure of spacecraft orientation in space at this time.

Figure 1-14 depicts the major subsystems of the G&N with subsequent figures illustrating the various modes of operation. In Fig. 1-14, the two optical instruments, the sextant and scanning telescope, are shown at the upper right together with the automatic star tracker and photometer. The optics are mounted on a common base, called the navigation base. This navigation base is also the support for the IMU and is flexibly mounted to the spacecraft. The base provides a rigid framework in which angles of

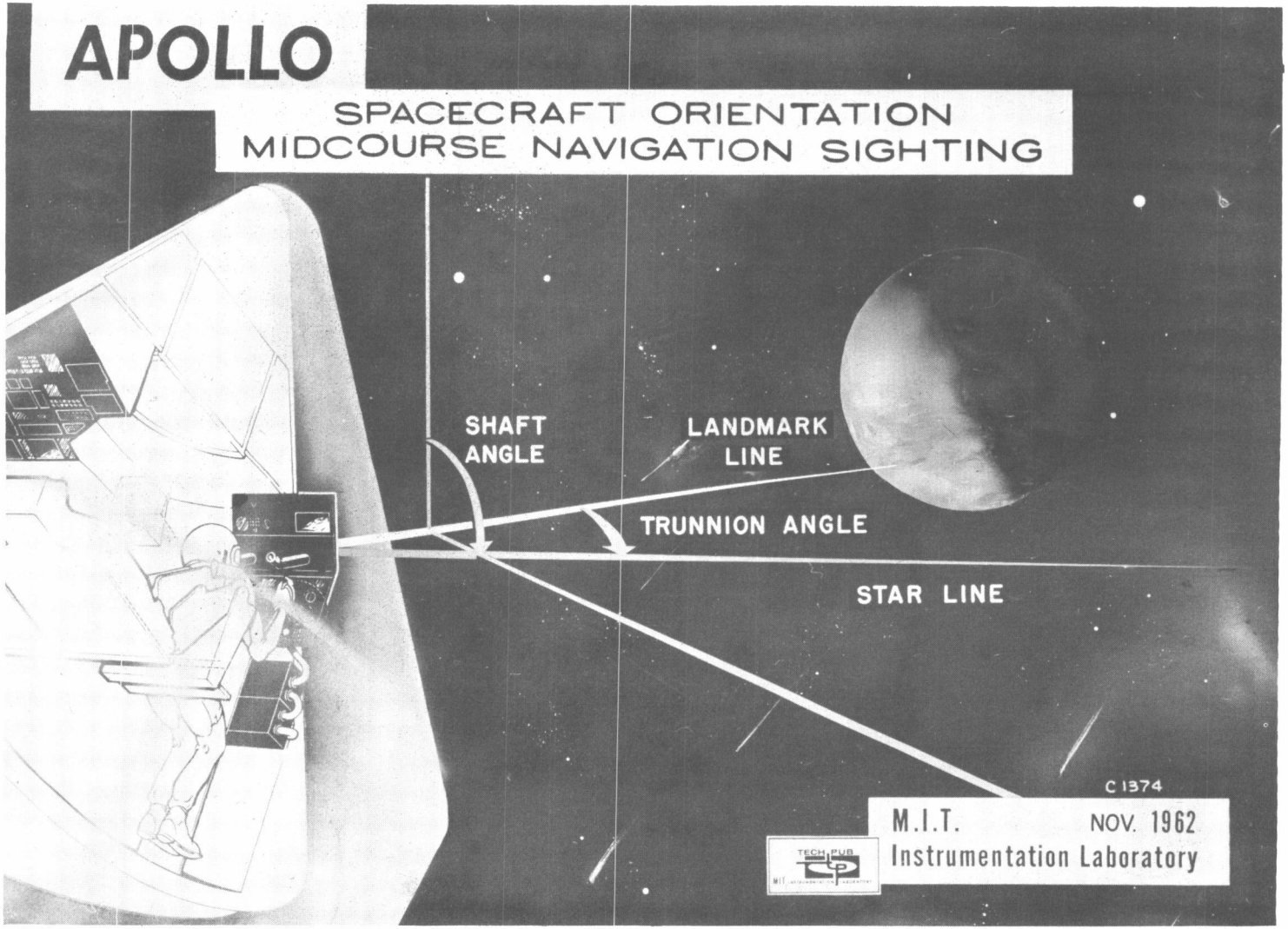
APOLLO
SPACECRAFT ORIENTATION
MIDCOURSE NAVIGATION SIGHTING
SHAFT ANGLE
LANDMARK LINE
TRUNNION ANGLE
STAR LINE
C 1374
M.I.T.
NOV. 1962
Instrumentation Laboratory

Fig. 1-10

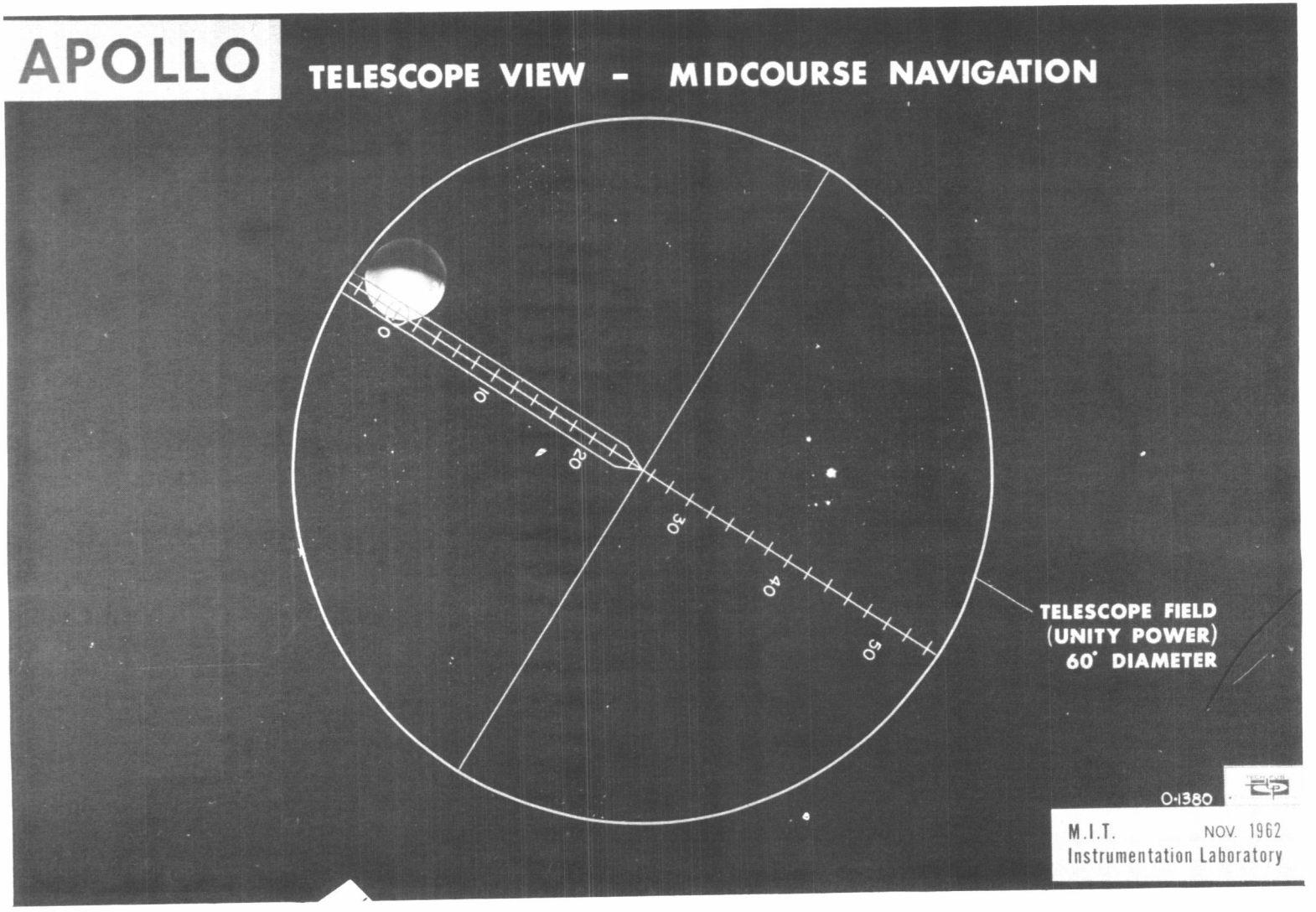
APOLLO
TELESCOPE VIEW - MIDCOURSE NAVIGATION
0
10
20
30
40
50
TELESCOPE FIELD
(UNITY POWER)
60° DIAMETER
0-1380
M.I.T.
NOV. 1962
Instrumentation Laboratory

Fig. 1-11

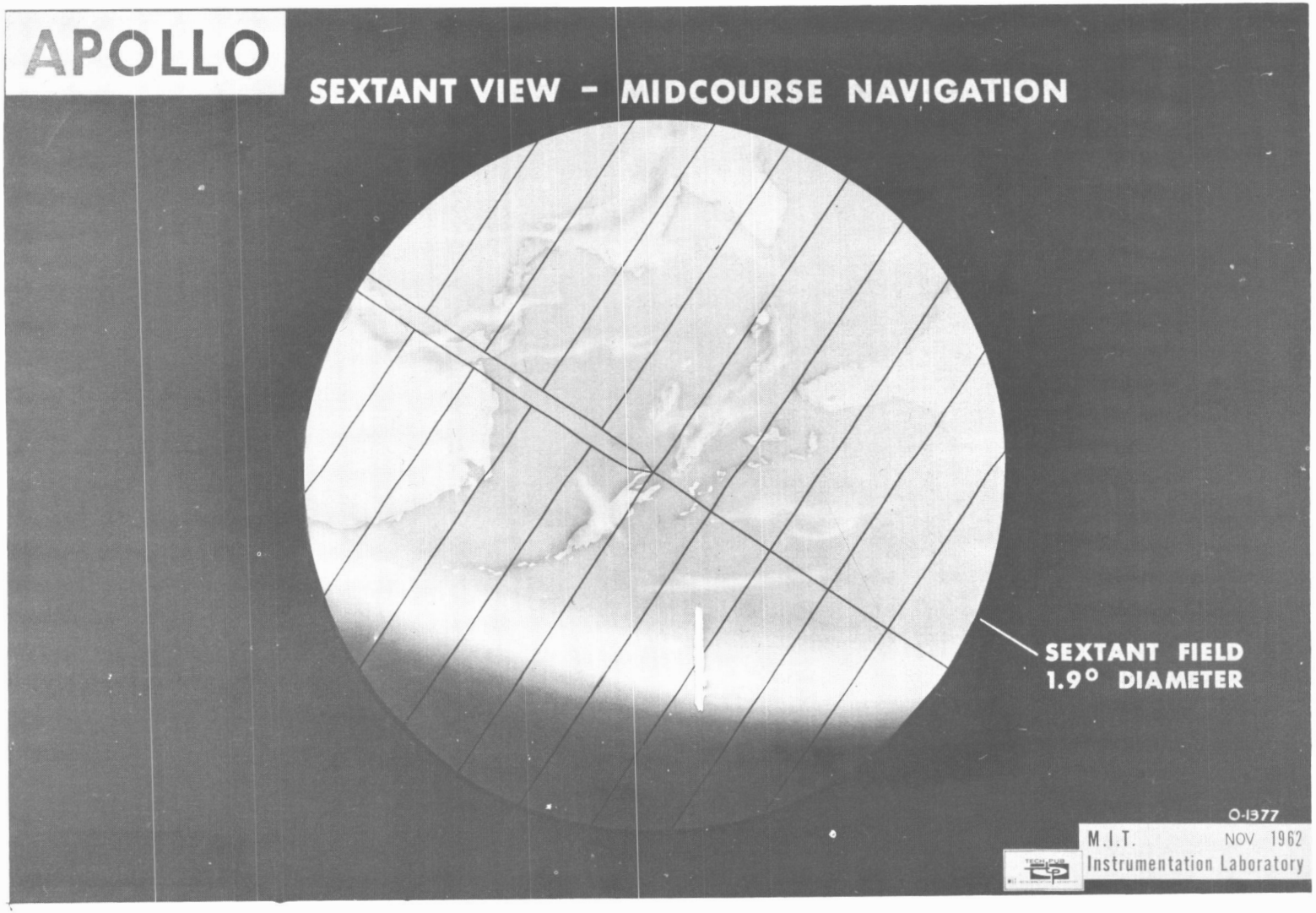
APOLLO
SEXTANT VIEW - MIDCOURSE NAVIGATION
SEXTANT FIELD
1.9° DIAMETER
O-1377
M.I.T.
NOV 1962
Instrumentation Laboratory

Fig. 1-12

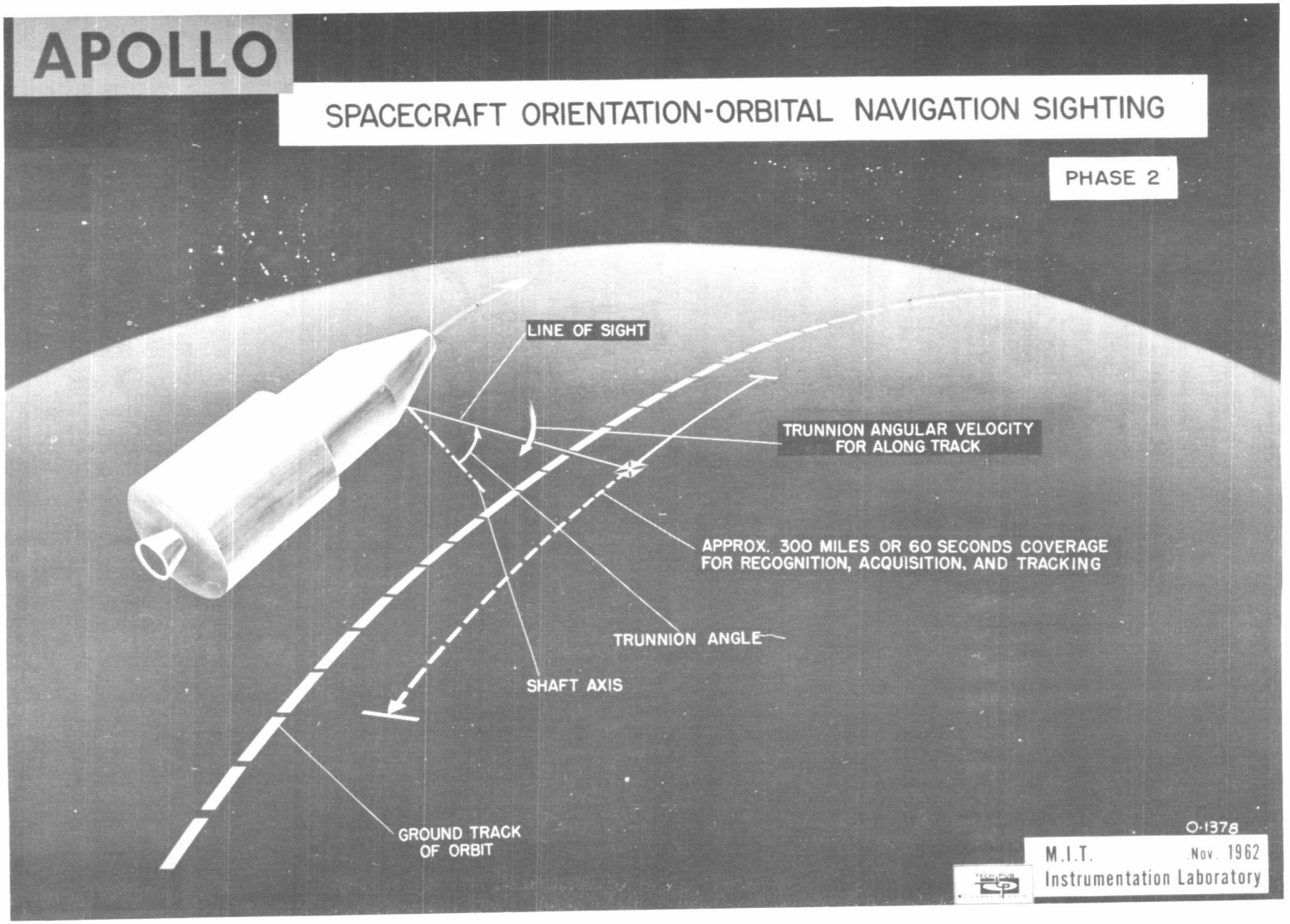
APOLLO
SPACECRAFT ORIENTATION-ORBITAL NAVIGATION SIGHTING
PHASE 2
LINE OF SIGHT
TRUNNION ANGULAR VELOCITY FOR ALONG TRACK
APPROX. 300 MILES OR 60 SECONDS COVERAGE FOR RECOGNITION, ACQUISITION, AND TRACKING
TRUNNION ANGLE
SHAFT AXIS
GROUND TRACK OF ORBIT
O-1378
M.I.T.
Nov. 1962
Instrumentation Laboratory

Fig. 1-13

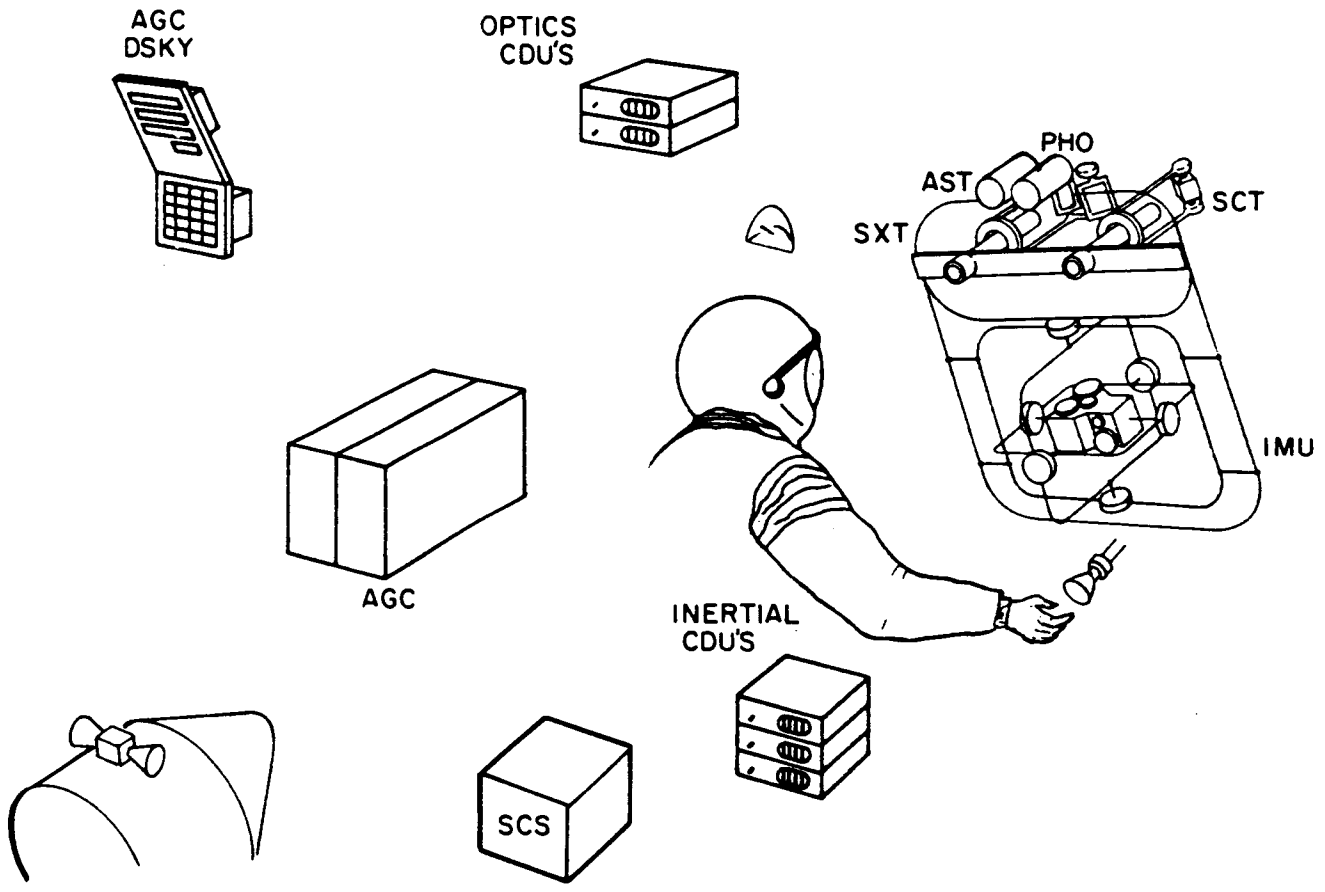

Fig. 1-14 Major subsystems.

the IMU and angles of the Optics can be related to each other without being disturbed by spacecraft flexure. Shown are two sets of identical coupling data units (CDUs) which are communication devices between measured angles, the computer, the stabilization and control system, and the astronaut. In the case of the inertial CDUs three units are associated with gimbal angles read out from the three-degree-of-freedom IMU. In the case of the optics, the two CDUs are associated with the optical shaft and trunnion angles. AGC in the figure represents the Apollo Guidance Computer. The AGC DSKY stands for Display and Keyboard which is the astronaut's communication with the computer. Using this format for description, the system may be used in the following ways.

To use the inertial equipment the inner member of the IMU has to be aligned to a specific spatial orientation. There are two phases of this alignment. Figure 1-15 shows the coarse alignment phase. Although other means are possible it is assumed here the astronaut has told the computer what the vehicle attitude is. The computer works out desired IMU gimbal angles that it wants the IMU to assume and transmits those via the inertial CDUs. The IMU gimbals then come around to the angle the computer desires within a second or so through a very fast servo. Those angles may be in error by several degrees because of spacecraft motion, poor knowledge of proper vehicle attitude, and possibly other reasons. The equipment is then put into the fine alignment phase shown in Fig. 1-16. In this case the astronaut, through the high-powered sextant tracks a star on the articulating line. He has a control stick which operates through the optical CDUs and changes mirror angles in a tracking loop as shown. When he is on the star he sends a "mark" signal to the computer which says the computer should read those star angles (angles of the star with respect to the navigation base). The computer can determine the orientation of the navigation base and then through the inertial CDUs read the present IMU gimbal angles. If those gimbal angles are not correct for the measured attitude, the computer determines what gyro precessional torquing is necessary to correct IMU orientation. Since one star gives only two degrees of freedom of orientation information, a second star sighting would be needed to complete the alignment.

Once the IMU is aligned it can be used for guidance and thrust control as shown in Fig. 1-17. Here acceleration signals from the accelerometers are operated upon in the computer by a set of stored equations which determine the commanded direction of the vehicle thrust desired. The attitude that is commanded is compared with the IMU measured attitude within the inertial CDUs. The difference or error is sent to the stabilization control system which effects a change in thrust direction. The resulting attitude and motion is fed back to the IMU to close the loop. When the correct velocity change is achieved the engine is shut down by command from the computer.

In midcourse, navigation measurements are made by using a star and a landmark, which is illustrated in Fig. 1-18. The sextant is used as a two-line-of-sight instrument. The astronaut has two tasks to perform, the first to command vehicle attitude through his

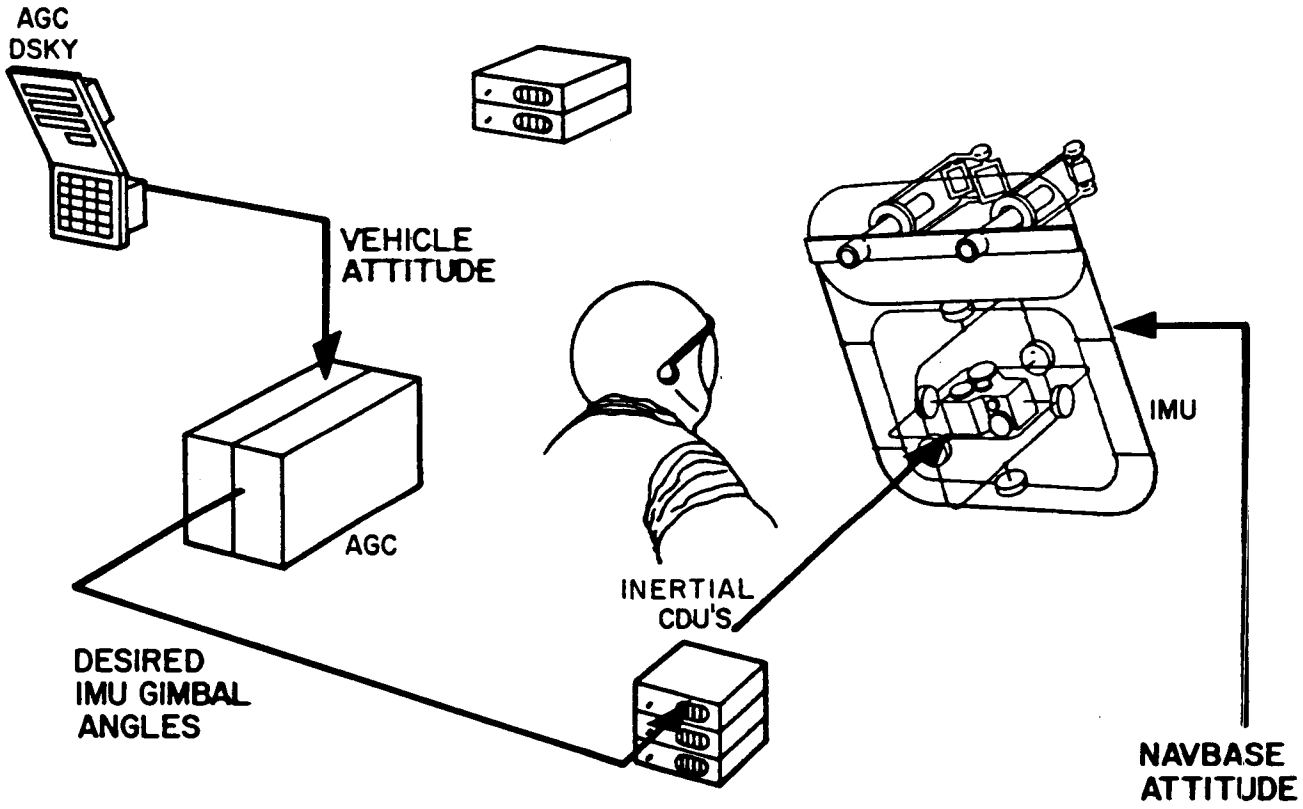

Fig. 1-15 IMU coarse alignment: manual.

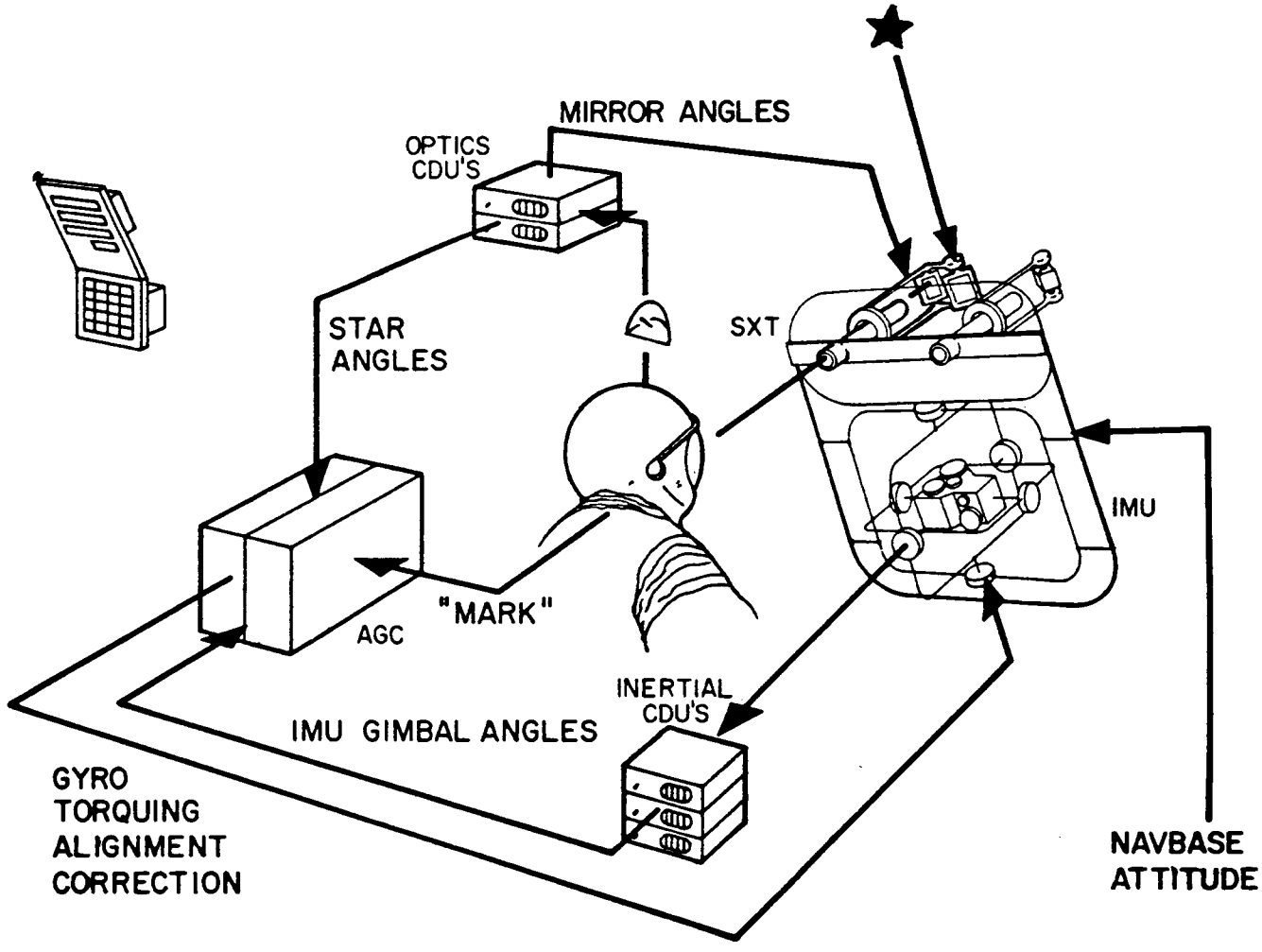

Fig. 1-16 IMU fine alignment: manual.

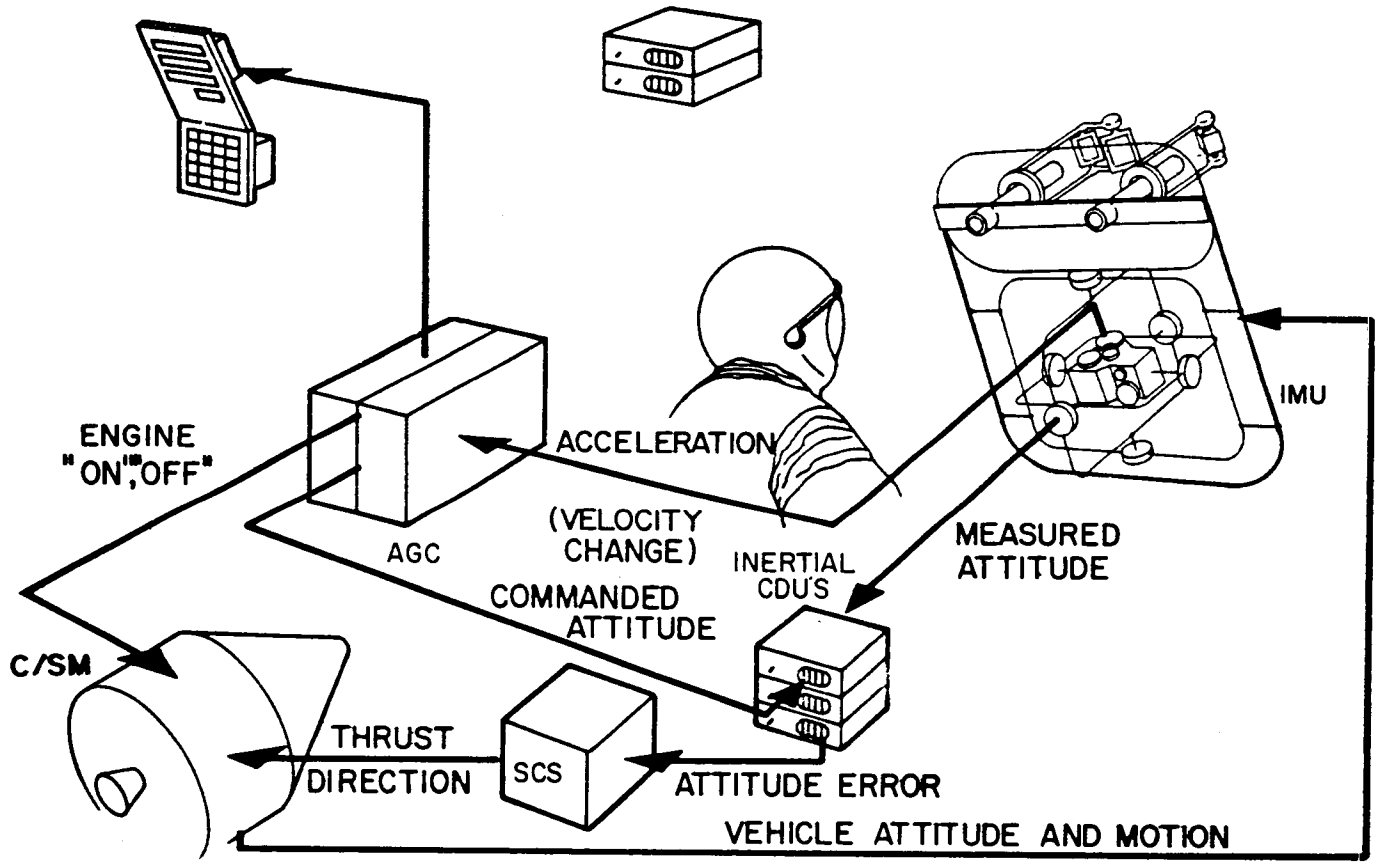

Fig. 1-17 Guidance thrust control.

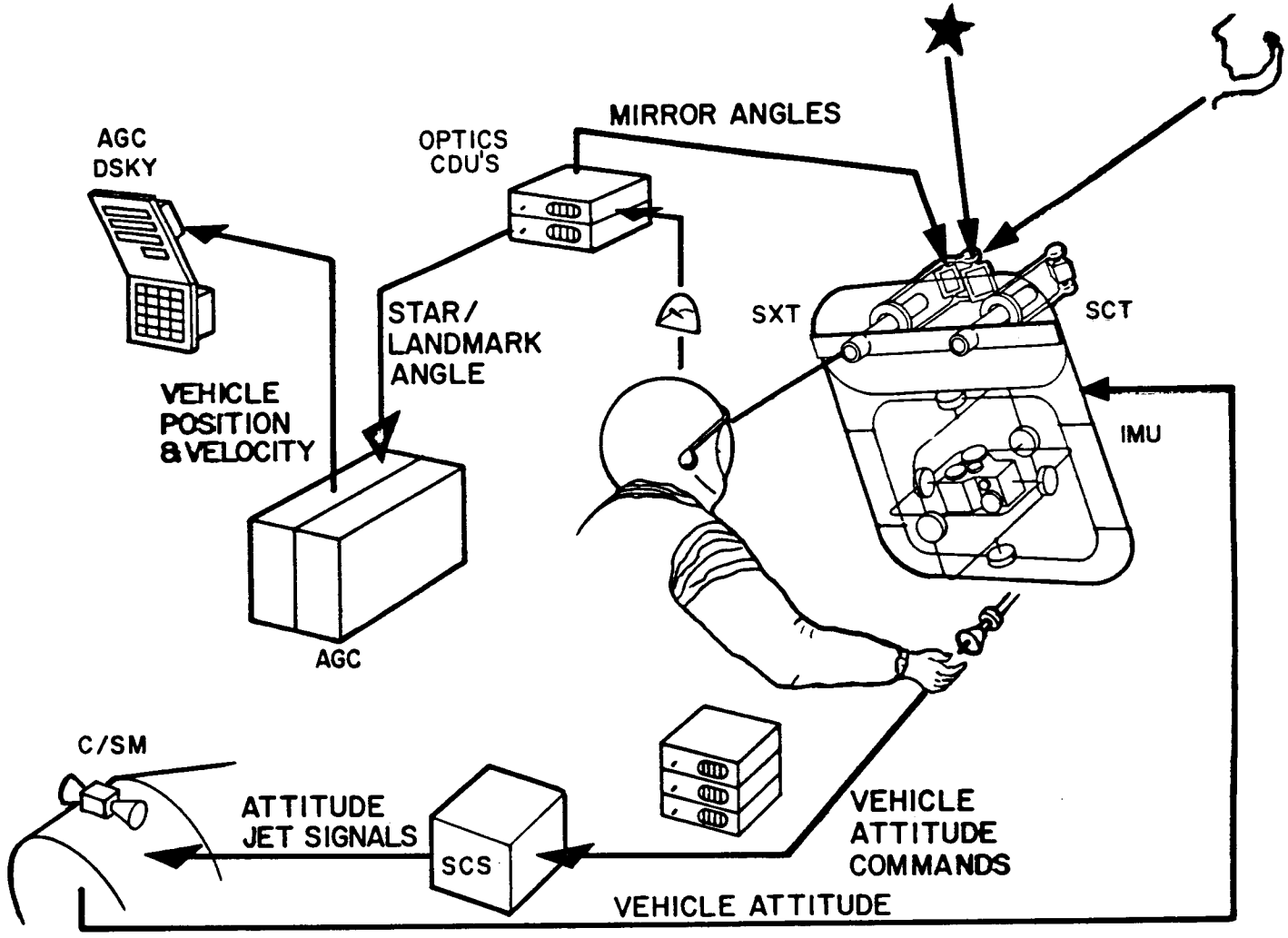

Fig. 1-18 Midcourse navigation: Manual star-landmark angle measurement.

control stick. This change in attitude is then fed back to the navigation base and rotates the landmark line so that the landmark is within the field of view of the instrument. Then, using his other hand to operate the optical CDU's, the second task is performed, that of changing the mirror angles until the star image and landmark image are superimposed. When he has done that successfully, he pushes a mark button (not shown) and tells the computer to read the angle. The computer reads that angle and reads time and then uses this single angle measurement to update the navigation.

The photometer shown in Fig. 1-19 is involved in the earth-illuminated horizon navigation. When the photometer has satisfied itself through its automatic features that it has the proper properties of the brightness of the local area of the horizon it sends a mark to the computer. The astronaut first acquires the star and the star tracker then automatically points to the star in a closed loop through the optical CDUs. The astronaut's task is to observe through the scanning telescope such as to set up the problem appropriately. He must be sure the plane of the angle being measured is perpendicular to the local horizon. He must achieve this by a spacecraft maneuver. When he has accomplished this task the computer will accept the automatic mark when it arrives, and then read the star horizon angle. In all cases the pertinent data can be displayed.

In low earth orbit or low lunar orbit the single-line-of-sight instrument is used as shown in Fig. 1-20. In this case the IMU is also involved as an altitude reference. It must be initially aligned (ref. Figs. 1-15 & 1-16) so that the computer can have knowledge of the orientation of the navigation base with respect to this prealigned coordinate frame. Utilizing the scanning telescope, the astronaut can perform the function of landmark tracking. Upon obtaining the landmark on the telescope cross hairs he "marks" this information into the computer, which causes the computer to read the angle of the landmark with respect to the navigation base and the angle of the aligned stable member with respect to the navigation base. The computer then processes the information as appropriate for navigation updating.

The next several figures refer to some automatic modes which will become particularly important in early unmanned flights. An automatic IMU alignment mode is possible. This requires the IMU be on and not have drifted any farther than the 1/2 degree provided in the field of sensitivity of the automatic star tracker. In the acquisition phase shown in Fig. 1-21, the IMU's present angles are measured by the computer from which the expected direction of the star is put into the star tracker mirror. When the star tracker is within this 1/2-degree field of view a "star present" signal is sent to the computer and the mode shifts over to the automatic tracking phase shown in Fig. 1-22. The star angles are sent to the computer. From a comparison of actual gimbal angles the correct torques are sent to the gyros to correct the alignment periodically. The automatic operation is dependent upon continuous IMU operation and alignment updating often enough as constrained by the sensitive acquisition field of the star tracker.

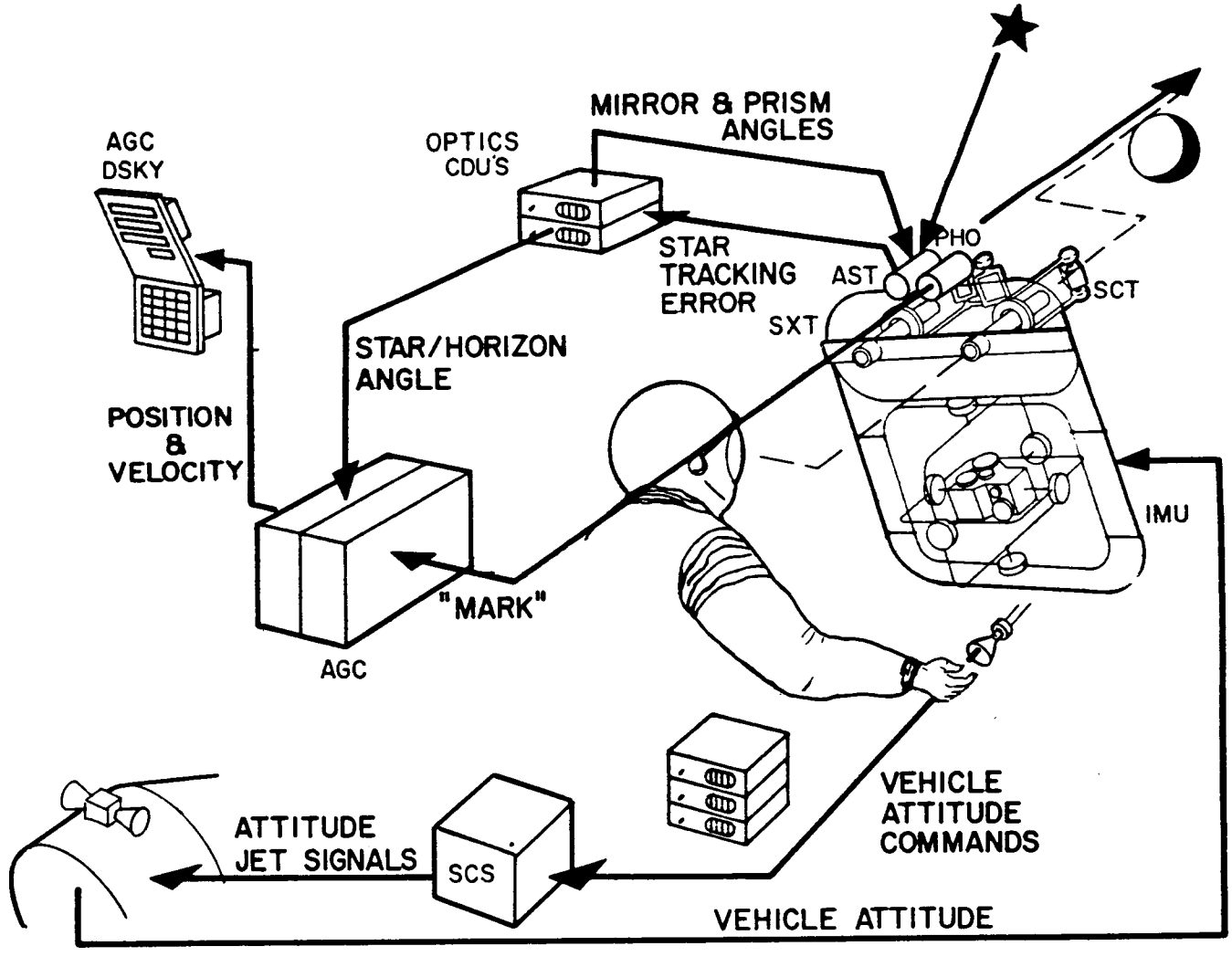

Fig. 1-19 Earth illuminated horizon navigation.

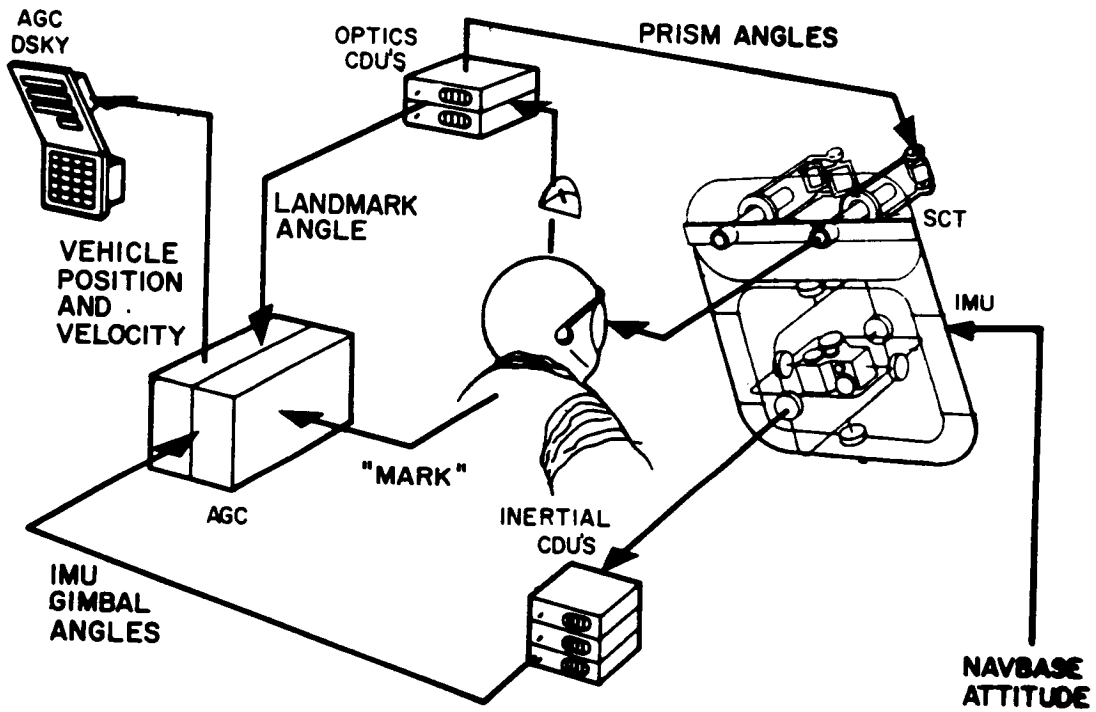

Fig. 1-20 Low orbit navigation landmark tracking.

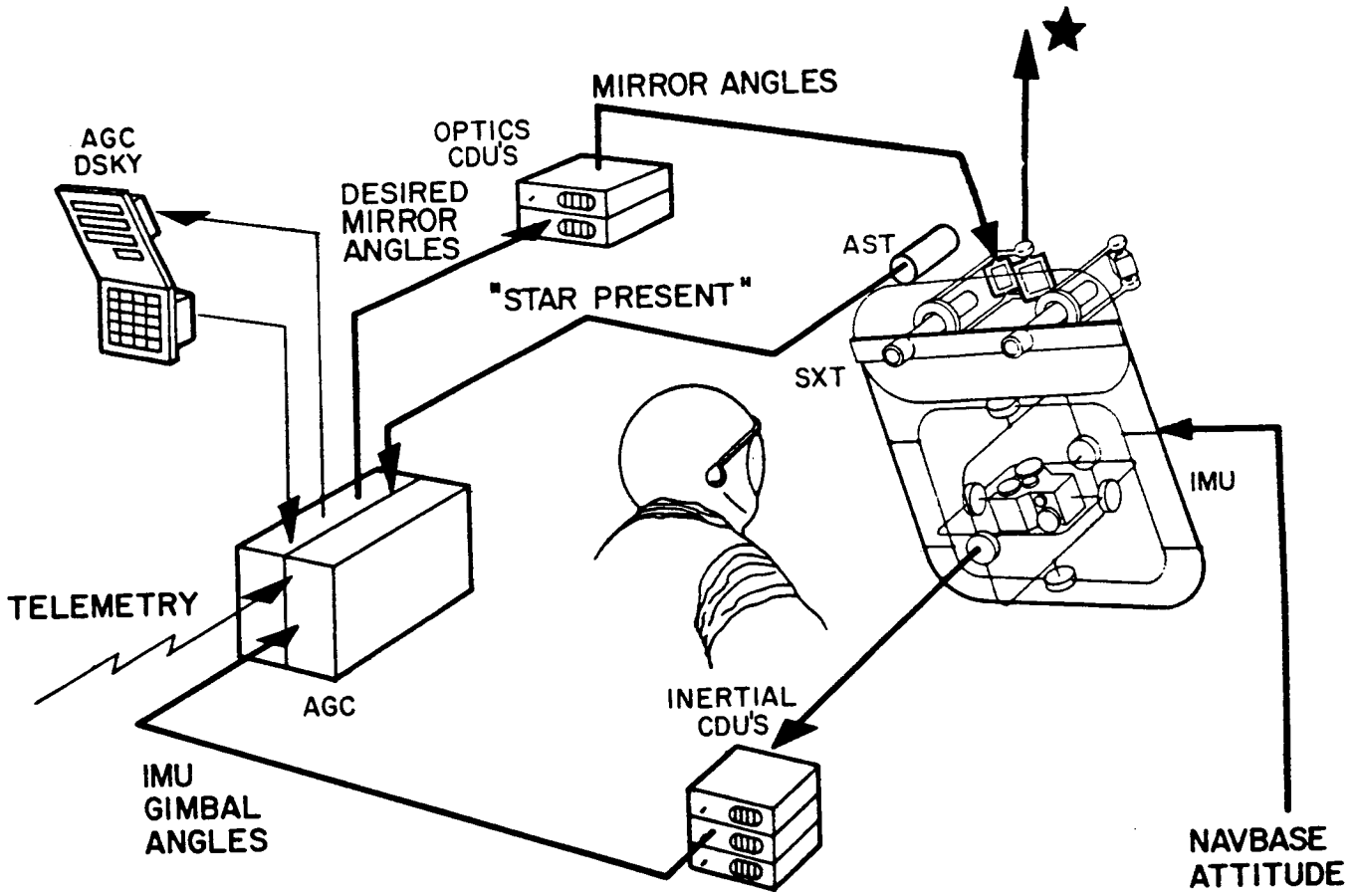

Fig. 1-21 IMU alignment: Automatic acquisition phase.

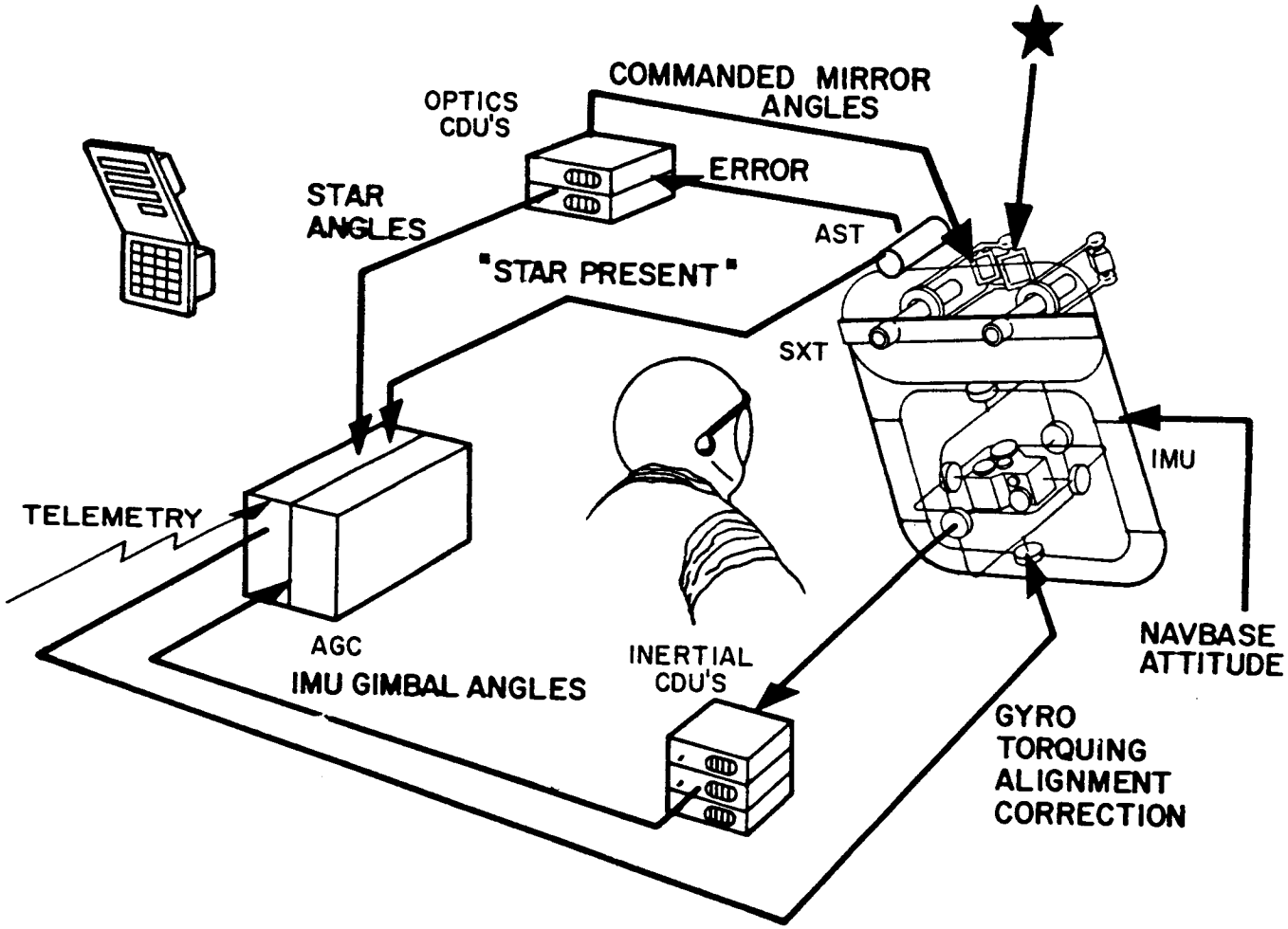

Fig. 1-22 IMU alignment: Automatic tracking phase.

With the IMU to do the control the astronaut would otherwise have to do, the attitude of the spacecraft can be controlled in a manner to achieve the photometer measurement shown in Fig. 1-23. That can be done using the illuminated earth horizon or also against the illuminated lunar horizon.

It is evident that star occultation with the moon time measurements can also be done using the star tracker as another automatic navigation measurement (not shown).

The chronological weight status of the G&N equipment is shown in Fig. 1-24. The weight scale is the ordinate; the abscissa is time, starting in September 1961 when MIT/IL made the requested proposal to develop the Apollo G&N. Intermittent reports were made until November 1962 at which time reporting was put on a monthly basis. This is a cumulative representation in which the top line is the total. The numbers on the chart represent the weight of each item to the nearest tenths of a pound. There is a vertical dashed line which represents the change from Block I to Block II in January 1964.

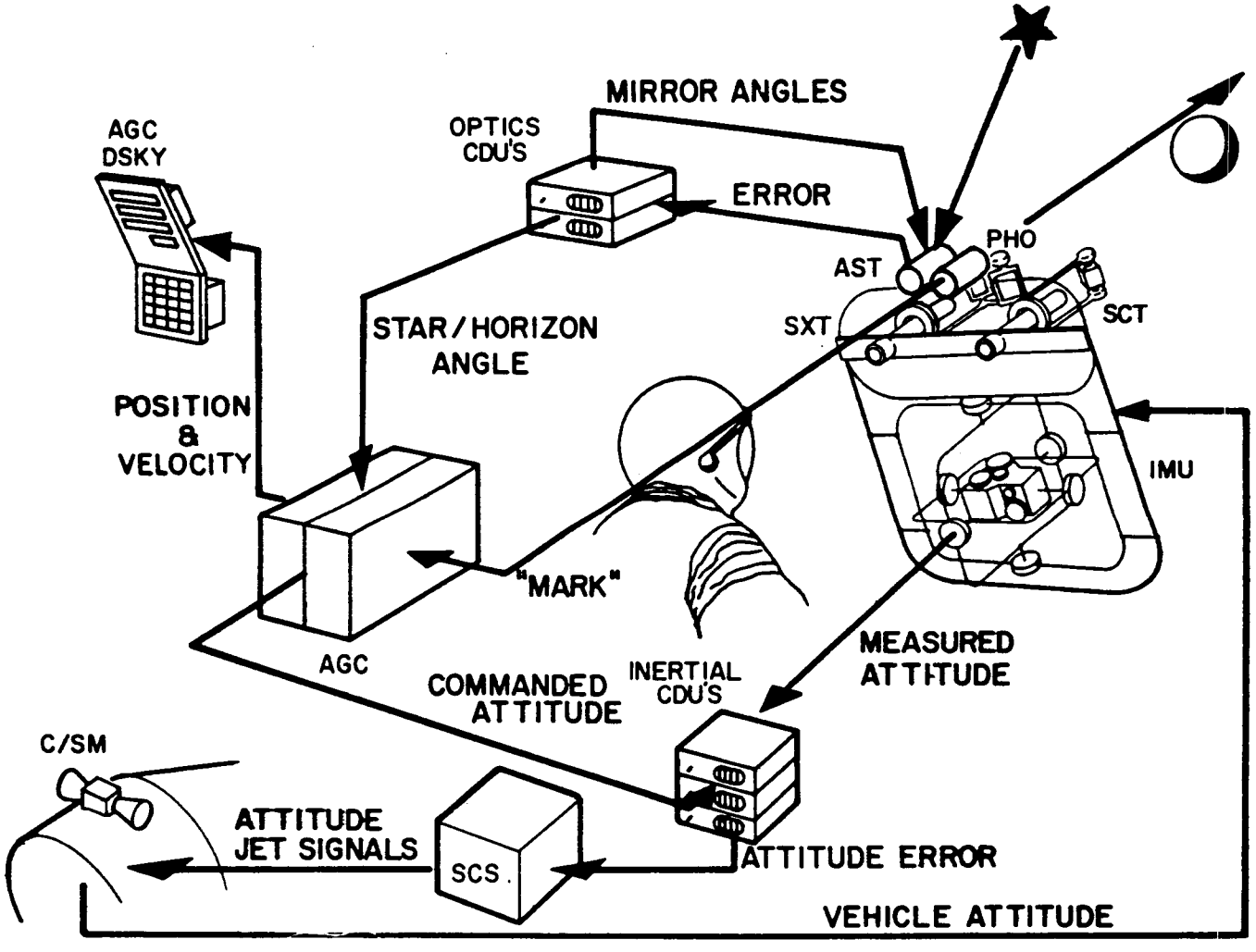

Fig. 1-23 Midcourse navigation: Automatic star-earth horizon measurement.

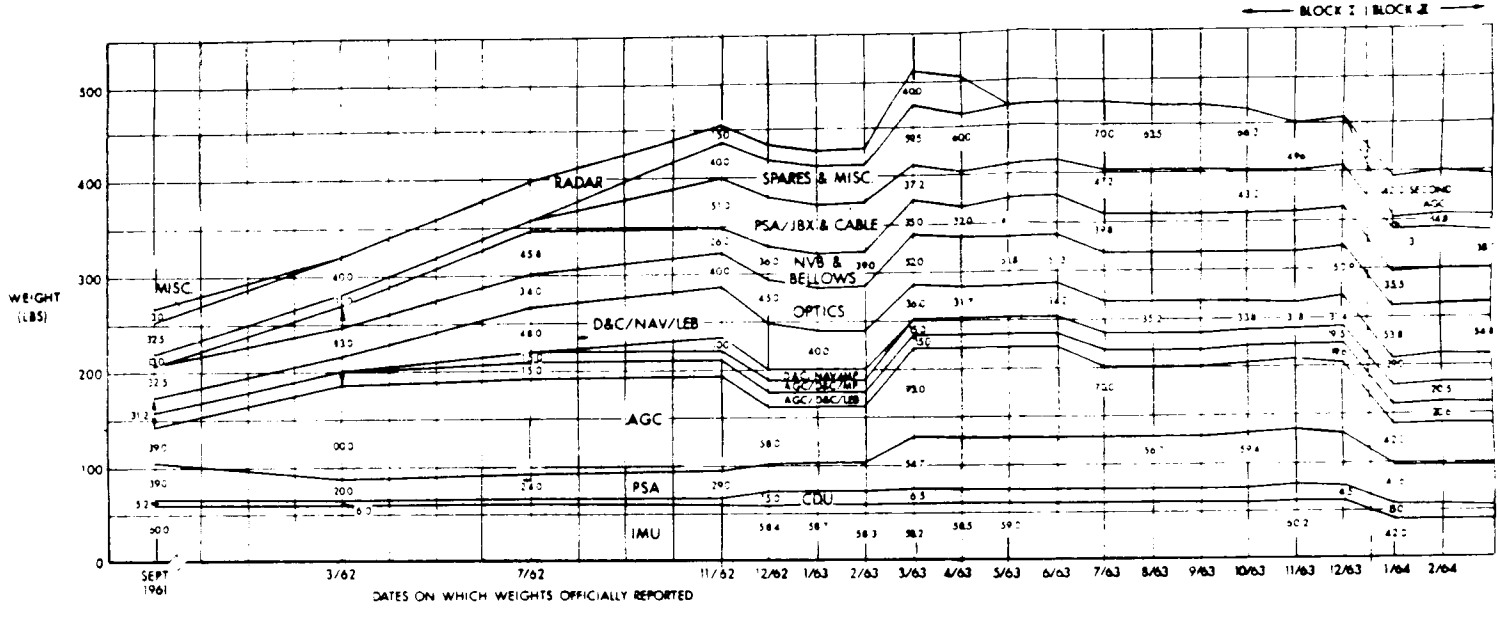

Fig. 1-24 Chronological Weight Status of G&N Equipment

Section 2

THE COMMAND MODULE INSTALLATION

R. W. Gras

Figure 2-1 shows the Command Module Lower Equipment Bay where the Guidance and Navigation (G&N) Equipment will be installed. Shown in this figure are the pressure vessel penetration holes for the Sextant and Scanning Telescope; also shown are the forward shock mounts installed and the beam to receive the rear shock mount. The spaces around the central space are for the Coupling and Display Units (CDU) and the Power and Servo Assembly (PSA), Computer and other electronic or control equipment.

Figures 2-2 and 2-3 prevent cause-and-effect flow grams. The numbers in circles indicate that the items so labeled are original requirements from which flow secondary requirements and the solutions used to meet the requirements.

Item (1), for example, starts with the requirement that the Sextant (SXT) and the Scanning Telescope shall be accurately aligned with the Inertial Measurement Unit (IMU) and with each other. The G&N solution used was to mechanically tie these units together with a rigid structure consisting of two parts, i.e. the Beryllium Nav. Base and the Beryllium Optics Base. Since the solution bulks these components together there is a secondary requirement imposed on the Command Module in the form of Bulk Space Allocation which necessitated a large compartment in the Command Module.

Items (2) through (8) are self-explanatory.

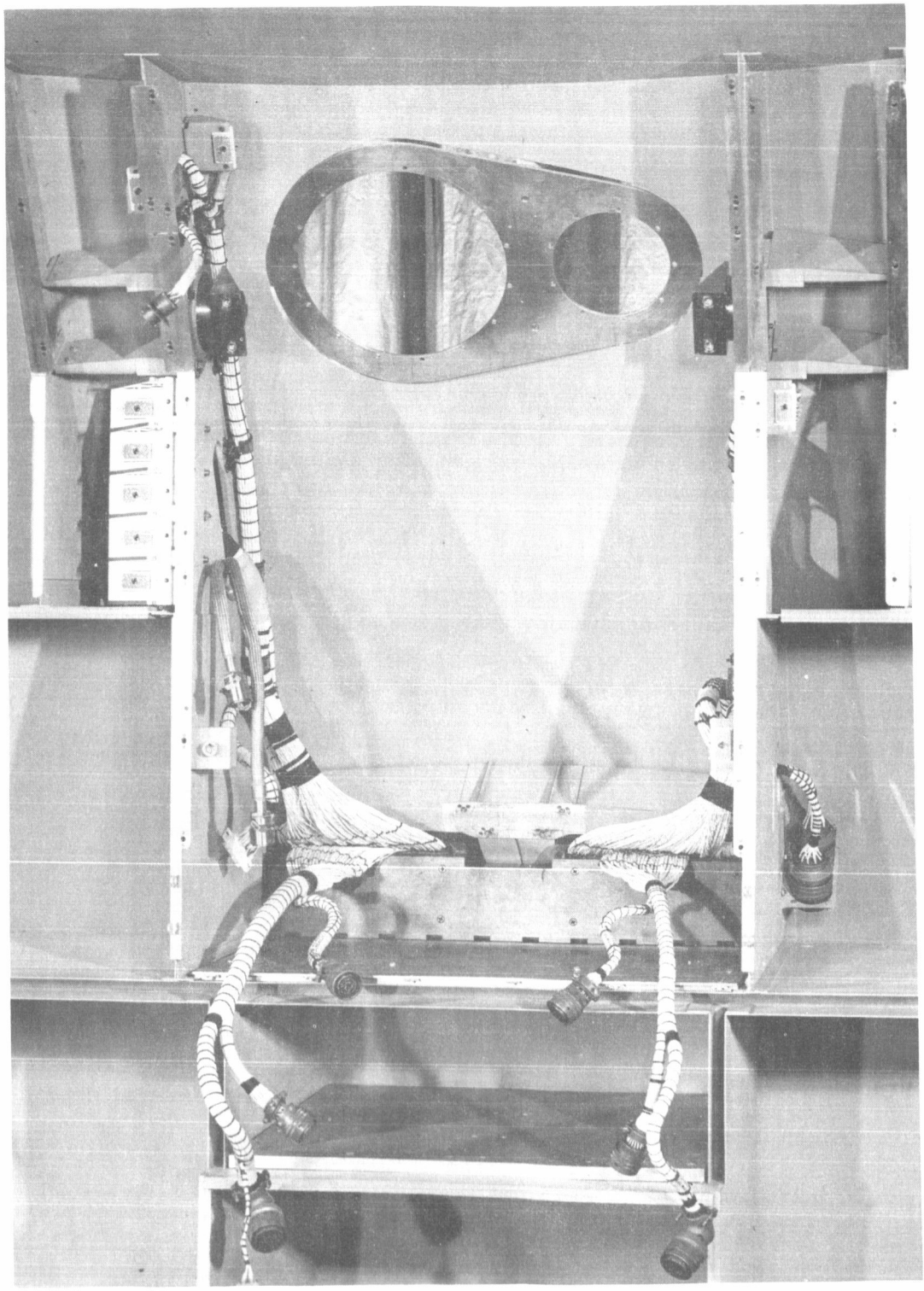

Fig. 2-1

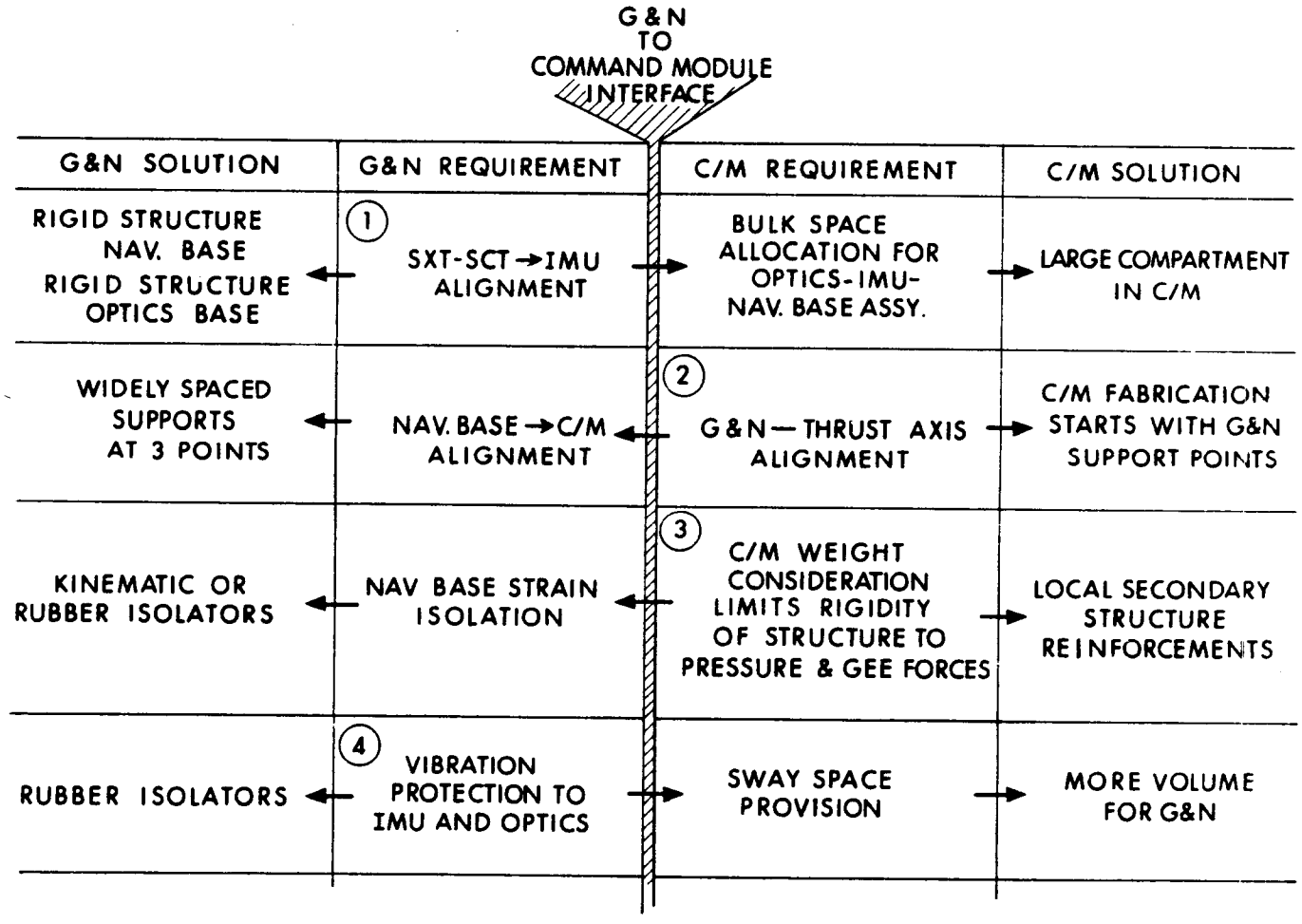
G&N
TO
COMMAND MODULE
INTERFACE
G&N SOLUTION
G&N REQUIREMENT
C/M REQUIREMENT
C/M SOLUTION
RIGID STRUCTURE
NAV. BASE
RIGID STRUCTURE
OPTICS BASE
1
SXT-SCT→IMU
ALIGNMENT
BULK SPACE
ALLOCATION FOR
OPTICS-IMU-
NAV. BASE ASSY.
LARGE COMPARTMENT
IN C/M
WIDELY SPACED
SUPPORTS
AT 3 POINTS
NAV. BASE→C/M
ALIGNMENT
2
G&N—THRUST AXIS
ALIGNMENT
C/M FABRICATION
STARTS WITH G&N
SUPPORT POINTS
KINEMATIC OR
RUBBER ISOLATORS
NAV BASE STRAIN
ISOLATION
3
C/M WEIGHT
CONSIDERATION
LIMITS RIGIDITY
OF STRUCTURE TO
PRESSURE & GEE FORCES
LOCAL SECONDARY
STRUCTURE
REINFORCEMENTS
RUBBER ISOLATORS
4
VIBRATION
PROTECTION TO
IMU AND OPTICS
SWAY SPACE
PROVISION
MORE VOLUME
FOR G&N

Fig. 2-2

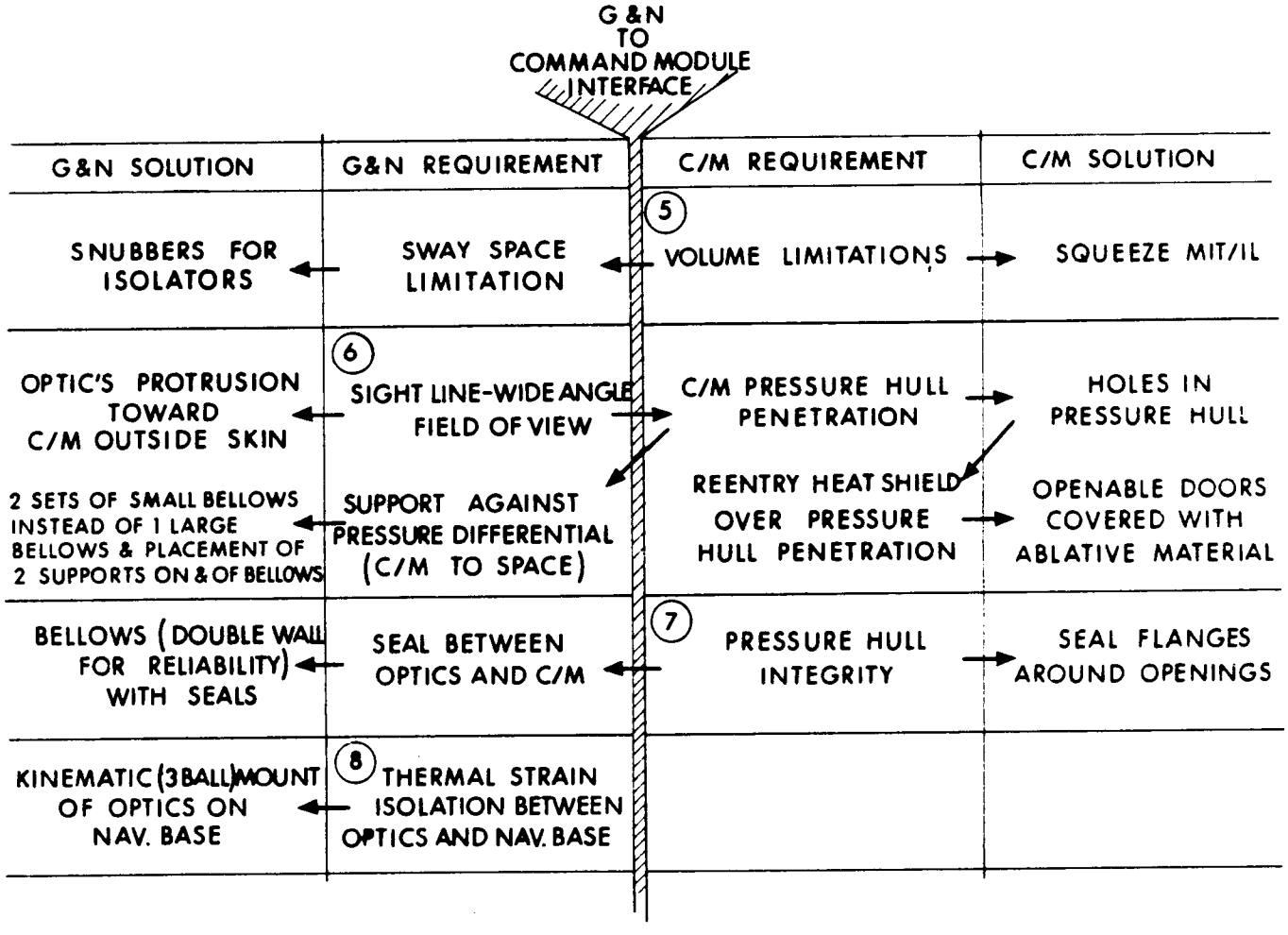
G&N
TO
COMMAND MODULE
INTERFACE
G&N SOLUTION
G&N REQUIREMENT
C/M REQUIREMENT
C/M SOLUTION
5
SNUBBERS FOR ISOLATORS
SWAY SPACE LIMITATION
VOLUME LIMITATIONS
SQUEEZE MIT/IL
6
OPTIC'S PROTRUSION TOWARD C/M OUTSIDE SKIN
SIGHT LINE-WIDE ANGLE FIELD OF VIEW
C/M PRESSURE HULL PENETRATION
HOLES IN PRESSURE HULL
REENTRY HEAT SHIELD OVER PRESSURE HULL PENETRATION
2 SETS OF SMALL BELLOWS INSTEAD OF 1 LARGE BELLOWS & PLACEMENT OF 2 SUPPORTS ON & OF BELLOWS
SUPPORT AGAINST PRESSURE DIFFERENTIAL (C/M TO SPACE)
OPENABLE DOORS COVERED WITH ABLATIVE MATERIAL
7
BELLOWS (DOUBLE WALL FOR RELIABILITY) WITH SEALS
SEAL BETWEEN OPTICS AND C/M
PRESSURE HULL INTEGRITY
SEAL FLANGES AROUND OPENINGS
8
KINEMATIC (3 BALL) MOUNT OF OPTICS ON NAV. BASE
THERMAL STRAIN ISOLATION BETWEEN OPTICS AND NAV. BASE

Fig. 2-3

Section 3

THE INERTIAL SUBSYSTEM

J. E. Miller

The Inertial Subsystem (ISS), one of the three major subsystems of the Apollo Guidance and Navigation system, consists of the Inertial Measurement Unit (IMU), the Power and Servo Assembly (PSA), the Coupling Data Unit (CDU), and the associated displays and controls. Other sections in this report will describe in detail each of these component parts.

The IMU has a stable member which has 360 degrees of freedom, with respect to its case, about each of its three axes. On each axis there are two DC torque motors. The angular deviation sensors are the size 25 IRIG's, and the accelerometers are three 16 PIP's. Both of these components will be described in more detail later. The angle information chain, which is used to determine the orientation of the stable member coordinates with respect to inertial space, consists of a 1-speed and a 16-speed resolver on each axis of the IMU. These resolvers, in conjuction with the CDU, serve to transmit angle increments of the stable member coordinates to the computer. The PSA consists of ten trays of electronics: eight of these trays are devoted to the IMU; two of the trays are devoted to the optical subsystem. The CDU's serve dually as an angle junction box between the IMU and the computer as well as between the optical subsystem and the computer. The display and controls associated with the IMU allow the astronaut to visually determine the mode of the ISS or to control the mode of the ISS through a series of manual buttons.

Most of the interfaces of the ISS between its subsystems and with the spacecraft are shown in Fig. 3-1. There is the mechanical interface, which will be described later; the astronaut has an interface with the Inertial Subsystem; the computer has an interface. The ISS generates the attitude signals and, in conjunction with the computer, steering signals which go to the stabilization and control system.

In order to frame the later presentations of the PSA, the moding control of the ISS, the mechanical design of the IMU, and a description of the gimbal servo power supplies, it is well to recall some of the ground rules when the design for the guidance and navigation system started.

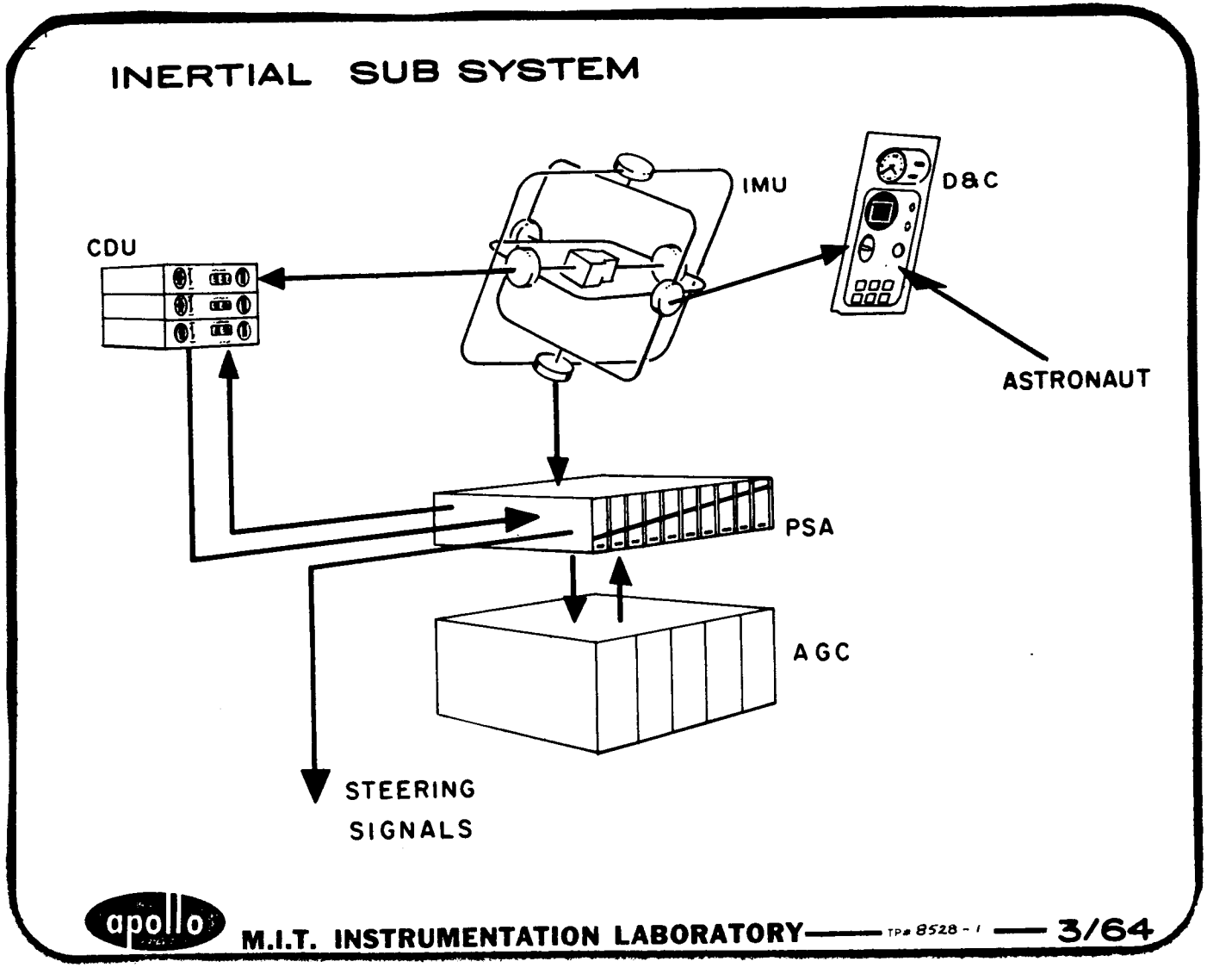
INERTIAL SUB SYSTEM
IMU
D&C
CDU
ASTRONAUT
PSA
AGC
STEERING
SIGNALS
apollo
M.I.T. INSTRUMENTATION LABORATORY
TP# 8528 - 1
3/64

Fig. 3-1

The first ground rule was to use state-of-the-art components. As an example, gyroscopes and accelerometers were used, which were then available, with little modification to their design. The system was designed for backup operation for a signal failure. As an example, power supplies were designed with a free-running multivibrator syncronized to the computer such that the loss of the computer would not cause a failure of the power supply. The system was to have a capability for inflight diagnosis of failure with module replacement in the PSA. The system was to have an emergency operation condition at zero pressure for three or four days. Like the modern woman the design was very weight-critical and power-conscious.

The system had a very rapid design-release schedule. At the time the program was started in 1961, the first flight was scheduled for November 1963. Also, early in the program the Command and Service Module was to land on the moon. Furthermore, after starting the design of the guidance and navigation system, the LEM concept was introduced. Much of the discussion to follow, about the components of the Apollo Guidance and Navigation system, will be framed around the Command Module interface constraints. The next series of presentations will frame the description of the present design including how the ground rules have affected the design, the present performance, the problems encountered, and the status today.

This section will begin with a description of the development cycle for the IMU. The same development cycle has been carried over throughout the guidance system. Five IMU's, designed for particular uses, have been built at MIT/IL. The first one, IMU #1, was a thermal system used for evaluation of the temperature control system of the IMU. This IMU was incomplete in a number of aspects, but it did contain the inertial components (gyros and pendulums) so that it was a thermally identical system to the operational IMU. IMU #2 was a mechanical system built for environmental testing. No real gyros and accelerometers were included with this system. Instead, it was used throughout the program of environmental testing, which included vibration. This will be described in detail later. System #3 was an electrical system used for the development of the gimbal servos. IMU #4 was the first inertial measurement unit to be completely married with the other parts of the Inertial Subsystem. This system actually started running in May 1963. There are many hours on this system as will be shown later. The fifth system is a flight-worthy configuration built to the Class A drawing releases designed at MIT/IL. This system is presently in operation.

The inertial components used in the IMU will be discussed next. The accelerometers used in the IMU are the 16 PIPA accelerometers as shown in Fig. 3-2. It uses, as its inertial sensor, a single-degree-of-freedom pendulum very similar to that which is used in the Polaris Mark II system. Those who are familiar with that pendulum might notice some of its differences. In particular, the Polaris pendulum has a one-gram-centimeter pendulosity, while in Apollo a one-quarter-gram-centimeter pendulosity is used.

APOLLO

16 PULSED INTEGRATING PENDULUM · MOD D

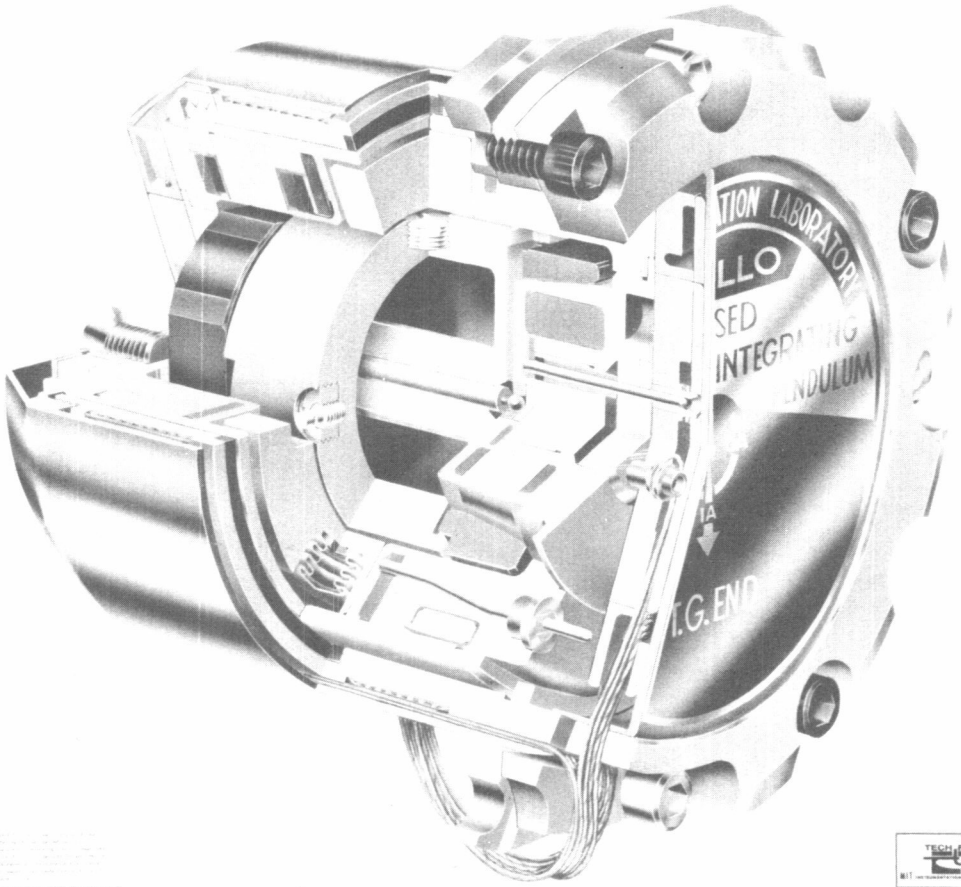

Fig. 3-2

The Polaris accelerometer gives a maximum g capability of about 4 g's whereas the Apollo accelerometer has a maximum g-capability of 19 g's. Figure 3-2 also shows that the 16 PIP contains a tapered rotor which gives both axial and radial suspension to the float with respect to the case. This pendulum is flange-mounted near the end and has a two-degree-of-freedom motion with respect to its mounting flange. This permits prealignment of the pendulum with respect to its mounting flange prior to its insertion into the stable member of the IMU.

Another significant difference between them is that the torque generator of the Apollo PIP contains a reset coil wound around the stator of the torque generator. This coil, excited by the microsyn excitation of 3200 cps, serves to reduce the stored residual magnetism in the circumference of the stator of the torque generator. Figure 3-3 shows an unpotted stator of the torque generator with the reset coil. The 16 PIP developed in the Miniature Components Group at MIT/IL is under contract to Sperry Rand Corporation for the production of these components. Figure 3-4 shows the Apollo PIP requirements and delivery schedules. As can be seen from this chart, the Sperry actual delivery date is very close to the readjusted schedule. The significant portion of this chart is that the actual delivery is considerably ahead of the system requirements for pendulums.

The accelerometer operation is shown in Figure 3-5. As has been previously stated, the 16 PIP is a prealigned assembly such that the orientation of the input axis with respect to its mounting flange is known with a high degree of accuracy. The portion of the accelerometer mounted in the IMU on the stable member is the 16 PIP and its suspension network. The operation of the accelerometer is best described as follows. It is a binary system. The signal information is generated from a signal microsyn excited from the 3200-cycle-per-second power supply which is clock-syncronized with respect to the computer. Angle information, the angle of the float of the pendulum with respect to its case, is transmitted from the signal generator to the PIP preamplifier also located on the stable member. A differential signal is transmitted from the stable member into the PSA to the AC differential amplifier. This amplified signal is transmitted to the interrogator where an interrogation pulse from the computer, phase-locked to the 3200-cycle microsyn excitation, is used to determine the phase of the angle of the pendulum with respect to the case. The interrogator asks only one question - is the torque applied in a direction to restore the float angle to zero? If not, switching networks inside the interrogator are set up so that when a switching pulse arrives a command is sent to the current switch to change the direction of the torque. The torque is applied through the PIPA calibration module into the V-type torquer located on the PIP. The command to the current switch is only to change the current from the odd poles to the even poles. Current is maintained constant through a DC current loop, whereby the current through the torque generator is compared to a precision voltage reference and its error signal is amplified through the DC differential amplifier to close the current loop. This is a

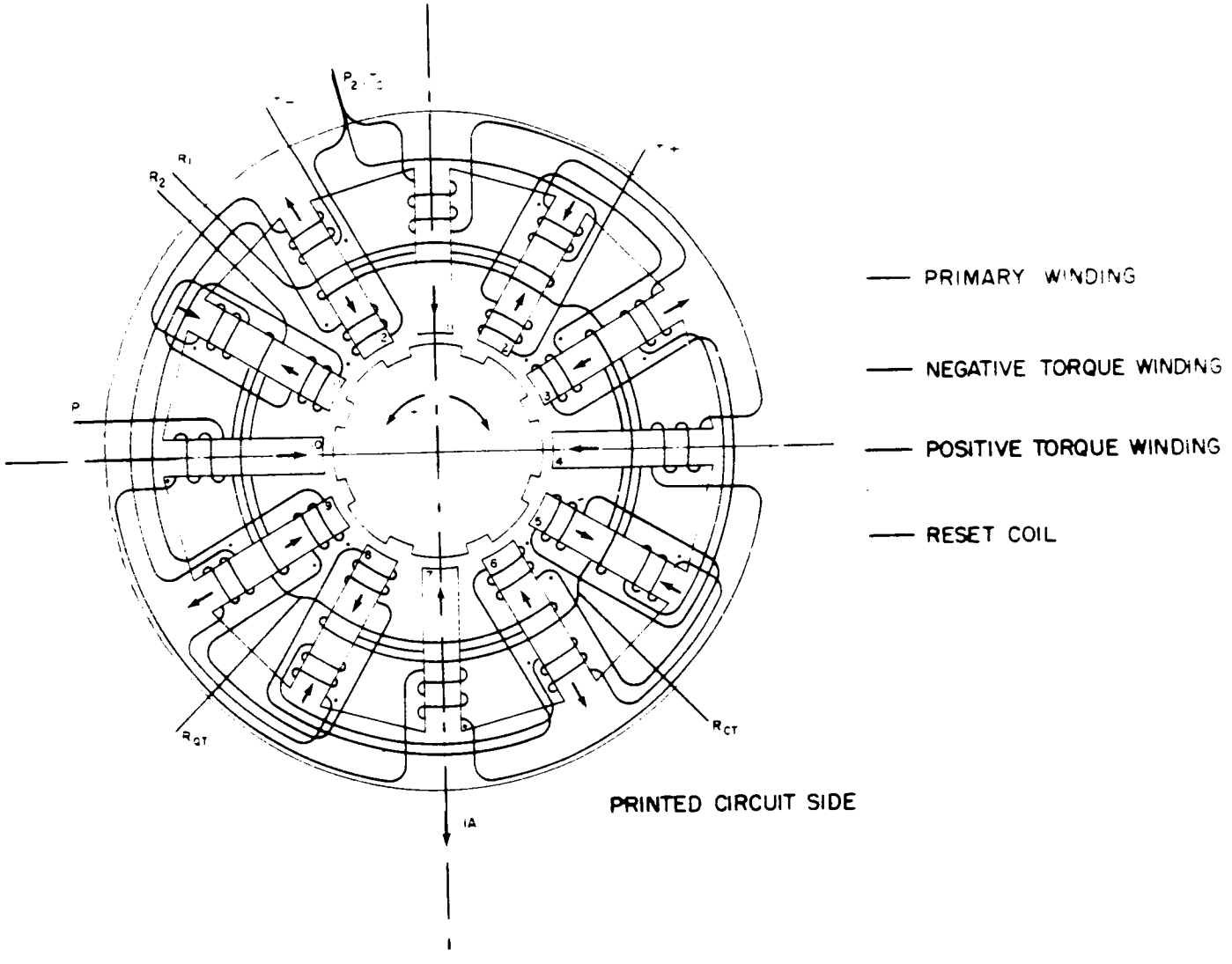

Fig. 3-3 Apollo II – Torque Generator Schematic

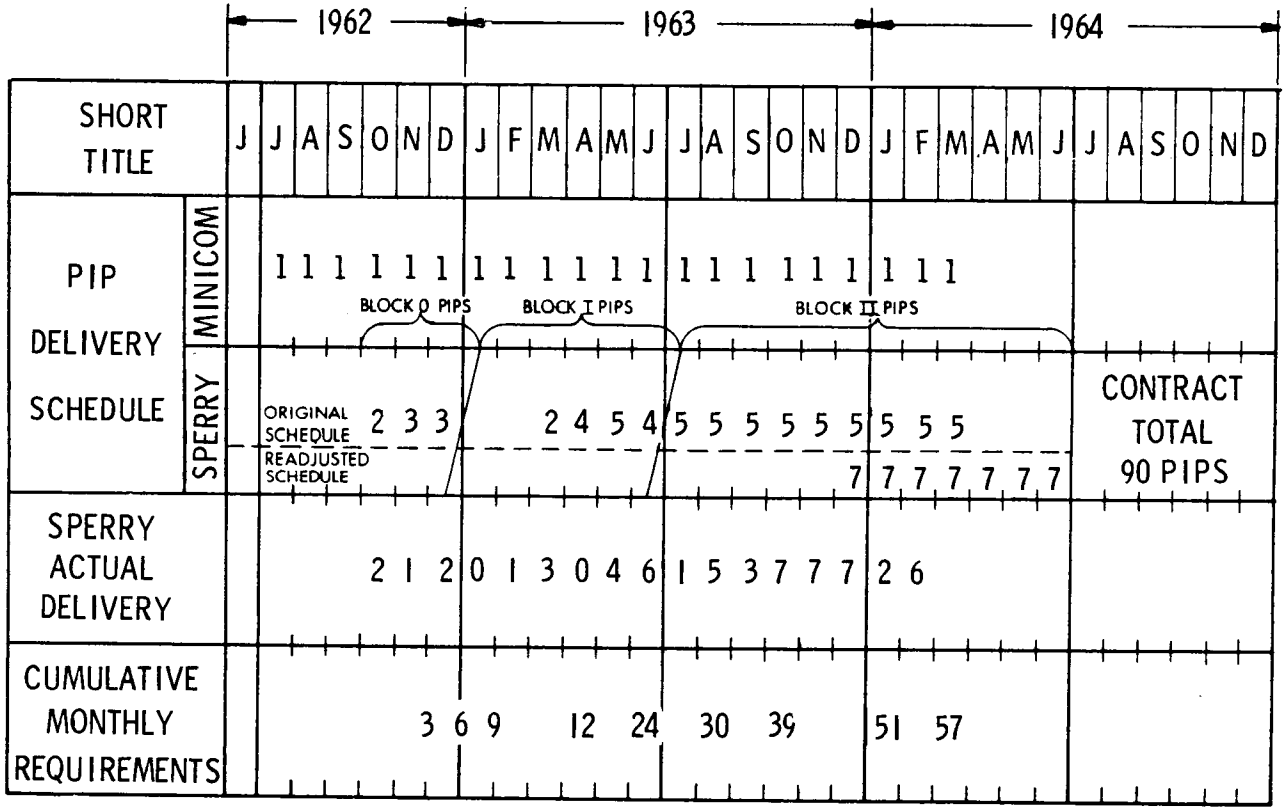

Fig. 3-4 Apollo PIP requirements & delivery schedules.

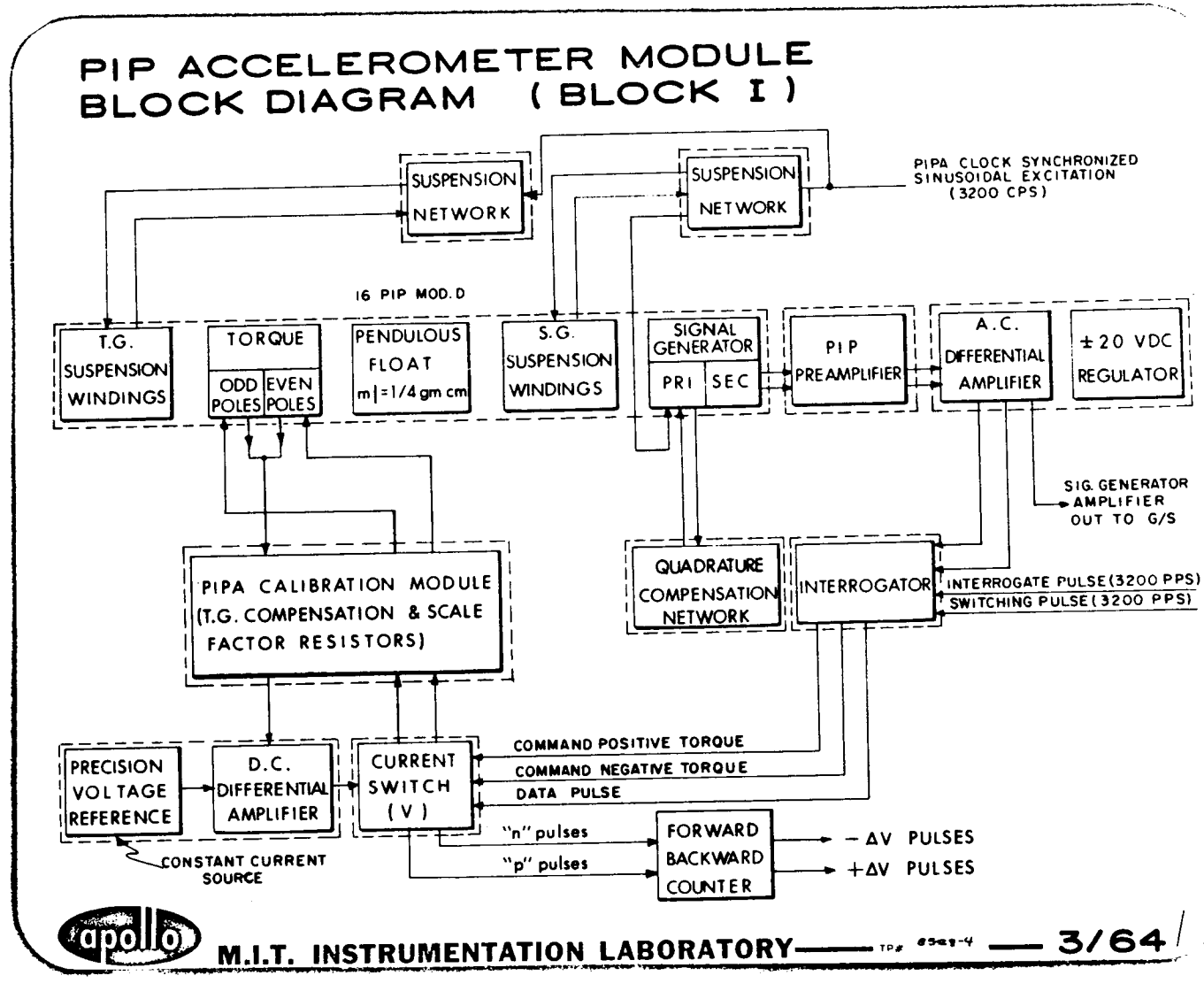
PIP ACCELEROMETER MODULE
BLOCK DIAGRAM (BLOCK I)
SUSPENSION NETWORK
SUSPENSION NETWORK
PIPA CLOCK SYNCHRONIZED SINUSOIDAL EXCITATION (3200 CPS)
16 PIP MOD. D
T.G. SUSPENSION WINDINGS
TORQUE
ODD POLES
EVEN POLES
PENDULOUS FLOAT
m|=1/4 gm cm
S.G. SUSPENSION WINDINGS
SIGNAL GENERATOR
PRI
SEC
PIP PREAMPLIFIER
A.C. DIFFERENTIAL AMPLIFIER
±20 VDC REGULATOR
SIG. GENERATOR AMPLIFIER OUT TO G/S
PIPA CALIBRATION MODULE (T.G. COMPENSATION & SCALE FACTOR RESISTORS)
QUADRATURE COMPENSATION NETWORK
INTERROGATOR
INTERROGATE PULSE (3200 PPS)
SWITCHING PULSE (3200 PPS)
PRECISION VOLTAGE REFERENCE
D.C. DIFFERENTIAL AMPLIFIER
CURRENT SWITCH (V)
COMMAND POSITIVE TORQUE
COMMAND NEGATIVE TORQUE
DATA PULSE
"n" pulses
"p" pulses
FORWARD BACKWARD COUNTER
−ΔV PULSES
+ΔV PULSES
CONSTANT CURRENT SOURCE
apollo
M.I.T. INSTRUMENTATION LABORATORY
3/64

Fig. 3-5

high-precision, ultrastable, DC source. The loop is thus closed to maintain at zero the net torque in this accelerometer. The electromagnetic torque is maintained constant and only time-switched synchronous with the interrogation pulses from the computer. Thus the net number of N-pulses minus P-pulses serve as velocity increments transmitted to the Apollo guidance computer. A forward-backward counter, with a capacity of three, is used to reduce to zero the moding as seen by the Apollo guidance computer.

The angular deviation sensor, used in the IMU, is the Apollo 25 IRIG, shown in Fig. 3-6. It is a modification of the Polaris MOD II gyro. Apollo has one source for the production of these gyroscopes, that is AC Spark Plug. Apollo gyro production started in December 1962 and should have ended by now, but deliveries are about two months behind schedule. The significant fact is that gyro procurement, while behind schedule, is nonetheless ahead of the system delivery requirements.

The Apollo gyro differs from Polaris in a number of minor ways. The only item of significance is in the torque generator. The torque generator is a V-connected torquer similar to that of the 16 PIP, such that, for the fine alignment mode, it can be pulse-torqued to align the inertial reference system to a desired orientation. What has been added to this gyroscope is a set of prealigned hardware, as shown in Fig. 3-7, which goes with the gyro and contains suspension capacitors, an end mount heater, normalization for the temperature sensors, and normalization for the transfer function of the gyroscope. The addition of this prealignment hardware has had significant bearing in our ability to obtain repeatable gyroscope performance from the component when on the test stand to that obtained when assembled in the system.

Figure 3-8 is typical of the results that have been obtained. The data for this gyro in ISS #4, made at MIT/IL, serial #66, had a bias drift of 24 meru at acceptance. The first time it was tested in ISS #4, its bias drift was measured at 23 meru. It should be noted that, at this time, there were 1525 hours on the wheel. The gyro was removed from the ISS and checked on the component level where the bias drift was measured at 27 meru. At this time there were 1700 hours on the gyro wheel. At the present time this gyroscope has 2281 hours on the wheel. Examination of the other two gyroscopes in ISS #4 will show the same type of result. In fact, the RMS values for all three gyro terms, for each of the three gyros, are within about 3 meru when comparing the system test with that of the component test. A reliability program is being conducted for both of the inertial components; that for the gyroscope at AC Spark Plug, and for the 16 PIP at Sperry Rand Corporation. The gyro reliability program, measuring gyro performance, has been underway for three months. The 16 PIP program at Sperry will not start to measure accelerometer performance until April. In addition to these two reliability programs there is a third inertial component data tabulation program being conducted by MIT/IL. This is a program which collects all data on all the gyros and accelerometers that are in the Apollo system. That is, any time a component is tested either as a

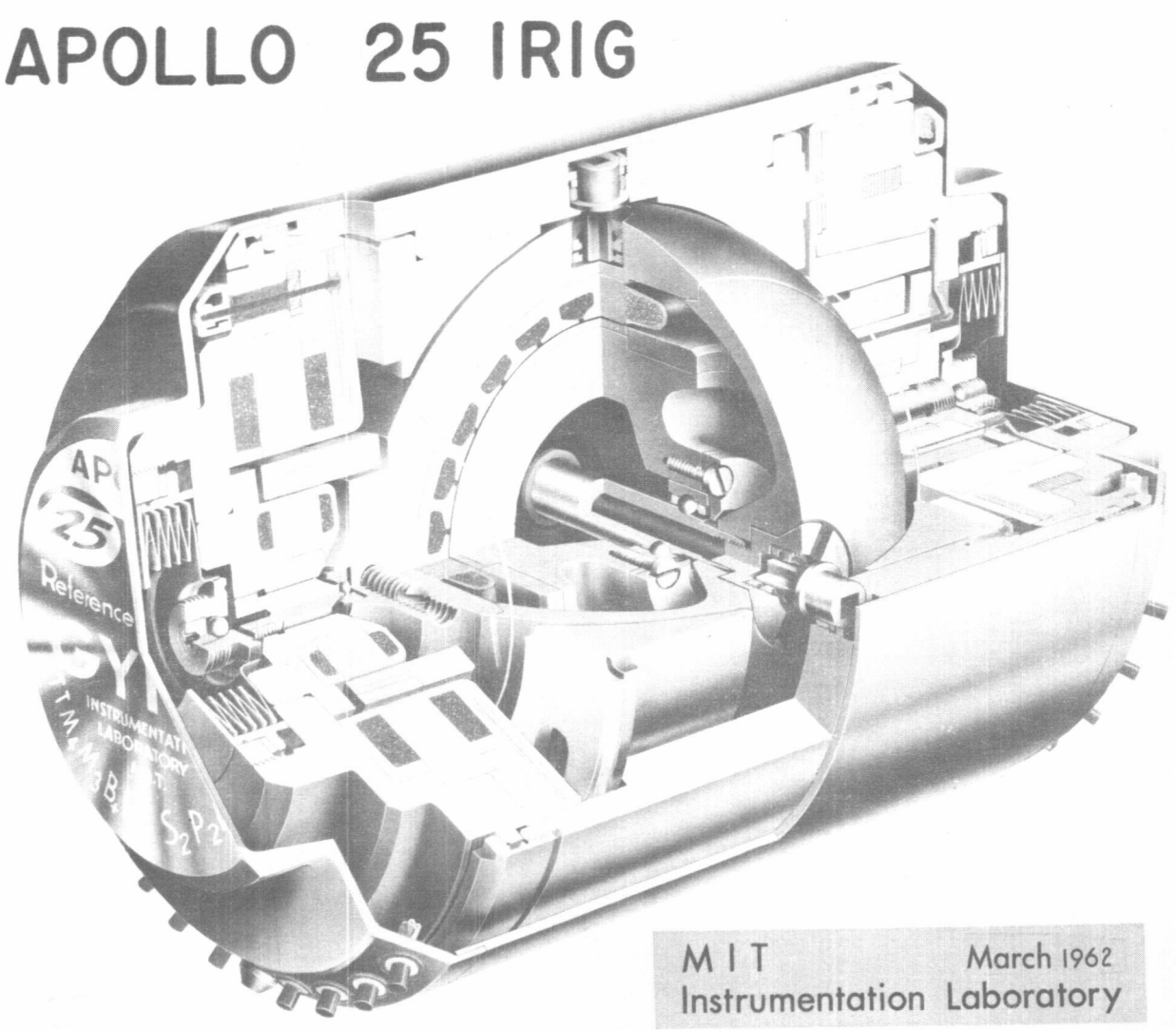

Fig. 3-5

CONFIDENTIAL

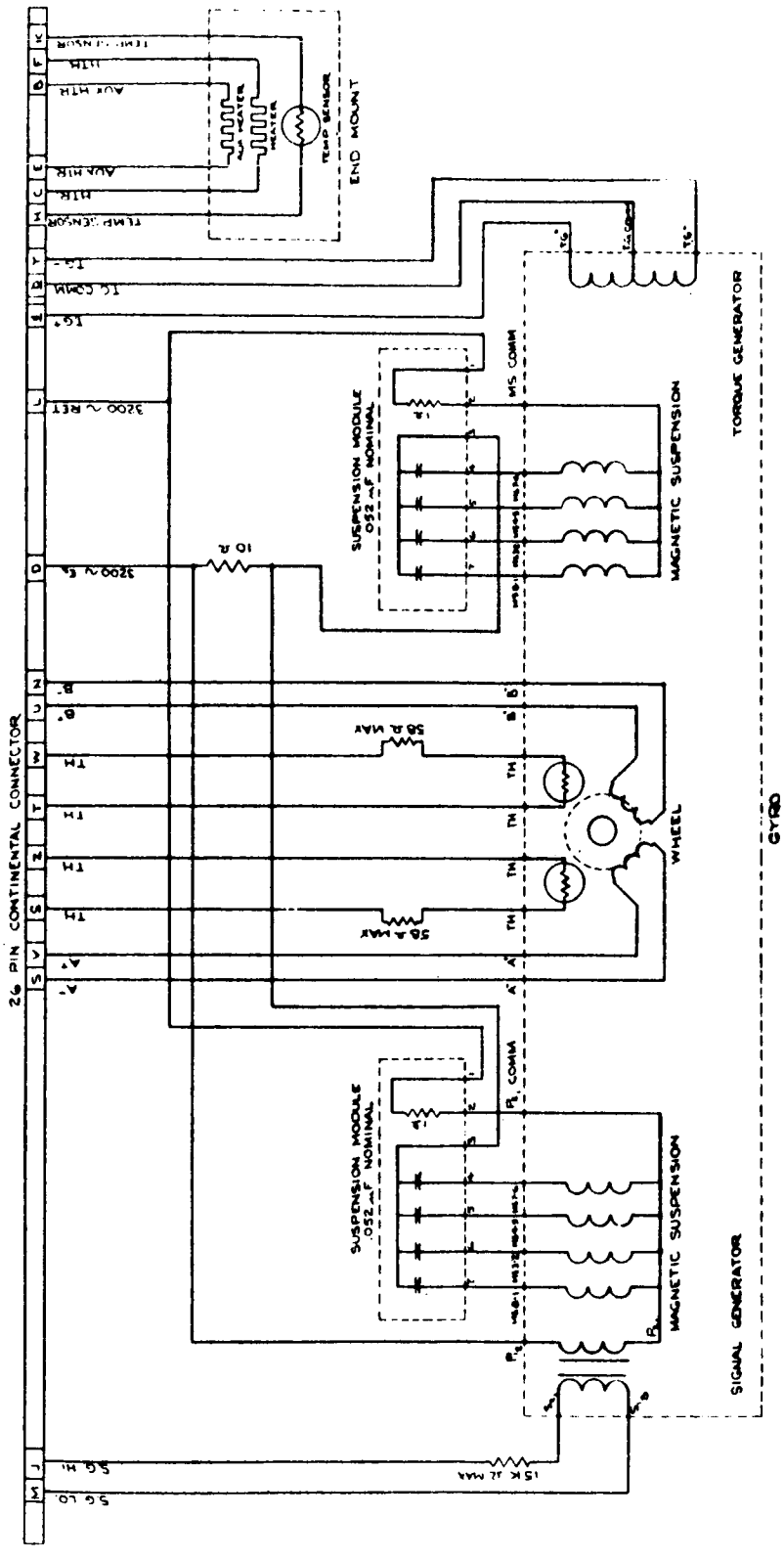

Fig. 3-7 Apollo 25 IRIG normalizing network.

INERTIAL SUBSYSTEM (ISS) #4

CONFIDENTIAL

PURPOSE : EVALUATE ISS TESTS, TEST EQUIPMENT AND INTERFACES AND TRAIN SUBSYSTEM TEST PERSONNEL

RESULTS FOR BIAS DRIFT (BD) IN MERU					
GYRO	MFR	ACCEPTANCE BD	ISS BD	GYRO TABLE RECHECK BD	TOTAL HOURS INCLUDING AGE #4
*66	MIT	+24	+23 at 1525 HRS.	+27 at 1700 HRS	2281
*1A2	ACSP	+5	+2 at 1700 HRS	+3 at 1825 HRS	2143
*1A3	ACSP	+6	+10 at 1600 HRS	+8 at 1650 HRS	1946

Fig. 3-8

component or in the guidance system, these data are reported directly to MIT/IL. Through this program and the reliability programs a performance prediction of the inertial components will be maintained. The capability of the Apollo 25 IRIG has yet to be demonstrated in its fullest capacity.

Figure 3-9 shows how stable the gyroscope can be made. This is a test on an Apollo 25 IRIG. The orientation of the gyroscope was with its input axis North and spin reference axis down. The gyro mounted on the single-degree-of-freedom table had a constant DC torque applied to balance the earth rate input and any bias drift and acceleration sensitive drift along the spin reference axis. Once this DC torque was established it was held constant and from then on the performance of the gyroscope was measured. The equivalent drift rate of this gyroscope over a period of 120 hours -- equivalent to a flight to the moon and back -- was less than 0.11 meru. This is equivalent to 720 seconds of arc drift over this 120-hour period.

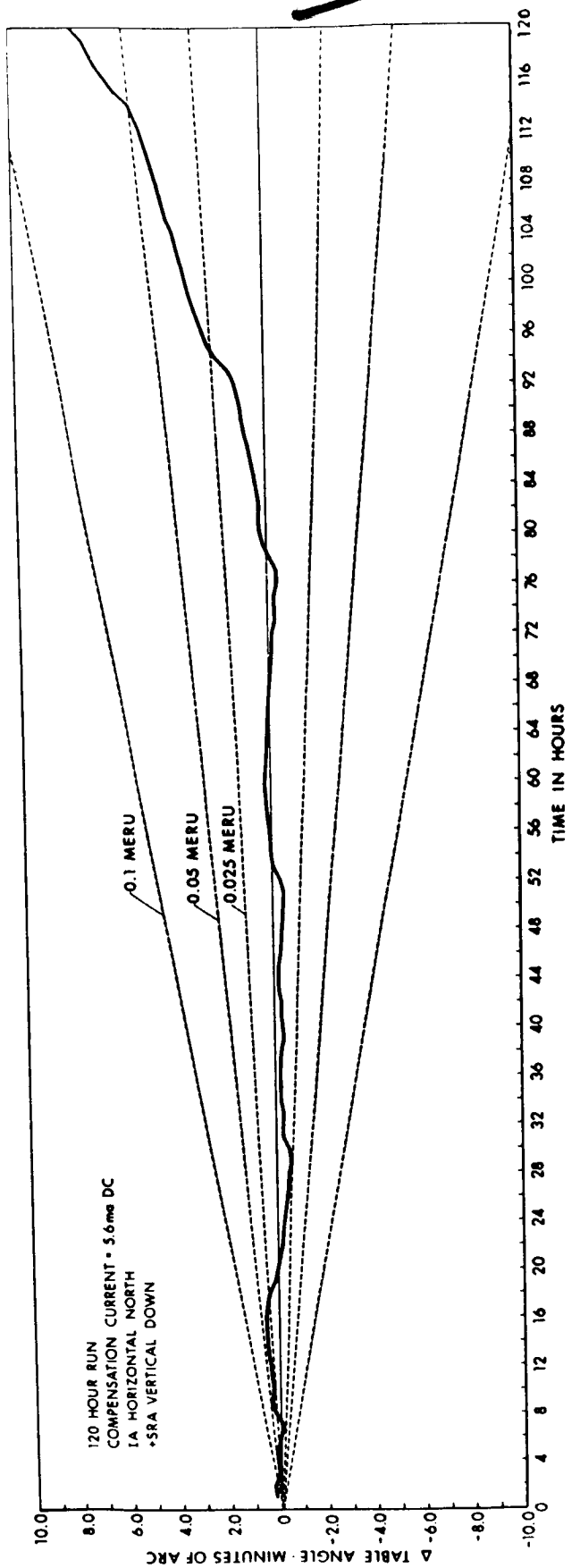

Fig. 3-9 Unit #AC-1A9-A stable azimuth drift test.

Section 4

IMU MECHANICAL DESIGN (BLOCK I)

A. J. Boyce

Figure 4-1 is a very brief description of the mechanical design of the Inertial Measurement Unit (IMU). It is a 3-axis system with unlimited motion on each axis. The inertial components and the resolvers on each axis are prealigned prior to assembly onto the IMU. It has a 14.1-inch spherical diameter, is 18.8 inches long and weighs 60 lbs. The rest of this really is a description of what the interface might be to somebody else. There is a case heat exchanger that carries the glycol water solution for coolant. It has two quick disconnects. This connection is made up by a flexible hose because of the sway of the shock mounts during accelerations. There are four 32-pin electrical connectors which connect the IMU to other parts of the G&N system, not directly with the spacecraft. It is aligned to the Nav base through four mounting pads which form a plane and two alignment pins which control the third axis of rotation.

Figure 4-2 shows IMU-5. There are four stainless steel, hardened pads, assembled to the case under the bottom flange. They are ground and lapped after all the other machining has been completed. This gives a plane reference parallel to the outer axis. The figure does not indicate it, but at the left end there is a slot and a hole aligned perpendicular to the outer axis. The alignment to the Optics is accomplished using this plane and a line through the center line of alignment pins in this slot and hole.

A cooling connection with the protective cover attached is shown in Fig. 4-3. From the quick disconnect the coolant flows through the integral coolant passages, over to the other side through a crossover tube, through another integral coolant passage, and then out through another connector on the other side. There are four electrical connectors, two at each end of the outer axis. At zero pressure the IMU will not operate because of temperature control problems. There are two blowers attached to the outer gimbal to circulate air to bring the heat from the stable member out to the heat exchanger. If there were an internal vacuum there would not be any heat transfer since the blower would have no air to circulate. There are "O" ring seals at each end cover and at each of the top and bottom covers. Also, the electrical connectors are hermetically sealed. The next step (Fig. 4-4) shows the middle axis and the inner axis; typical gimbal wiring is clearly shown as are two ADA's and their preamplifiers for the middle and outer axes. Finally, Fig. 4-5 has half the middle gimbal removed showing the three gyros assembled on the

DESCRIPTION OF INERTIAL MEASUREMENT UNIT - IMU

1. 3 Axes, Unlimited Motion
   Inertial Components & Resolvers Prealigned.
2. 14.1" Spherical Diameter
   18.8" Long
   60 Pounds
3. Case Heat Exchanger
   Glycol Water
   2 Quick Disconnects
   Flexible Hose
4. 4 - 32 Pin Electrical Connectors
5. Aligned to Navigation Base - Optics

apollo M.I.T. INSTRUMENTATION LABORATORY — IP# 8534-1 — 3/64

Fig. 4-1

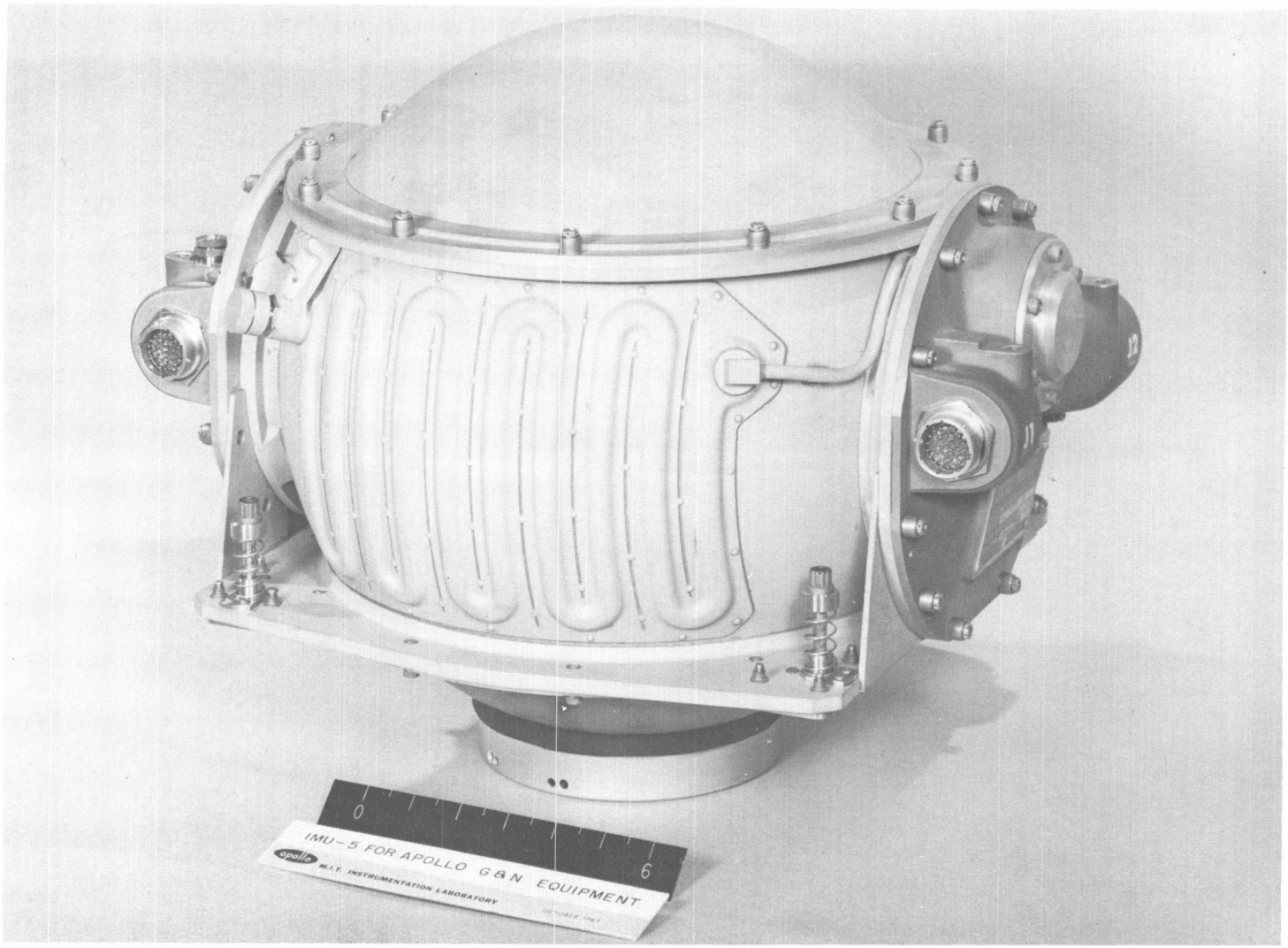
0
6
IMU-5 FOR APOLLO G&N EQUIPMENT
apollo
M.I.T. INSTRUMENTATION LABORATORY

Fig. 4-2

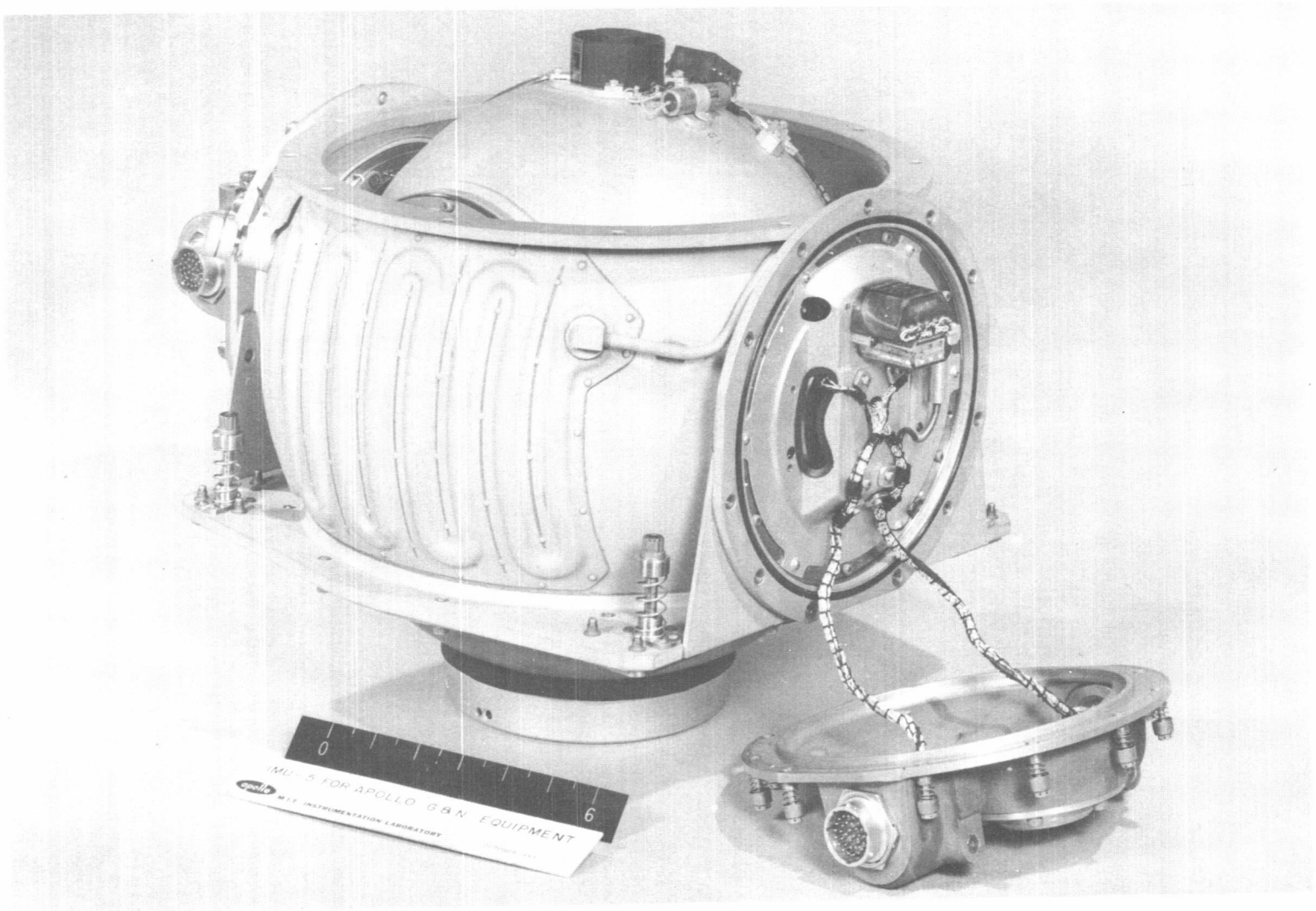

Fig. 4-3

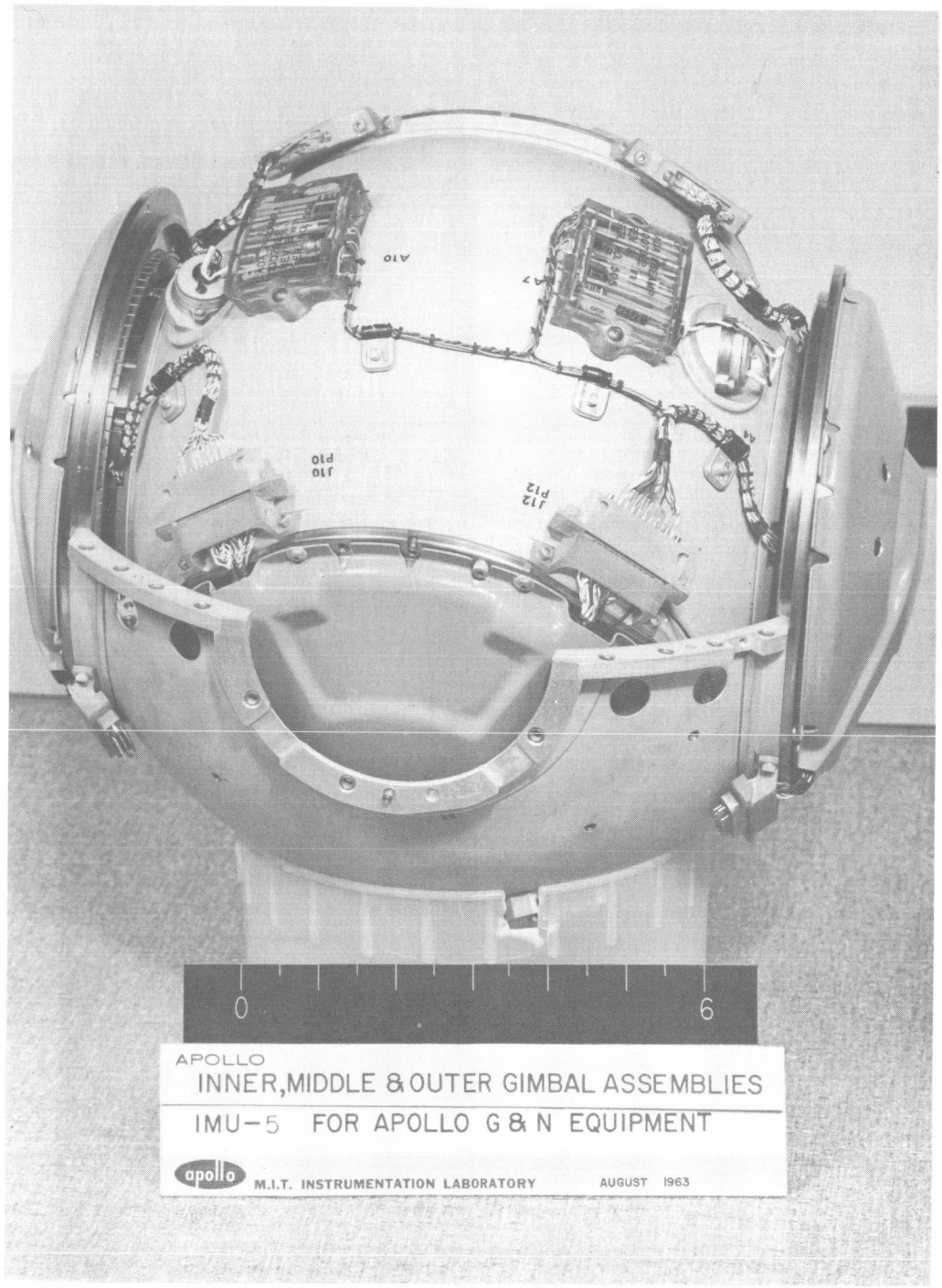
0
6
APOLLO
INNER, MIDDLE & OUTER GIMBAL ASSEMBLIES
IMU-5 FOR APOLLO G & N EQUIPMENT
apollo
M.I.T. INSTRUMENTATION LABORATORY
AUGUST 1963

Fig. 4-4

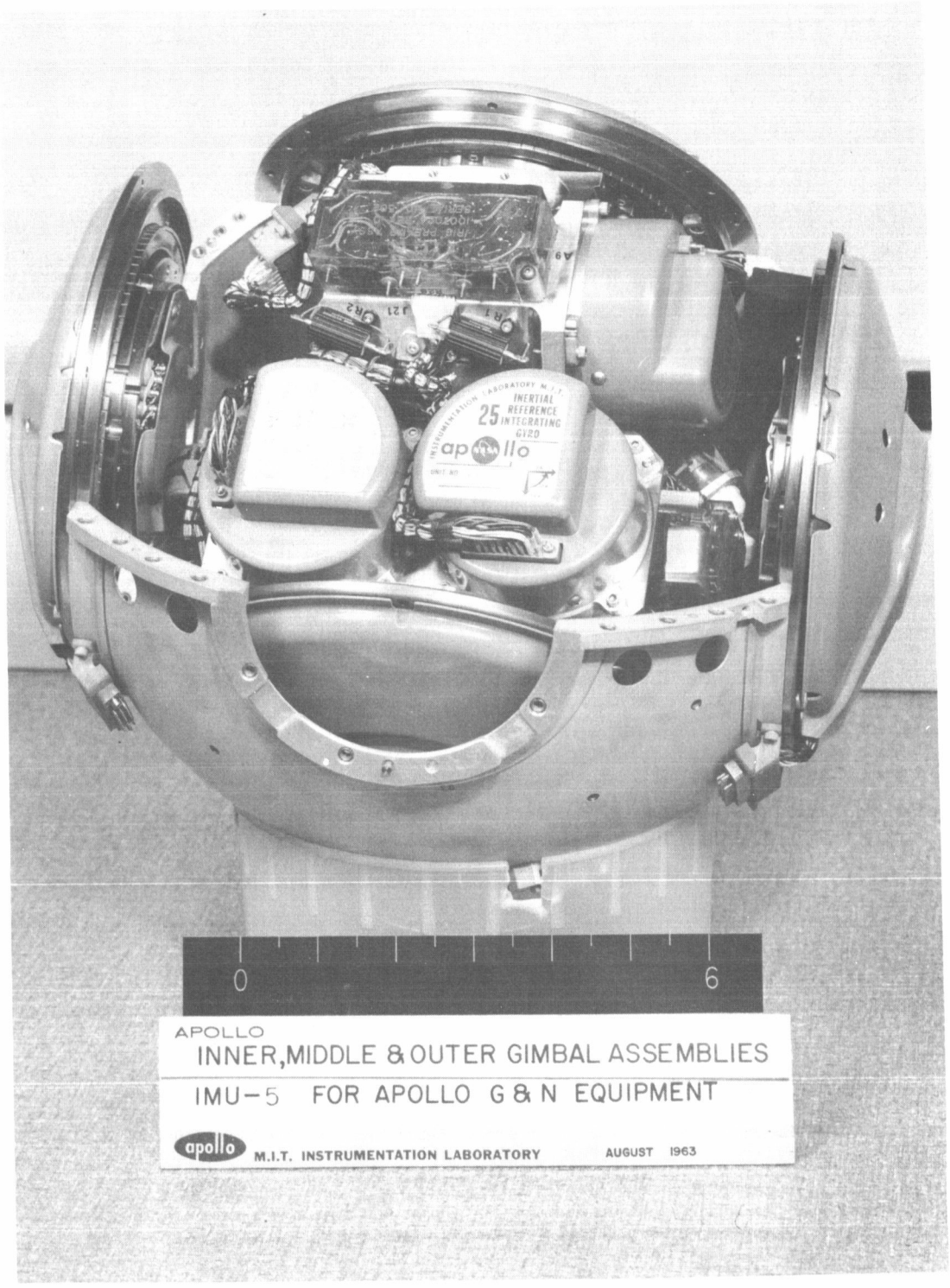
INSTRUMENTATION LABORATORY M.I.T.
INERTIAL
25 REFERENCE
INTEGRATING
GYRO
apollo
UNIT NO
0
6
APOLLO
INNER, MIDDLE & OUTER GIMBAL ASSEMBLIES
IMU-5 FOR APOLLO G & N EQUIPMENT
apollo
M.I.T. INSTRUMENTATION LABORATORY
AUGUST 1963

Fig. 4-5

stabilized member. The three PIPs are not visible in this view, but there is a clear picture of some of the gimbal-mounted electronics, and one of the IRIG prealignment pins.

The present status of the Block I IMU is shown in Fig. 4-6. All the drawings have been released to the participating contractor. All Procurement Specifications, the Assembly Test Procedures, Final Test Methods, etc., have been released, or are in process of being released, through design review or change control. MIT/IL has completed the display model, the vibration model and the thermal model. These early units are not as detailed as the mechanical integrity unit or the thermal systems. They are made up with the stable member just being a representative mass of the stable member in the final system, but can be fabricated faster with substitute materials so that very early information may be obtained. Systems 1 through 5 have also been assembled. AC Spark Plug has a learner model and their System 6 completely assembled with Systems 7, 8, and 9 in progress.

The mechanical problem areas being worked on now are given in Fig. 4-7. On case brazing, the problem is maintaining the specified leak rate which is a NAA requirement of 5×10^{-8} cc of helium maximum. The unit previously shown in Fig. 4-2 has the coolant coils fully brazed to the case. The area around the coupling is where the greatest problem has been found. In checking after the brazing and heat treatment of the case we have been unable to meet the required leak rate; consistently we have been meeting about 1×10^{-5} cc in four cases out of five. It is questionable as to whether 5×10^{-8} is a realistic requirement; there has been some work done in the thermal ICD area to reduce this leak requirement to 1×10^{-6}, in which case there would be less rejects, but we would not expect to meet this in every one of the cases.

It has been proven that it does hold pressure over some 10 to 12 hours, but will not hold helium. If the procedures cannot be worked out for maintaining this pressure, using brazing techniques, there are two things that could be done. One, use the roll bonding material which originally was to be used, but because of various problems was not used in these first Block I systems. At this point the roll-bond material could be incorporated. Another thing that ACSP has been looking at is pre-forming an aluminum tube into a serpentine shape and brazing it to the case. There are now two hydroformed pieces brazed together with the brazed joint making up the seal between the atmosphere and the coolant passage. Integral tubes are being recommended, that are formed and brazed to this case. Further discussions on this problem are scheduled with ACSP.

The case insulation is not a requirement for temperature control, but is required because of the cold surfaces on the case and the high relative humidity in the spacecraft interior to prevent condensation from dripping or floating through the atmosphere. There is not at this time a drawing or design specification as far as surface temperature or dew point.

IMU PROGRESS — MARCH 1964

1. All Drawings Released
2. All Specifications, Test Procedures, Etc. Released or in Process.
3. Completed Assemblies

MIT - Display, Vibration, & Thermal Models
NAA Mock-up & GAGE
-1 Thermal
-2 Mechanical Integrity
-3 Servo
-4 Functional
-5 Flight

ACSP - -LM Learner Model
-6

Fig. 4-6

IMU MECHANICAL PROBLEM AREAS

1. Case Brazing
   - A. HX Leaks
2. Case Insulation
   - A. Condensation
3. Vibration
   - A. High Magnification - Low Damping
   - B. Stub Shafts - Failure & Redesign
   - C. Bearing Nuts - Vibration Damper
   - D. Stabilized Member - Vibration Damper

Fig. 4-7

There is a vibration problem in the IMU because of high magnifications in the system at the resonant frequency of about 130 cps. This high magnification is due to low natural damping in the assembly.

The first time the vibration model was shaken there was a fairly high magnification at the resonant frequency. Then the mechanical integrity system, IMU-2, was shaken and a magnification of about 15 was measured on the stabilized member with a 1 g, 20-2000 cps, sinusoidal sweep input to the case flange. After some rework on the vibration model, it was shaken again, and during this test the assembly did not have this high magnification.

It was found, while shaking IMU-2 and IMU-5, that each had about the same resonant frequency of about 130 cps, which indicates that both have about the same magnification.

Because of the high transmissibility of the assembly, there are higher loads on some of the parts than had been anticipated, in particular the stub shafts. There were stub shaft failures on IMU-2; these were fatigue cracks. Two things can be done to correct this; one is to make the parts stronger, the second is to eliminate the problems of vibration by adding vibration dampers. We have been concentrating on the second method, but immediately made a change to improve the parts by eliminating three holes which caused a stress concentration and increasing the web thickness. At the same time we started looking at various vibration dampers, built into the nuts at one end of each axis or an absorber on the stabilized member.

Many tests have been run on the vibration model to determine why the transmissibility changed from one test to the next. It has been found that, by shaking along the Z axis, with a load applied perpendicular to the outer axis, on the floated end, the friction damping between the two parts is changed and as a result the transmissibility has been varied from approx. 6 to 35 with the resonant frequency varying from approx. 150 to 100 cps. If the floated end is fixed, we have gotten the 35 magnification at 100 cps.

The results of the tests on the vibration model show that the transmissibility is very high with no radial load, it drops to approximately 6 as the radial load is increased to 70 lbs., and it again increases as the radial load is increased above the 70-lb level. This indicates that a damper built into the bearing nut will theoretically control the damping to give the lowest transmissibility. It remains to be demonstrated that a device can be fabricated in the volume available to do this job.

A tuned vibration absorber on the stabilized member with a 1/4-lb resonating mass will theoretically reduce the transmissibility. Tests on IMU-2 with a preliminary absorber design mounted on the stabilized member have resulted in a reduction in transmissibility from approx. 15 to 10.

IMU-2 will be rebuilt from what has been learned on the vibration model and tests will be run next month.

The entire vibration problem may be eliminated when results are complete on vibration tests on a Nav base, optics, IMU assembly mounted on shock mounts. Early tests have shown that the shock mounts reduce the 1-g input to approximately 1/8-g at the IMU flange in the frequency range of 100 to 150 cps when there is no thrust load on the mounts. Additional tests will be run in about a month during which thrust loads will be added to the mounts during the vibration. The results of the tests will determine the maximum vibration input to the IMU flange.

Section 5

BLOCK I INERTIAL SUBSYSTEM (ISS)

J. H. Flanders

This presentation of the Block I Inertial Subsystem will encompass two areas. The first will be a description of the Operational Modes, the Coupling and Display Units (CDU), and their associated resolver chain. The second will relate to ISS operational performance and will include an appraisal of its current status compared to Block I performance objectives.

In addition to the Block I ground rules cited by John Miller, it is important when considering the Apollo Inertial Subsystem to remember three factors that make it different from the inertial equipment in the typical ballistic mission. First, in the Apollo mission the inertial measurements are used intermittently to monitor relatively short velocity changes between comparatively long, free-fall trajectories. If the first propulsion phase does not achieve final mission Circular Error Probability (CEP) there will be an opportunity to correct these errors later in flight. Secondly, the inertial reference is needed to supply an attitude reference for a series of untried manuevers, such as the entry maneuver, the lunar orbit rendezvous, and the safe landing of the LEM in a hard vacuum. Finally, the inertial subsystem is not fully automatic; the astronauts play a key part in initiating and executing the maneuvers.

The CDU is an ideal location to start the discussion of the operational modes. Figure 5-1 schematically represents a CDU, showing its various components, particularly the slew switch and thumb adjustment wheel which permit the astronaut to set a dial indication in the manual CDU mode. The digital pick-off gear and the digital pickoff head are the means of informing the computer what is happening to the two sextant angles and the three IMU angles which are being tracked by the five CDU's mounted on the panel shown in Fig. 5-2.

The basic electro-mechanical nature of the CDU is a consequence of the Block I ground rule which called for existing techniques and components. Also interchangeability of the CDU's in the Optics and in the IMU was a requirement for reliability.

In the sextant trunnion axis of the optics application, a 1-speed and 64-speed ratio is used which, combined with the encoder scaling, gives a trunnion axis bit size of 4.95 seconds of arc per bit. The sextant shaft axis of the optics application has the same bit size as the IMU application, namely 39.6 seconds of arc per bit. In order to provide

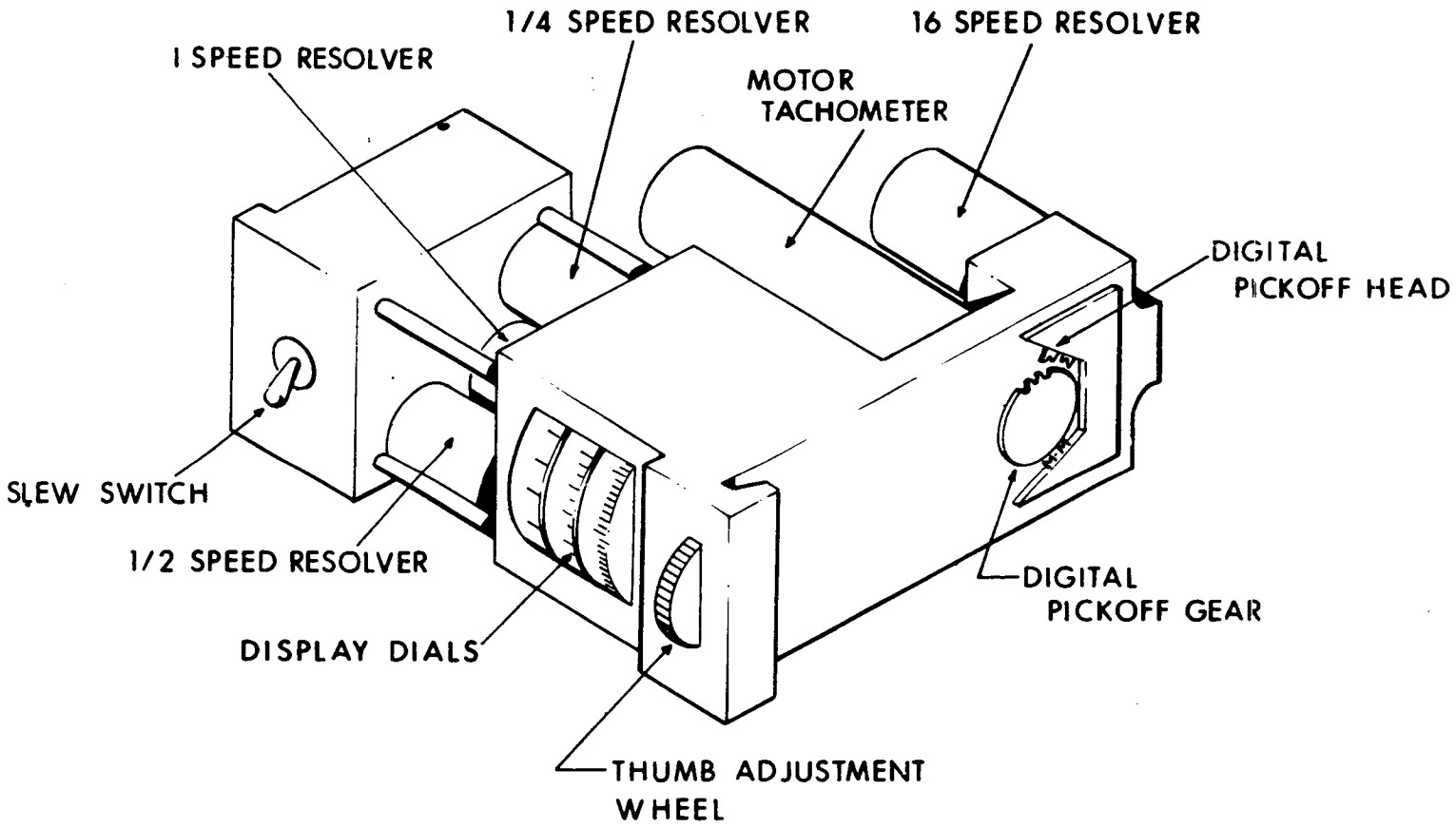

Fig. 5-1 Coupling display unit.

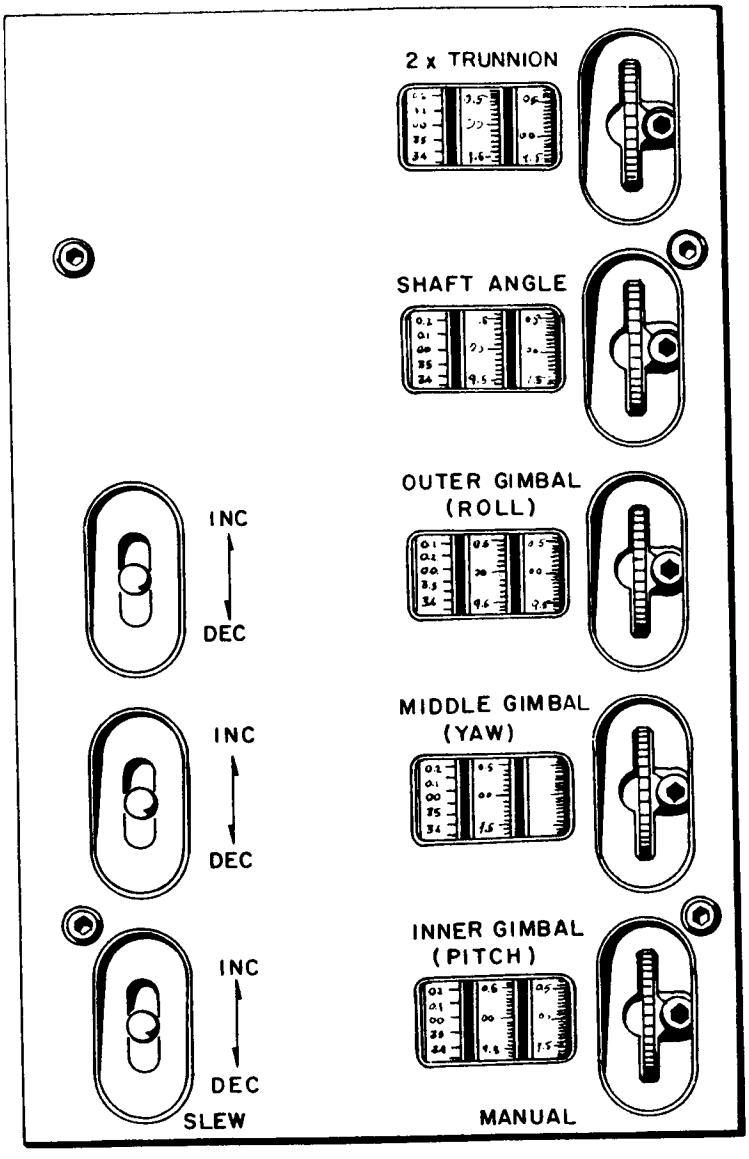

Fig. 5-2 CDU panel.

manual slewing capability of the sextant line of sight by the astronaut it is desirable to resolve his drive commands into up-down and left-right in the field of view. This is achieved by cosecant resolution of the trunnion axis and resolving the drive signals through the shaft axis angle.

Each CDU has a motor-tach unit with a dynamic range of 1200 to 1. The minimum line-of-sight rate of the trunnion drive is 25 seconds of arc per second of time.

The Block I CDU's have been subjected to several qualification tests. Five CDU's have been vibrated in a 10-g rms environment in a standard rack assembly similar to that in the command module. They have been subjected at ambient pressures to temperatures ranging from -50°C to +100°C. They have passed these tests, except for some minor wiring failures which are being corrected. Two qualification tests still to be done are the life test and the minimum pressure (vacuum) operation.

Having described the individual CDU, the operational modes can now be explained. In the Fine Align Mode shown schematically in Fig. 5-3, the CDU acts basically as a repeater. The 16-speed and 1-speed resolvers in the IMU act as transmitters to the resolvers on the CDU's shafts separated by a 16 to 1 gear ratio. Any error signal thus generated passes through a selection circuit to an amplifier that drives a motor-tachometer combination until the CDU position matches that of the IMU. Meanwhile, the encoder, with a quantization of about 40 arc sec per pulse, sends pulses to the AGC to keep the AGC informed of the angles.

Using the same figure, the Zero-CDU Mode can be illustrated. Its purpose is to synchronize the AGC registers and the CDU's. The Zero-CDU Mode switch is energized, informing the AGC of the new operating mode. The inputs to the CDU's are removed and an electrical zero placed on the CDU stator windings. The CDU's slew to their zero positions, putting the encoder and the AGC, which has cleared its registers, into synchronization. If any different mode is now commanded, the CDU's will start to count to the IMU gimbal positions and the AGC will track the CDU's correctly. To recapitulate, in the Fine Align Mode the CDU's are slaved to the IMU resolvers; in the Zero-CDU Mode, the CDU's are held at their own electrical nulls.

In the Coarse Align Mode shown in Fig. 5-4 the positions of the CDU shafts are controlled by the AGC. Pulses with the same quantization of about 40 arc sec per bit, mentioned previously, are sent out by the AGC to the three IMU CDU's. The difference between these commanded pulses and the actual position pulses from the CDU's go through a digital to analog conversion to produce an 800-cycle error signal that moves the CDU shaft to the position commanded by the AGC. This error is not used for steering purposes but is rerouted to the IMU gimbal servo. This is the basis for the Coarse Align Mode wherein the objective is to set the IMU gimbal angles with respect to the spacecraft to within a tolerance of about one degree. When the 1-speed resolver on the IMU gimbal and the 1-speed resolver on the CDU are in approximate synchronization, the coarse alignment has been completed.

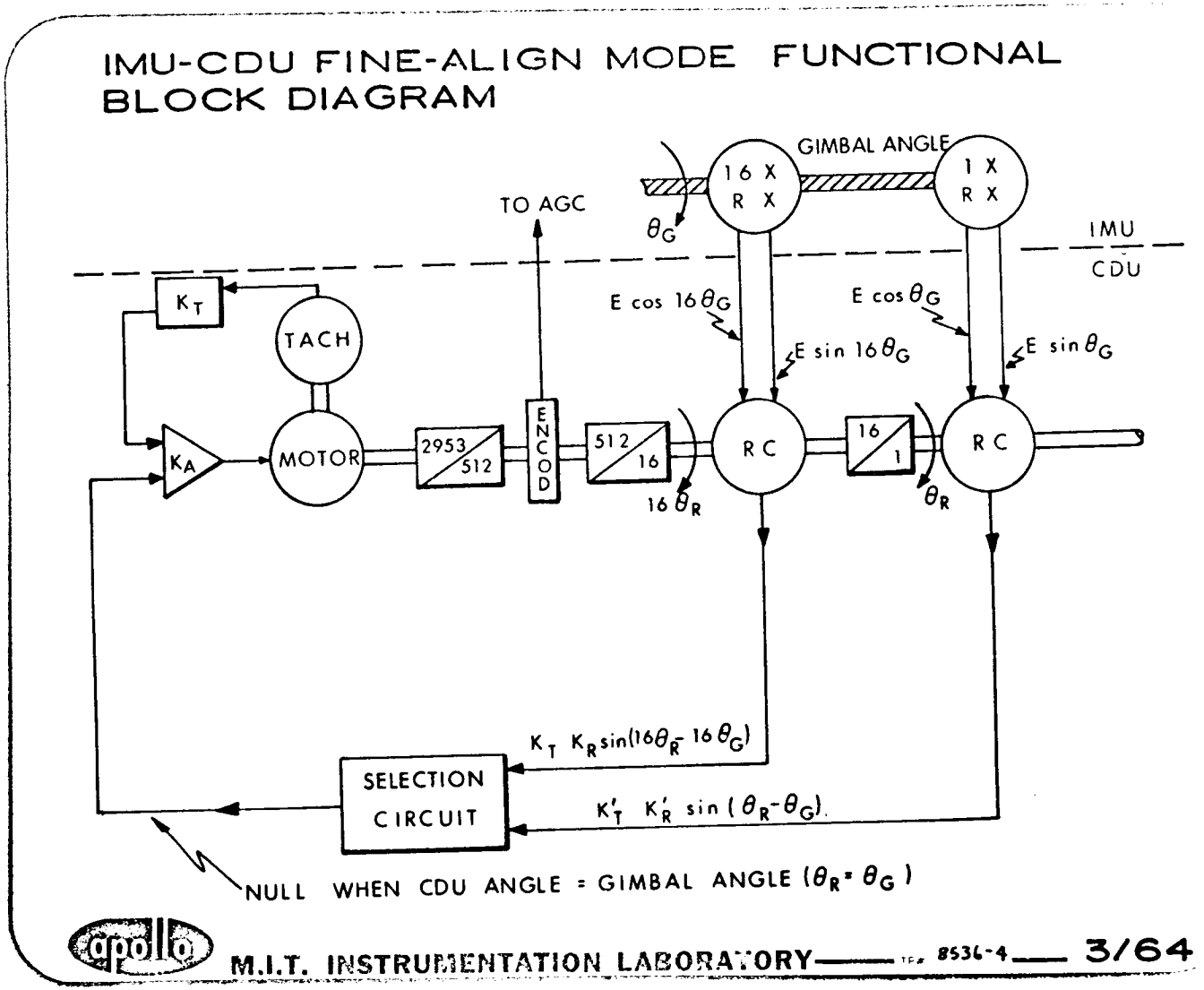
IMU-CDU FINE-ALIGN MODE FUNCTIONAL BLOCK DIAGRAM
GIMBAL ANGLE
16 X R X
1 X R X
TO AGC
θ_G
IMU
CDU
K_T
TACH
E cos 16θ_G
E sin 16θ_G
E cos θ_G
E sin θ_G
K_A
MOTOR
2953/512
ENCOD
512/16
16 θ_R
RC
16/1
θ_R
RC
K_T K_R sin(16θ_R - 16θ_G)
SELECTION CIRCUIT
K'_T K'_R sin (θ_R - θ_G)
NULL WHEN CDU ANGLE = GIMBAL ANGLE (θ_R = θ_G)
M.I.T. INSTRUMENTATION LABORATORY
E 8536-4
3/64

Fig. 5-3

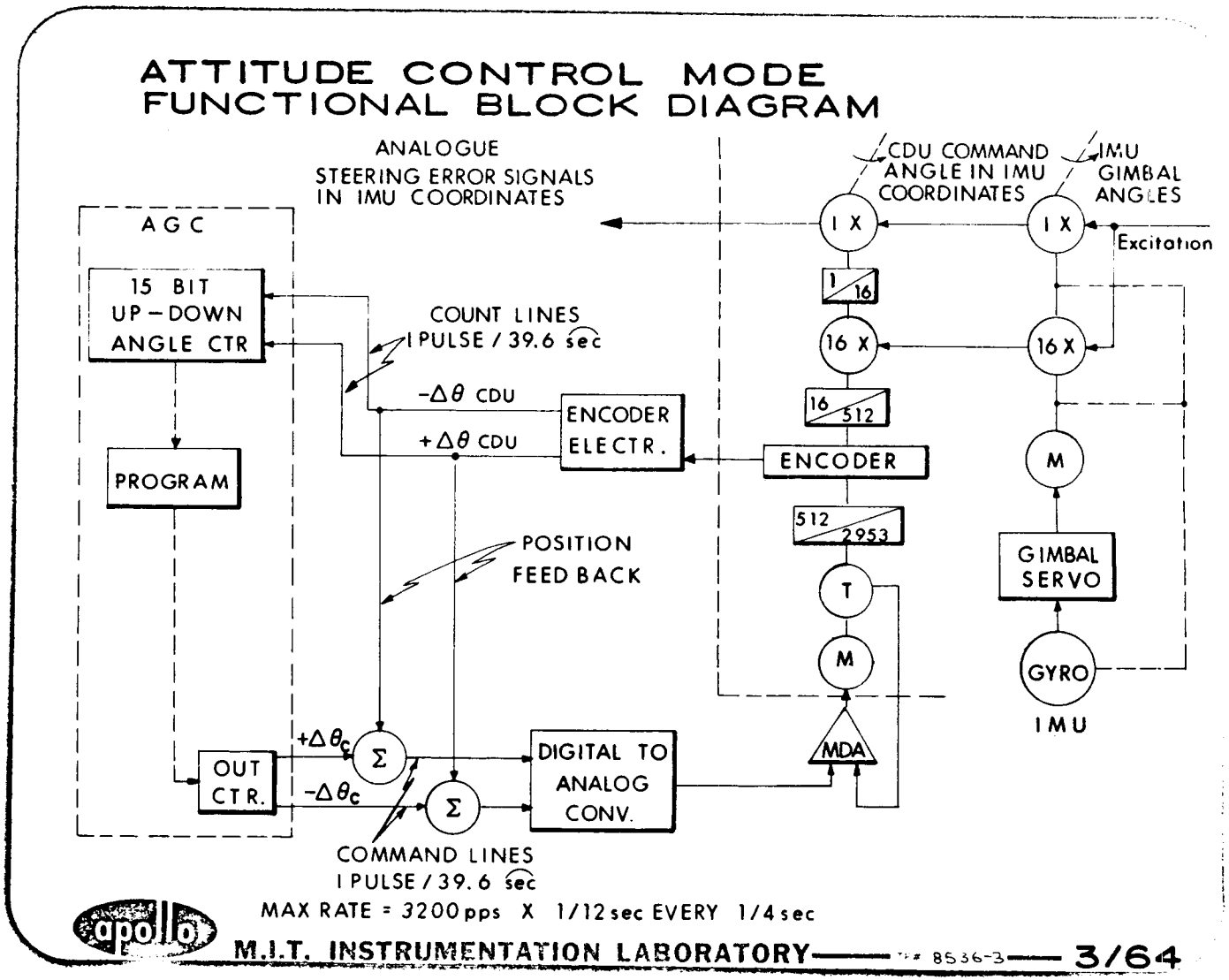
ATTITUDE CONTROL MODE
FUNCTIONAL BLOCK DIAGRAM
ANALOGUE
STEERING ERROR SIGNALS
IN IMU COORDINATES
CDU COMMAND
ANGLE IN IMU
COORDINATES
IMU
GIMBAL
ANGLES
AGC
1 X
1 X
Excitation
15 BIT
UP – DOWN
ANGLE CTR
1/16
COUNT LINES
1 PULSE / 39.6 sec
16 X
16 X
-Δθ CDU
16/512
ENCODER
ELECTR.
+Δθ CDU
ENCODER
M
PROGRAM
512/2953
POSITION
FEED BACK
GIMBAL
SERVO
T
M
GYRO
IMU
+Δθc
Σ
DIGITAL TO
ANALOG
CONV.
MDA
OUT
CTR.
-Δθc
Σ
COMMAND LINES
1 PULSE / 39.6 sec
MAX RATE = 3200 pps X 1/12 sec EVERY 1/4 sec
apollo
M.I.T. INSTRUMENTATION LABORATORY
TM 8536-3
3/64

Fig. 5-4

In the Attitude Control Mode, Fig. 5-5 shows the resolver chain functional diagram to obtain steering control. The 1-speed resolver signal is used as a steering error signal to the command module stabilization and control system. This steering signal is in IMU coordinates and is transformed through the resolver chain into useful steering signals. The computer, in response to a variety of steering programs, generates in IMU coordinated angles the desired commands to the CDU's. Any differences between the spacecraft attitude angles and the pickoffs by the 1-speed resolvers generate properly coordinated steering signals. Because of the half-cone angle that the IMU occupies in the spacecraft, these steering signals must pass through a fixed transformation into spacecraft X, Y, and Z coordinates. After the inner and middle gimbal steering errors have been resolved through the outer gimbal angle, the outer and middle gimbal steering errors are resolved into the roll error body and yaw error body coordinates. Thus the pitch error, yaw error, and roll error are delivered as attitude error signals to the S/C system.

The Entry Mode differs from the preceding in two ways. First a different coordinate system is used because the principle rotations in the entry maneuver occur about the steady-state velocity vector which is aligned along the X-axis of the navigation base. This need not be resolved through the fixed transformation process but is used in the so-called offset axis system. The pitch attitude is not handled any differently than before. Also the pitch and yaw error signals are still resolved through the outer gimbal angle. Once this is done, the roll and yaw errors are in the offset axis system. But, because of the required rapid roll rates for path and entry control, a gain change of 16 to 1 is obtained by switching over to the 16-speed resolver in the CDU to generate the error signal. The computer also is switched to a 16 to 1 scale factor to get the necessary increase in the command rate.

In the Manual CDU Mode, the astronaut can position the CDU to any desired position with the combination of the slew switch and thumb wheel. This motion of the CDU has no effect on the inertial stabilization of the IMU until an "align" button is actuated to position the gimbal angles to the values set in the CDU, similar to the manner of operation in the Coarse Align Mode.

The performance of the Inertial Subsystem (ISS) is covered by an Assembly Test Procedure that was released Class B in May 1963 and Class A in January 1964 (Fig. 5-6). Both System 5 at MIT/IL and System 6 at ACSP are being tested in accordance to this document. There are three broad categories of tests. The system is operated to see that it conforms to specifications. The alignment is checked to determine gimbal orthogonalities, 16-speed resolver accuracies, and the alignment of the gyros and accelerometers with respect to the stable member coordinate system. The inertial performance of the ISS with respect to gyro coefficients and the PIPA scale factors, and bias, is again checked for correlation with previous history with particular emphasis on stability.

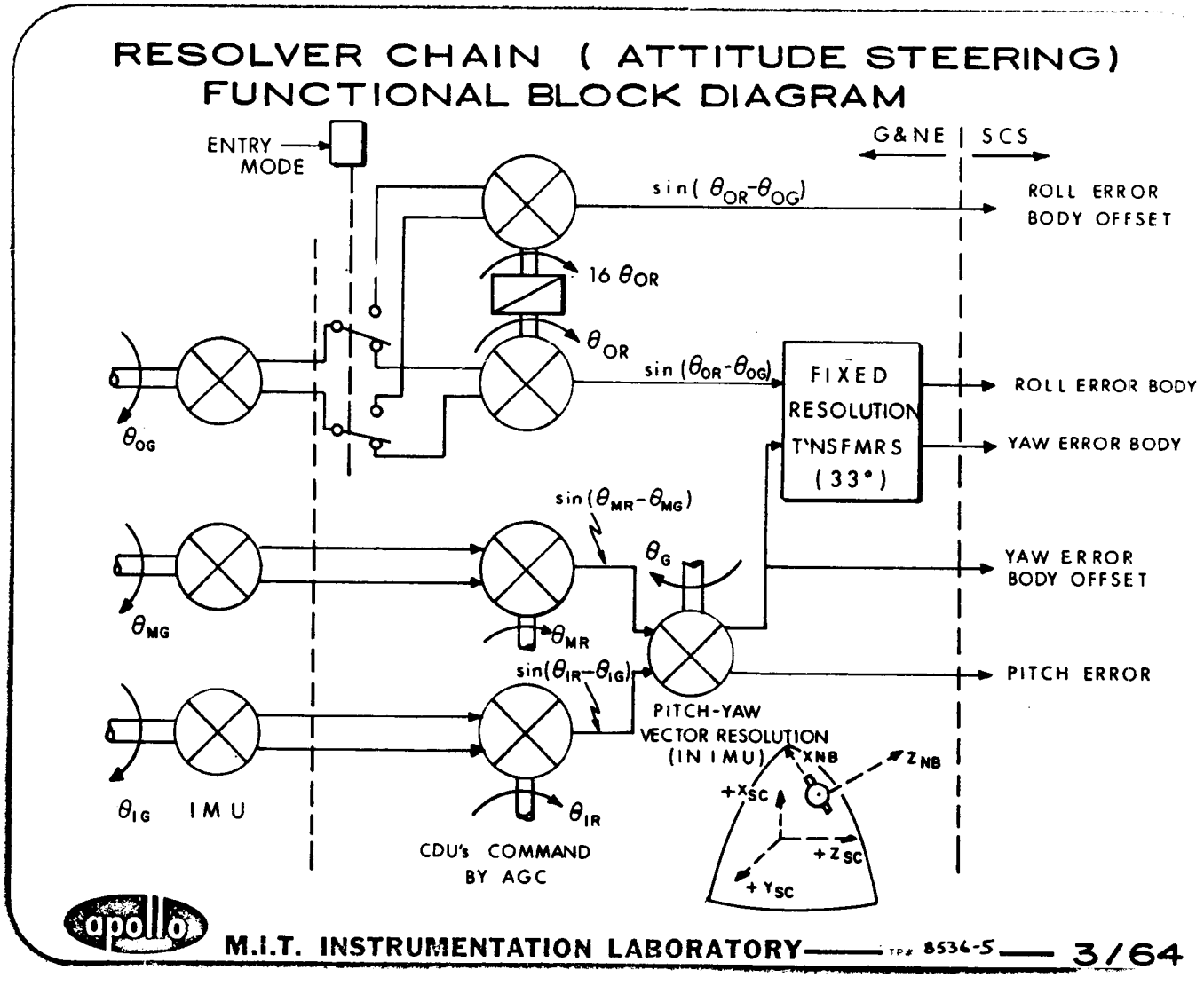
RESOLVER CHAIN (ATTITUDE STEERING)
FUNCTIONAL BLOCK DIAGRAM
ENTRY MODE
G&NE
SCS
sin(θOR-θOG)
ROLL ERROR BODY OFFSET
16 θOR
θOR
sin (θOR-θOG)
FIXED RESOLUTION T'NSFMRS (33°)
ROLL ERROR BODY
YAW ERROR BODY
θOG
sin (θMR-θMG)
θG
YAW ERROR BODY OFFSET
θMG
θMR
sin(θIR-θIG)
PITCH ERROR
PITCH-YAW VECTOR RESOLUTION (IN I MU)
XNB
ZNB
+XSC
+ZSC
+YSC
θIG IMU
θIR
CDU's COMMAND BY AGC
apollo
M.I.T. INSTRUMENTATION LABORATORY
TP# 8536-5
3/64

Fig. 5-5

INERTIAL SUBSYSTEM ASSEMBLY TEST PROCEDURE

(ISS/ATP # 1,015,947)

Class B Release, May 1963 for ISS # 4
Class A Release, January 1964 for ISS # 5 On

BROAD CATEGORY OF TESTS

OPERATIONAL

ALIGNMENT

CALIBRATION

Fig. 5-6

The results of some tests on ISS-5 are shown in Fig. 5-7. After about 700 hours of operation ISS-5 was subjected to a shake test of about 3-1/2 g's rms between 10 and 1000 cps to determine how much the orthogonality of the unit might shift. As shown in Fig. 5-7, the non-orthogonality remained well within specifications both before and after the shake test.

The zero-shift of the 16-speed resolvers due to shift and/or inspections is shown in Fig. 5-8. While the units were approximately within specifications before the shake and no special effort was taken to resolve this difference, it is questionable that the discrepancies after the shake were caused by the shake. The gimbal covers were removed after the shake to check for any loose parts or possible damage. It appears that the removal of the covers and reassembly might be the source of the shifts because this same effect was observed on another set of resolvers when subjected to inspection only and not to any shake. So there is less concern about the effects of the shake than there is about the possibility that the alignment measurements might have to be repeated if the gimbal covers are removed for inspection.

The PIPA scale factor stability is shown in Fig. 5-9. The nominal values are shown for each axis (X, Y, and Z) as well as the values before shake, after shake, and later as a factor of time, together with the departure of each from the nominal value. Effort is continuing to reduce these departures below the 1-sigma value of 100 parts per million.

The noncompensated bias drift (NBD) of the gyros in ISS-5 are shown in Fig. 5-10. The acceptance figures were taken in January 1964, the shake figures in February, and the last column figures are for March.

These inertial components, both the PIPA's and the gyros, are to be removed and returned to their respective test stations to attempt to repeat correlation between the subsystem test data, and the component test station data. After re-installation of the inertial components in IMU-5, the subsystem tests will be repeated.

QUANTITY	SPEC.	BEFORE SHAKE	AFTER SHAKE
OUTER TO MIDDLE GIMBAL NON-ORTHOGONALITY ($\mathbf{E}_{MGA}$)	±60"	-15" ± 5"	-11" ± 5"
MIDDLE TO INNER GIMBAL NON-ORTHOGONALITY ($\mathbf{E}_{IGA}$)	±60"	-13" ± 7"	-11" ± 7"

Fig. 5-7 Gimbal non-orthogonality (Seconds of Arc).

	SPEC.	BEFORE SHAKE	AFTER SHAKE
OUTER GIMBAL (E_{OGR})	±8"	+6" ± 8"	+56.4" ± 8"
MIDDLE GIMBAL (E_{MGR})	±7"	+27" ± 7"	-43" ± 7"
INNER GIMBAL (E_{IGR})	±4"	-4" ± 4"	-23" ± 4"

Fig. 5-8 16X Resolver zero shift due to shake and/or inspection (Second of Arc)

	X	Y	Z
NOMINAL	5.850,000	5.850,000	5.850,000
PRESHAKE (FEB.)	5.849,195 (-308 PPM)	5.849,292 (-121 PPM)	5.851,121 (+207 PPM)
POSTSHAKE (FEB.)	5.847,632 (-405 PPM)	5.849,219 (-134 PPM)	5.848,880 (-193 PPM)
MARCH	5.848,302 (-290 PPM)	5.849,698 (-52 PPM)	5.849,229 (-132 PPM)

Fig. 5-9 ISS #5 PIPA scale factor stability $\frac{\text{cm/sec}}{\text{pulse}}$.

HISTORY OF GYRO NONCOMPENSATED BIAS DRIFT (NBD) IN MERU

AXIS	GYRO	MFG.	ACCEPT	PRESHAKE	POSTSHAKE	MARCH
X	#69	MIT	+13	+13	+16	+11
Z	#73	MIT	+2	-6	-5	-3
Y	#1A10	ACSP	-4	+2	+1	+3

Fig. 5-10 Inertial subsystem (ISS) #5

Section 6

GIMBAL SERVOS, POWER SUPPLIES & IMU #3 DEMONSTRATION

M. Kramer

The function of Inertial Measurement Unit (IMU) #3 is to evaluate and optimize the electronic circuits that were designed to instrument the electro-mechanical components of the IMU; viz., the three platform servos, the AC and DC power supplies, and the failure indicator. A special test table, capable of driving the case of the IMU at a rate of up to 100 rpm around an axis perpendicular to the IMU outer axis, supports the case. The design-released circuits were packaged on plug-in boards to facilitate evaluation measurements and maintenance.

The circuits are interlocked so that the system comes on coarse-aligned while the Inertial Reference Integrating Gyro (IRIG) wheels are coming up to speed. In "coarse align" the gimbal orientations are controlled by command angles generated in manually operated Coupling and Display Units (CDU). When the wheels are up to approximately 80% of their synchronous speed, the system can be switched over to the "inertial reference" mode.

Absolute values and variation in wheel speed, temperature control, clock frequency and IRIG alignment are not critical for the evaluation of the servo loops since the precision and dynamic response of the servo system is measured as electrical signals and not as absolute space-referenced angles. The electronics themselves were designed to tolerate rather large variations in the above-mentioned parameters as well as to reject other environments; such as, DC supply variation, heat-sink temperature, vibration, etc.

In the "inertial reference" mode, the stable member is held fixed to its prealigned inertial coordinate system and the gimbals rotate to provide the geometric isolation of the stable member with respect to the case. Angular motion of the stable member is sensed by the IRIG's, amplified in the servo amplifier and drives the appropriate gimbal torque motor, which opposes the torque which initially disturbed the platform. Disturbing torques arise from gimbal bearing friction, gimbal mass unbalance, and reactions to angular acceleration which are a natural consequence of some gimbal orientations.

Very high angular spacecraft rates (50 rpm) can be tolerated when the gimbals are aligned mutually orthogonal. They are limited only by the back emf generated in the gimbal torque motors.

Maximum spacecraft rates for 80 degrees of middle gimbal angle are 60 degrees per second. To accommodate higher rates for this large gimbal angle it would be necessary to dissipate more power in the gimbal servo amplifier.

A new component, the ADA, is used to improve the gimbal servo response. It is essentially a "space tachometer" which is used in conjunction with the IRIG to provide data necessary to drive the gimbal torque motors. Its main feature is that it has a high signal-to-noise ratio for platform rate data over the frequency range where it is used and its sensitivity is independent of temperature. Using this component it is possible to design a broad-band servo loop with large gain margin.

The AC power supplies are run from local oscillators which in turn are synchronized, rather than triggered, from the AGC clock. Thus a loss or absence of the AGC will not result in complete inoperability of the IMU attitude reference capability. Should the AGC fail, it will retain all its dynamic capability with accurate frequency but will run merely with a reduced IRIG drift performance.

It is not the intent to allow all these various environmental disturbances to exist, but it is usually characteristic of a reliable system to be able to operate in spite of an unfavorable environment.

Section 7

PSA PACKAGING, INSTALLATION & MECHANICAL DESIGN

D. R. Test

The emphasis of this section will be in the area of the PSA mechanical design; where the PSA is in the spacecraft, and what effect the installation requirements and other interface constraints have on the final design. Since there are several good packaging techniques available and many new techniques possible, it is pertinent to note that the ground rules and Command Module interface are primarily responsible for the final mechanical design of the PSA. Changes in these ground rules will have significant effect on the Block II PSA installation and all other packaged electronics in the G&N.

The ground rules which have had primary influence on PSA mechanical design for Block I are:

(1) In-flight diagnosis and module replacement.

(2) C/M interface constraints.

(3) Existing components and techniques.

The effect of these constraints will be evident in the following discussion.

Figure 7-1 shows the Block I Power and Servo Assembly. The PSA is located on the structural shelf below the IMU, just above the Computer. The PSA consists of ten (10) removable trays, each containing a number of replaceable module assemblies. Each tray jacks into an end connector assembly. A wedge at the connector end and guide pins at the front end of each tray serve to locate the tray and cam the tray down on the NAA compressible thermal interface material while it is being jacked into place. The AGE harness is an integral part of the PSA End Connector Assembly. Each of the ten trays contains a test connector for pre-flight and in-flight test. Also, Tray 7 includes a connection for a portable temperature controller to maintain the IMU at temperature during the factory and field checkouts.

The PSA overall configuration, therefore, results from the in-flight diagnosis and replacement ground rule which requires test connectors on trays, and removable trays and modules. It also results from the C/M interface: the compressible thermal interface on the NAA coldplate, and the envelope available in the spacecraft. From the amount of electronics to be packed into the assigned installation volume, it was determined that two levels of modules were required in each tray.

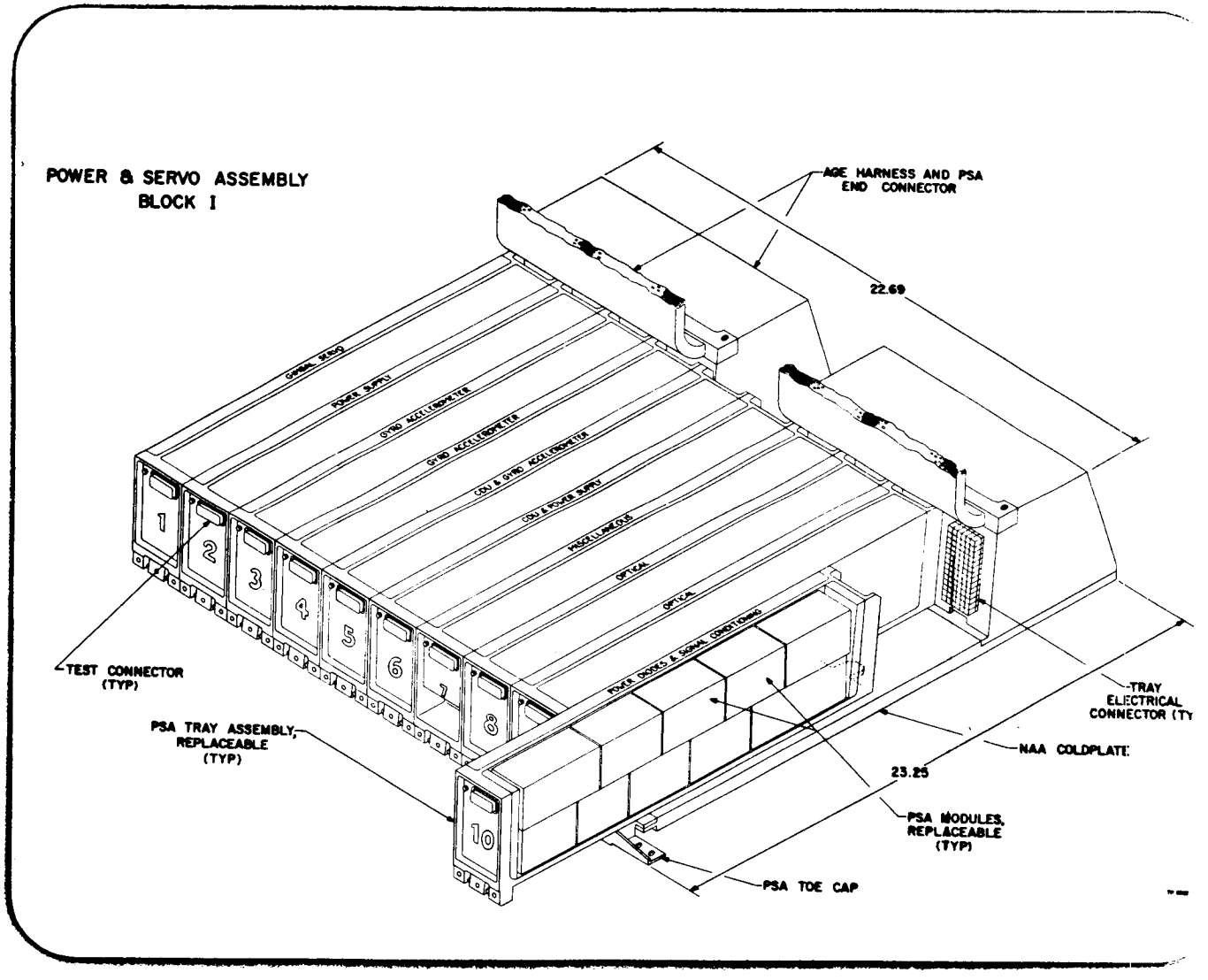
POWER & SERVO ASSEMBLY
BLOCK I
AGE HARNESS AND PSA
END CONNECTOR
22.69
TEST CONNECTOR
(TYP)
PSA TRAY ASSEMBLY,
REPLACEABLE
(TYP)
TRAY
ELECTRICAL
CONNECTOR (TY
NAA COLDPLATE
23.25
PSA MODULES,
REPLACEABLE
(TYP)
PSA TOE CAP
1
2
3
4
5
6
7
8
10

Fig. 7-1

The end connector in Fig. 7-2 is shown prior to attachment of the harness and final potting. It contains interwiring between trays and provides the major focal point of electrical signals to and from all G&N equipment above the PSA. The AGE Harness, which transmits these signals, in an integral part of the end connector, thus eliminating a removable connector interface. Two connectors at the base of the PSA attach to the Computer Harness Tray below the PSA. These connectors interface with the computer and with the spacecraft with the exception of power. The power cable is a pigtail from the end connector attaching to spacecraft connectors adjacent to the end connector.

Figure 7-3 is a rear view of the same end connector showing the interwiring between trays and the two terminal boards to which will be attached the AGE Harness. Interwiring will be accomplished by the "wire-wrap" technique proven in Polaris. This view shows the end connector before attachment of the harness.

Figure 7-4 shows the PSA tray configuration. Each tray contains a varying number of replaceable modules, each of standard height and width. Module mounting screws are captive in the tray frame, and act as jacking screws.

The tray is T-shaped. Heat is conducted to the coldplate down the vertical web and out along the base flange. Inter-module wiring is contained in the shallow, encapsulated volume on one side of the verticle web. The tray frames are magnesium to reduce weight, and they are nickel-plated to resist corrosion and to improve thermal conductivity.

Figure 7-5 shows a functional tray assembly for PSA-4 now on test. The modules have not been encapsulated. They would normally appear as solid blocks mounted on the tray. This is a typical tray. Intermodule harnesses are terminated at the tray connector at the end of the tray.

Figure 7-6 shows the configuration of the lowest replaceable unit, the module. The ground rule which specified existing components and techniques is reflected in the typical module design. Except for the fact that the module is replaceable, the design is similar to welded module assemblies used on Polaris: aluminum or magnesium heatsinks (depending on heat dissipation), tape-drilled to receive the component parts and connectors. Point-to-point welded interconnections are made on both sides of the module and foam potted. On Block I modules, test points were located on the surface opposite the mounting face.

For low heat dissipating modules, average weight densities may be reduced. The components are contained in a conventional cordwood arrangement between two fiberglass waferboards inside a metallic mounting frame, and foam potted.

PSA END CONNECTOR-FRONT VIEW
(SHOWN PRIOR TO ATTACHMENT OF AGE HARNESS)

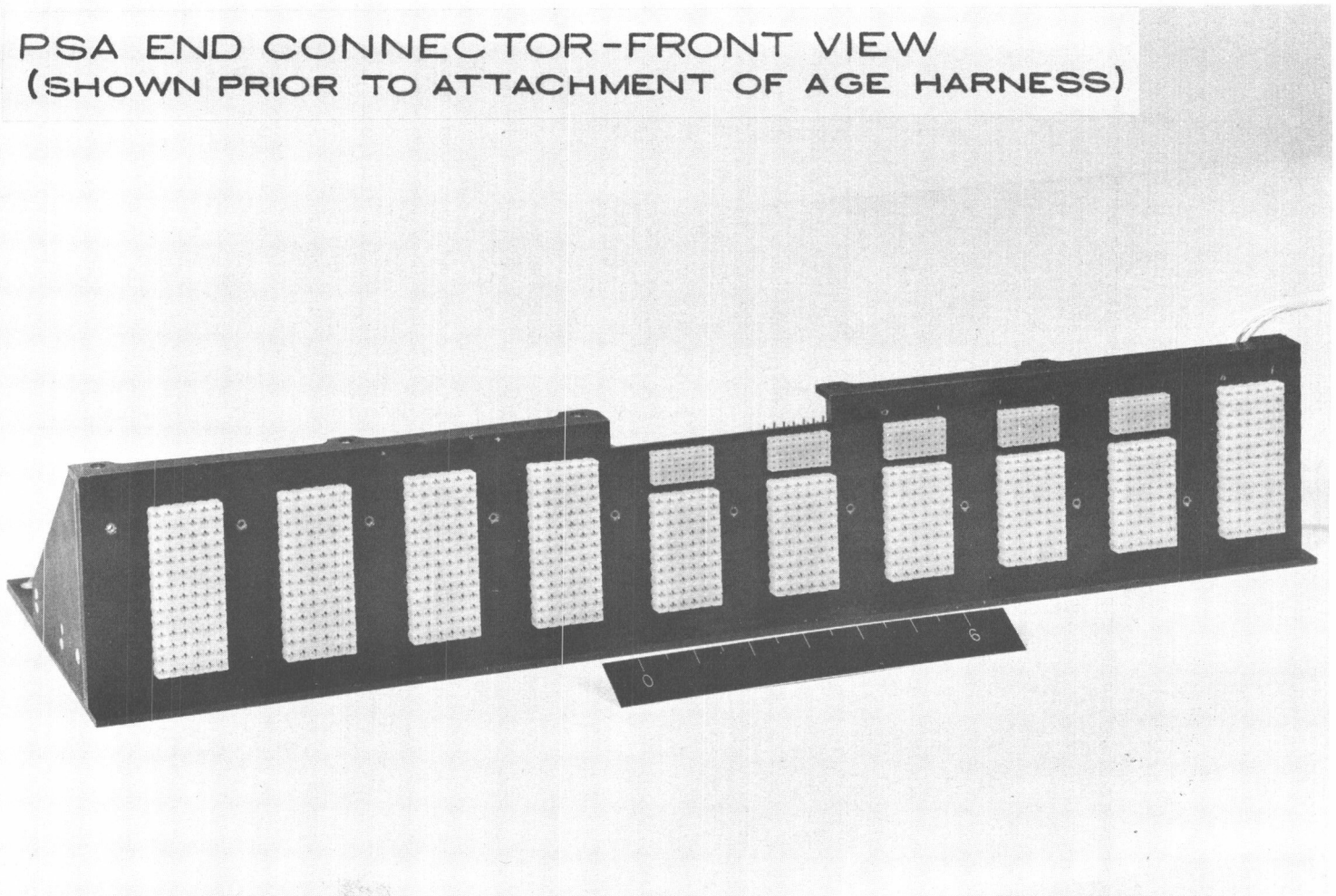

Fig. 7-2

PSA END CONNECTOR - REAR VIEW
(SHOWN PRIOR TO ATTACHMENT OF AGE HARNESS)

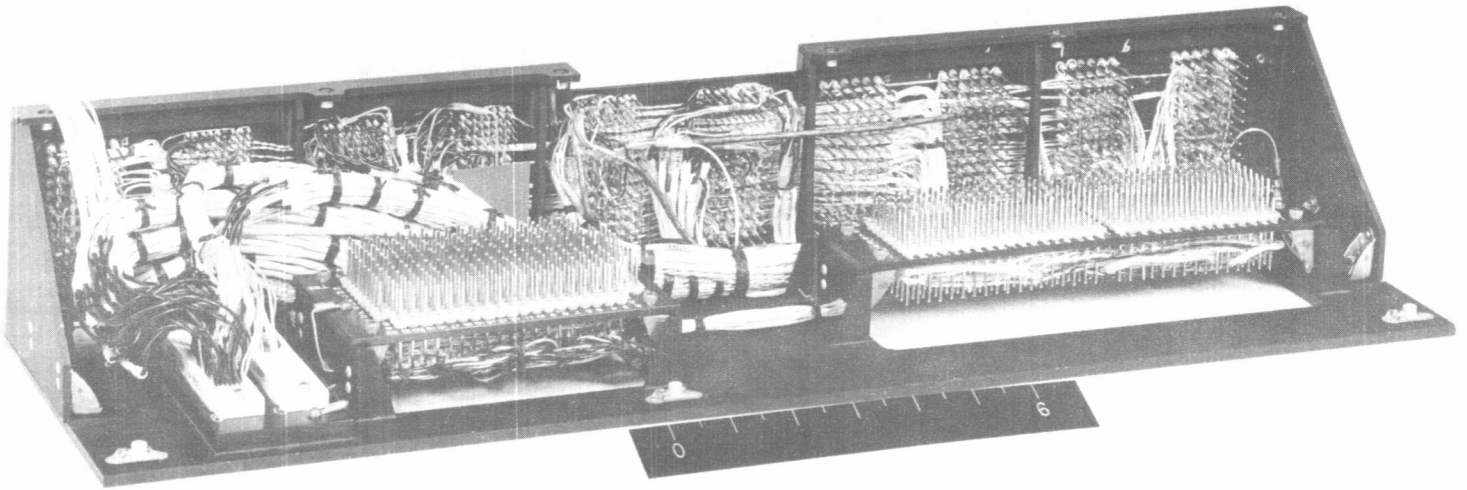

Fig. 7-3

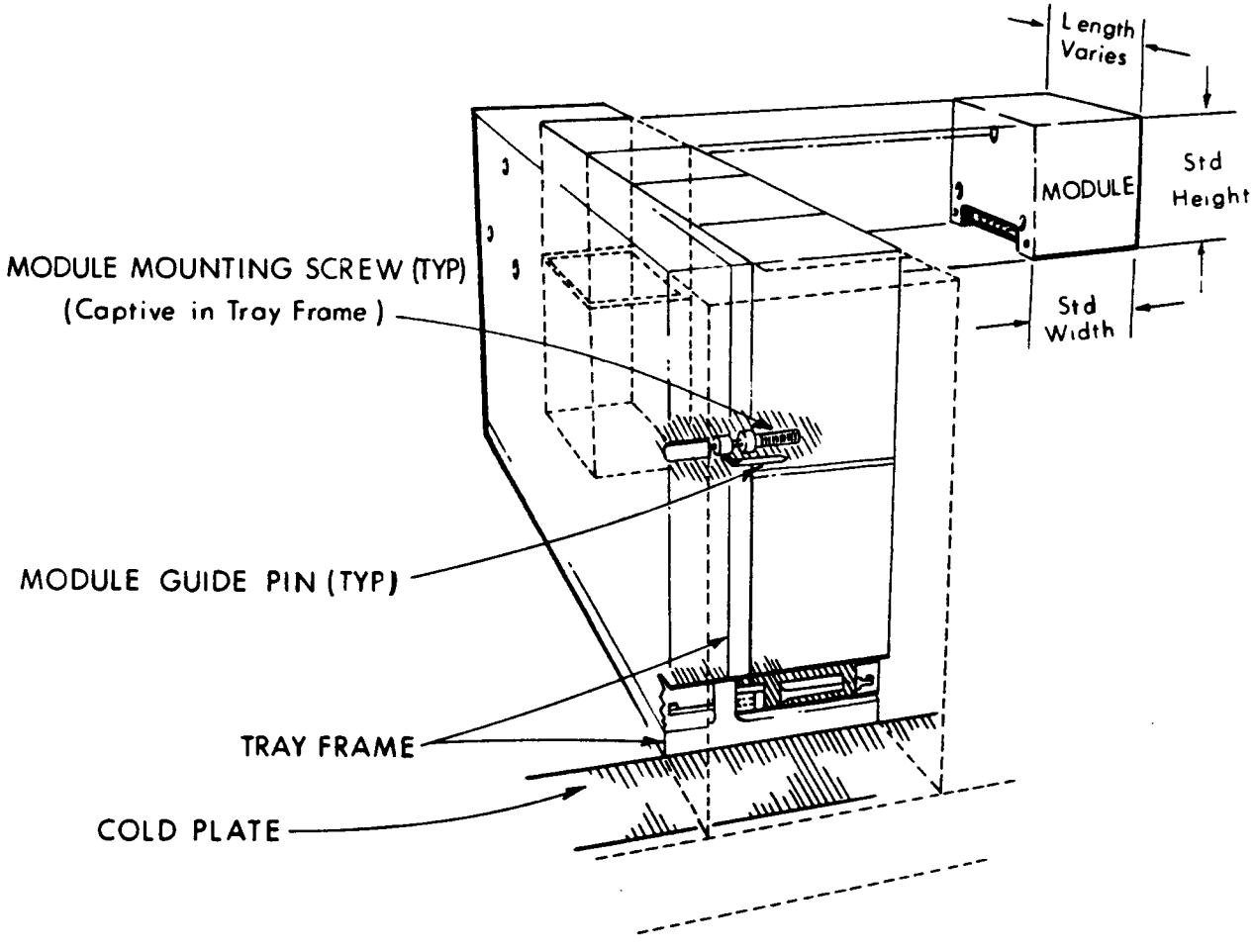

Fig. 7-4 PSA tray configuration.

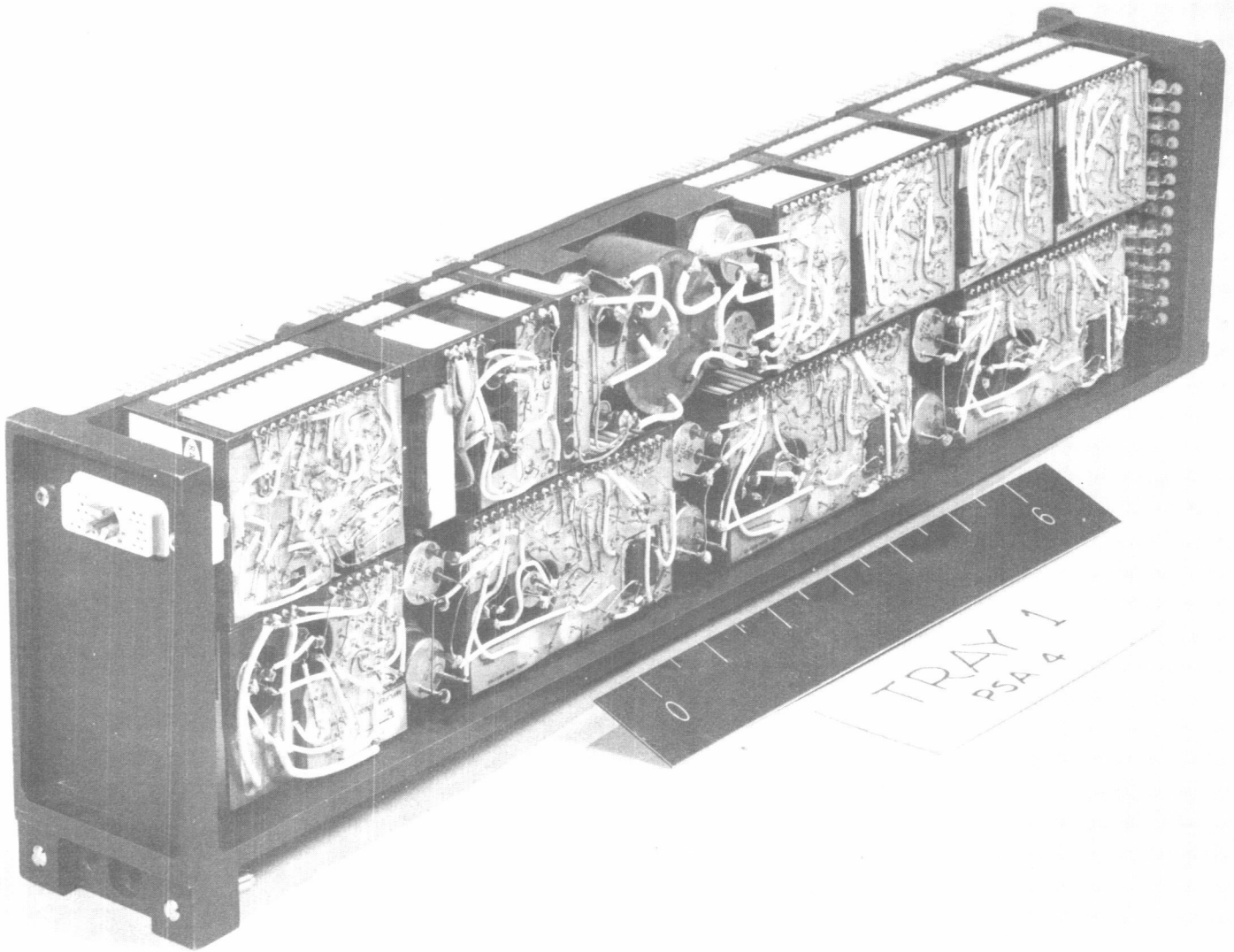

Fig. 7-5

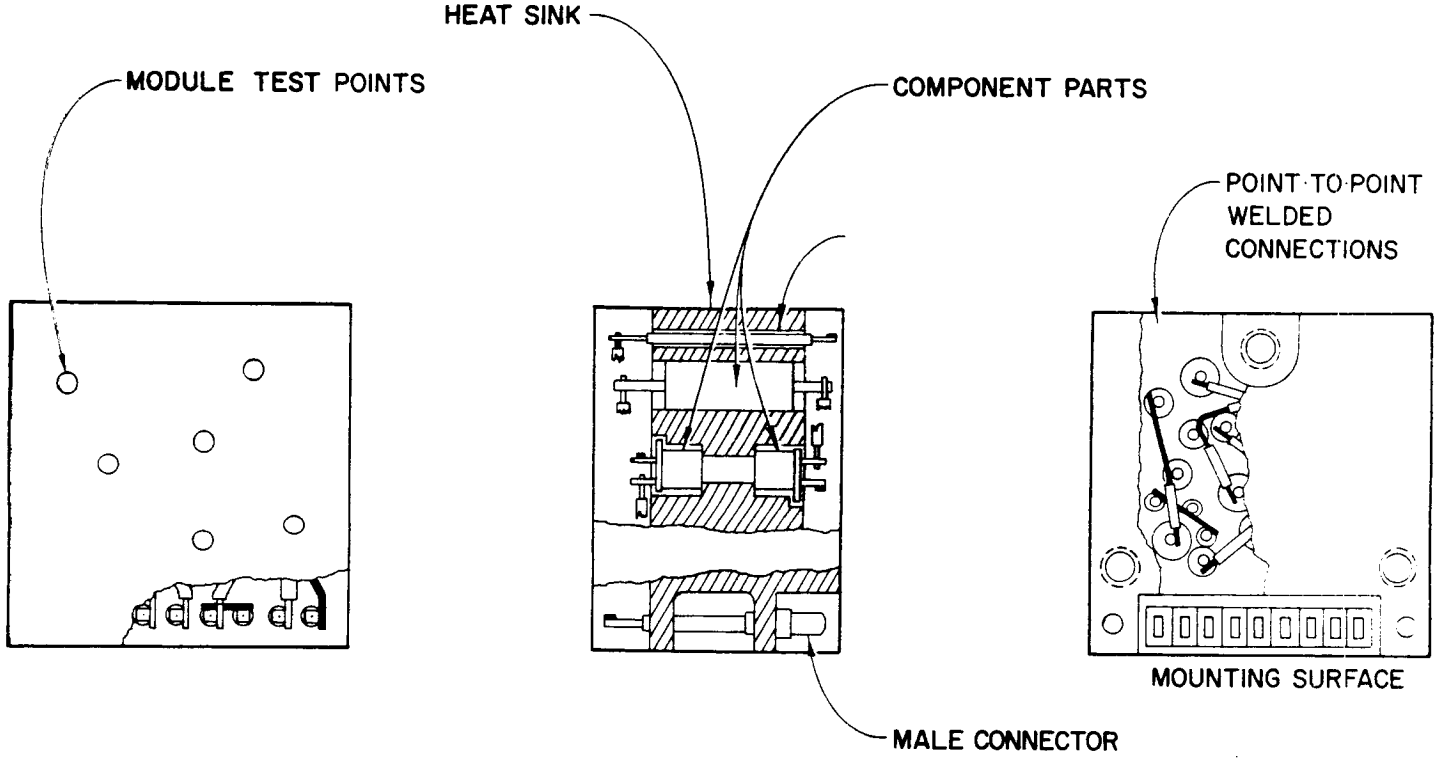

Fig. 7-6 PSA module configuration.

Figure 7-7 shows a typical heatsink type of module. The actual, unpotted module is shown in the background. A plexiglass model of the same module is in the foreground, showing component orientation and interwiring. Two, three, or four screws in the tray frame hold the module in place.

The chart in Fig. 7-8 shows those considerations from which module size is derived:

1. Function
2. Reliability
3. Serviceability
4. Producibility

The only point to be made here is that the trade-offs are not difficult. There are not a large number of choices. Block I experience indicates that the functional circuit, as breadboarded and drawn as a schematic by the circuit designers, is almost always the best compromise. Normally, package design has affected the initial schematic only when module size was too small. In those instances, several circuits were combined to create a module of reasonable size.

With regard to PSA design status, all drawings are released including SCD's for the component parts. Release of the final test methods and procurement specifications for PSA modules are almost complete.

The largest mechanical problem has been the thermal interface with the NAA cold plate. In order to achieve the design value for conductivity across the thermal interface, the compressive forces of the trays on the NAA interface material are much larger than originally anticipated. This causes bowing of the trays and toe cap, thereby reducing conductivity across local areas on the interface. Discussion are proceeding with NAA to resolve the problem.

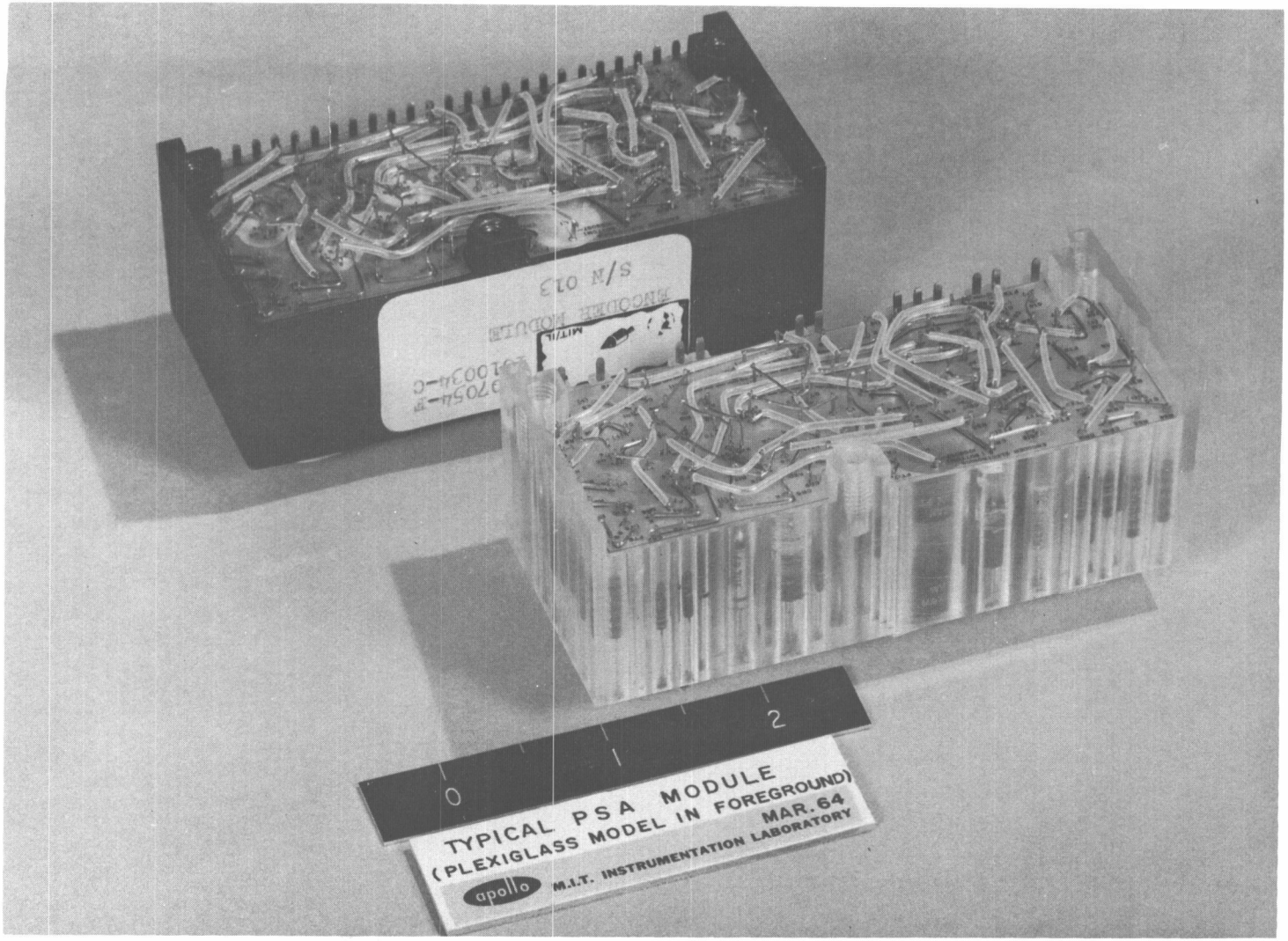
0
2
TYPICAL PSA MODULE
(PLEXIGLASS MODEL IN FOREGROUND)
MAR. 64
apollo
M.I.T. INSTRUMENTATION LABORATORY

Fig. 7-7

1.	FUNCTION:	CIRCUIT INTEGRITY
		MAXIMUM CAPABILITY FOR INDEPENDENT CHECKOUT & TRIM ADJUSTMENT
2.	RELIABILITY:	MINIMUM INTER-MODULE CONNECTIONS
3.	SERVICEABILITY:	SIMPLICITY OF MALFUNCTION DETECTION
		MINIMUM NUMBER OF MODULES CONSISTANT WITH MAXIMUM INTERCHANGEABILITY OF MODULES, I.E. MINIMUM WEIGHT OF SPARES
4.	PRODUCIBILITY:	MINIMUM COST FROM IN-PROCESS REJECTION OF MODULES
		EASY INCORPORATION OF CHANGES
		SIMPLICITY OF RETROFIT
		EASY HANDLING

Fig. 7-8 Module size considerations.

Section 8

G&N THERMAL INTERFACE WITH SPACECRAFT AND IMU TEMPERATURE CONTROL SYSTEM

E. S. Hickey

I. G&N Thermal Interface with Spacecraft

The thermal interface with North American Aviation (NAA) has been negotiated and is about 90% completed. Results of this negotiation appear on Thermal ICD (Interface Control Document) No. MH01-01049-416. G&N equipment cooling is achieved by three methods: direct contact with an ethylene-glycol coolant, indirect contact with the coolant via a NAA supplied coldplate and metallic conduction to the secondary structure. The Navigation Base Assembly (NBA) which contains the Inertial Measurement Unit (IMU) and the Optical Base Assembly (OBA) contains plumbing which terminates in two quick disconnect coupling halfs mating with matching halfs on NAA plumbing. The Power and Servo Assembly (PSA), Apollo Guidance Computer (AGC) and the Coupling and Data Unit Junction Box (CDUJB) are mounted on NAA coldplates utilizing grease as a thermal interface material. The rest of the equipment is cooled by conduction to its mounting structure. All equipment must be capable of operating at nominal ambient conditions of $75^{\circ}F \pm 5^{\circ}F$ with a gas pressure of 5 psia. Under emergency conditions the equipment is subjected to an ambient pressure of 10^{-4} mm Hg and structure temperature variations from 0 to $160^{\circ}F$.

Figure 8-1 represents the CM glycol-water coolant loop; 200 lbs/hr of coolant at approximately $45^{\circ}F$ comes from the water boiler, 167 lbs/hr is circulated through the suit circuit, cabin heat exchanger and another coldplate while the remainder of 33 lbs/hr is circulated through a parallel branch which contains the NBA and CDU's. These parallel loops are joined together after the CDU's whereupon it is piped through the AGC, PSA, and one other coldplate in parallel and proportioned according to heat load. The discharge from these coldplates goes to 15 other coldplates in a series parallel arrangement.

The most serious problem in the thermal interface area is that of NAA's thermal interface material. A photograph of this material is shown in Figure 8-2. It consists of silicone tubing approximately 0.160 inch in diameter with a helix of copper foil 0.002 inch thick wrapped on the individual tubes. These tubes are all soldered to a copper base plate. The idea is that the equipment will contact this tubing and compress it approximately 0.025 inch in order to yeild a conductance of 100 BTU's/hr-ft^2-$^{\circ}$F.

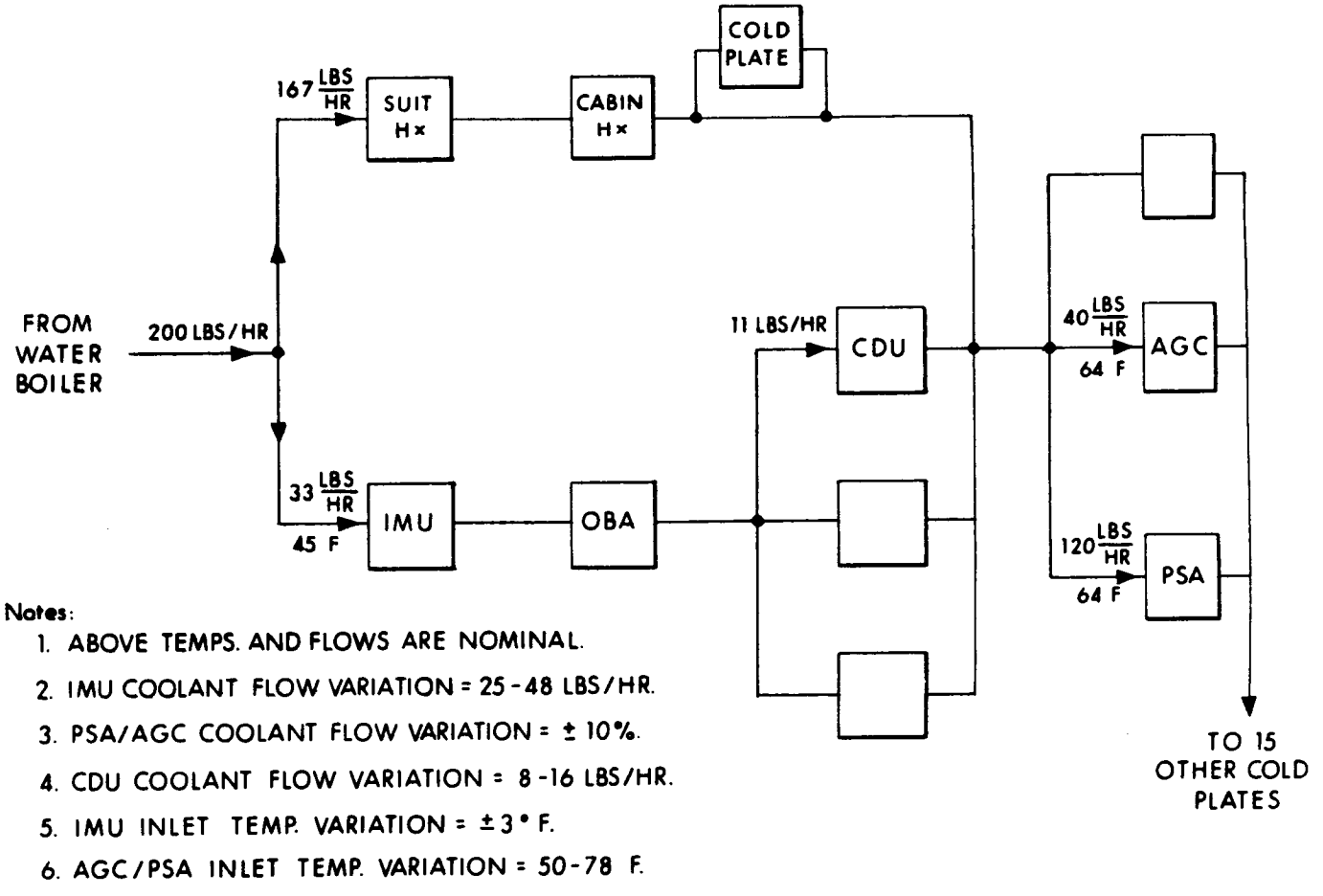

Fig. 8-1 Command module ECS glycol-water coolant flow diagram

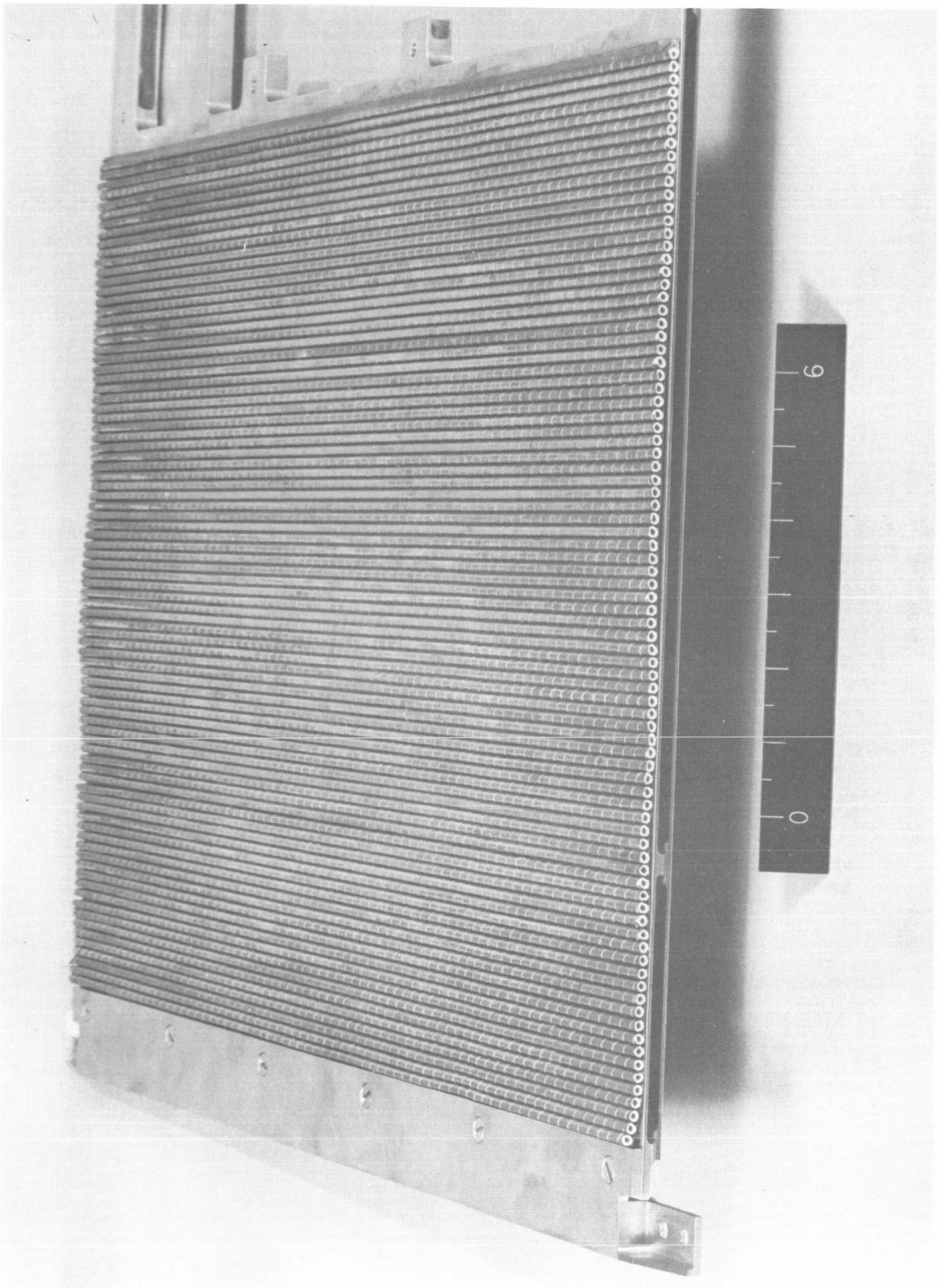

Fig. 8-2

NAA's original design goal was to achieve a conductance of 100 with a compressive force on the interface material of 1 psi. NAA further stated that for design purposes MIT/IL should assume a max. pressure to achieve this conductance would be 2 psi. A test program was recently initiated at MIT/IL to evaluate this thermal interface material. These tests yielded the following results: It takes approximately 14.5 psi to compress the thermal interface material 0.025 inch, and the thermal conductance with a compressive force of 10 psi is 100 at 1 atm pressure. NAA has recently revised their design goal of a conductance of 100 at 1 psi to a conductance of 100 at 10 psi. Figure 8-3 is a plot of conductance vs. pressure. The NAA Process Specification indicates that a conductance of 125 should be measured at 1 atmospheric pressure in order to realize a conductance of 100 at a cabin pressure of 10^{-4} mm Hg. Figure 8-4 plots the compressive force vs. deflection of the interface material. NAA's new design point of 10 psi is indicated, and results show that a compressive force of 14.5 psi is required. This excessive pressure bows the frames in the AGC and both the frames and the toeplate in the PSA. In the case of the PSA this excessive toeplate bowing results in frame contact with the interface material for only about two-thirds of its length.

Another problem in this area is the maximum temperature requirements at the thermal interface. This interface is defined by a thermal map indicating local heat flux and upper temperature limits in these local areas. NAA has been having difficulty meeting these temperature requirements even with the assumption of a conductance of 100 through the interface material and nominal coldplate inlet temperatures and flow rates. These temperature requirements are presently exceeded in some areas by as much as 20°F.

II. IMU Temperature Control

The IMU temperature control ground rules for Block I are listed in Figure 8-5.

There are two significant differences between the Apollo IMU Temperature Control System and other gimbal assembly temperature control systems. These are that the six inertial components are temperature-controlled utilizing one controller and that the thermal resistance from the stable member to the case is a controlled variable via blower speed. The latter technique greatly extends the operating range and conserves temperature control power.

Figure 8-6 shows the IMU Temperature Control System Block Diagram. There are basically three temperature control systems: primary, backup and emergency. The primary system senses and controls the Inertial Reference Integrating Gyro (IRIG) end mount temperature via a proportional controller and inertial component heaters, and indirect control of the blower speed is achieved by sensing the heater current and varying the blower voltage as an inverse function of it. Additional protection is achieved via

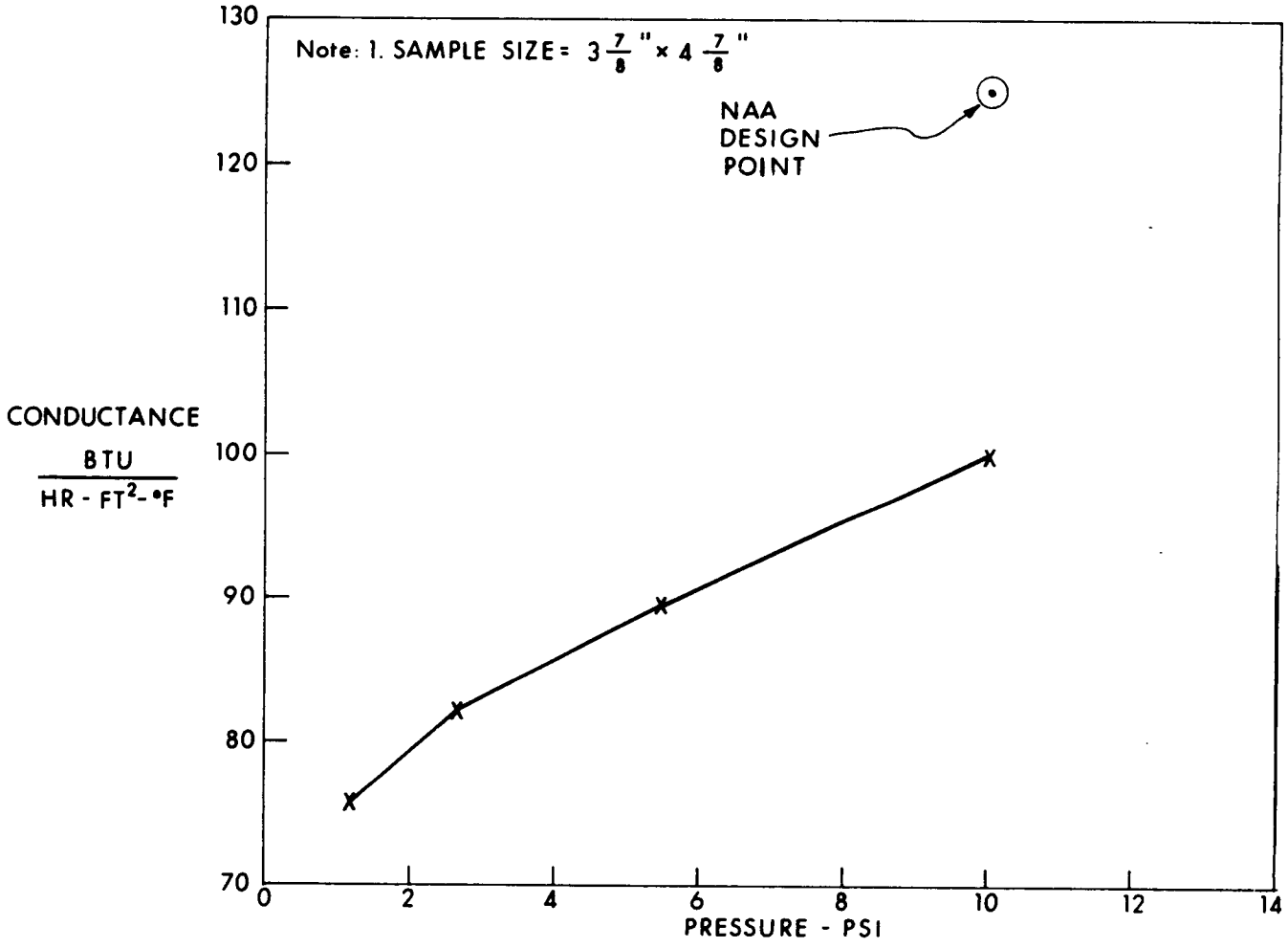

Fig. 8-3 NAA thermal interface material-conductance vs. pressure at 1 atmosphere

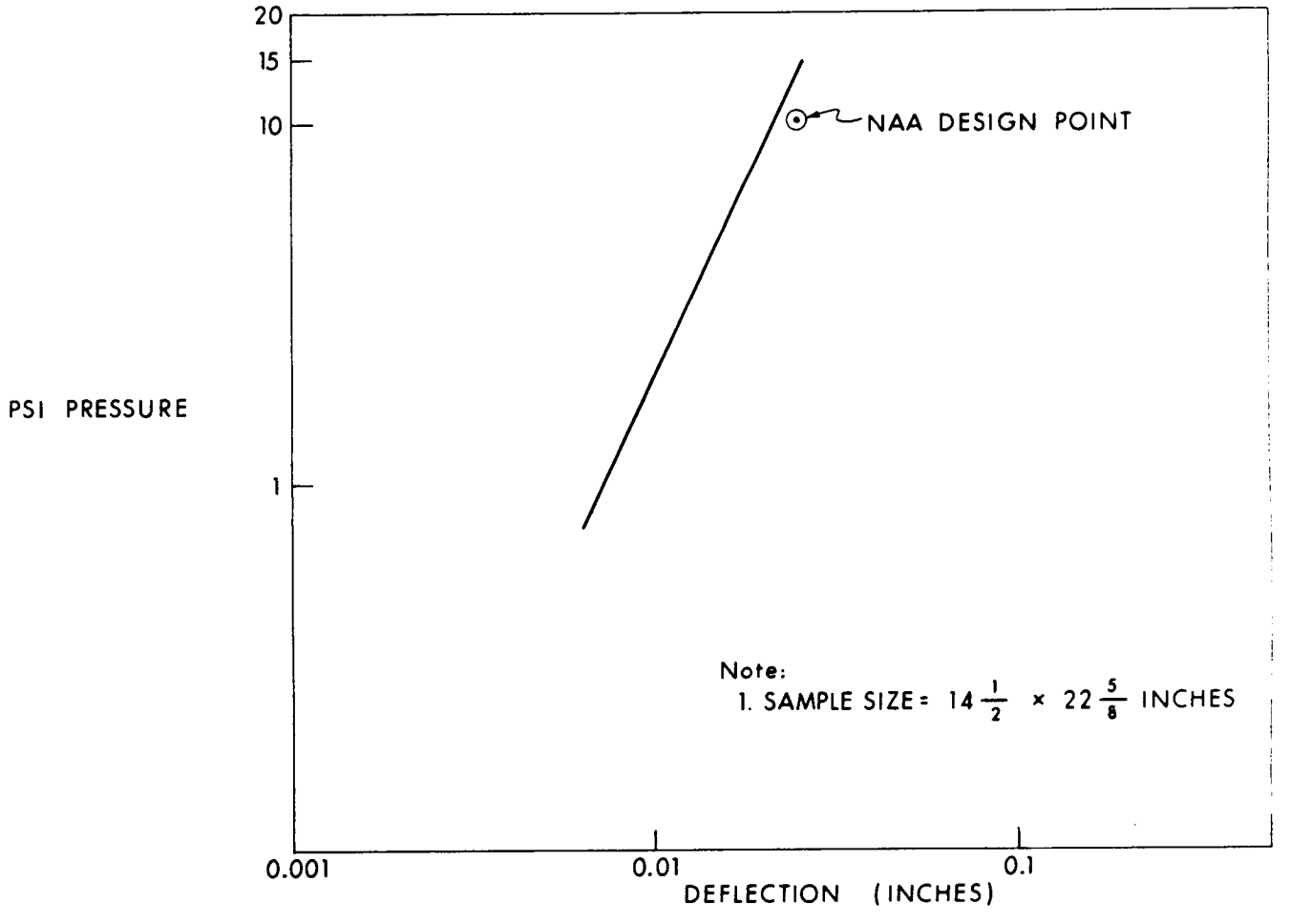

Fig. 8-4 NAA thermal interface material-compressive force vs. deflection of material.

1. INERTIAL COMPONENT TEMP. CONTROL SPECS

   a. IRIG ABSOLUTE TEMP. = 135° F ± 1° F

   b. PIP ABSOLUTE TEMP. = 130° F ± 1° F

   c. MAX. TEMP. DEVIATION = 0.5° F

   d. STANDBY TO OPERATE CONDITIONS IN 15 MINUTES.

2. DESIGN TO BE CAPABLE OF HANDLING IRIG WHEEL POWER FROM 3 TO 15 PSIA.

3. AIR PRESSURE VARIATIONS FROM 3 TO 15 PSIA.

4. AMBIENT AND STRUCTURE TEMPERATURE VARIATIONS FROM 0° F TO 160° F.

5. MINIMIZE TEMPERATURE CONTROL POWER.

Fig. 8-5 Block I IMU thermal design ground rules.

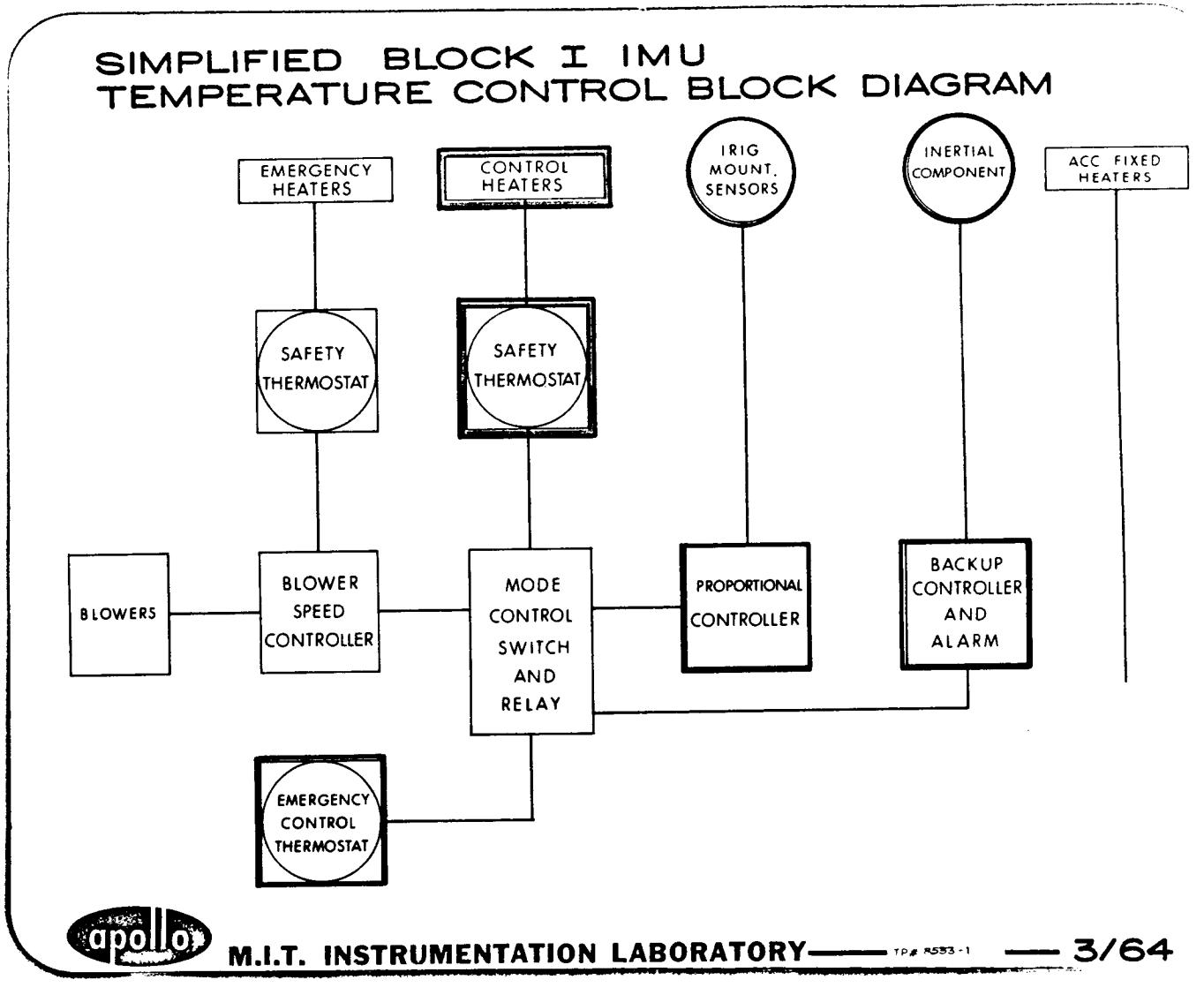
SIMPLIFIED BLOCK I IMU
TEMPERATURE CONTROL BLOCK DIAGRAM
EMERGENCY HEATERS
CONTROL HEATERS
IRIG MOUNT. SENSORS
INERTIAL COMPONENT
ACC FIXED HEATERS
SAFETY THERMOSTAT
SAFETY THERMOSTAT
BLOWERS
BLOWER SPEED CONTROLLER
MODE CONTROL SWITCH AND RELAY
PROPORTIONAL CONTROLLER
BACKUP CONTROLLER AND ALARM
EMERGENCY CONTROL THERMOSTAT
apollo
M.I.T. INSTRUMENTATION LABORATORY
TP# R583-1
3/64

Fig. 8-6

high temperature safety thermostats in the heater circuits. Backup operation is achieved by utilizing the monitor circuits and limit cycling the inertial components over a narrow temperature band. This backup system protects against any failure in the primary system except for heaters or blowers. The emergency system consists of mercury in glass thermostat mounted on the stable member which functions as both a temperature sensor and controller.

Figure 8-7 contains a thermal diagram of the IMU. Heat transfer is achieved from the stable member to the middle gimbal via gas and metallic conduction with some natural convection existing during ground operation. (Heat is transferred from the middle gimbal to the water-glycol cooled case via a closed loop air circuit.) The thermal resistance from the middle gimbal to the case is a function of the blower speed and internal gas pressure.

Figure 8-8 is an electrical analog representation of the thermal system. This analog indicates the fixed and variable heat sources together with the fixed and variable thermal resistances. It is interesting to note that the thermal coupling with the structure, ambient and coolant can be represented by three parallel resistors. Test data to date indicates that the accuracy of this simplification is extremely good.

Figures 8-9 through 8-12 are the results of thermal tests on IMU No. 4. These results are indicative of the type of performance to be expected from the three temperature control systems.

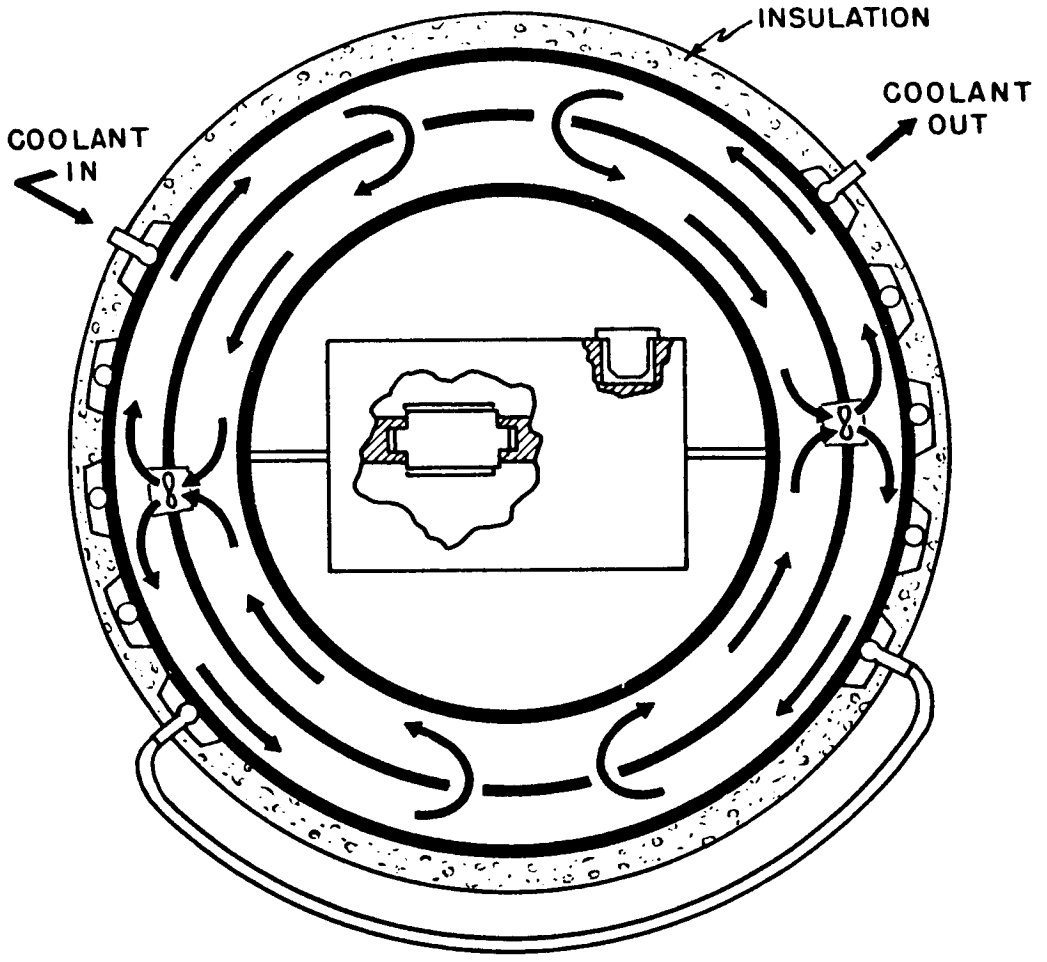

Fig. 8-7 IMU heat transfer diagram.

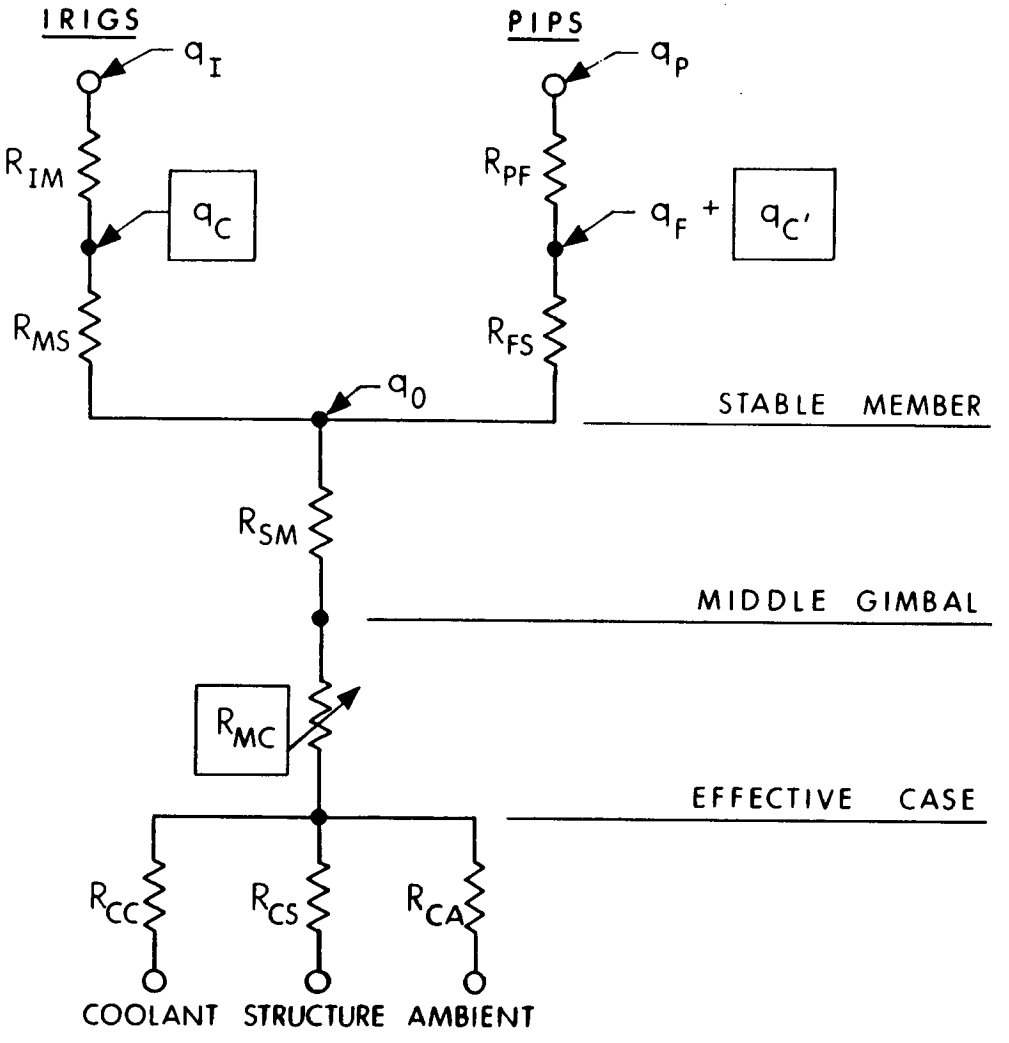

Fig. 8-8 Simplified IMU heat transfer analog.

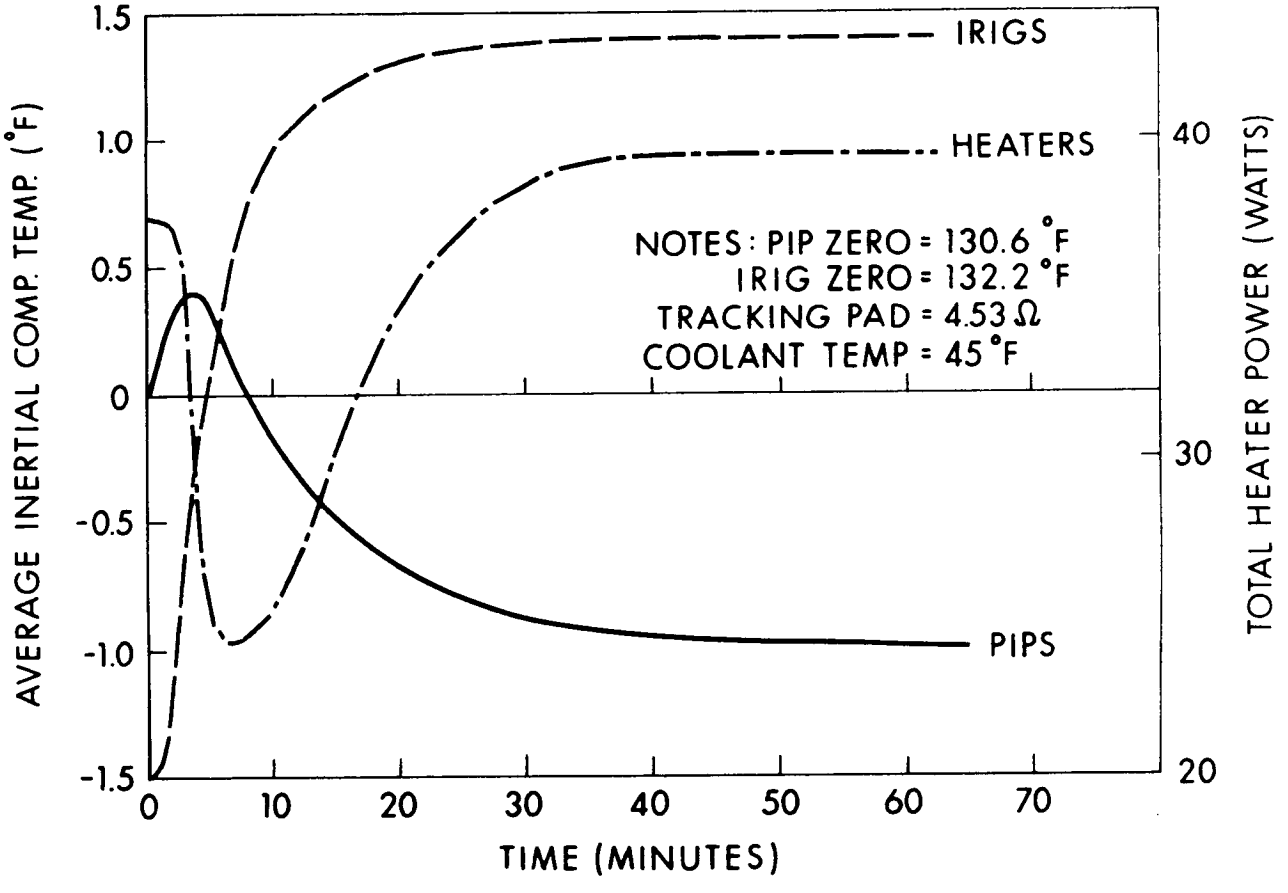

Fig. 8-9 IMU #4 Standby to operate test proportional mode.

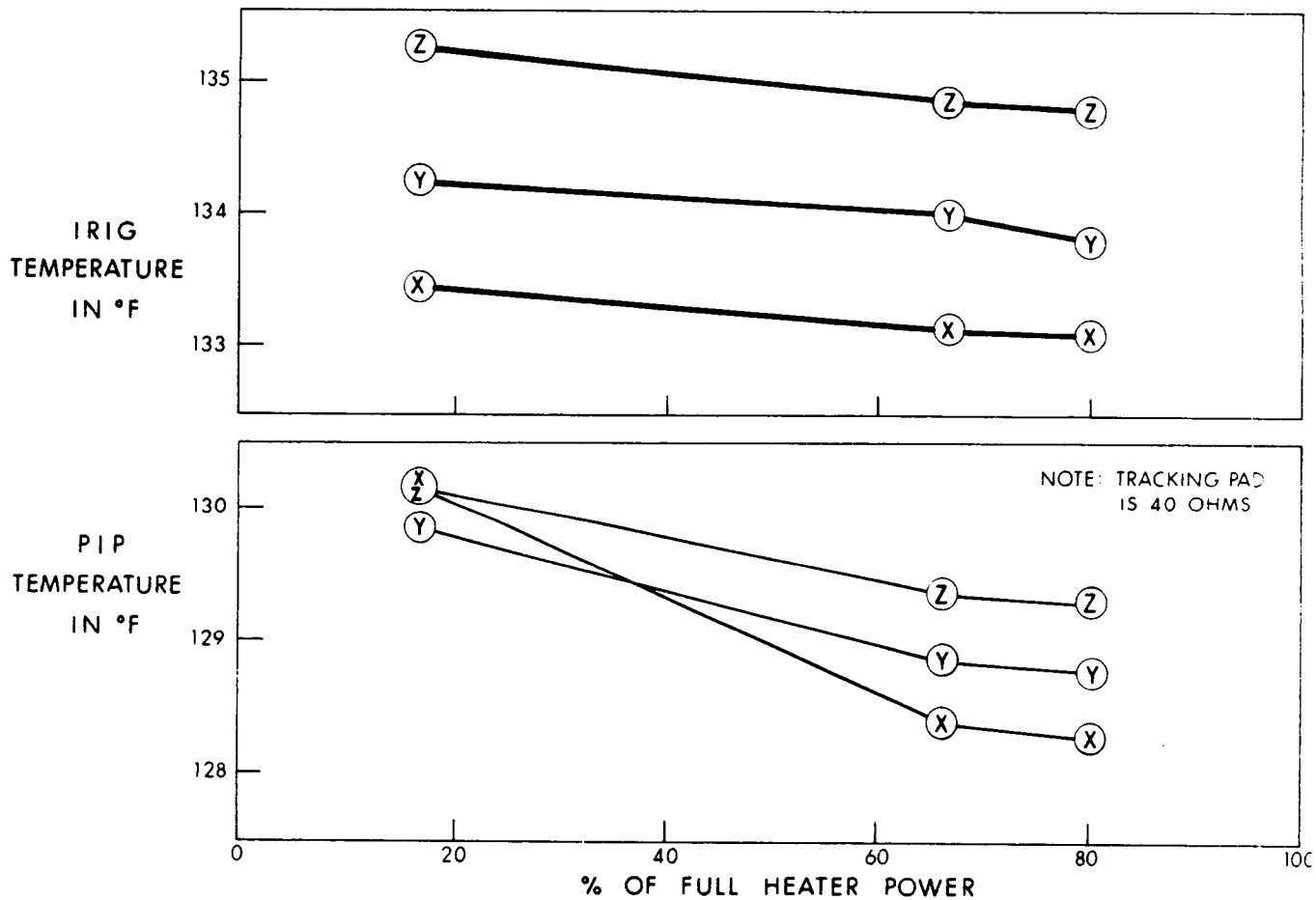

Fig. 8-10 IMU #4 Inertial component temperature vs. heater power.

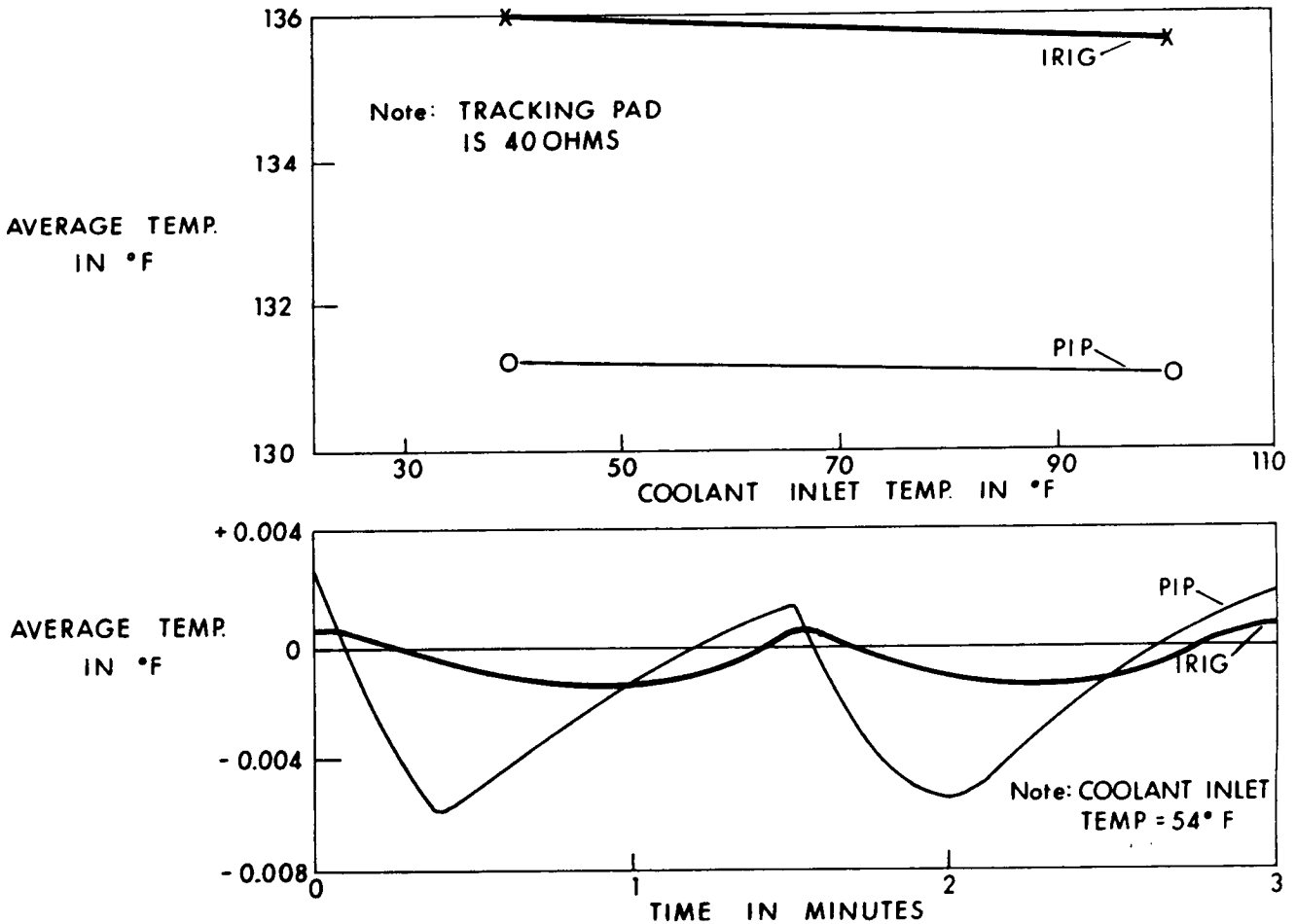

Fig. 8-11 IMU #4 Emergency temperature control system characteristics

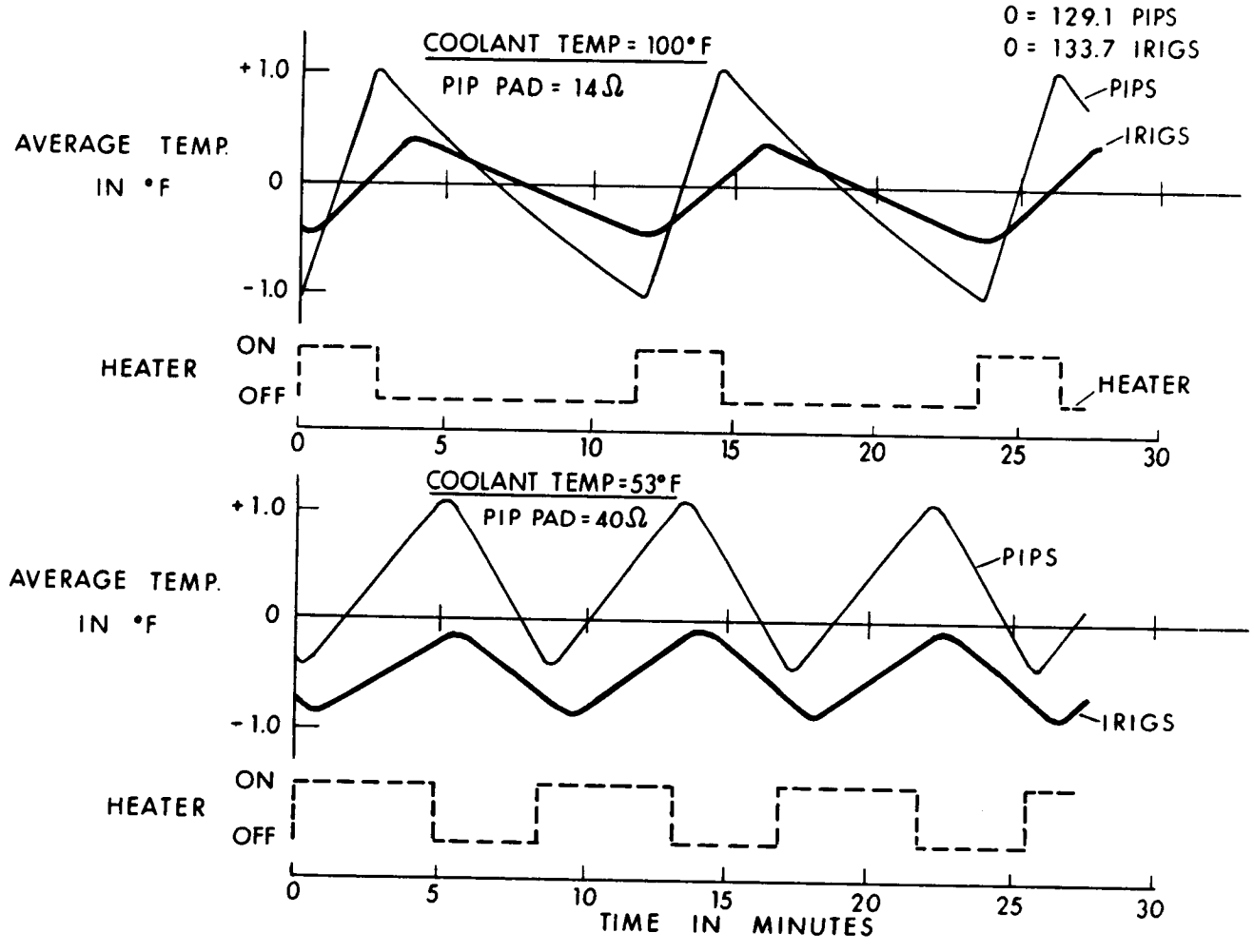

Fig. 8-12 IMU #4 Backup temperature control system characteristics

Section 9

APOLLO GUIDANCE COMPUTER (AGC) - MECHANICAL DESIGN

E. J. Duggan

The Block I computer reflects the design ground rules established for this unit early in this program. The ground rules were that (1) there would be a single operating AGC on-board the command module and (2) this single AGC could experience in-flight repair necessitating; (a) rapid fault isolation to module level, (b) accessable-on-board-spare modules, and (c) ability to change module during emergency conditions (in pressurized suit).

Figure 9-1 shows the Block I AGC-C/M configuration which weighs 70 lbs exclusive of harness. It occupies 0.8 cu. ft. and consumes 100 watts of power. It is located in the C/M directly below PSA in a double bay opening 7-1/2 x 20 inches.

Finalization of the Block I design has demonstrated the feasibility of carrying a full spare computer in tray form mounted in the space originally negotiated with NAA for a single AGC.

This fact, coupled with the complexity and time involved in fault isolation to the module level, subsequently resulted in the concept of tray replacement as the lowest level of in-flight repair.

NASA has recently directed that a single AGC be flown in Block I, and we are configuring accordingly. A bay close-out panel will be provided.

The astronaut interface with the AGC is through the Display and Keyboard Assembly (Fig. 9-2). Two such units each weighing about 22 lbs appear as peripheral to the computer. The electronic modules for each are identical; however, their arrangement is altered to fit either the lower equipment bay or the main panel shown here.

The basic computer is functionally separated into two active units, the dual tray. Tray A contains the logic and interface segments and Tray B contains the fixed and erasable memory, the oscillator, and power supplies. Intra-tray information transfer is accomplished by use of an end connector assembly which is hard mounted to the cold plate.

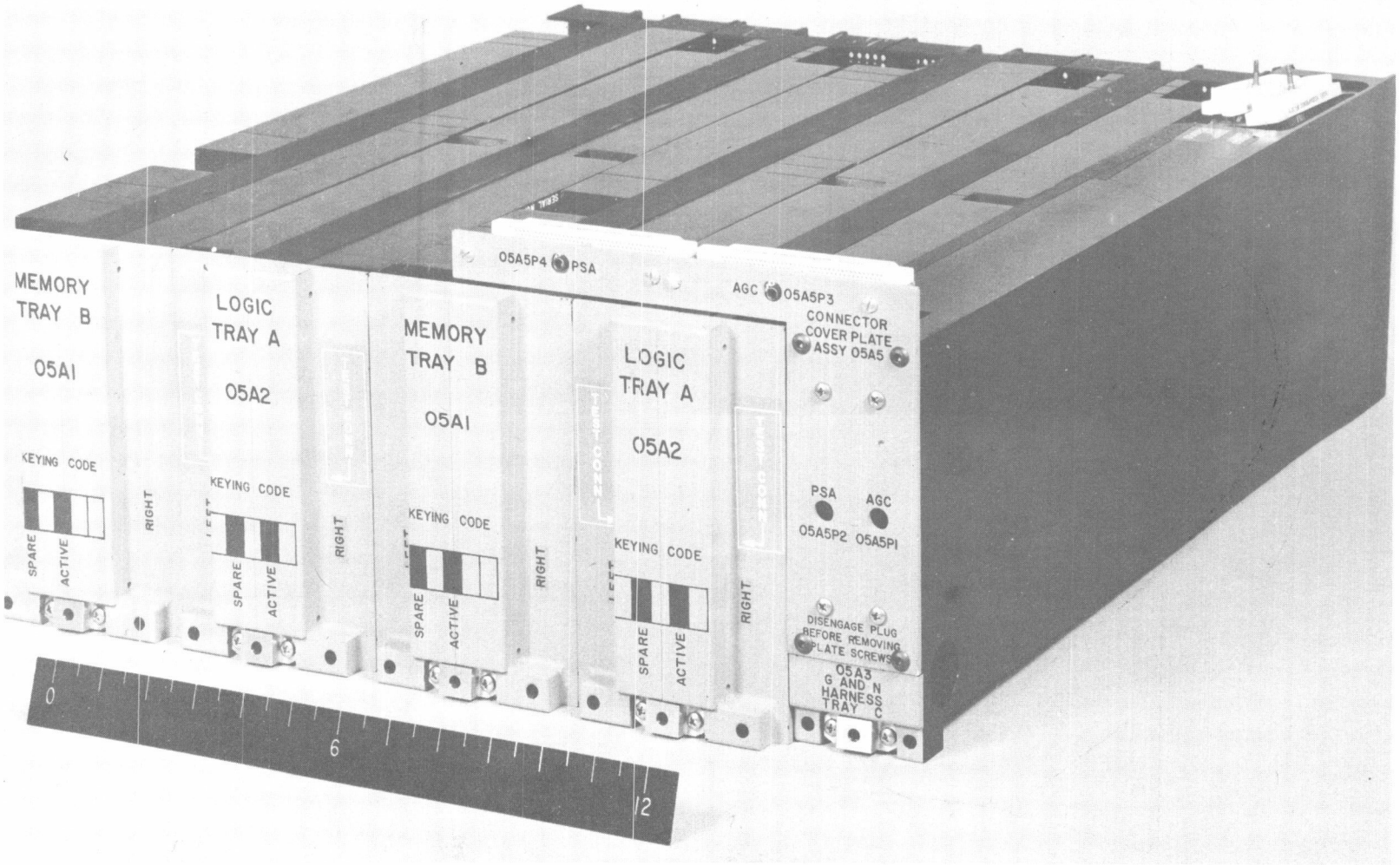
MEMORY
TRAY B
05A1
KEYING CODE
SPARE
ACTIVE
RIGHT
LOGIC
TRAY A
05A2
KEYING CODE
SPARE
ACTIVE
RIGHT
MEMORY
TRAY B
05A1
KEYING CODE
SPARE
ACTIVE
RIGHT
LOGIC
TRAY A
05A2
KEYING CODE
SPARE
ACTIVE
RIGHT
05A5P4 PSA
AGC 05A5P3
CONNECTOR
COVER PLATE
ASSY 05A5
PSA
AGC
05A5P2 05A5P1
DISENGAGE PLUG
BEFORE REMOVING
PLATE SCREWS
05A3
G AND N
HARNESS
TRAY C
0
6
12

Fig. 9-1 AGC 5A.

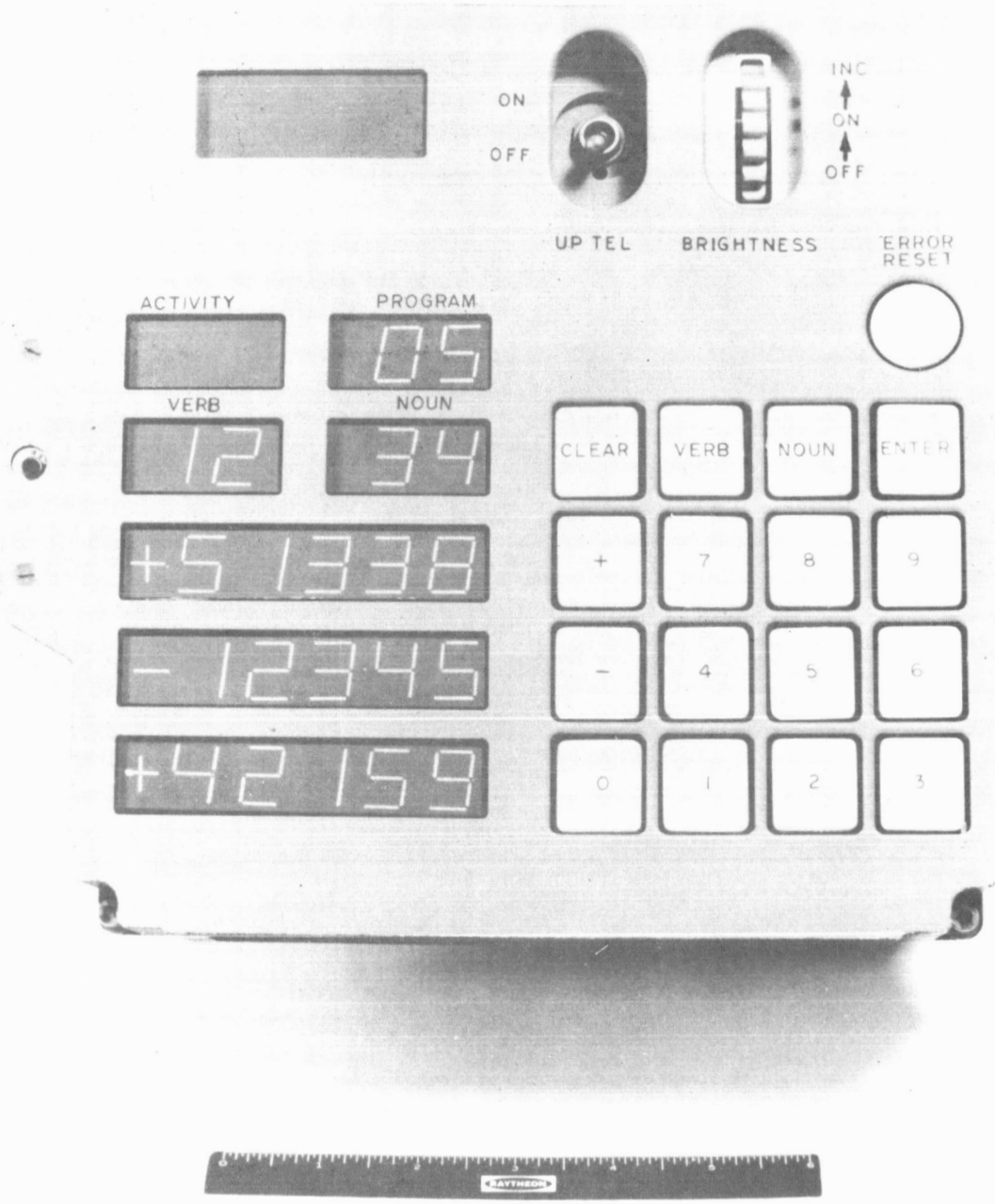
ON
OFF
INC
ON
OFF
UP TEL
BRIGHTNESS
ERROR RESET
ACTIVITY
PROGRAM
05
VERB
NOUN
12
34
+51338
-12345
+42159
CLEAR
VERB
NOUN
ENTER
+
7
8
9
-
4
5
6
0
1
2
3

Fig. 9-2

Tray C while not actually an AGC component, also plugs into the end connector at the rear and distributes signals to and from the computer to the spacecraft (S/C) and PSA. All other G&N signals that interface with the S/C are combined and routed in this assembly to the front connector.

The power dissipated within the computer is routed thermally via the tray frame assembly to thermal interface material atop a S/C cold plate. This is a water glycol heat exchanger upon which is mounted an interface material. This is the current material used by NAA where a compressible thermal conductor is required because of removal of units for service. This arrangement is designed to give a worst case temperature at the bottom of the tray of 40.5°C. This yields a 70°C micrologic junction temperature and a 105°C silicon device junction temperature as the worst case design.

The AGC arithmetic and control section is located in tray A (Fig. 9-3). Its logical design is accomplished entirely through the use of some 4200 nor elements --- (36 modules of 120 gates each).

The nor circuit is a single integrated circuit made using planar diffusion transistor techniques and housed in a round TO-47 size can (Fig. 9-4).

The unit shown in Fig. 9-5 is mounted in a plastic holder. Power wiring and logical interconnection are added and the sub-module mounted into a magnesium header plug assembly.

Since all nor gates are identical, the logical interconnection is what makes each stick specific. A device to appropriately wire these units in accordance with the logic diagrams, with complete machine repeatable accuracy, is the heart of successful logic module production. This is done by the so-called matrix welder which was developed by Raytheon at MIT/IL direction. This machine fabricates matrices by tape-controlled welding of interconnection wiring (Fig. 9-6).

In the Tray B side of the computer the P.S. oscillator memory drivers are constructed of common type electronic parts with specially weldable leads. The components are mounted in drilled block and point-to-point wired in what is becoming classic cordwood welded module construction. After test, each module then plugs into appropriate location in the tray.

Of unique interest is the core rope unit (Fig. 9-7). This form of fixed storage is programmed by the rating of 128 sense wires through or around each of 512 tape wound cores. This combination of cores and wires yields 8 (16 BIT) words/core or a module size of 4000 words of memory. Six (6) such fixed program modules (24K words of memory) are carried in AGC.

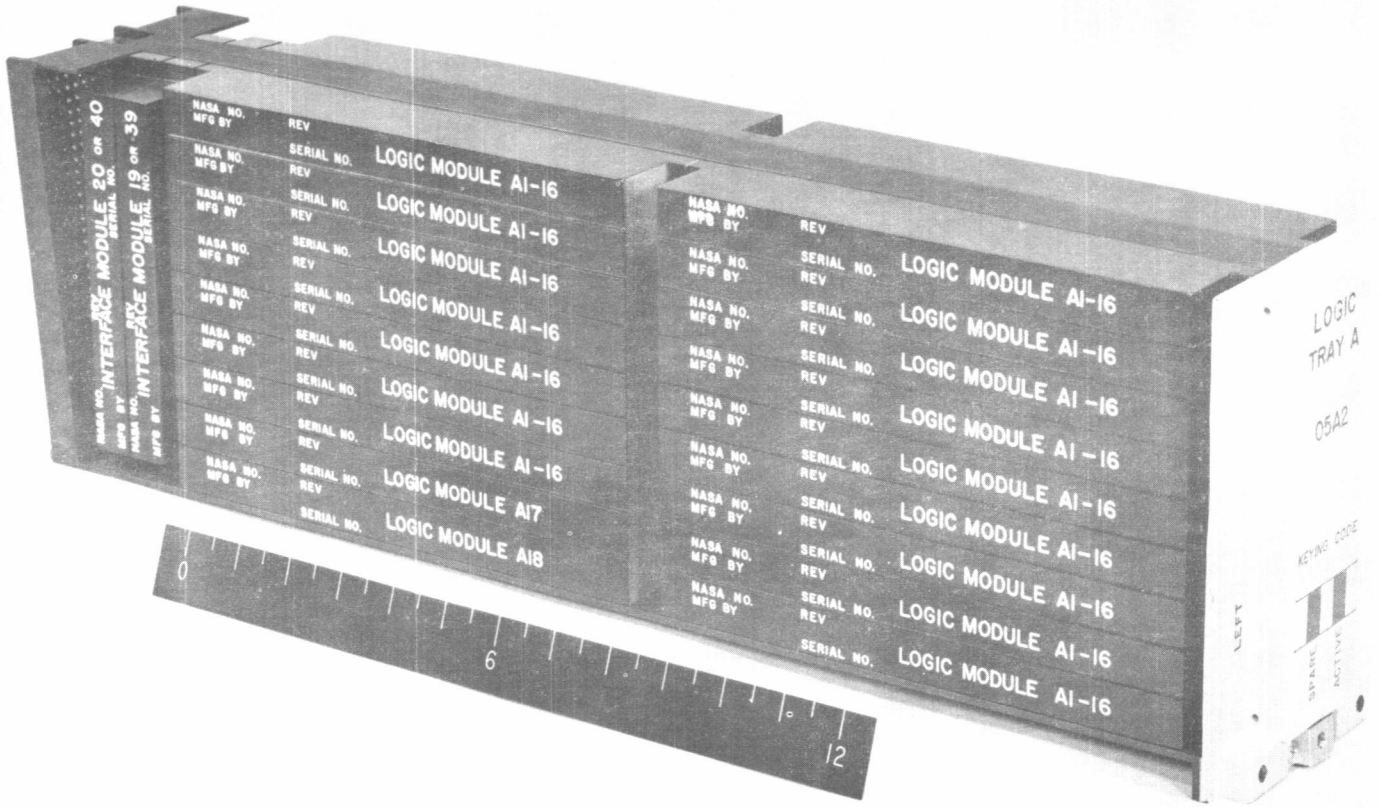
INTERFACE MODULE 20 OR 40
INTERFACE MODULE 19 OR 39
LOGIC MODULE A1-16
LOGIC MODULE A17
LOGIC MODULE A18
LOGIC
TRAY A
05A2
KEYING CODE
LEFT
SPARE
ACTIVE
0
6
12

Fig. 9-3

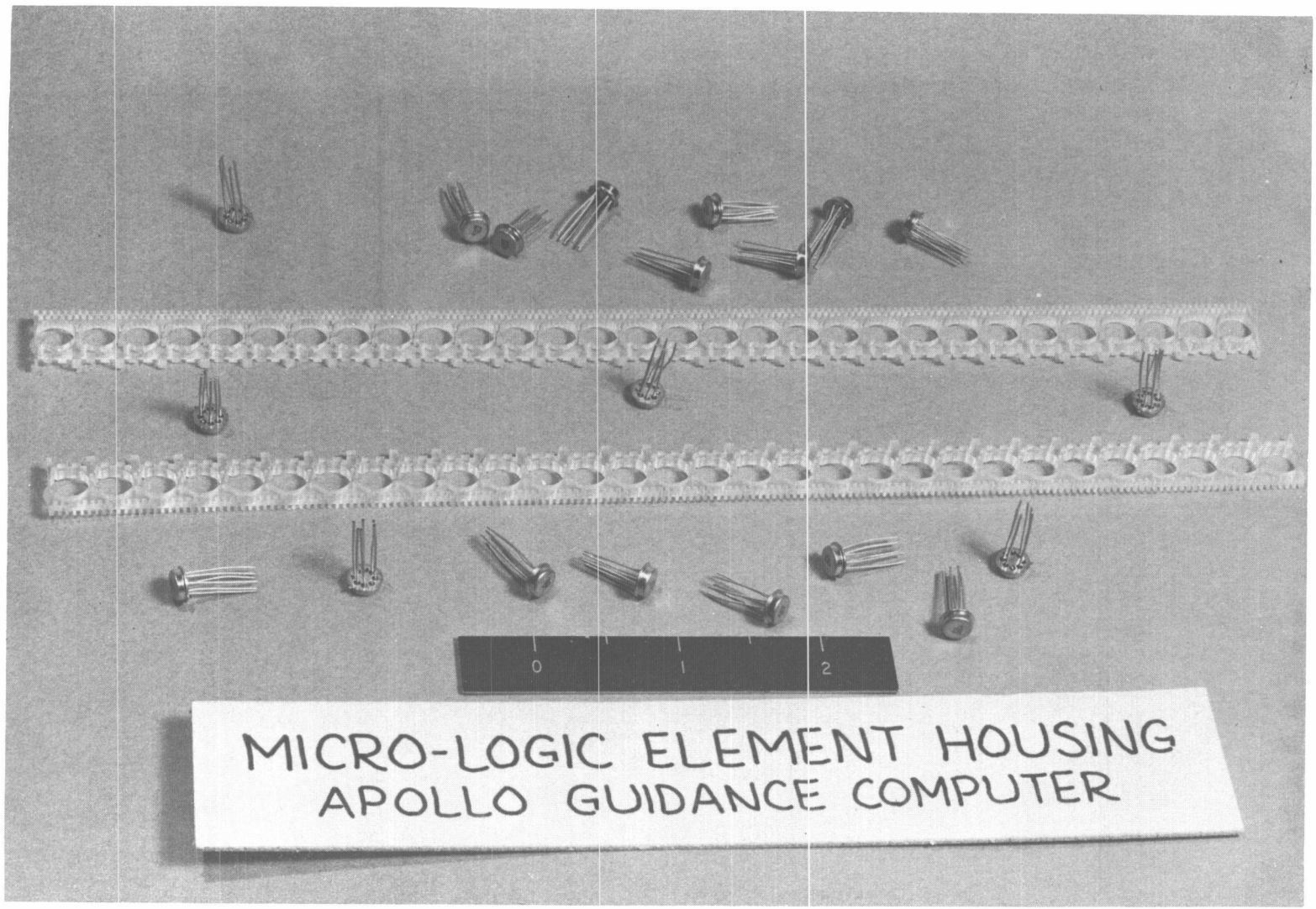

Fig. 9-4

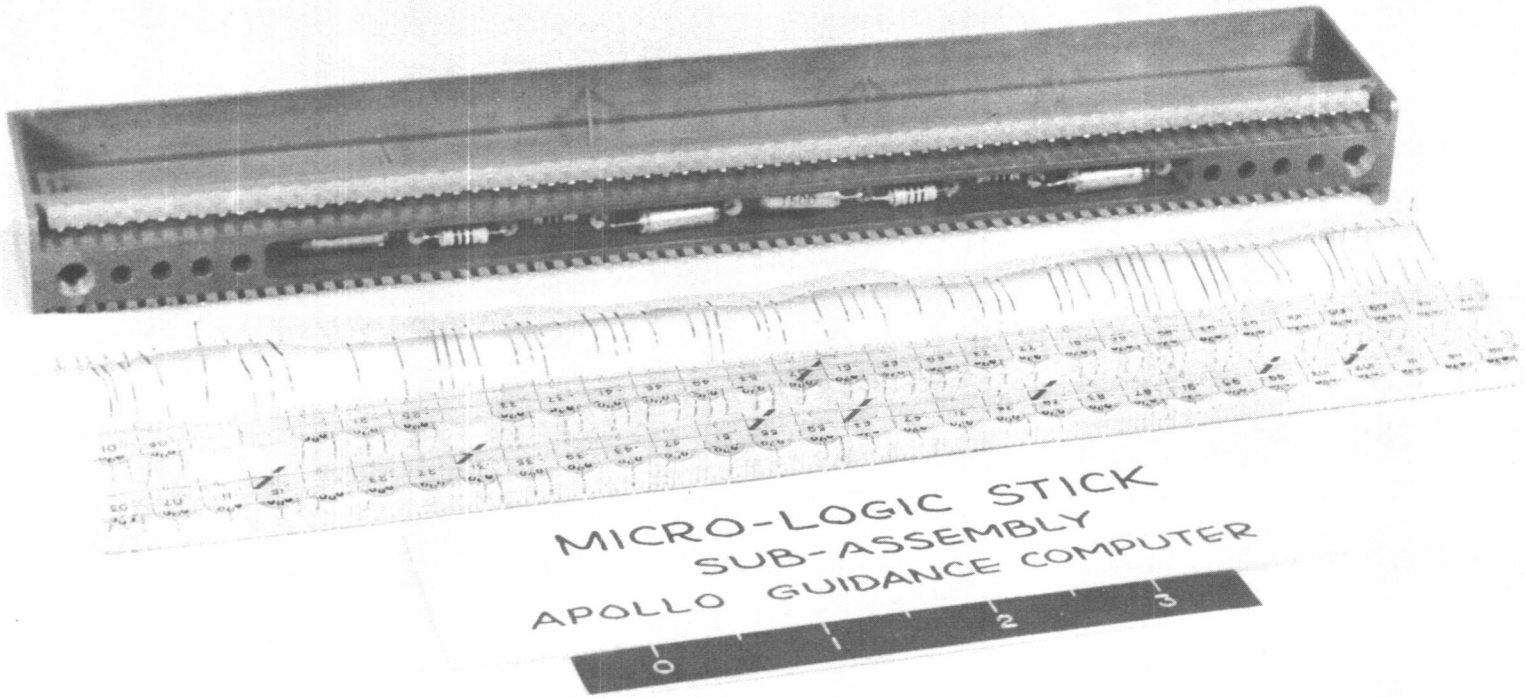
MICRO-LOGIC STICK
SUB-ASSEMBLY
APOLLO GUIDANCE COMPUTER
0
1
2
3

Fig. 9-5

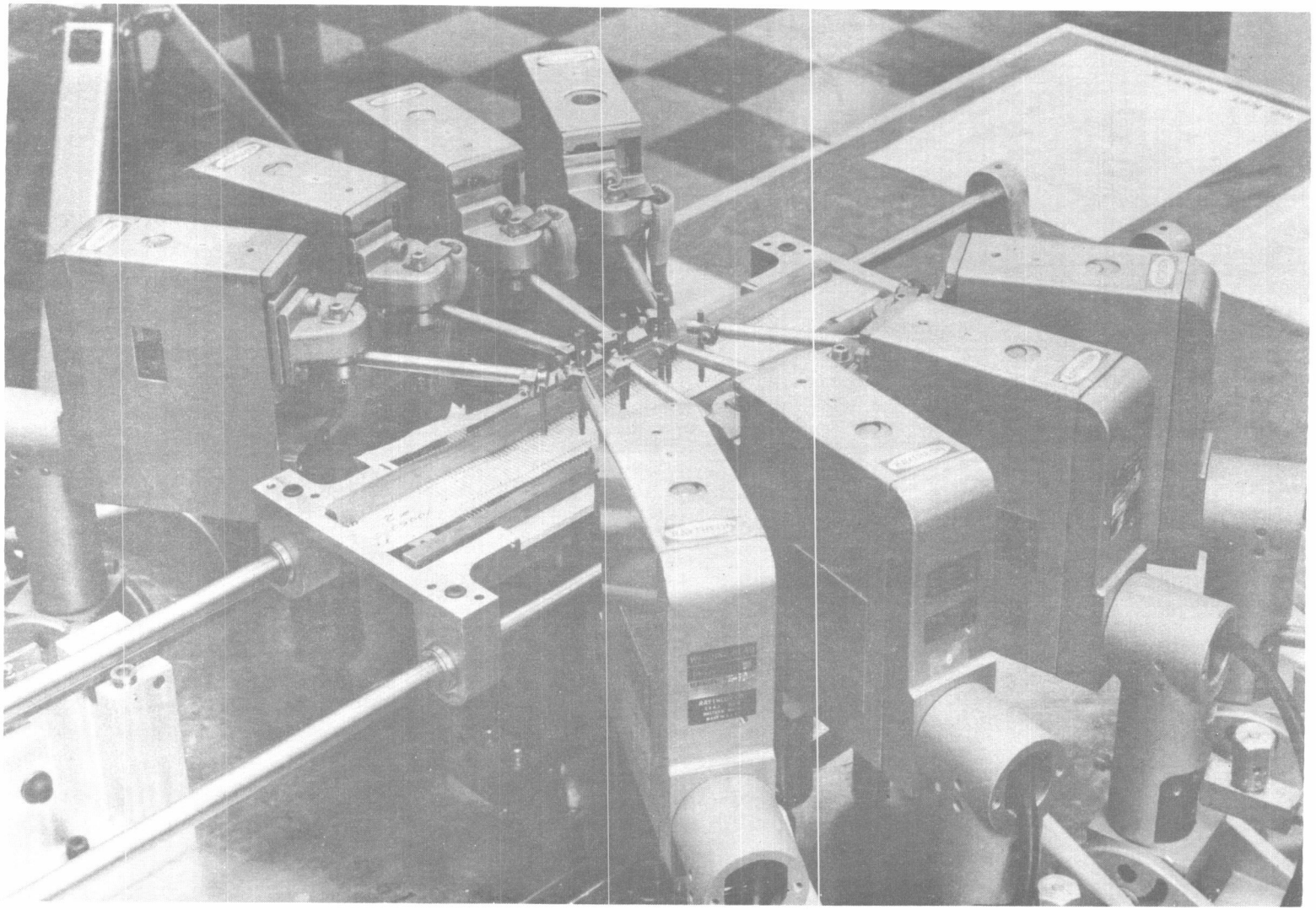

Fig. 9-6

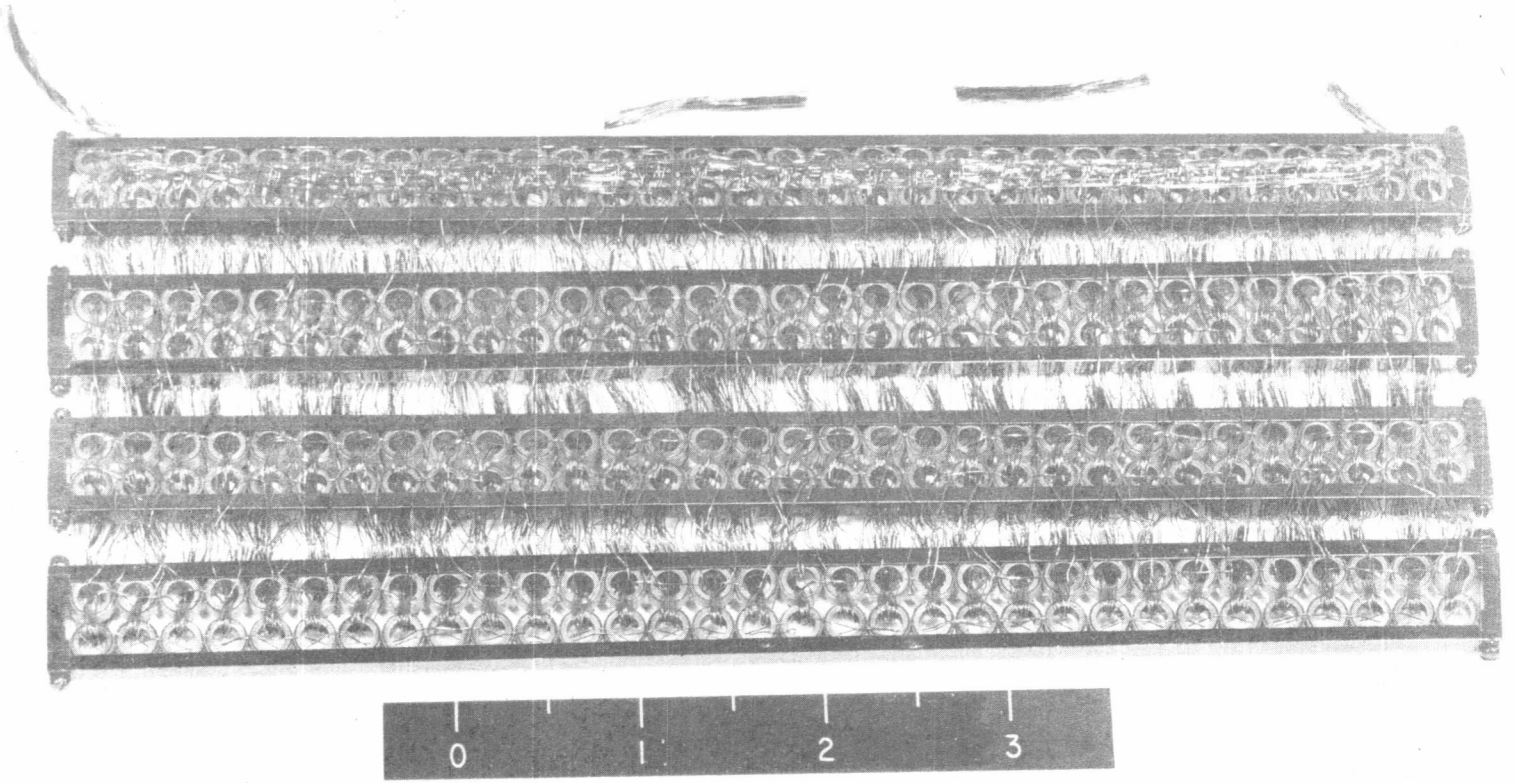

EXPERIMENTAL 256 CORE ROPE
MADE BY RAYTHEON

apollo M.I.T. INSTRUMENTATION LABORATORY

Fig. 9-7

To fabricate such a unit, 256 cores are arranged in each of two-side frames. Twenty-one ft. of 2-mil diameter wire is coiled into a door spring spiral and inserted into a 12-inch hyperdermic needle. The tape programmed fixture positions cores in proper sequence for a given wire path in the wiring aperture. The needle supply is then passed through the core and the wire coiled inside is splayed out behind. Upon completion of a pass, the supply needle touches a switch generating a control signal causing the tape to index the fixture to the next aperture position. Upon installation of 128 sense lines and 21 inhibit set-reset wires properly terminated to pins of the header, the unit is tested functionally.

Removing and folding the frames into the header, final test and pot completes this unit.

The tray frame itself carries out the duality seen in the two trays per computer by itself being dowled together in two halves and match profiled; then re-opened for wiring potting and test.

There are over 20,000 tape-controlled mill moves involved in making this part. In addition to intricate profiling, thin wall sections, there are many highly accurate holes located to 0.002 true positioning. Porosity and lower thermal conductivity of cast material would be intolerable hence this unit is machined from solid on tape-controlled equipment. The use of tape, if not justified in volume, is certainly defendable when one thinks of the decision time and error probability implicit in drilling 1800 holes in the end connector, 3000 holes in Tray B, and 6000 holes in Tray A. If the number of holes in the computer presents a looming statistic it must only be expanded to the insertion of the same number of electrical connector pins to create the imposing task of point-to-point wiring of these pins, in a pre-determined manner, with exact reproducible accuracy and testability. To do this, automatic wire wrapping was chosen as the interconnection mechanism. Used successfully on Polaris fire control and flight computers, using standard wrapost sizes, the method has been extrapolated by Gardner-Denver to a miniature pin on a 1/8-inch center.

MIT/IL wrote programs which converted the interconnection list of the computer into control punch cards for the newly developed universal wire wrapped machine. In addition, this program selects wiring patterns and routing to optimize wire densities in the wrap field.

If one is armed with a deck of cards, a computer tray, 2600 ft. of 0.010-diameter teflon coated wire and access to the pneumatic marvel, it is possible to put a wire securely between 2 pins every 6 seconds and repeat this process with machine accuracy throughout the 11,000 connections required by AGC. Ground busses and connections to the front of the tray are installed by hand after machine wrapping. Clearly a design that obviated this hand operation would be desirable. It is felt that this is a design deficiency in the Block I configuration.

In the light of shifting ground rules, other characteristics of the Block I AGC bear re-examination. Current planning requires switch-over from one AGC to a second, with dual operation of both during critical phases, through the addition of certain logical changes to the Block I design. This, in effect, generates electronic in-flight repair without the necessity of mechanically removing units in effecting exchange. In view of this the weight of structure jacking hardware, tray pins, toe plates and end connector assemblies loom large.

Problems of compressible interface material could be eliminated with its removal and hard mounting with the computer. Improved form factors in micrologic design, namely flat pack, allow twice the logic in the same volume. Finally, and perhaps most importantly, the AGC Block I has no sealed connectors. Requiring sealing on Block I would necessitate a redesign.

In the light of this electronic in-flight maintenance ground rule, I would like to describe the Block II solution to the problems just mentioned. Despite slightly more logic, it is comfortably possible to install two computers in the same allocated volume used in Block I. These computers are referred to as AGC's 12 on this front panel moding control. Dual or alternate operation is offered with manual selection of mode. Details of operation will appear in other presentations.

To provide improved thermal paths and single wire wrap operation for each machine the modules are arranged on a single flat end connector. All module connections are then made automatically in one assembly including those to the outside world connector. One thousand connectors are eliminated by not requiring tray connectors, as well as eliminating the hand installation they require.

Tray C, the interconnection tray, is replaced by a cable assembly which plugs into the two computers and the S/C and PSA. One fixed memory unit is adjacent to the interface connector and readily removable by stripping the silastic plug seal and jacking it out of the end connector. As the cold plate supplied by S/C loses its center support upon being shifted upward for the Block II configuration it can no longer support the lighter combined Block II weight. Rather than add structure to this assembly a bridging arrangement has been added to the AGC to transmit its load directly to secondary structure at each edge of the cold plate. This is done at a weight penalty of 3#/computer.

A fringe benefit is derived, however, in that the bridging, with the addition of side plates, provides a cover for all modules. It is now possible to fill this cover with silastic to effect a moisture seal to all computer module pins. The addition of a thin sheet metal top, electrically bonded to the frame, provides additional interfering shielding. The entire computer with cover weighs 44 lbs vs 70 in Block I. Module design in the B section, memory, oscillator, power supply is virtually identical to Block I.

This allows production techniques, test equipment and personnel training in the areas of rope erasable memory, oscillators, drivers, etc., to continue into Block II. Logic module design differs in that twice the number of gates can be fitted in the same width and length stick with the flat form factor.

We are, however, using 16 less than twice the number of gates due to the location of the filter condensers in the stick ends. Flat micrologics carry two nor gates per package and are mounted once again on a plexiglass header assembly. The back of this assembly will have been matrix interconnected and tested for accuracy and continuity prior to installing the flat unit. No new process is involved in the fabrication. Once again this assembly is mounted into a magnesium header and potted.

This model reflects the state of the Block II hardware design at this time. It should be pointed out that all parts of the two machines shown are in metal and the logic module has been configured completely.

Milling tapes exist to fabricate a complete end connector and can be released for production as soon as thermal analysis is complete and final logic allocation made.

Wire wrapping programs are being overhauled to generate control decks to the flat configuration. Interface with NAA structures people is scheduled for meetings soon.

A note in conclusion should be made of the fact that a single AGC of the flat design would fit on the existing Block I cold plate with the use of an MIT/IL aluminum adaptor. Such a Block II mechanical design could carry Block I logic and interface and provide the answer to a sealed connector requirement with 26 lbs reduction in computer weight.

Section 10

APOLLO GUIDANCE COMPUTER (AGC)

E. C. Hall

According to the tasks listed in Fig. 10-1, the AGC must perform the steering calculations for ΔV corrections. It provides digital communications to and from the ground. It displays to the astronaut, gives attitude commands, and controls the thrust by turning it off and on. In some respects it does system testing. The clock in the computer provides the frequency reference for all of the spacecraft subsystems.

The computer is 0.8 cu. ft. in size, weighs 70 pounds, and requires 100 watts of 28 volts dc prime-power from the fuel cells. Although originally designed into Block I, it will not have the capability of going into the idle mode. This is the condition wherein the computer keeps track of time but does not do any other computations. Block II will have this "idle mode" capability, and it could be in Block I if required.

Figure 10-2 describes very briefly the organization of the AGC. On the left-hand side various types of input circuits are shown. There is interrupt capability so a signal from the outside world can interrupt whatever is going on in the computer, and the computer will process that particular input. It has counter inputs from the CDU's, from the PIPA's, and from various outside inputs. There are other input registers and output registers. The clock provides the reference for the complete spacecraft. There are approximately 24,000 words of fixed memory and 1000 words of erasable memory.

Some AGC characteristics are as follows. It has a 16-bit word, consisting of 15 bits plus parity. One's complement with overflow correction is the number system. The memory cycle time of 11.7 microseconds describes to some extent the speed of the computer. The erasable memory is the normal coincident-current ferrite-type memory; however, it uses non-temperature-sensitive ferrite cores. The computer has 11 normal code instructions, such as add, subtract, etc. In addition it has has 8 involuntary instructions, among which are interrupt increment, load, and start. There are 6 possible interrupts. The add instruction time is 23 microseconds; this gain is representative of the speed of the computer. The time to multiply is 93.6 microseconds; this is one of the normal instructions. A double precision add, or a double precision multiply, are subroutines that have to be programmed. To add in the counter incrementing of any incoming pulses requires only one memory cycle time. Because of incrementing and interrupts, considerable speed of operation of the computer is achieved with real time requirements from outside functions.

AGC TASKS

Supervision of other navigation components

Steering calculations

Digital communication to and from ground

Displays to Astronaut

Thrust and attitude commands

System tests

Frequency reference to spacecraft systems

Fig. 10-1

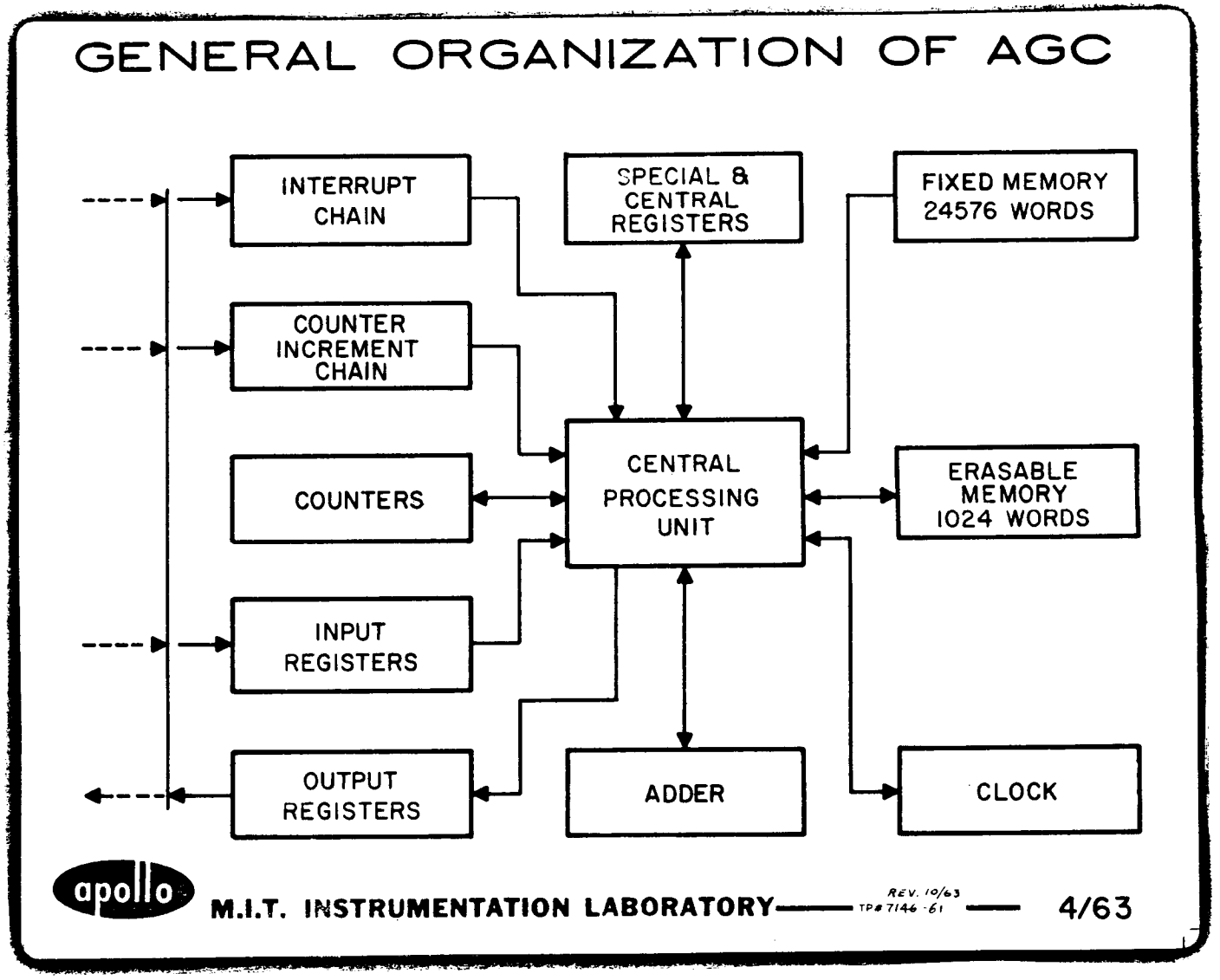
GENERAL ORGANIZATION OF AGC
INTERRUPT CHAIN
SPECIAL & CENTRAL REGISTERS
FIXED MEMORY 24576 WORDS
COUNTER INCREMENT CHAIN
COUNTERS
CENTRAL PROCESSING UNIT
ERASABLE MEMORY 1024 WORDS
INPUT REGISTERS
OUTPUT REGISTERS
ADDER
CLOCK
apollo
M.I.T. INSTRUMENTATION LABORATORY
REV. 10/63
TP# 7146-61
4/63

Fig. 10-2

The computer has 20 counters which are used for the various operations previously mentioned, for instance, the encoders, the PIPA's, or the telemetry. The 4 discrete input registers and the 5 output registers each have 15 bits. These registers in some cases are used to provide programmed numbers of pulses out. To drive the CDU's for example, the AGC has to put out a pre-selected number of pulses. The pulses are controlled through these output registers. The actual number of such outputs is 25. There are also 16 pulsed outputs not under program control. The telemetry is used for processing of down telemetry data. Up-telemetry is handled in the same fashion as the astronaut's key code.

Figure 10-3 shows a schematic diagram of the core rope memory. By applying currents I_{1B}, and I_{2B} all cores are saturated except core 1; thus applying current I_{SR} switches core 1 only. The memory sense wires may either go through the core or not; if it does, it is defined as a one; if outside, a zero.

The flow diagram for rope design and construction is shown in Fig. 10-4. Programming feeds into simulations, into a program review board, and then through the Change Control Board. For these releases paper tapes are generated at Raytheon and documented. Ropes are manufactured and tested against tapes specifically generated for test. After passing the test, the rope goes into real AGC hardware for simulation and, if proved here the result is a verified program.

Figure 10-5 shows the fabrication at Raytheon. The tape which controls the process is visible. The operator merely passes a needle containing the wire through the aperture. The wire either goes through or does not go through a core in accordance with the tape program.

Another new application is the one of integrated circuits, such as the micro nor gate shown in Fig. 10-6. A total of 4200 are used in the system. The lighter areas are aluminum interconnecting wires and the module contains resistors and transistor elements.

AGC interfaces are shown in Fig. 10-7. The keyboard and display is important since this is the way the astronaut communicates with the computer, and in many cases, with the complete system. The Display and Keyboard, or DSKY, panels are shown in Fig. 10-8 and Fig. 10-9. The Navigation DSKY is to be located in the lower equipment bay and is used for normal navigation. The Main DSKY is located on the main C/M panel.

Figure 10-10 is a drawing of the AGC-S/C interface. The only connections with the S/C are those wires which run between the upper and lower connectors. The radar interface section will undergo minor changes from the description laid down some 8 months ago; these will be LEM requirements and not C/M requirements. The S/C interfaces are primarily concerned with stabilization and control. The only signal used here

4 CORE ROPE SELECTION (SENSE LINES NOT SHOWN)

TO SWITCH CORE 1 APPLY I_{1B} AND I_{2B} AND I_{SR}

TO SWITCH CORE 2 APPLY I_{1A} AND I_{2B} AND I_{SR}

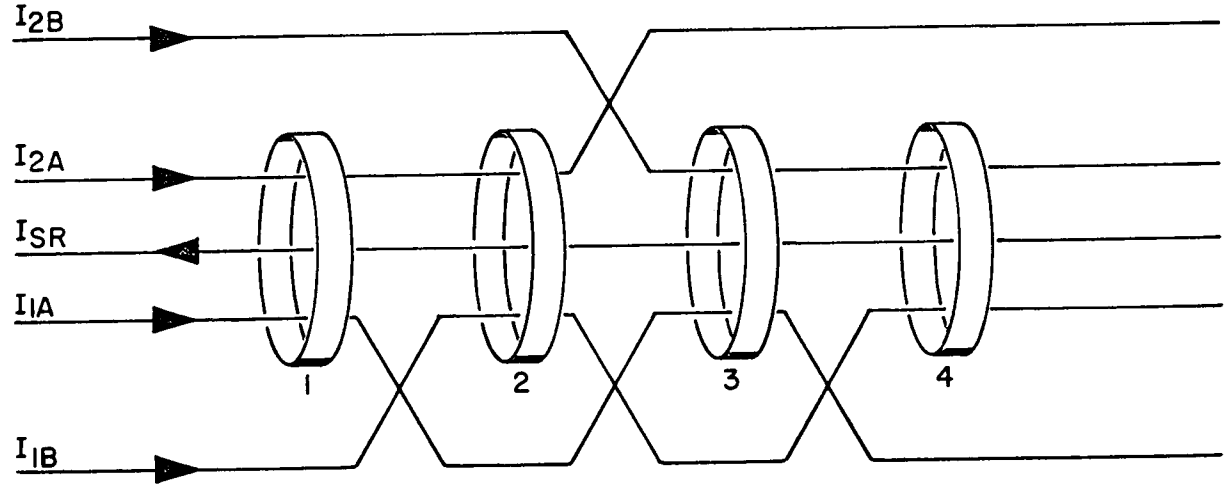

TO SWITCH CORE 3 APPLY I_{1B} AND I_{2A} AND I_{SR}

TO SWITCH CORE 4 APPLY I_{1A} AND I_{2A} AND I_{SR}

Fig. 10-3

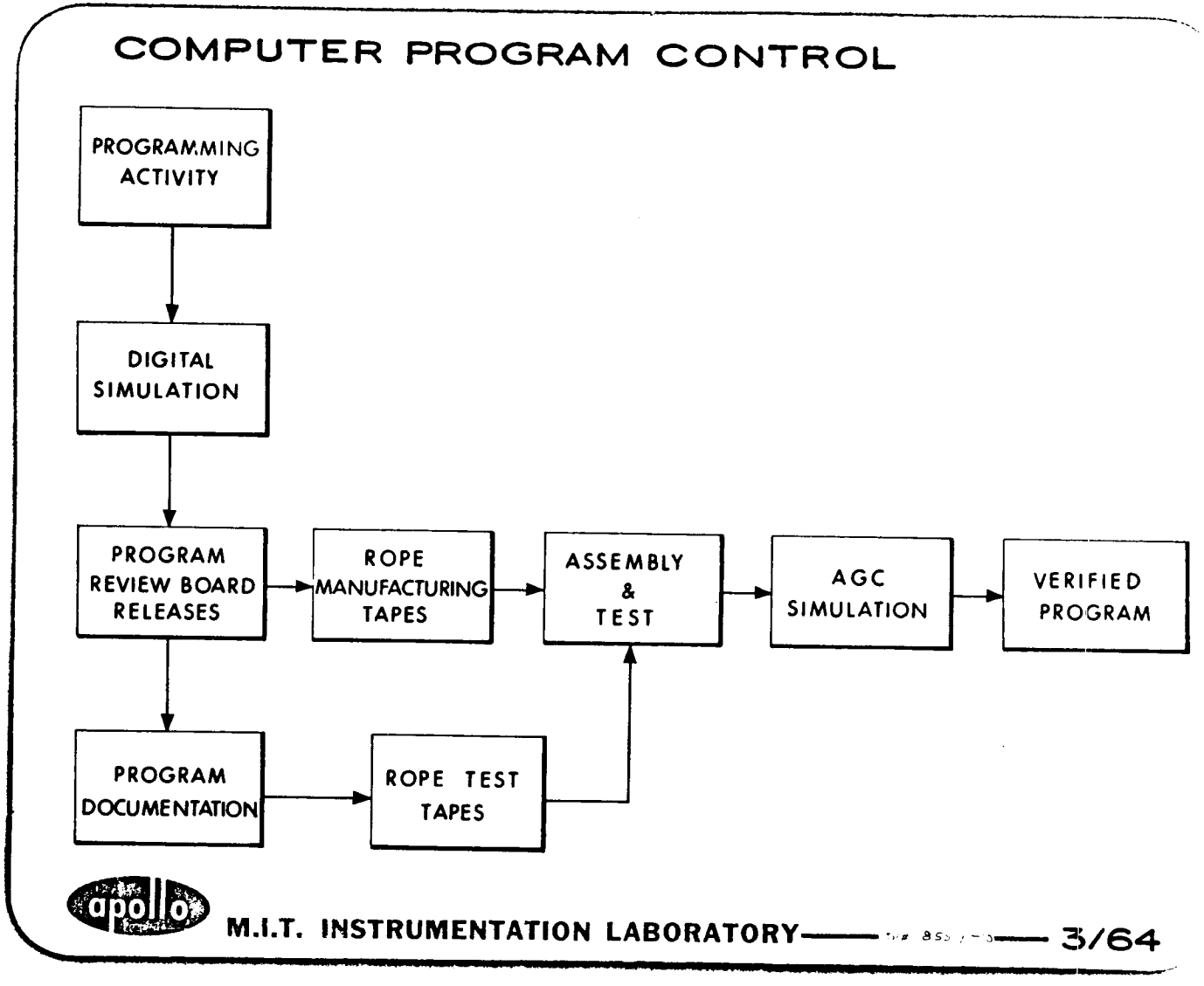
COMPUTER PROGRAM CONTROL
PROGRAMMING ACTIVITY
DIGITAL SIMULATION
PROGRAM REVIEW BOARD RELEASES
ROPE MANUFACTURING TAPES
ASSEMBLY & TEST
AGC SIMULATION
VERIFIED PROGRAM
PROGRAM DOCUMENTATION
ROPE TEST TAPES
apollo
M.I.T. INSTRUMENTATION LABORATORY
3/64

Fig. 10-4

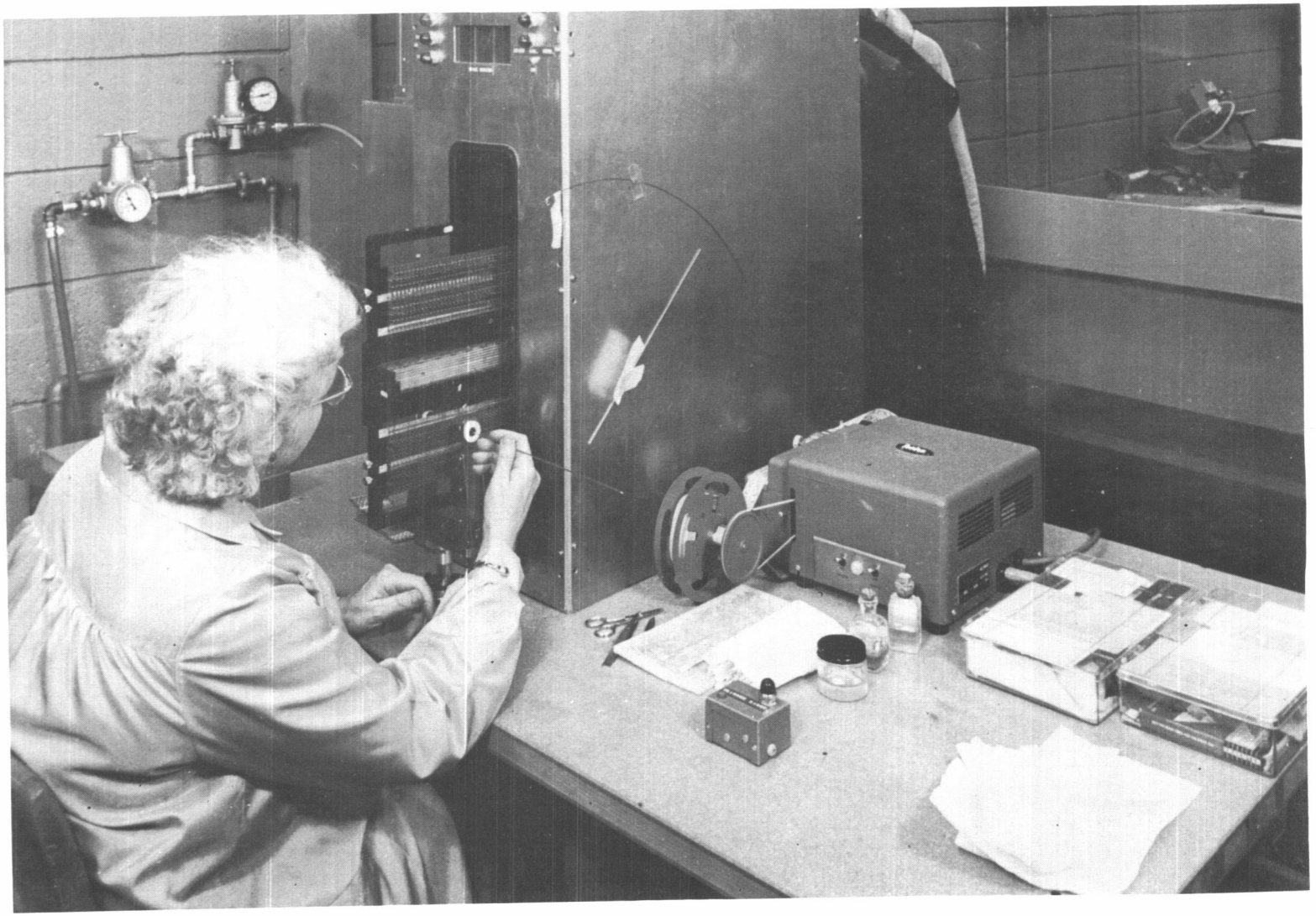

Fig. 10-5

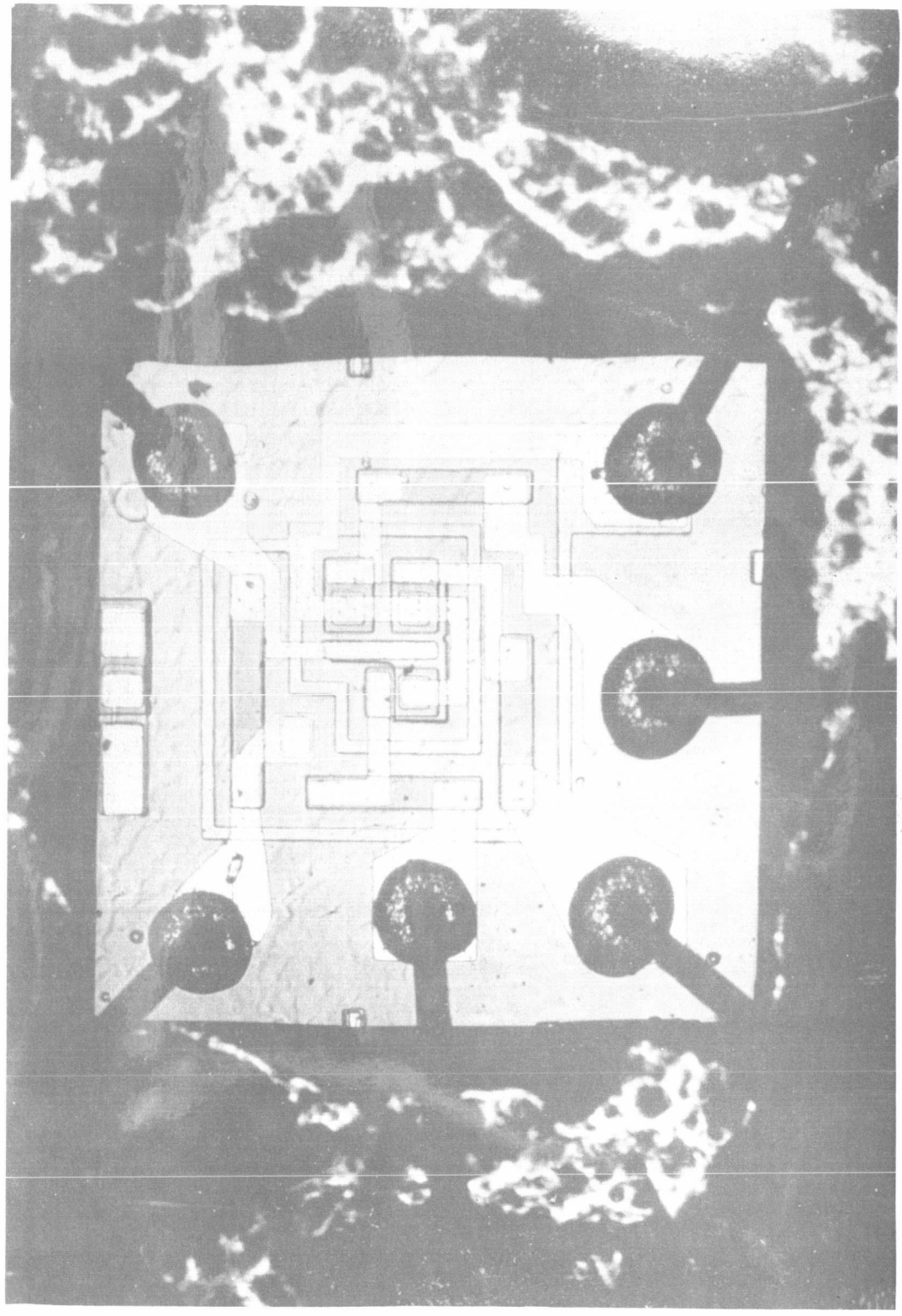

Fig. 10-6

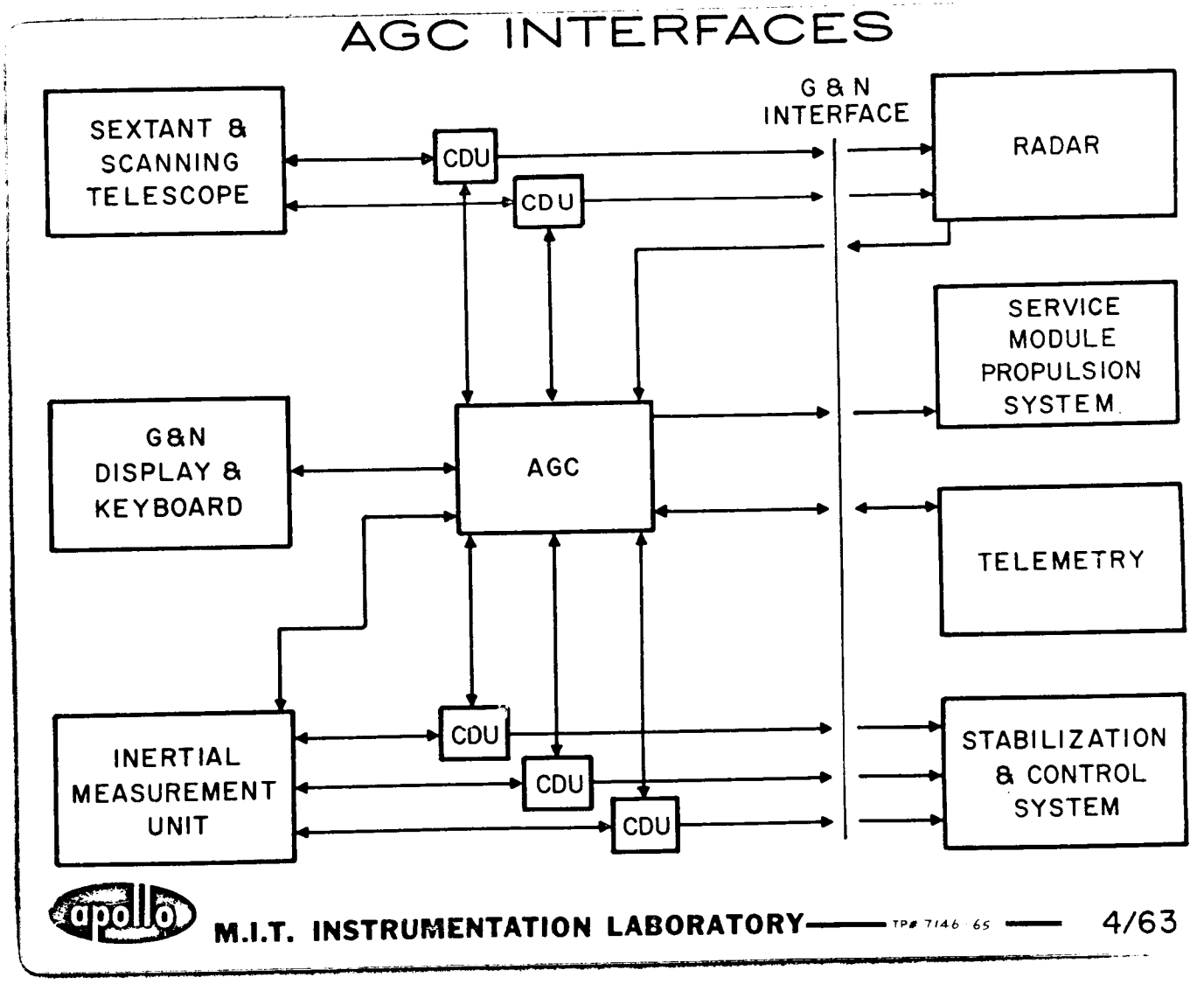
AGC INTERFACES
SEXTANT & SCANNING TELESCOPE
CDU
CDU
G & N INTERFACE
RADAR
SERVICE MODULE PROPULSION SYSTEM
G&N DISPLAY & KEYBOARD
AGC
TELEMETRY
INERTIAL MEASUREMENT UNIT
CDU
CDU
CDU
STABILIZATION & CONTROL SYSTEM
apollo
M.I.T. INSTRUMENTATION LABORATORY
TP# 7146 65
4/63

Fig. 10-7

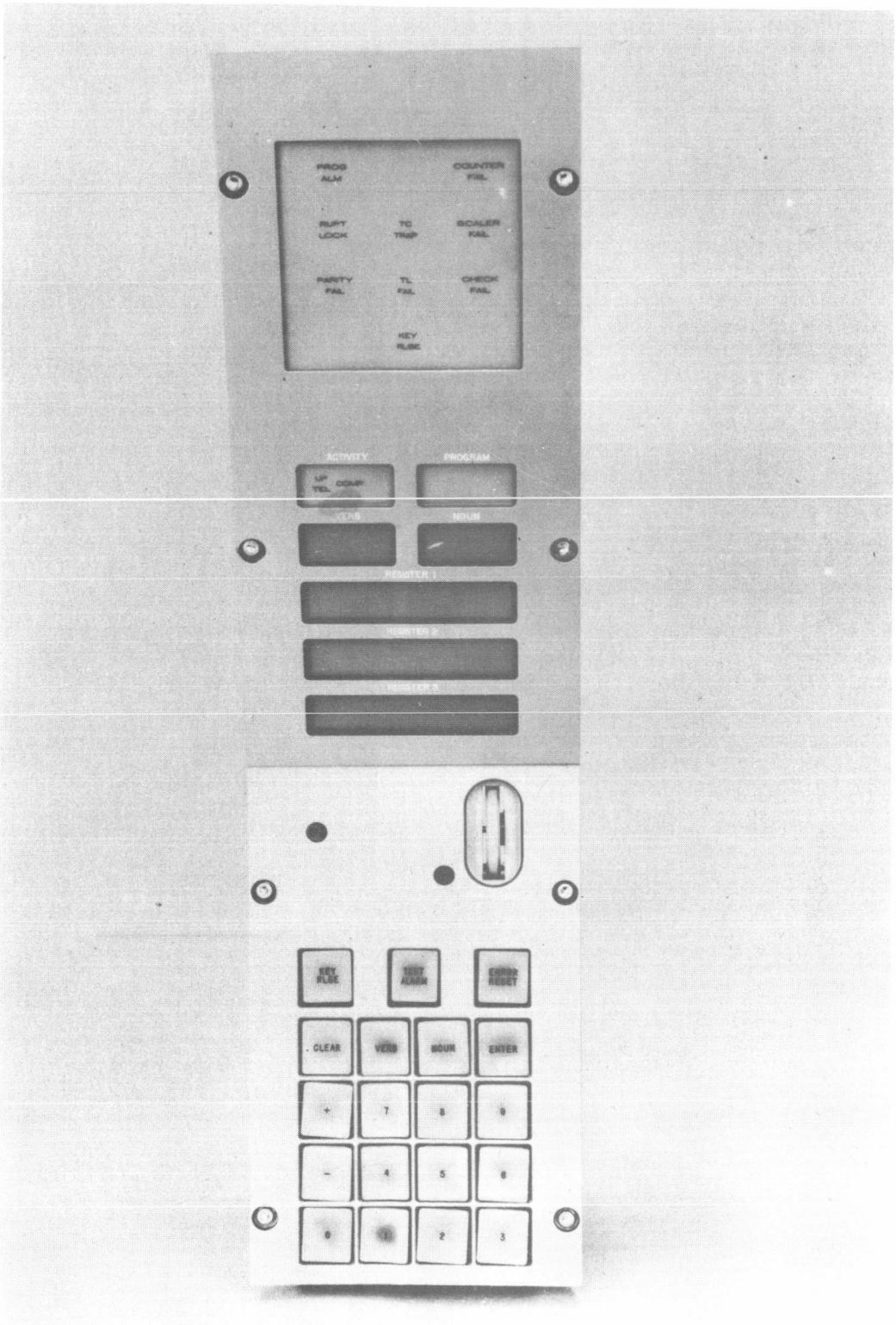
PROG ALM
COUNTER FAIL
RUPT LOCK
TC TRAP
SCALER FAIL
PARITY FAIL
T/L FAIL
CHECK FAIL
KEY REL
ACTIVITY
PROGRAM
VERB
NOUN
REGISTER 1
REGISTER 2
REGISTER 3
KEY REL
TEST ALARM
ERROR RESET
CLEAR
VERB
NOUN
ENTER
+
7
8
9
-
4
5
6
0
1
2
3

Fig. 10-8

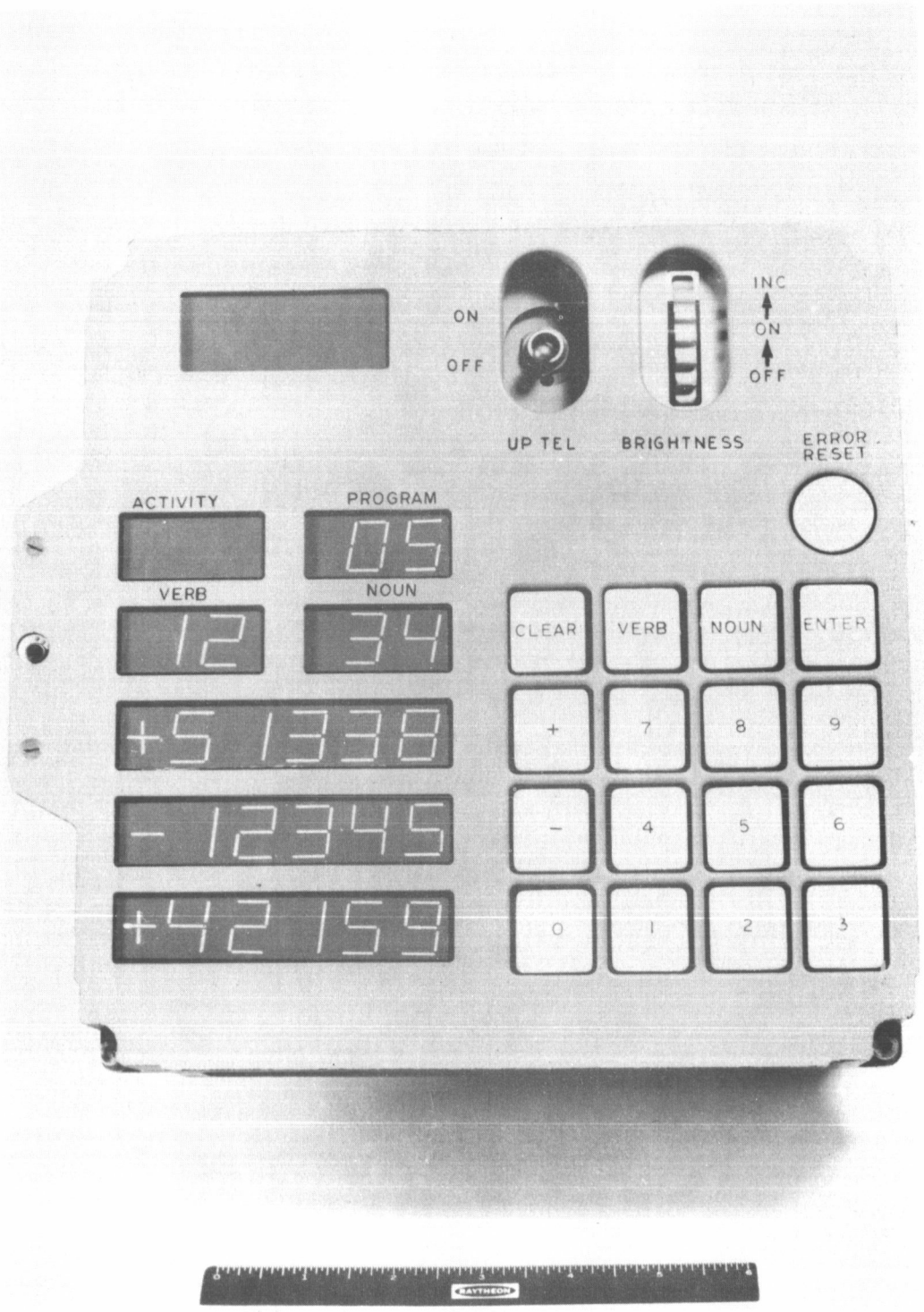
ON
OFF
INC
ON
OFF
UP TEL
BRIGHTNESS
ERROR RESET
ACTIVITY
PROGRAM
05
VERB
12
NOUN
34
+5 1338
- 12345
+42 159
CLEAR
VERB
NOUN
ENTER
+
7
8
9
-
4
5
6
0
1
2
3
RAYTHEON

Fig. 10-9

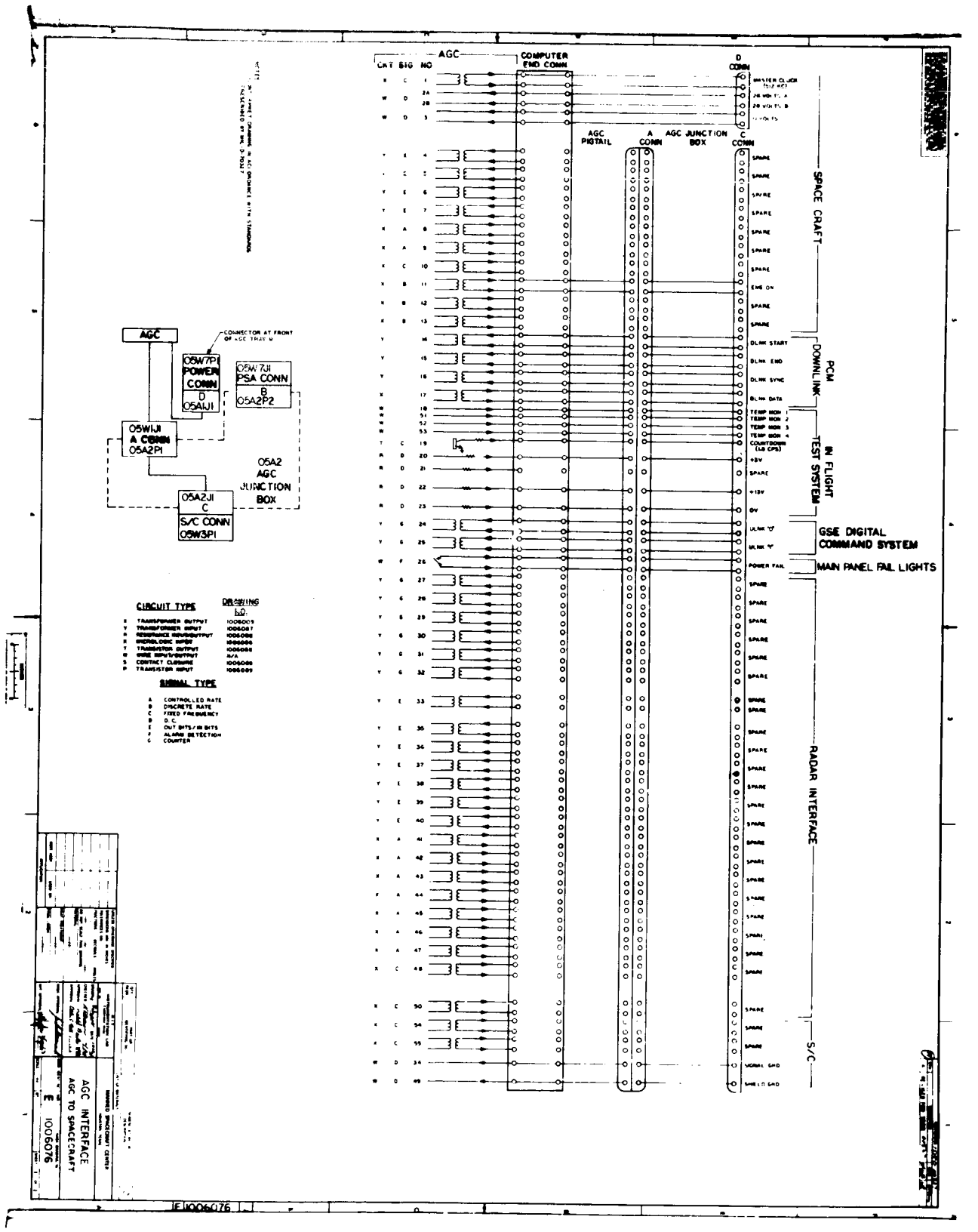
AGC
COMPUTER END CONN
D CONN
AGC PIGTAIL
A CONN
AGC JUNCTION BOX
C CONN
SPACE CRAFT
PCM DOWNLINK
IN FLIGHT TEST SYSTEM
GSE DIGITAL COMMAND SYSTEM
MAIN PANEL FAIL LIGHTS
RADAR INTERFACE
S/C
05W7P1 POWER CONN D 05A1J1
05W7J1 PSA CONN B 05A2P2
05W1J1 A CONN 05A2P1
05A2 AGC JUNCTION BOX
05A2J1 C S/C CONN 05W3P1
CIRCUIT TYPE
SIGNAL TYPE
AGC INTERFACE
AGC TO SPACECRAFT
1006076

Fig. 10-10

turns the engine off and on. Negotiations may lead to putting other signals in this interface regarding the moding of the SCS system. Ground rules specify manual functions, which makes these unnecessary if the astronaut does all the checking. For example, if the astronaut puts the G&N system into the G&N ΔV mode, he pushes a button on the main panel; he would then have to go down to the lower equipment bay and so notify the computer. The keyboard is not that easy to operate, and this delay would certainly be undesirable when fast reaction time is needed, such as in abort.

The signals have been signed off on ICD's, but information is lacking on the ICD. Shielding and grounding is a problem area. The Mil. Spec. on EMI is being followed as far as possible, but once their recommendations are not followed, one must be careful. For instance, transformer coupling at both ends is recommended, and the figure shows this on the AGC side. But on the other side transformers are not used and there may be problems with other kinds of grounding.

Figure 10-11 shows AGC-4 which is now being used to operate system 4 and to check programs. The next illustration (Fig. 10-12) shows the rope simulator which allows conversion of any one module into an erasable memory. Thus the program can be read in and changed readily.

Figure 10-13 shows AGC-4B with the racks of equipment from AGC-4 compressed into two trays. The status of AGC-4B is shown in Fig. 10-14; it has been used for computer subsystem checkout. There have been no failures in either AGC-4 or AGC-4B.

AGC-5 is in final assembly (Fig. 10-15 and 10-16) and power has just been turned on.

Figure 10-17 shows the AGC-5 fabrication schedule. Raytheon has delivered everything except for Tray C, called the G&N harness tray, which is not necessary for checking.

System 6 modules are now in test (Fig. 10-18). All of Tray A is under test. Most of Tray B has finished subsystem testing. All the modules for Tray B have not been finished so a complete testing cannot be done. There is a problem of cutting the gear off the main panel and changing the wiring. How that reflects in this particular schedule is in the main DSKY. It has slipped quite a distance; note that it is delivered the 12th of June. It will be necessary to use DSKY 5, which will not have this change, to checkout the system at this point and then sell off all but the DSKY.

System 7 is getting very close to test all the way down the line (Fig. 10-19). A summary status chart for all the hardware, and DSKY's, is shown in Fig. 10-20. Computer test set No. 3 (Fig. 10-21) has been delivered. No. 4 will come out next and will go to Raytheon for processing and test. An operation console, used to mount the computer, is undergoing tests and the first one is due to be delivered. All of the components

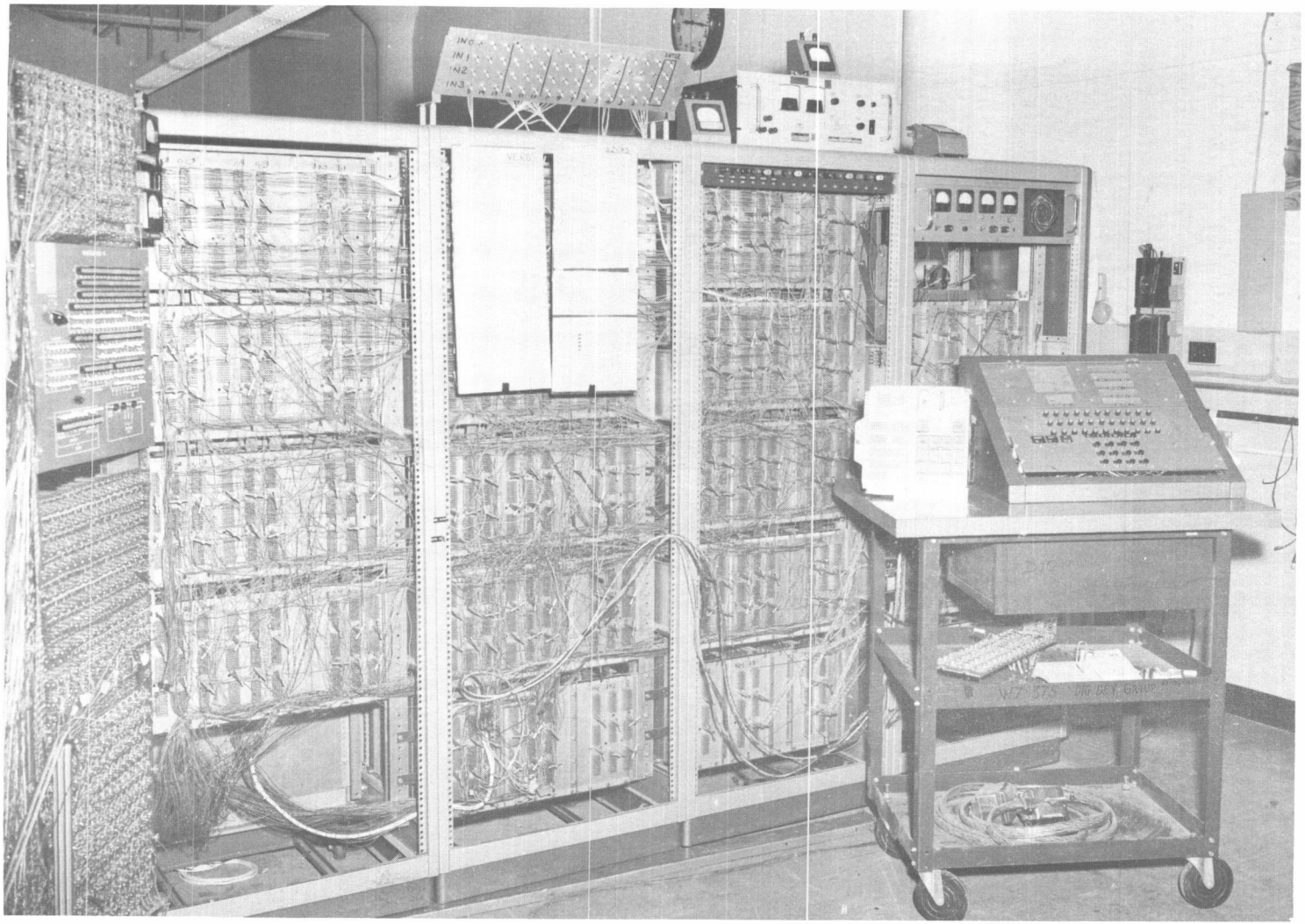

Fig. 10-11

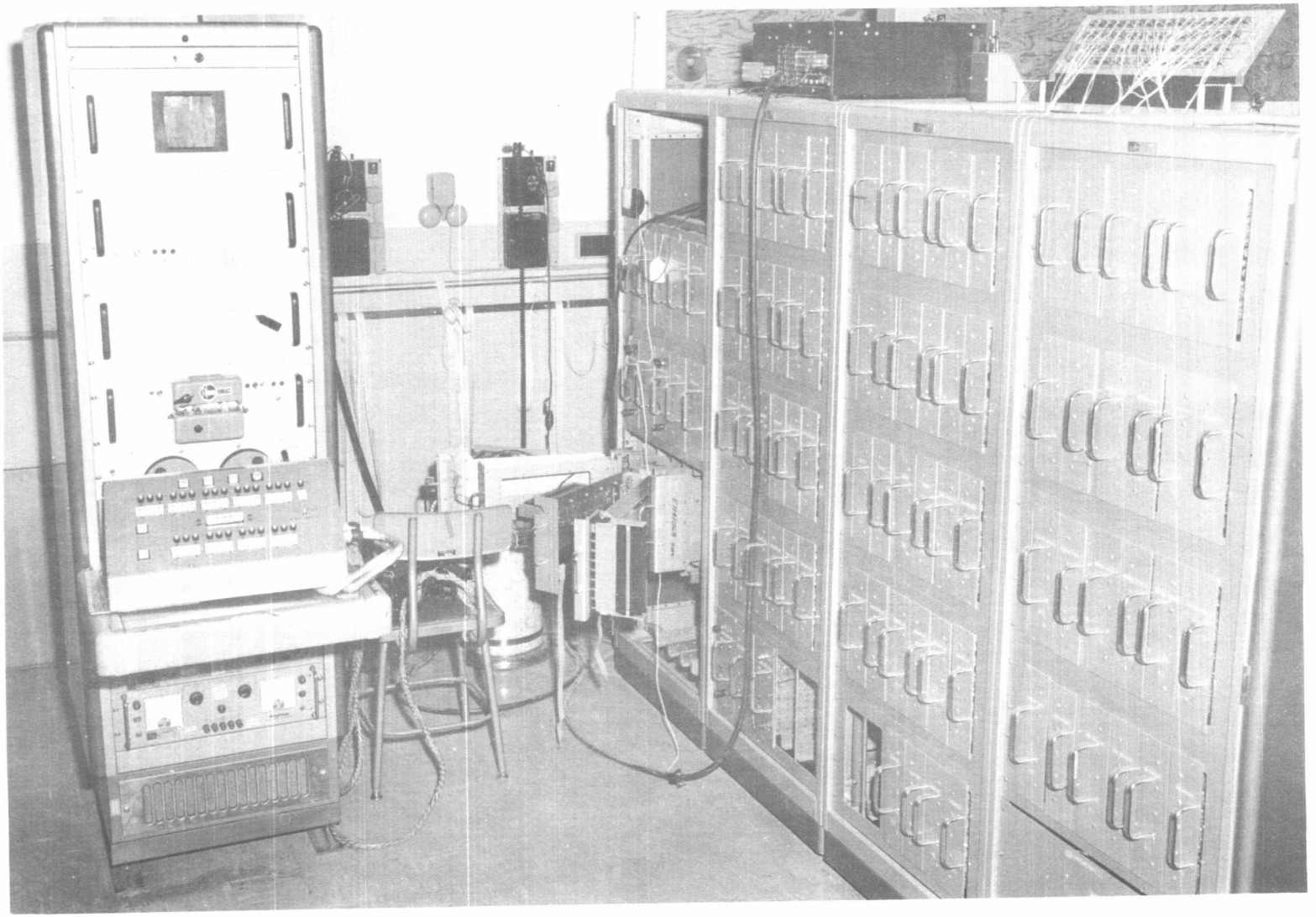

Fig. 10-12

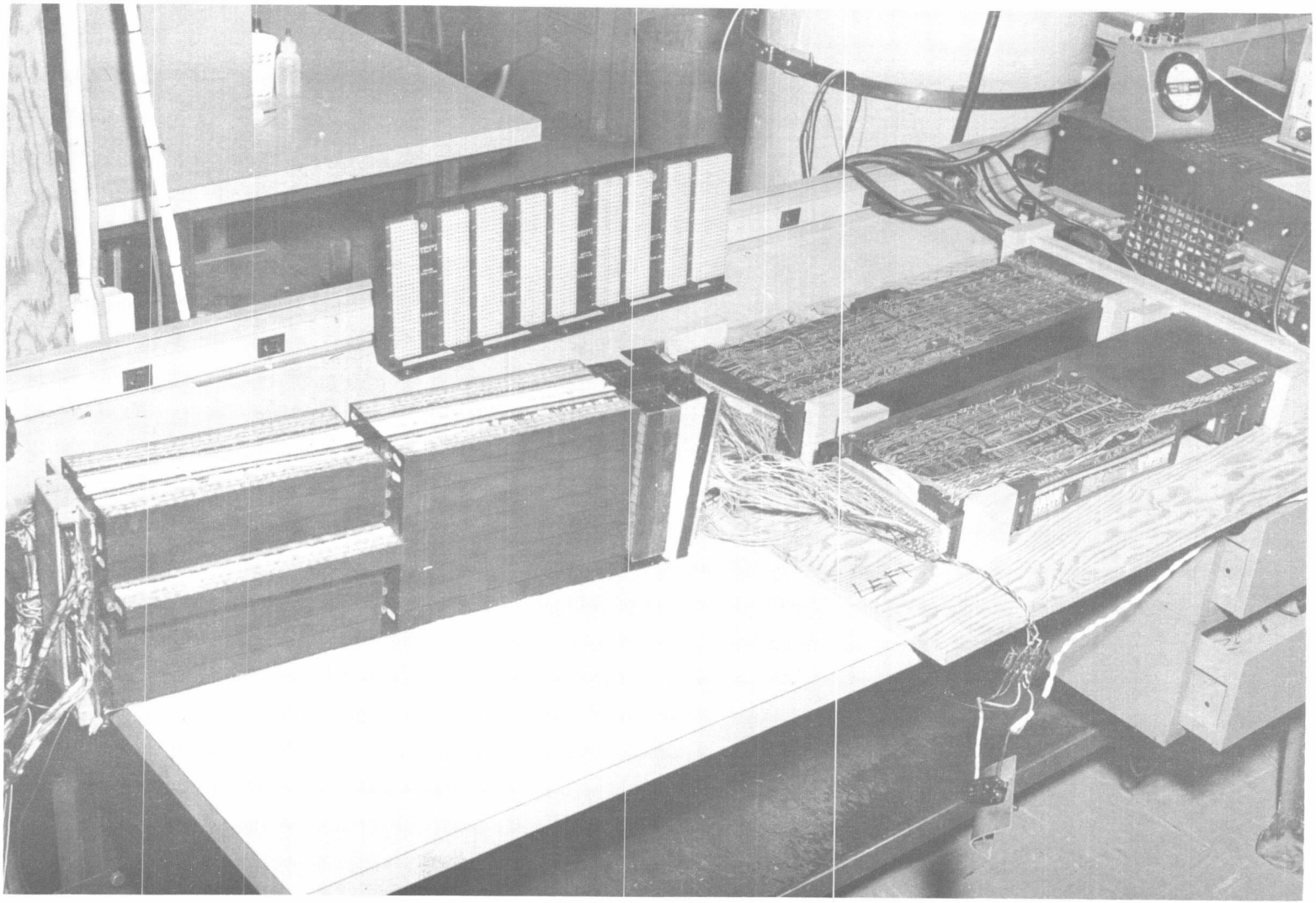

Fig. 10-13

EQUIPMENT STATUS

	STATUS	OPERATIONAL	OPERATING (hrs)
AGC 4	1. SYSTEM 4 Checkout 2. PROGRAMMING	JULY 1963	5700
AGC 4B	1. SUBSYSTEM Checkout 2. Computer Test Set check	FEB 1963	960
AGC 5	FINAL ASSEMBLY & TEST	———	———

Fig. 10-14

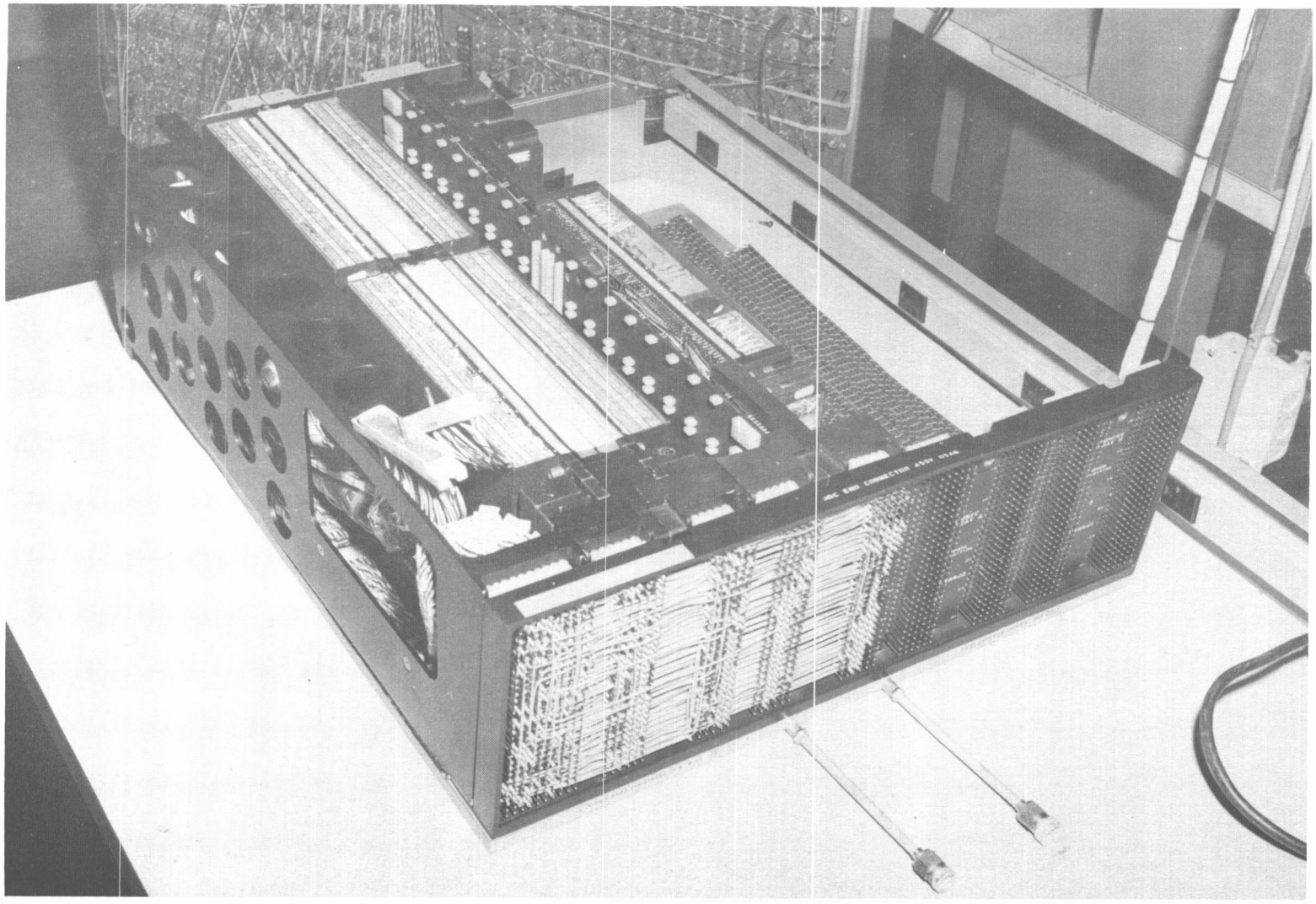

Fig. 10-15

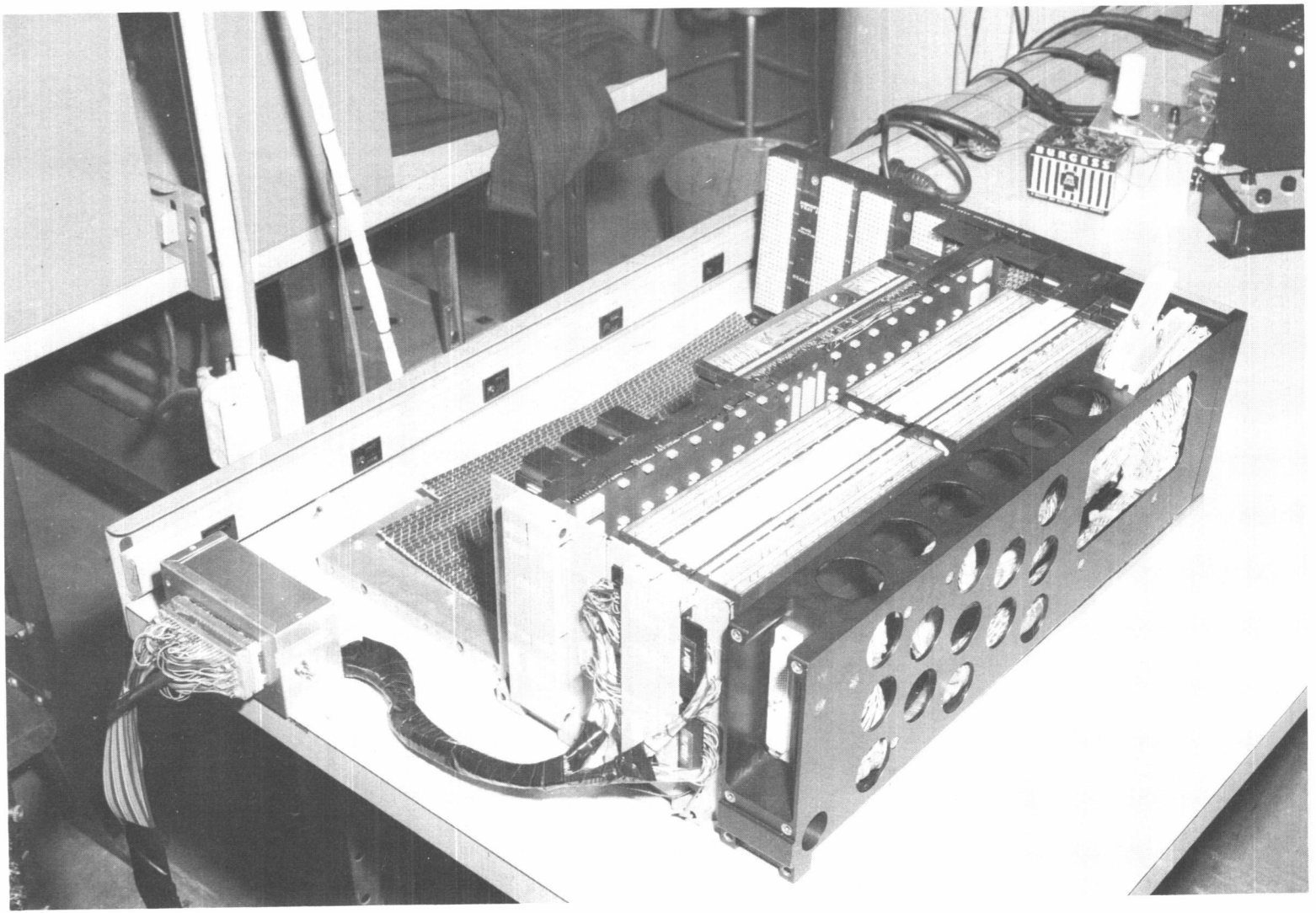

Fig. 10-16

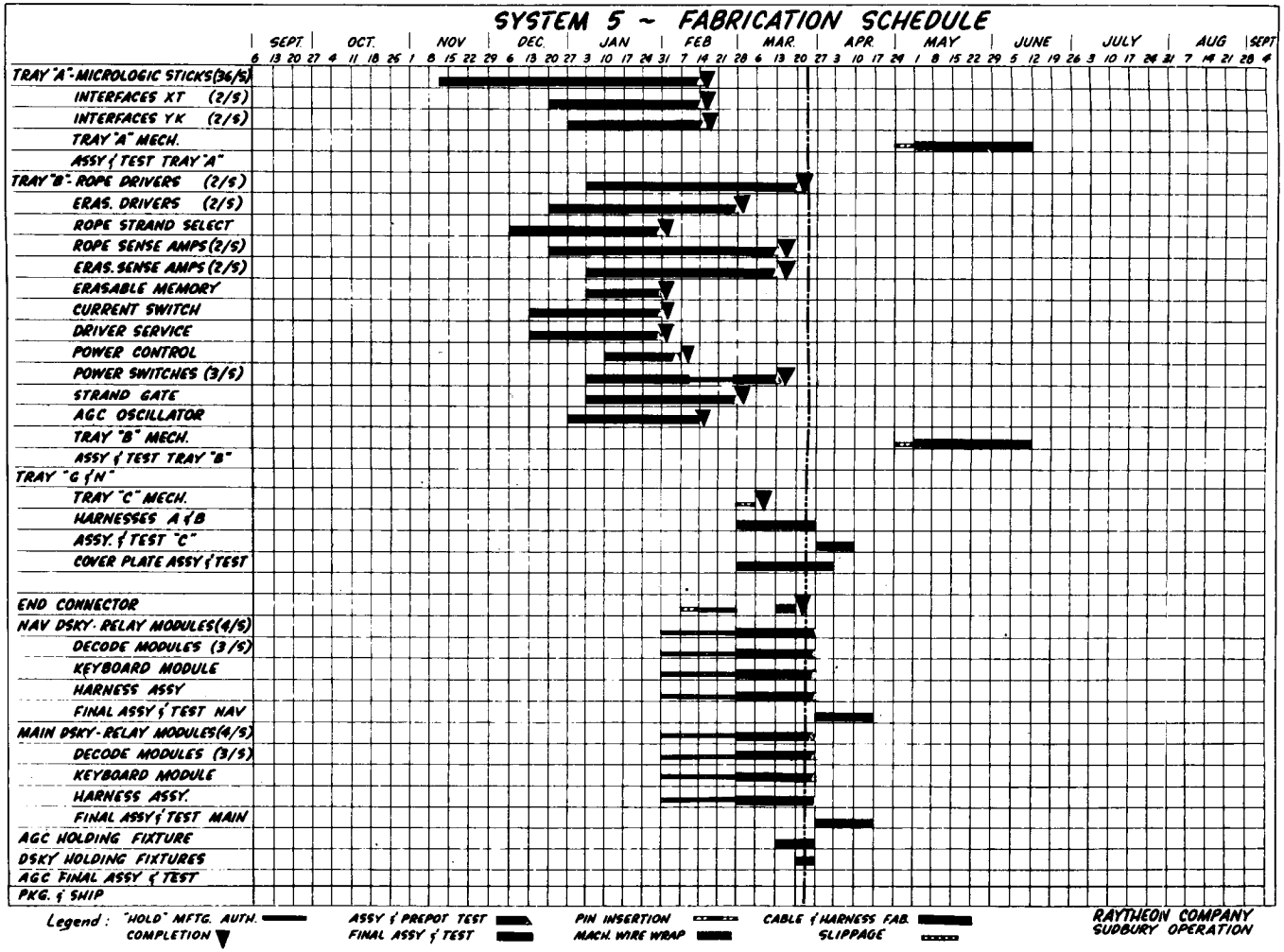
SYSTEM 5 ~ FABRICATION SCHEDULE
SEPT
OCT.
NOV
DEC.
JAN
FEB
MAR.
APR.
MAY
JUNE
JULY
AUG
SEPT
6 13 20 27 4 11 18 25 1 8 15 22 29 6 13 20 27 3 10 17 24 31 7 14 21 28 6 13 20 27 3 10 17 24 1 8 15 22 29 5 12 19 26 3 10 17 24 31 7 14 21 28 4
TRAY "A"-MICROLOGIC STICKS(36/S)
INTERFACES XT (2/S)
INTERFACES YK (2/S)
TRAY "A" MECH.
ASSY & TEST TRAY "A"
TRAY "B"- ROPE DRIVERS (2/S)
ERAS. DRIVERS (2/S)
ROPE STRAND SELECT
ROPE SENSE AMPS (2/S)
ERAS. SENSE AMPS (2/S)
ERASABLE MEMORY
CURRENT SWITCH
DRIVER SERVICE
POWER CONTROL
POWER SWITCHES (3/S)
STRAND GATE
AGC OSCILLATOR
TRAY "B" MECH.
ASSY & TEST TRAY "B"
TRAY "G & N"
TRAY "C" MECH.
HARNESSES A & B
ASSY. & TEST "C"
COVER PLATE ASSY & TEST
END CONNECTOR
NAV DSKY- RELAY MODULES(4/S)
DECODE MODULES (3/S)
KEYBOARD MODULE
HARNESS ASSY
FINAL ASSY & TEST NAV
MAIN DSKY- RELAY MODULES(4/S)
DECODE MODULES (3/S)
KEYBOARD MODULE
HARNESS ASSY.
FINAL ASSY & TEST MAIN
AGC HOLDING FIXTURE
DSKY HOLDING FIXTURES
AGC FINAL ASSY & TEST
PKG. & SHIP
Legend : "HOLD" MFTG. AUTH.
COMPLETION
ASSY & PREPOT TEST
FINAL ASSY & TEST
PIN INSERTION
MACH. WIRE WRAP
CABLE & HARNESS FAB.
SLIPPAGE
RAYTHEON COMPANY
SUDBURY OPERATION

Fig. 10-17

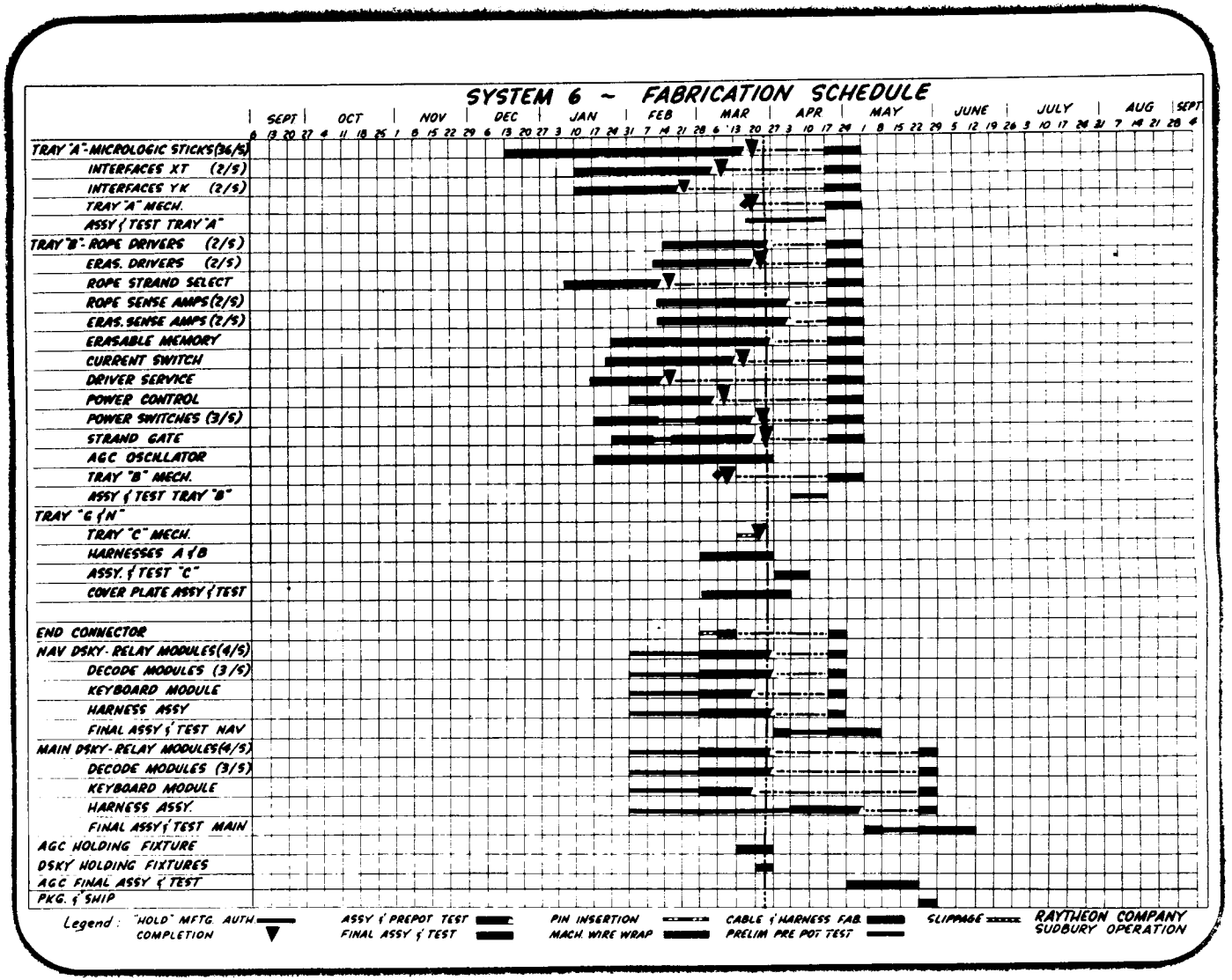
SYSTEM 6 ~ FABRICATION SCHEDULE
SEPT
OCT
NOV
DEC
JAN
FEB
MAR
APR
MAY
JUNE
JULY
AUG
SEPT
TRAY "A"- MICROLOGIC STICKS (36/S)
INTERFACES XT (2/S)
INTERFACES YK (2/S)
TRAY "A" MECH.
ASSY & TEST TRAY "A"
TRAY "B"- ROPE DRIVERS (2/S)
ERAS. DRIVERS (2/S)
ROPE STRAND SELECT
ROPE SENSE AMPS (2/S)
ERAS. SENSE AMPS (2/S)
ERASABLE MEMORY
CURRENT SWITCH
DRIVER SERVICE
POWER CONTROL
POWER SWITCHES (3/S)
STRAND GATE
AGC OSCILLATOR
TRAY "B" MECH.
ASSY & TEST TRAY "B"
TRAY "C & N"
TRAY "C" MECH.
HARNESSES A & B
ASSY. & TEST "C"
COVER PLATE ASSY & TEST
END CONNECTOR
NAV DSKY- RELAY MODULES (4/S)
DECODE MODULES (3/S)
KEYBOARD MODULE
HARNESS ASSY
FINAL ASSY & TEST NAV
MAIN DSKY- RELAY MODULES (4/S)
DECODE MODULES (3/S)
KEYBOARD MODULE
HARNESS ASSY.
FINAL ASSY & TEST MAIN
AGC HOLDING FIXTURE
DSKY HOLDING FIXTURES
AGC FINAL ASSY & TEST
PKG. & SHIP
Legend: "HOLD" MFTG. AUTH
COMPLETION
ASSY & PREPOT TEST
FINAL ASSY & TEST
PIN INSERTION
MACH. WIRE WRAP
CABLE & HARNESS FAB.
PRELIM PRE POT TEST
SLIPPAGE
RAYTHEON COMPANY
SUDBURY OPERATION

Fig. 10-18

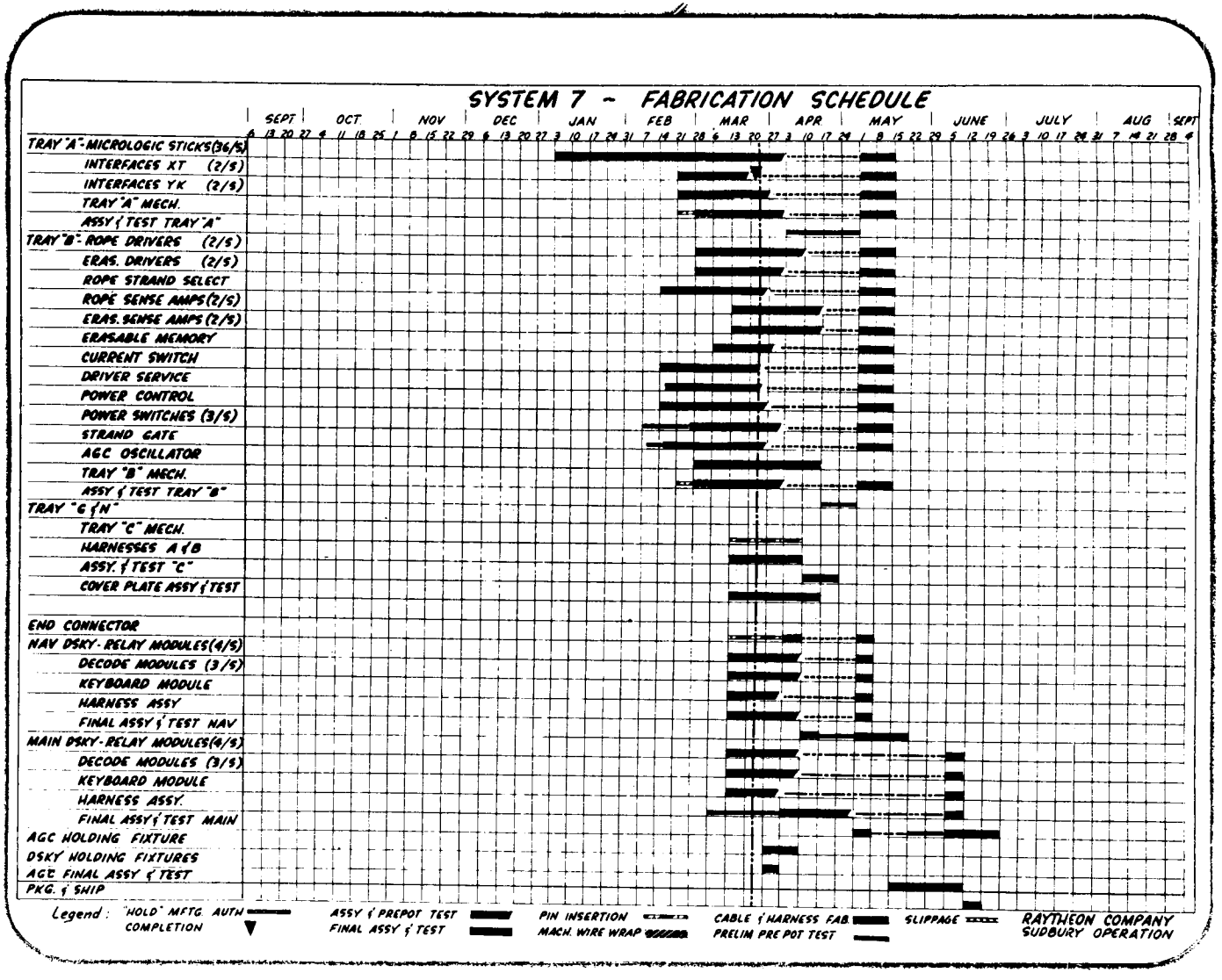
SYSTEM 7 - FABRICATION SCHEDULE
SEPT
OCT
NOV
DEC
JAN
FEB
MAR
APR
MAY
JUNE
JULY
AUG
SEPT
TRAY "A" - MICROLOGIC STICKS (36/S)
INTERFACES XT (2/S)
INTERFACES YK (2/S)
TRAY "A" MECH.
ASSY & TEST TRAY "A"
TRAY "B" - ROPE DRIVERS (2/S)
ERAS. DRIVERS (2/S)
ROPE STRAND SELECT
ROPE SENSE AMPS (2/S)
ERAS. SENSE AMPS (2/S)
ERASABLE MEMORY
CURRENT SWITCH
DRIVER SERVICE
POWER CONTROL
POWER SWITCHES (3/S)
STRAND GATE
AGC OSCILLATOR
TRAY "B" MECH.
ASSY & TEST TRAY "B"
TRAY "C & N"
TRAY "C" MECH.
HARNESSES A & B
ASSY. & TEST "C"
COVER PLATE ASSY & TEST
END CONNECTOR
NAV DSKY - RELAY MODULES (4/S)
DECODE MODULES (3/S)
KEYBOARD MODULE
HARNESS ASSY
FINAL ASSY & TEST NAV
MAIN DSKY - RELAY MODULES (4/S)
DECODE MODULES (3/S)
KEYBOARD MODULE
HARNESS ASSY.
FINAL ASSY & TEST MAIN
AGC HOLDING FIXTURE
DSKY HOLDING FIXTURES
AGC FINAL ASSY & TEST
PKG. & SHIP
Legend: "HOLD" MFTG. AUTH
COMPLETION
ASSY & PREPOT TEST
FINAL ASSY & TEST
PIN INSERTION
MACH. WIRE WRAP
CABLE & HARNESS FAB.
PRELIM PRE POT TEST
SLIPPAGE
RAYTHEON COMPANY
SUDBURY OPERATION

Fig. 10-19

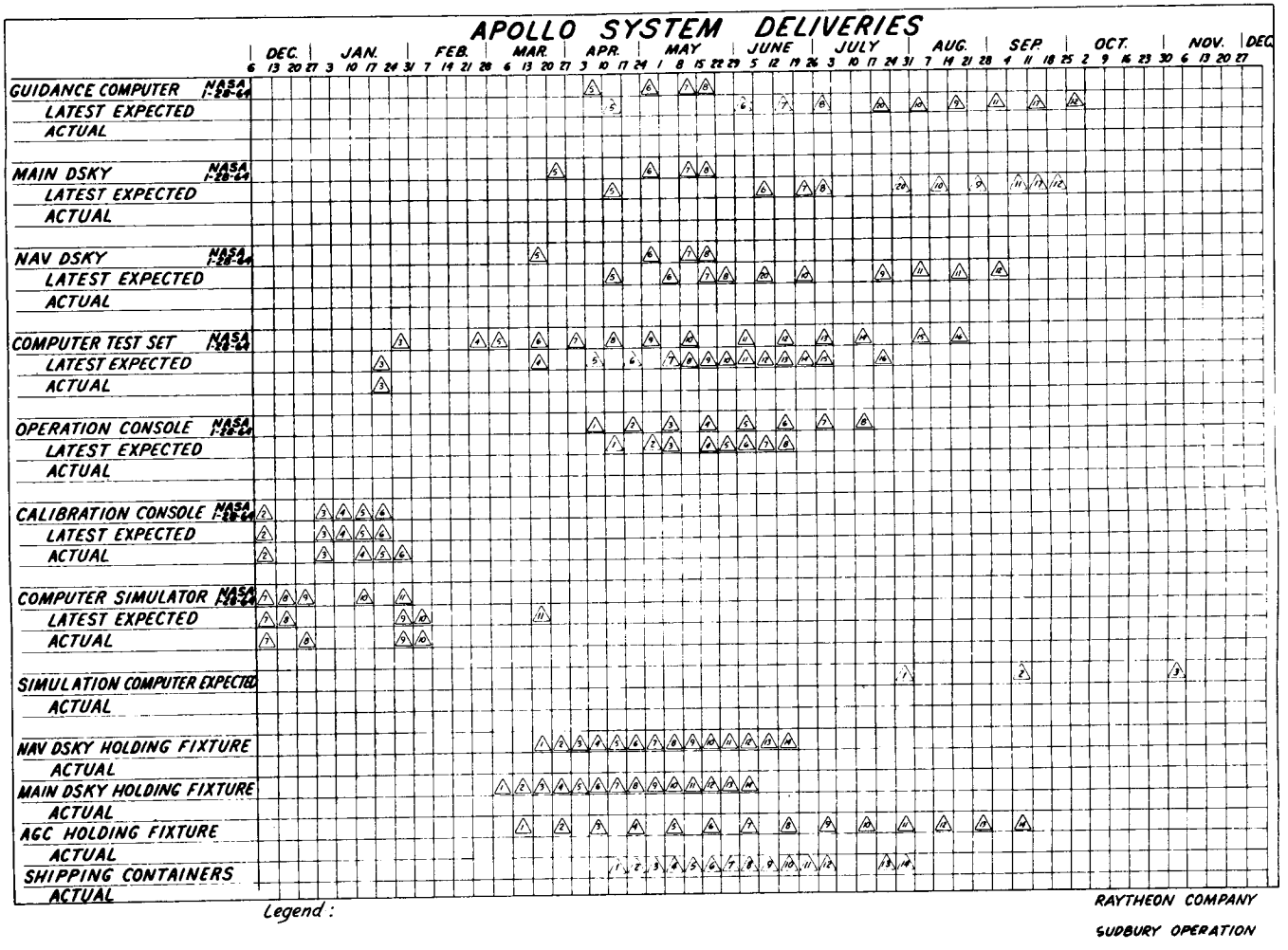
APOLLO SYSTEM DELIVERIES
DEC.
JAN.
FEB.
MAR.
APR.
MAY
JUNE
JULY
AUG.
SEP.
OCT.
NOV.
GUIDANCE COMPUTER NASA 1-28-64
LATEST EXPECTED
ACTUAL
MAIN DSKY NASA 1-28-64
LATEST EXPECTED
ACTUAL
NAV DSKY NASA 1-28-64
LATEST EXPECTED
ACTUAL
COMPUTER TEST SET NASA 1-28-64
LATEST EXPECTED
ACTUAL
OPERATION CONSOLE NASA 1-28-64
LATEST EXPECTED
ACTUAL
CALIBRATION CONSOLE NASA 1-28-64
LATEST EXPECTED
ACTUAL
COMPUTER SIMULATOR NASA 1-28-64
LATEST EXPECTED
ACTUAL
SIMULATION COMPUTER EXPECTED
ACTUAL
NAV DSKY HOLDING FIXTURE
ACTUAL
MAIN DSKY HOLDING FIXTURE
ACTUAL
AGC HOLDING FIXTURE
ACTUAL
SHIPPING CONTAINERS
ACTUAL
Legend :
RAYTHEON COMPANY
SUDBURY OPERATION

Fig. 10-20

Fig. 10-21

will be out in time to test check the computer. The rope fabrication schedule is shown in Fig. 10-22. The ropes shown are test modules. The first group of ropes is to go in AGC-4B. They are all prototype ropes and are not folded or potted.

Some test equipment at Raytheon is now in operation. Figure 10-23 is a DITMCO machine used to check the wiring on the trays.

The operation console which mounts the computer subsystem for test is shown in Fig. 10-24. This particular artist's concept shows the four modules in the computer, with one module out on an extender, presumably to do some testing. The operation console provides coolant and power for the computer when it is in a subsystem test configuration.

A typical program to qualify components is shown in Fig. 10-25. The initial micro nor gate activity started about two years ago, when a few were procured and tested. It was established that the vendor had the capability of producing. Then vendor qualification was established, as was process control, and a specification control document was written to procure larger quantities. The lab tests are the data received from the prototype computers AGC's 4 and 4B. From the information obtained from the stress testing, etc., we go into data analysis and failure mode analysis and feed back information to correct the documentation and control of the product. Then the procurement process begins from the specification control document as shown in Fig. 10-26.

This specification control document requires the vendor to do part rejection. Then the parts come into Raytheon and they go through a 100% mechanical and leak test. Everything from this point on is a 100% test within Raytheon. From there they go to the first electrical test, to a bake, centrifuge, thermal, shock, and a second electrical test (all of this is a 100%), then a power burn in and a third electrical test before it goes to the computer. From each of these points information is sorted for both data and fail units and fed into data failure analyses at Raytheon, after which the information is fed back into the vendor qualification list.

Figure 10-27 shows the production screening and burn in test results by vendor. Sample size is number of units that have gone through, and the percentage of rejects is shown for each vendor. Vendor C does not appear too satisfactory when compared with A & B. A & B are being used in flight hardware.

The results of step stress testing are shown in Fig. 10-28. Again vendors A & B performed better than C. Stress level I is essentially the same test as performed at screening and burn in: level II is more rigid; more temperature cycles, larger ranges, higher shocks: and level III is higher than II. The results shown are for 100 units tested.

The next step is to predict a failure rate for nor gates. In February and March 1963, 0.2 failures per 30×10^6 component hours was predicted. Calculated values based on operating times of AGC's 4 and 4B are shown on the Fig. 10-29. While failures have

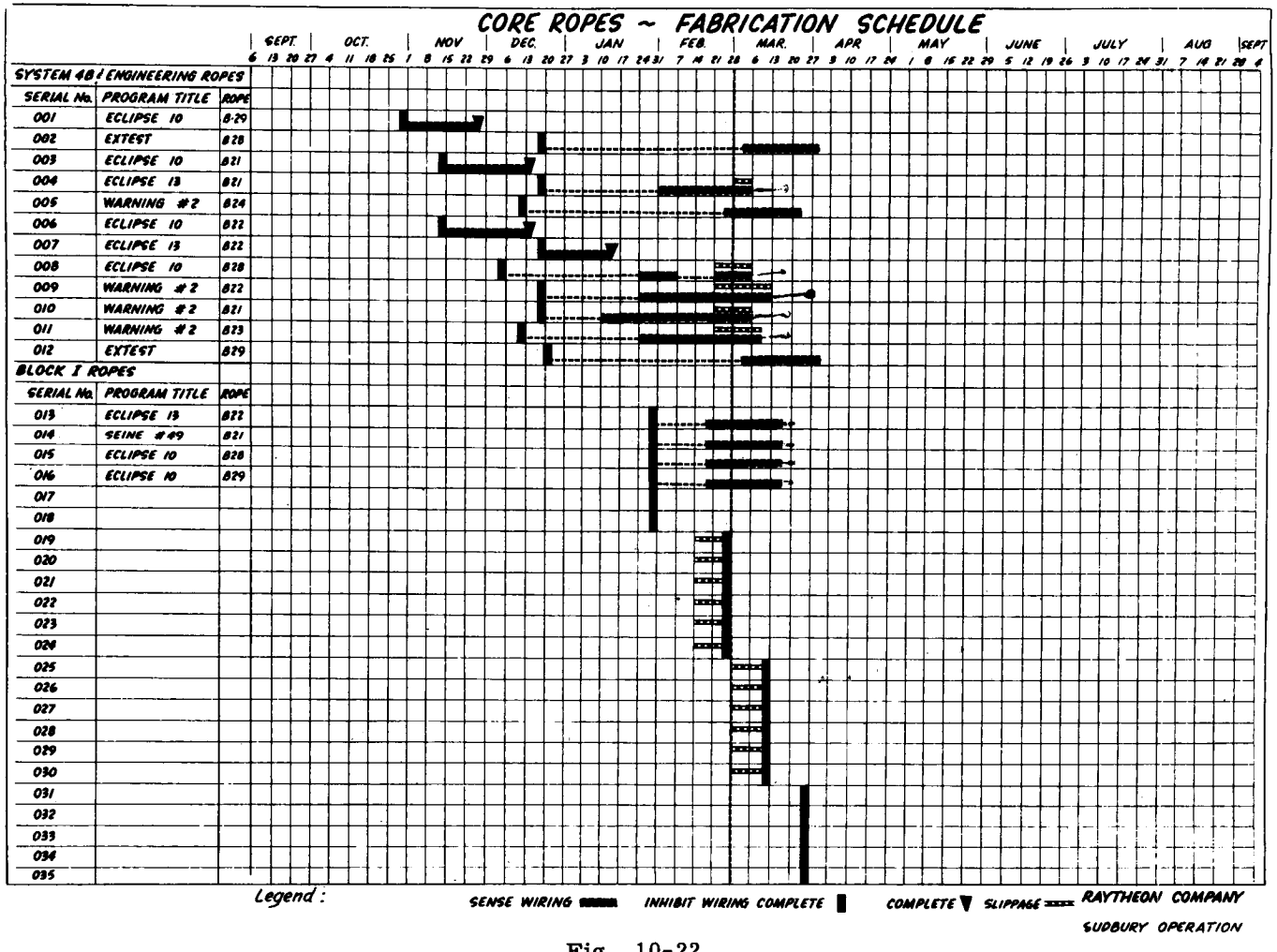
CORE ROPES ~ FABRICATION SCHEDULE
SEPT. OCT. NOV DEC. JAN FEB. MAR. APR MAY JUNE JULY AUG SEPT
SYSTEM 48 / ENGINEERING ROPES
SERIAL No. PROGRAM TITLE ROPE
001 ECLIPSE 10 B-29
002 EXTEST B28
003 ECLIPSE 10 B21
004 ECLIPSE 13 B21
005 WARNING #2 B24
006 ECLIPSE 10 B22
007 ECLIPSE 13 B22
008 ECLIPSE 10 B28
009 WARNING #2 B22
010 WARNING #2 B21
011 WARNING #2 B23
012 EXTEST B29
BLOCK I ROPES
SERIAL No. PROGRAM TITLE ROPE
013 ECLIPSE 13 B22
014 SEINE #49 B21
015 ECLIPSE 10 B28
016 ECLIPSE 10 B29
017
018
019
020
021
022
023
024
025
026
027
028
029
030
031
032
033
034
035
Legend :
SENSE WIRING
INHIBIT WIRING COMPLETE
COMPLETE
SLIPPAGE
RAYTHEON COMPANY
SUDBURY OPERATION

Fig. 10-22

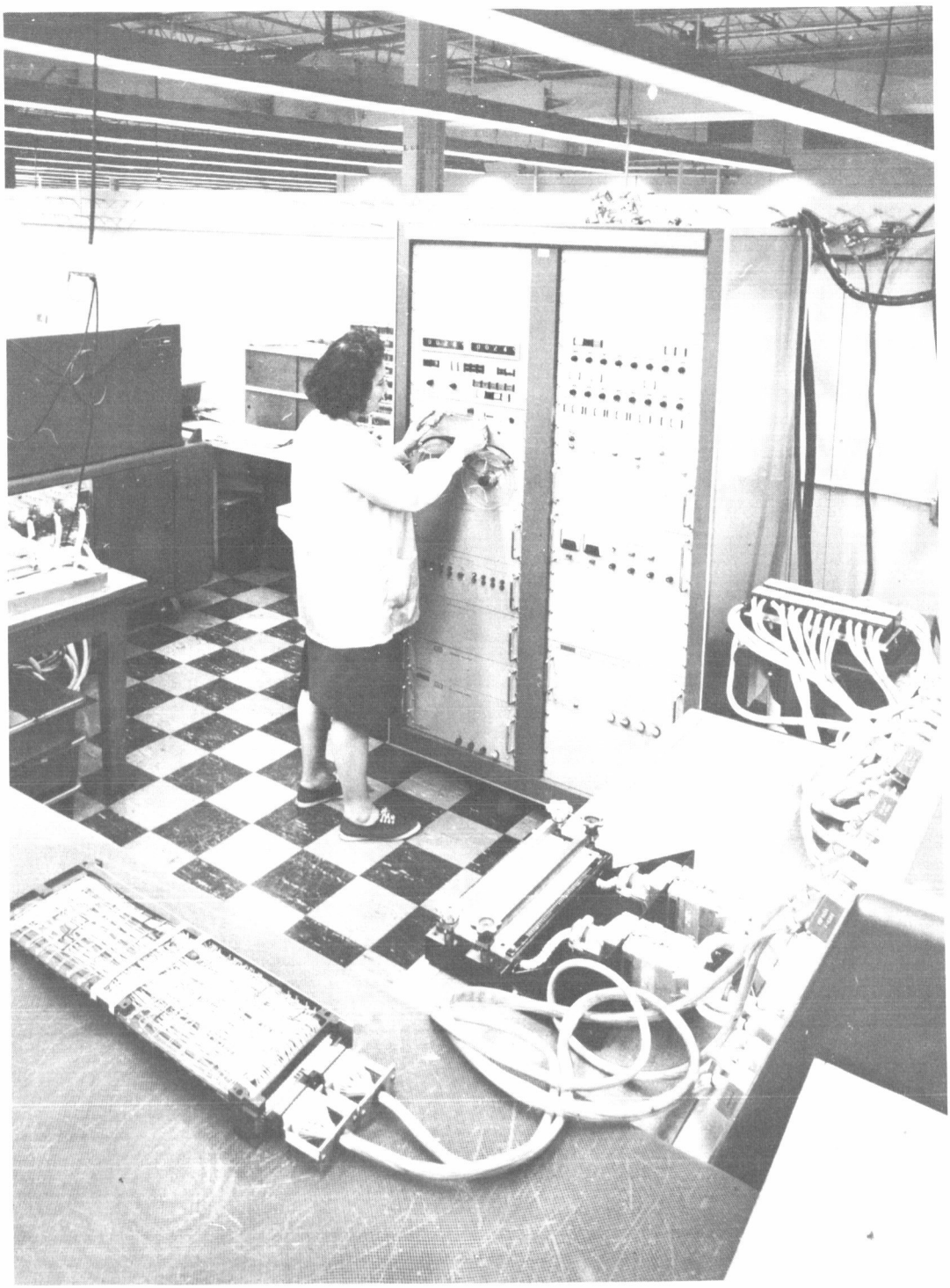

Fig. 10-23

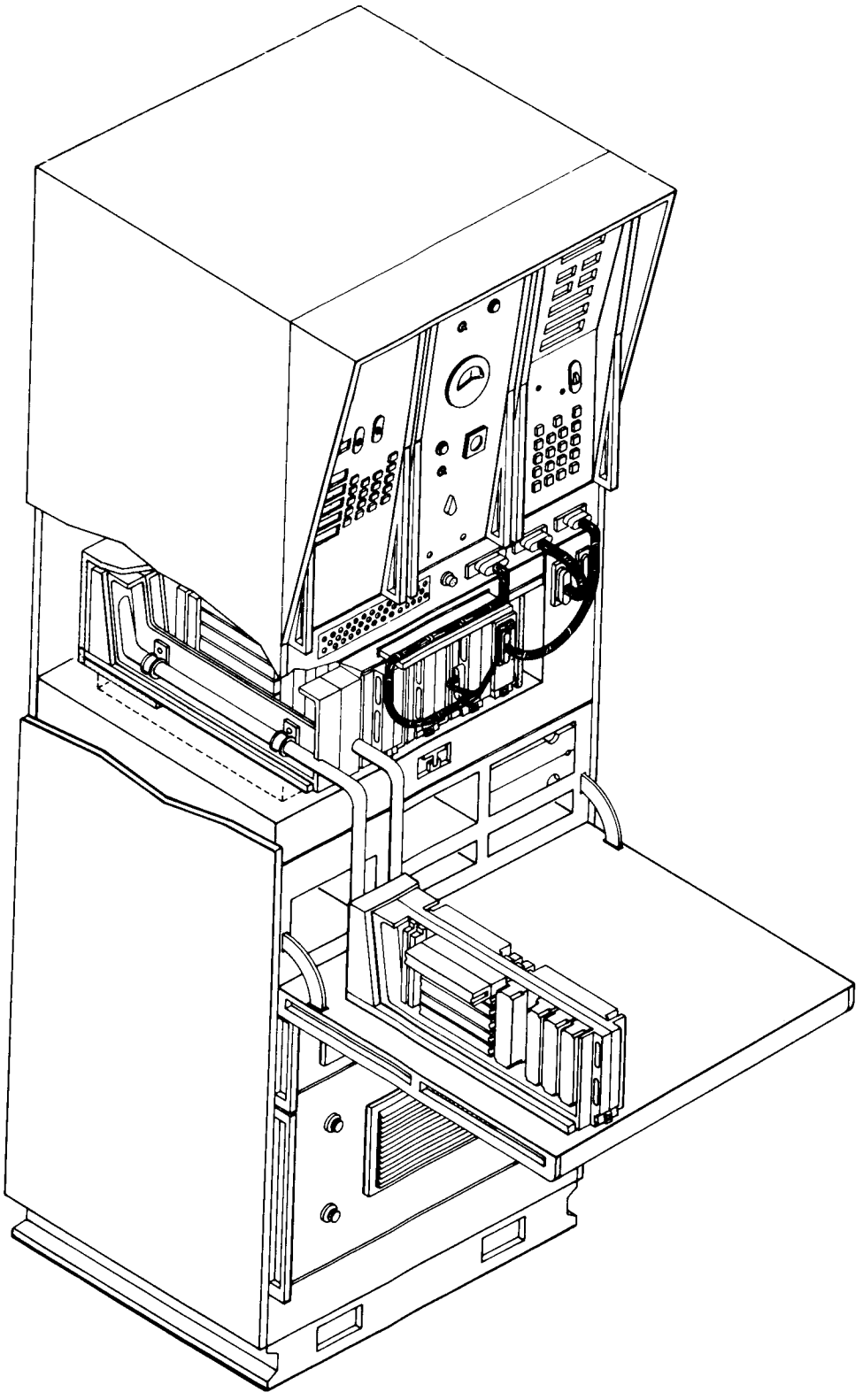

Fig. 10-24

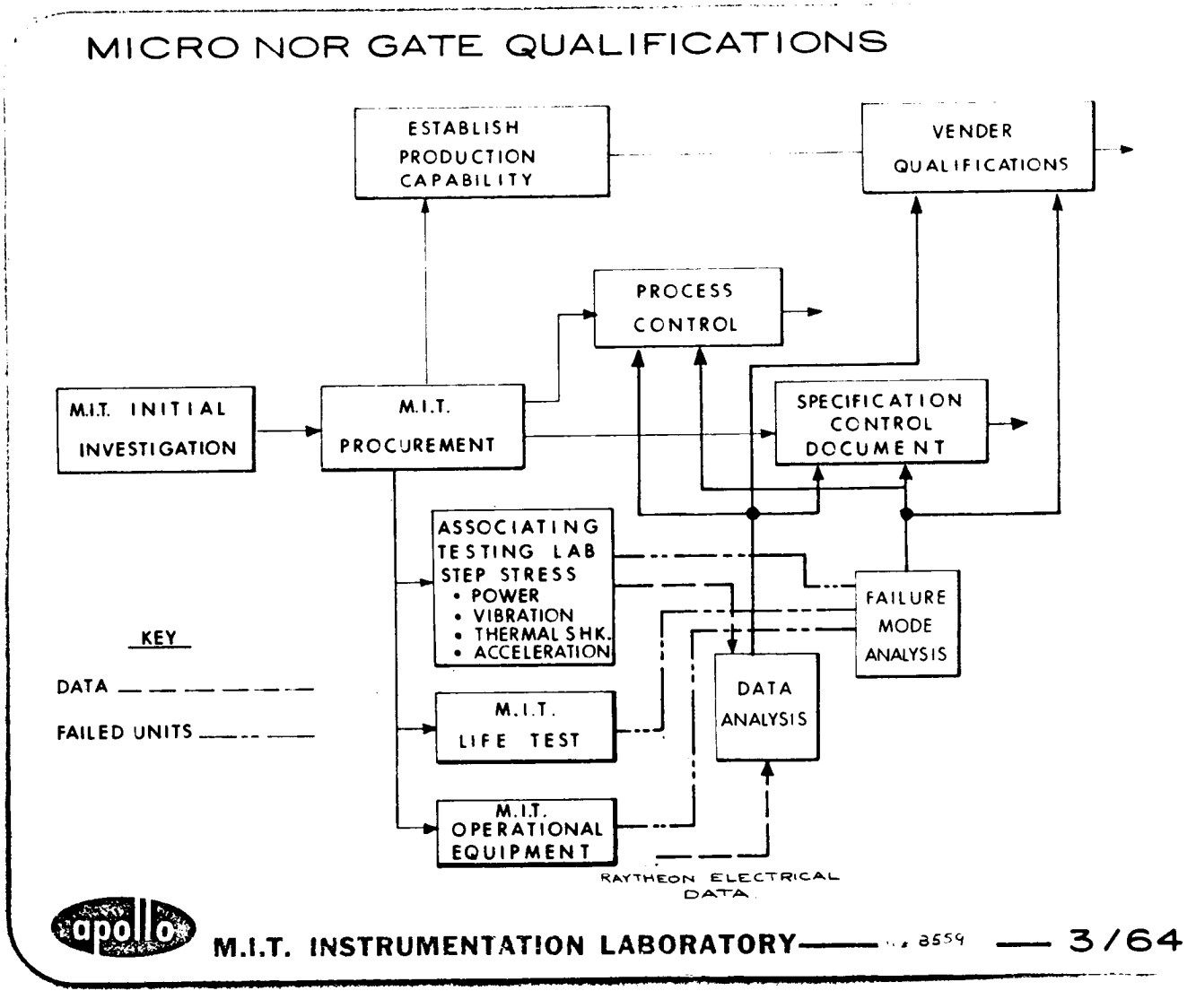
MICRO NOR GATE QUALIFICATIONS
ESTABLISH PRODUCTION CAPABILITY
VENDER QUALIFICATIONS
PROCESS CONTROL
M.I.T. INITIAL INVESTIGATION
M.I.T. PROCUREMENT
SPECIFICATION CONTROL DOCUMENT
ASSOCIATING TESTING LAB STEP STRESS
• POWER
• VIBRATION
• THERMAL SHK.
• ACCELERATION
FAILURE MODE ANALYSIS
KEY
DATA
FAILED UNITS
M.I.T. LIFE TEST
DATA ANALYSIS
M.I.T. OPERATIONAL EQUIPMENT
RAYTHEON ELECTRICAL DATA
apollo
M.I.T. INSTRUMENTATION LABORATORY
8559
3/64

Fig. 10-25

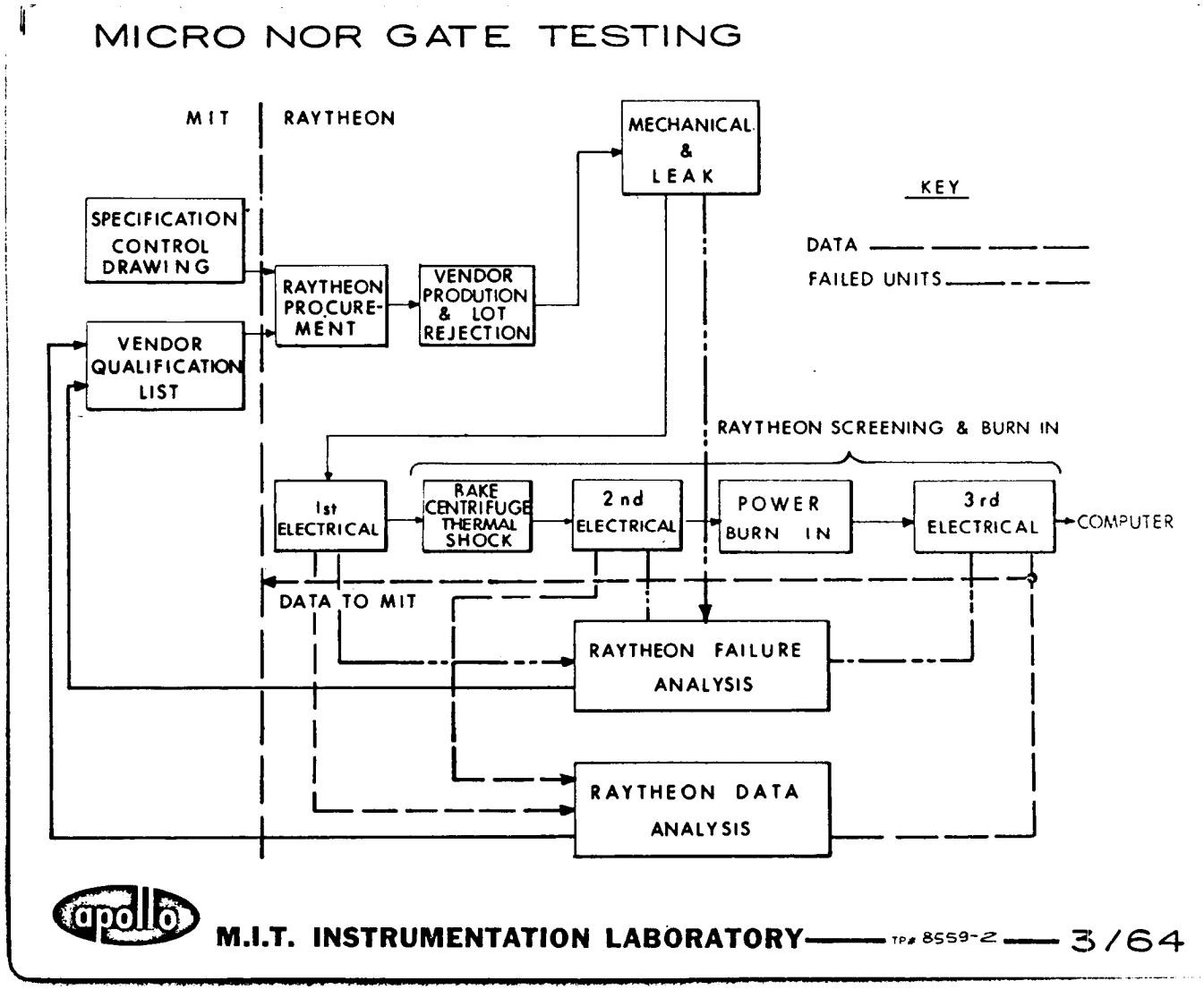
MICRO NOR GATE TESTING
MIT
RAYTHEON
MECHANICAL & LEAK
KEY
DATA
FAILED UNITS
SPECIFICATION CONTROL DRAWING
RAYTHEON PROCURE-MENT
VENDOR PRODUTION & LOT REJECTION
VENDOR QUALIFICATION LIST
RAYTHEON SCREENING & BURN IN
1st ELECTRICAL
RAKE CENTRIFUGE THERMAL SHOCK
2nd ELECTRICAL
POWER BURN IN
3rd ELECTRICAL
COMPUTER
DATA TO MIT
RAYTHEON FAILURE ANALYSIS
RAYTHEON DATA ANALYSIS
apollo
M.I.T. INSTRUMENTATION LABORATORY
TP# 8559-2
3/64

Fig. 10-26

PRODUCTION SCREENING AND BURN IN

	VENDOR A		VENDOR B		VENDOR C	
	Sample Size	% Rejects	Sample Size	% Rejects	Sample Size	% Rejects
MECH.	33,755	1.3	1538	4.7	4033	2.6
LEAK	33,755	0.3	1538	0	4033	0.2
1st ELEC.	33,755	0.3	1538	0.7	4033	0.9
2nd ELEC.	17,249	0.21	1538	0.85	2577	2.8
3rd ELEC.	17,249	0.12	1538	0.5	2577	0.1

SUMMARY OF RAYTHEON'S INCOMING INSPECTION AND SCREEN AND BURN IN MICRO NOR GATE

M.I.T. INSTRUMENTATION LABORATORY——— [illegible] ——— 3/64

Fig. 10-27

STEP STRESS TESTING

STRESS LEVEL	VENDOR A	VENDOR B	VENDOR C
I	2	3	6
II	0	0	8
III	2	0	11

COMPARISON OF ELECTRICAL FAILURES GENERATED AMONG VENDORS DURING TESTING AT ASSOCIATED TESTING LABS

Fig. 10-28

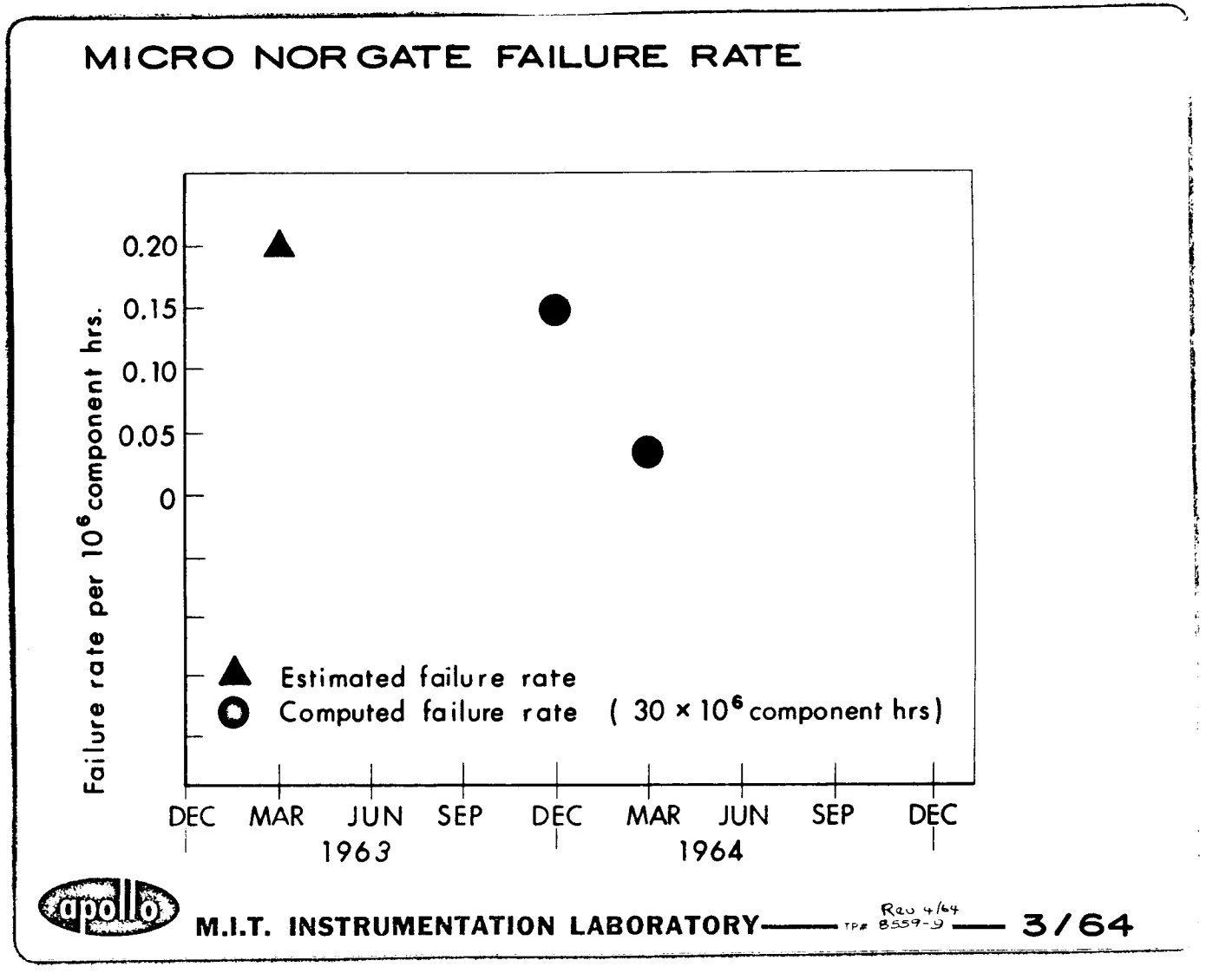
MICRO NOR GATE FAILURE RATE
Failure rate per 10^6 component hrs.
0.20
0.15
0.10
0.05
0
Estimated failure rate
Computed failure rate (30×10^6 component hrs)
DEC
MAR
JUN
SEP
DEC
MAR
JUN
SEP
DEC
1963
1964
apollo
M.I.T. INSTRUMENTATION LABORATORY
TP# 8559-9 Rev 4/64
3/64

Fig. 10-29

occurred on System 4, they would have been picked up by screening if the components used had been screened, so those failures are not included in the failure rate. Redesign has eliminated another failure mode. The latest calculated failure rate is 0.037.

Electromagnetic interference is also being tested. This is shown in Fig. 10-30. This shows interference generated in the computer which can effect the outside world. The procedure is to go through normal MIL Spec interference document using the applicable sections.

Figure 10-31 shows the susceptibility of the computer to interference generated outside. Transient and some sinusoidal tests have been performed. Other tests await the proper equipment.

Figure 10-32 shows the computer test program. Thermal mock-ups of trays are undergoing test now. Module qualification tests have not begun. Computer qualification tests have not started yet. At subsystem level special programs are used for comprehensive electrical checking of the computer. Environmental and mechanical tests will follow at different levels.

ELECTROMAGNETIC INTERFERENCE TESTING

1. INTERFERENCE GENERATION

A. CONDUCTED

1. POWER LINES
2. SIGNAL LINES

B. CROSS COUPLED

1. POWER LINES
2. SIGNAL LINES

C. RADIATED

1. HIGH IMPEDANCE ELECTRIC FIELDS
2. LOW IMPEDANCE MAGNETIC FIELDS

M.I.T. INSTRUMENTATION LABORATORY—— TP# 8559-3 —— 3/64

Fig. 10-30

ELECTROMAGNETIC INTERFERENCE TESTING

II. INTERFERENCE SUSCEPTIBILITY

A. CONDUCTED

1. TRANSIENT
2. SINUSOIDAL
   a. AUDIO FREQUENCY
   b. RADIO FREQUENCY

B. RADIATED

1. HIGH IMPEDANCE ELECTRIC FIELDS
2. LOW IMPEDANCE MAGNETIC FIELDS

Fig. 10-31

COMPUTER TEST PROGRAM

1. COMPUTER SUBASSEMBLY QUALIFICATION
   - a. THERMAL MOCK-UP OF TRAYS
   - b. MODULE QUALIFICATIONS TEST

2. COMPUTER QUALIFICATIONS
   - a. THERMAL
   - b. VIBRATION, SHOCK
   - c. LIFE

3. COMPUTES FTM FOR SELL OFF
   - a. COMPREHENSIVE ELECTRICAL
   - b. ENVIRONMENTAL TEST
     - (1) THERMAL CYCLE
     - (2) VIBRATION
   - c. MECHANICAL & ELECTRICAL
   - d. LONG TERM TEST (200 hrs)
   - e. COMPREHENSIVE ELECTRICAL & MECHANICAL

Fig. 10-32

Section 11

OPTICS MECHANICAL DESCRIPTION AND THE DESIGN QUALIFICATION TESTING PROGRAM*

P. N. Bowditch

The AGE-3 optical unit is shown in Fig. 11-1, installed on the precision test fixture. The sextant (SXT) is to the left and the scanning telescope (SCT) to the right. The two instruments have different functions. The sextant has two lines of sight, one fixed at an angle of 57^{o} from the vehicle thrust vector; the other movable in altitude and azimuth. The fixed line is the landmark line of sight (LLOS), the movable line is the star line of sight (SLOS). The SXT, which has 28X magnification and a 1.8^{o} field of view is used for midcourse and lunar orbital navigational sightings and for IMU erection. The SCT, a single-power, 60^{o} field of view fully-articulating telescope, is used as a target finder for the sextant and for orbital landmark tracking.

Figure 11-2 shows the bellows vacuum seals which separate the S/C interior from outer space. The unit shown is a mechanical gauge used at NAA.

Figure 11-3 shows the optics penetration of spacecraft (S/C) hull, and the doors which cover the opening during re-entry. The total field of view is a 100^{o} conic scan centered 57^{o} from the vehicle thrust axis. The constraints limiting this field of view were that the instrument be stationary with respect to secondary structures, be sealed to the C/M, and have covers for boost and re-entry. This field of view is adequate for required sightings.

The two lines of sight were intentionally put outside in the vacuum to eliminate optical windows which introduce scatter and distortion. The instruments are physically shielded from waste contamnation and from solar radiation scatter. To permit adequate shielding without impeding equipment operation, the shrouds are pulled out as far as possible without interfering with closing of the S/C doors. The covers serve a dual purpose; they shield against thermal radiation, and reduce solar scatter and radiation.

The optical requirements of this precise instrument dictate a stable and accurate assembly. Diligent efforts were made in the instrument design to minimize vacuum and

*Edited transcription of a design review presentation made to NASA (MSC) technical staff members on 3-26-64.

Fig. 11-1 Optics 3.

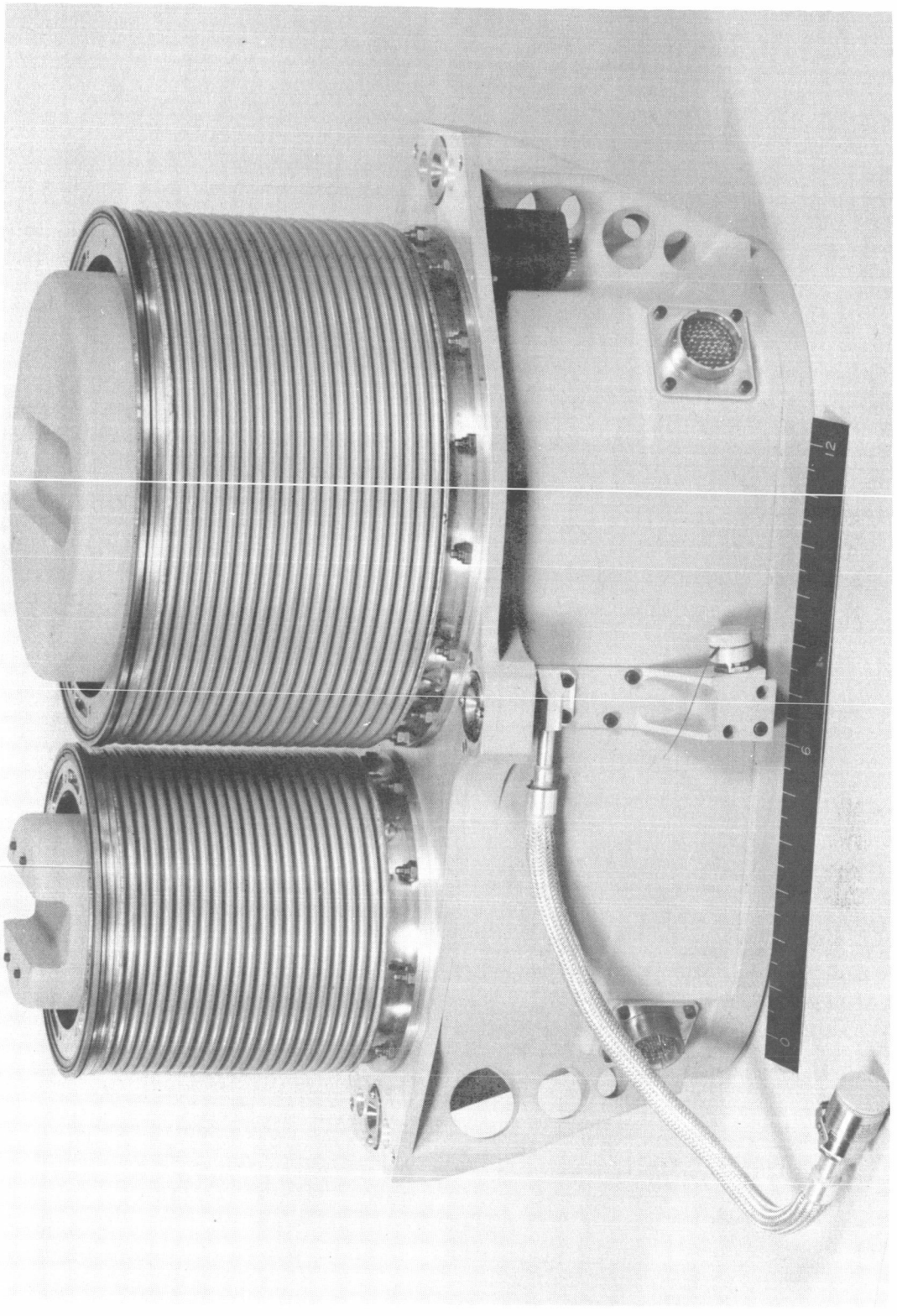

Fig. 11-2

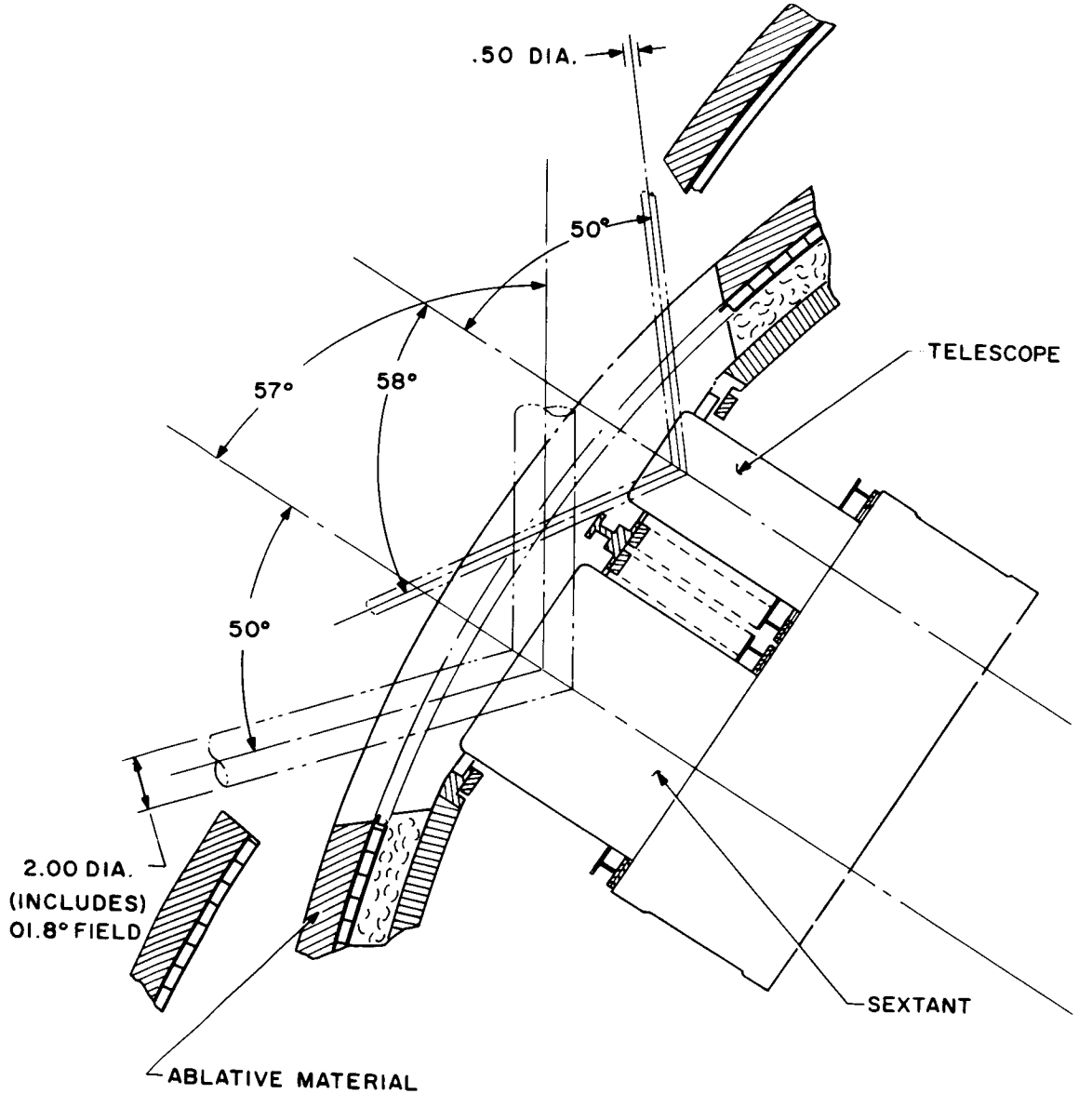
.50 DIA.
50°
57°
58°
50°
TELESCOPE
2.00 DIA.
(INCLUDES)
Ø1.8° FIELD
SEXTANT
ABLATIVE MATERIAL

Fig. 11-3

outer-space effects. Thermal stability must be controlled by conduction and radiation in a vacuum. The thermal shroud and bellows seal strain-isolate any motion of the vehicle relative to the optics base and act as a high thermal impedance to any temperature influence from the S/C, and constitute a vacuum seal. The bellows are double convoluted about each instrument to provide redundancy for vacuum integrity.

The unit is mounted to the Navigation Base on three steel balls for kinematic strain isolation. To preserve the accuracy of the instruments, the optical base is extremely rugged. The bellows and the vacuum seal are required to withstand a differential force of 5 psi between the S/C interior and the outside vacuum which totals some 800 pounds. This force must be considered in the alignment accuracy of the instrument.

Construction has been simplified as much as possible to provide maximum reliablity. Figure 11-4 shows schematic views of the instruments. Sextant operation is identical to a marine or any other kind of sextant. The beam splitter has on its surface a polarizer to obscure the fixed line of sight. This obliterates stars which might appear in the landmark line of sight to confuse the operator. There are limit stops to prevent damage to internal connectors. The instrument may move $\pm 270^{o}$ about the landmark line-of-sight axis; the star line-of-sight may go from 0^{o} (parallel to landmark LOS) to 90^{o} (self-collimating position).

The SCT has a double-dove redirection element which may be rotated about an axis parallel to the SXT trunnion axis. Motions of the two units are phased together.

Fixed to the head of the SXT is an automatic star/landmark tracking unit, the horizon photometer and star tracker. The star tracker uses the same mirror as the star LOS. Thus, one precision angle transducer-resolver is sufficient for all measurements made either visually or automatically. Star target tracking is accomplished by crossed reeds in the star tracker.

Figures 11-5 and 11-6 show optical elements of the SXT and the SCT, respectively. In each figure the eyepiece window is the seal between the interior of the S/C and the instrument. The cutaway drawing of the SXT in Fig. 11-7 shows its mechanization. A flexprint cable takes all leads into and out of the head; there are no slip-rings. Resolvers drive both trunnion and shaft to desired angles.

On the SCT there are manual drives which are not engaged unless there is a power failure. The cutaway of the SCT is shown in Fig. 11-8.

The double dove prism, in Fig. 11-9, is a single reflection element which inverts the image. In order to re-invert the image an odd number of reflections must be introduced into the optical path. This is done by the pechan prism of Fig. 11-10.

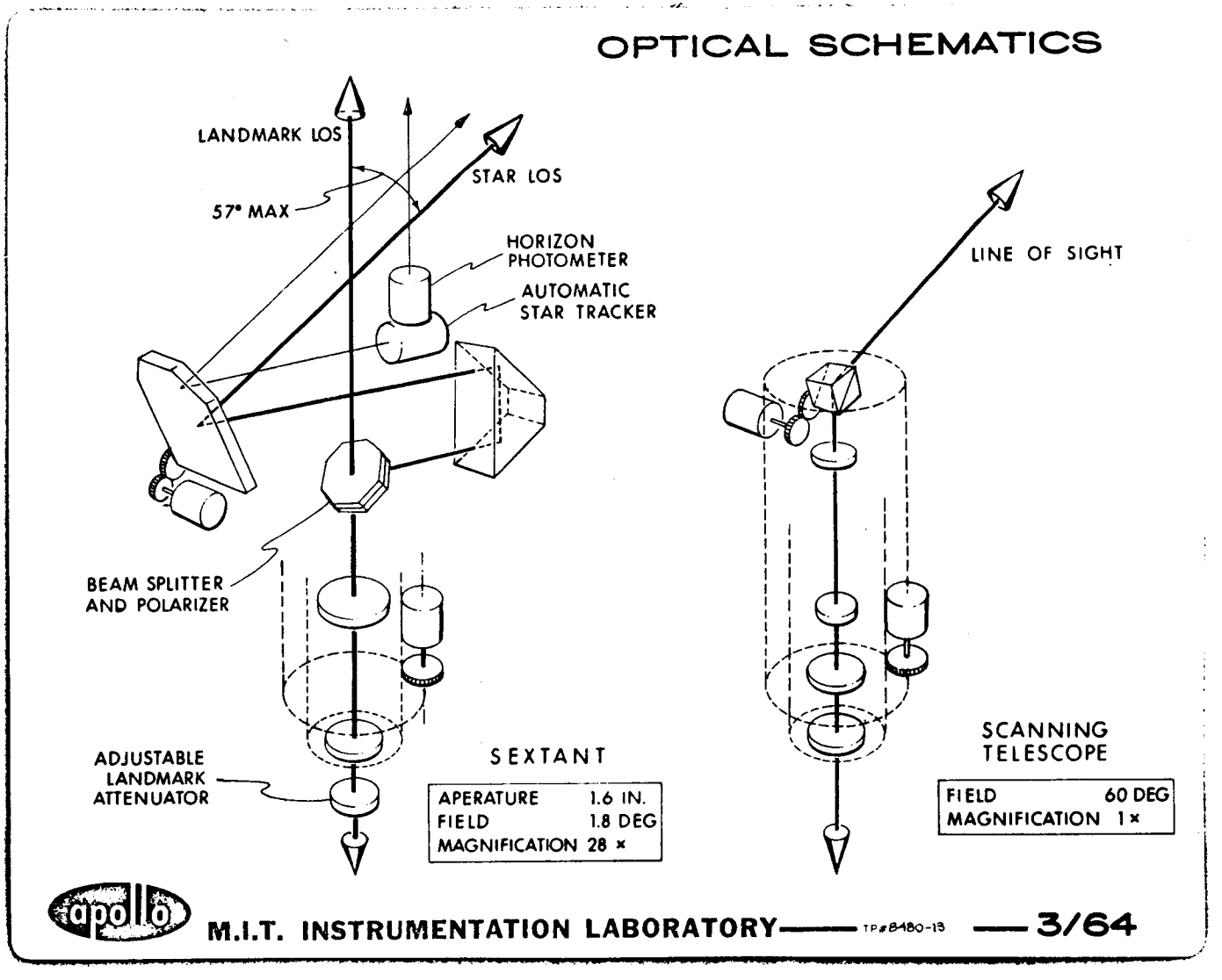
OPTICAL SCHEMATICS
LANDMARK LOS
STAR LOS
57° MAX
HORIZON PHOTOMETER
AUTOMATIC STAR TRACKER
BEAM SPLITTER AND POLARIZER
ADJUSTABLE LANDMARK ATTENUATOR
SEXTANT
APERATURE 1.6 IN.
FIELD 1.8 DEG
MAGNIFICATION 28 ×
LINE OF SIGHT
SCANNING TELESCOPE
FIELD 60 DEG
MAGNIFICATION 1×
apollo
M.I.T. INSTRUMENTATION LABORATORY
TP#8480-13
3/64

Fig. 11-4

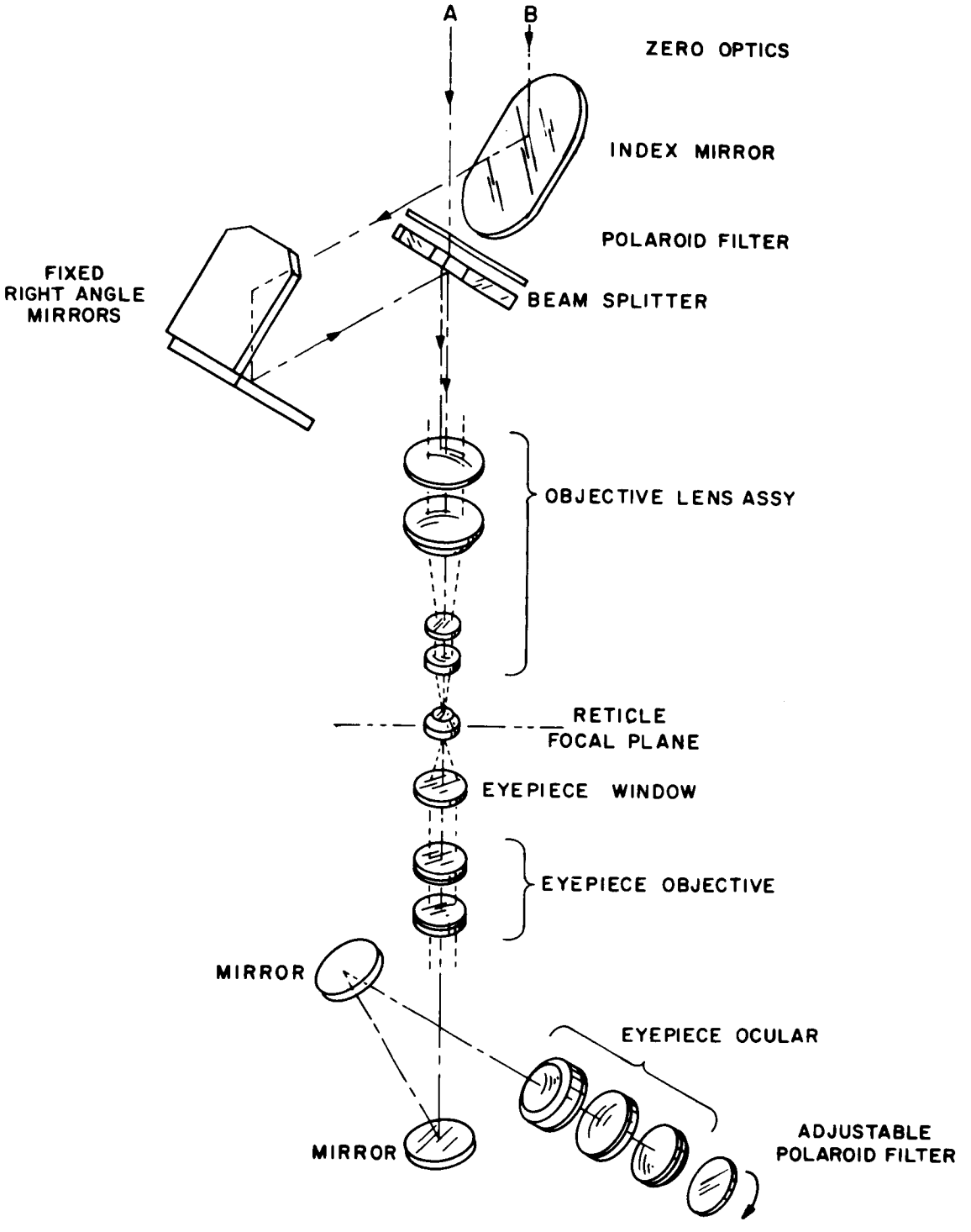
A
B
ZERO OPTICS
INDEX MIRROR
POLAROID FILTER
FIXED
RIGHT ANGLE
MIRRORS
BEAM SPLITTER
OBJECTIVE LENS ASSY
RETICLE
FOCAL PLANE
EYEPIECE WINDOW
EYEPIECE OBJECTIVE
MIRROR
EYEPIECE OCULAR
MIRROR
ADJUSTABLE
POLAROID FILTER

Fig. 11-5

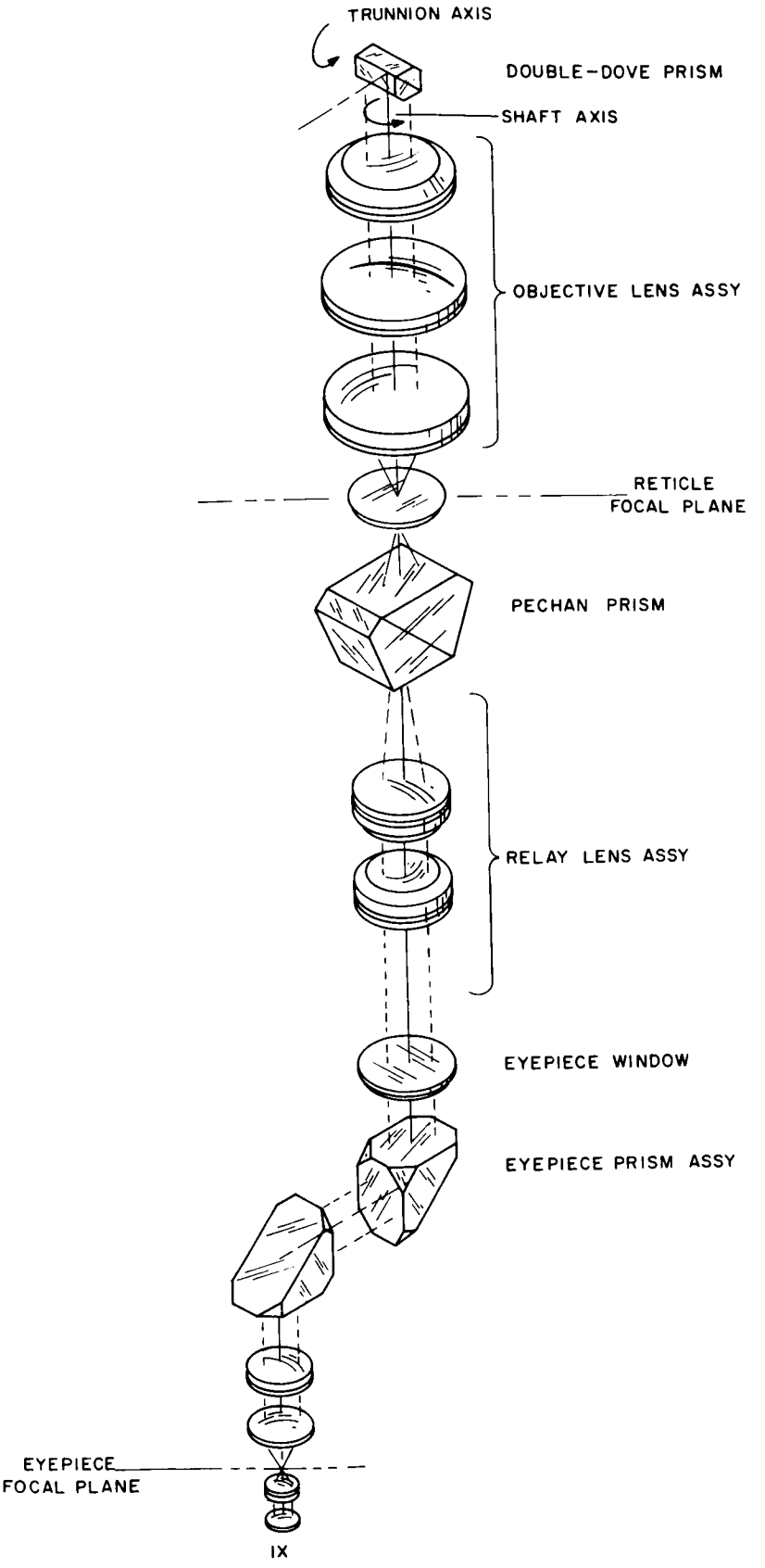
TRUNNION AXIS
DOUBLE-DOVE PRISM
SHAFT AXIS
OBJECTIVE LENS ASSY
RETICLE
FOCAL PLANE
PECHAN PRISM
RELAY LENS ASSY
EYEPIECE WINDOW
EYEPIECE PRISM ASSY
EYEPIECE
FOCAL PLANE
IX

Fig. 11-6

1. OPTICAL BASE
2. COOLANT CONNECTIONS
3. BALL MOUNT
4. STUD HOLES FOR MOUNTING BELLOWS
5. FIXED RIGHT-ANGLE MIRRORS
6. TRUNNION AXIS RESOLVER
7. COVER-FASTENING ROD
8. INDEXING MIRROR
9. BEAM SPLITTER
10. TRUNNION DRIVE GEAR BOX
11. OBJECTIVE LENS ASSEMBLY
12. SHAFT AXIS DRIVE MOTOR
13. RETICLE
14. LIGHT-TRANSMITTING TUBE
15. RETICLE LAMP
16. SHAFT-AXIS RESOLVER
17. SHAFT DRIVE GEAR BOX
18. EYEPIECE WINDOW
19. EYEPIECE OBJECTIVE LENS
20. EYEPIECE MIRRORS
21. EYEPIECE OCULAR

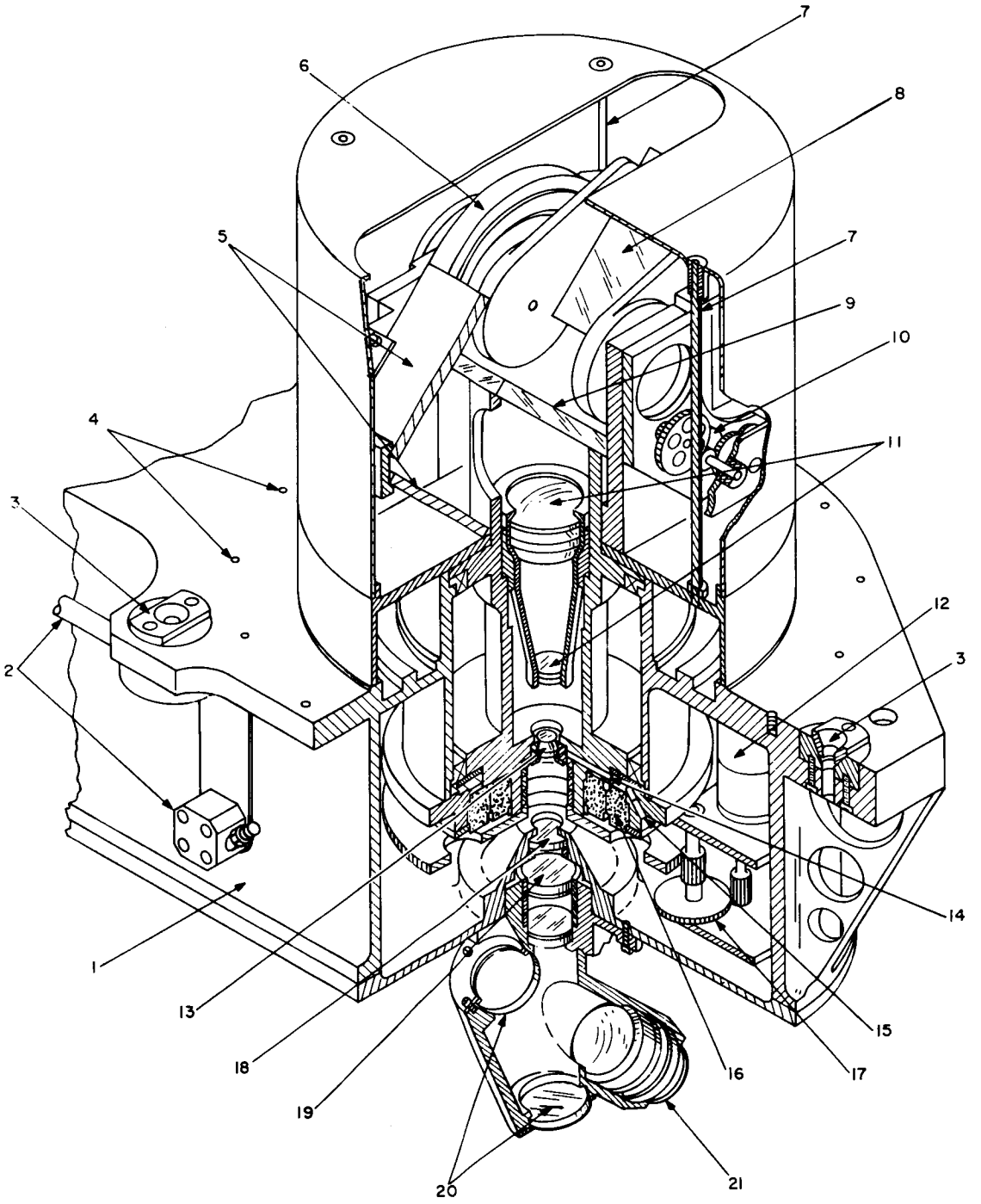

Fig. 11-7

1. EYEPIECE WINDOW
2. ELECTRICAL CONNECTOR
3. RELAY LENS ASSEMBLY
4. OPTICAL BASE
5. PECHAN PRISM
6. BALL MOUNT
7. TRUNNION DRIVE WORMSHAFT
8. PRISM & MOUNT ASSEMBLY
9. CAM
10. SPRING & CAMFOLLOWER (ANTIBACKLASH)
11. OBJECTIVE LENS ASSEMBLY
12. RETICLE
13. RETICLE ILLUMINATION TUBES
14. STUD HOLES FOR BELLOWS
15. SHAFT DRIVE GEAR BOX
16. HEAT EXCHANGER CHANNELS
17. COUNTER (SHAFT AXIS)
18. EYEPIECE ASSEMBLY

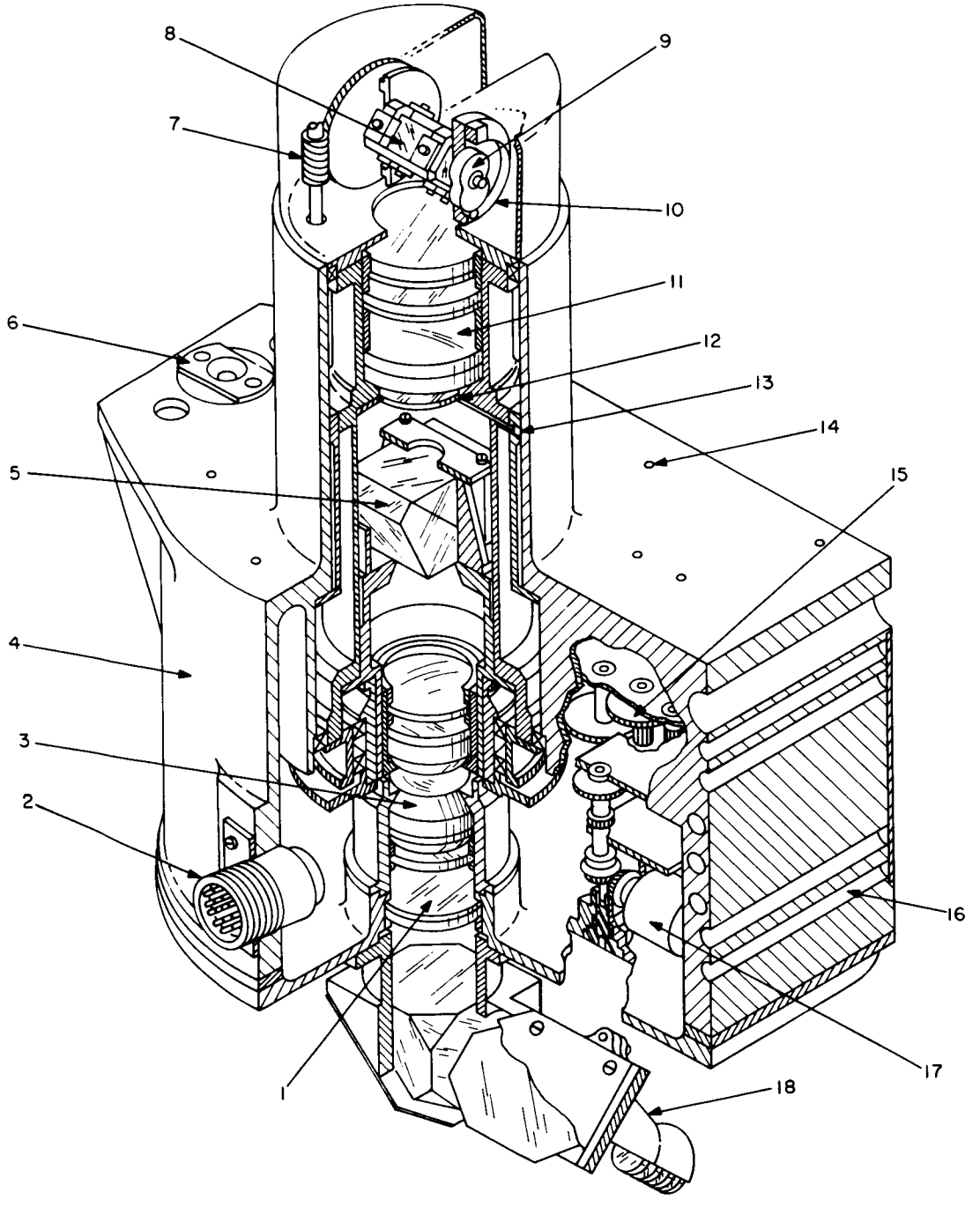

Fig. 11-8

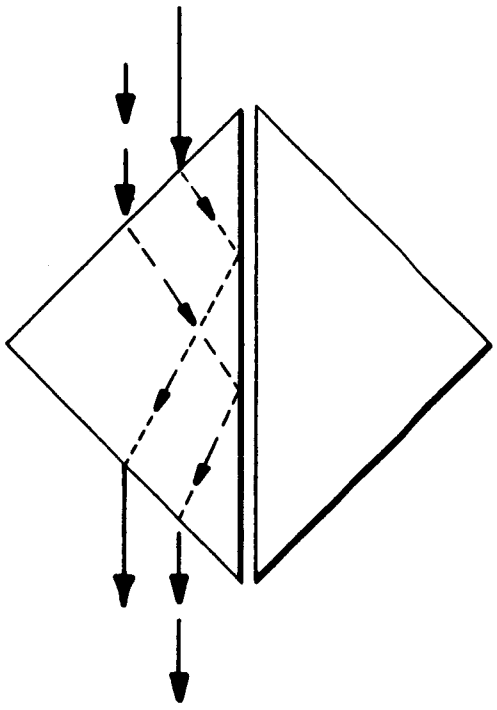

Fig. 11-9 Double dove prism.

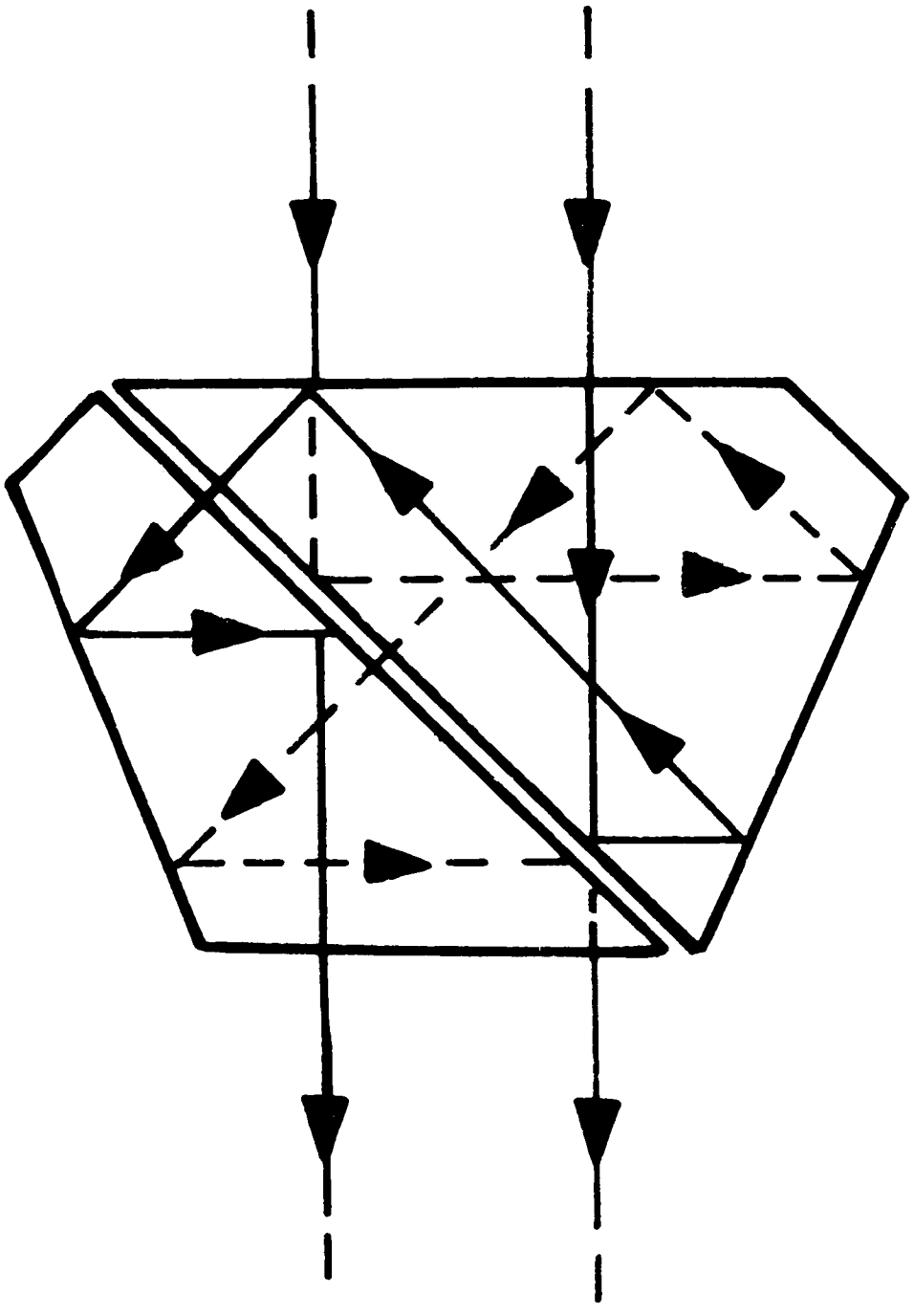

Fig. 11-10

Figure 11-11 shows the SCT gear system. Shown in this design are two universal tool inputs; normally these would not be engaged until power has failed. The astronaut may then turn the instrument manually. Labyrinth seals have been employed wherever any elements are exposed to the space vacuum; no gears or moving parts are exposed. This seal prevents evaporation of the lubricant. The glass elements have also been protected from the mission environment. However, this environment has not been adequately defined.

There are three major design evaluation tests. AGE-3 is at MIT/IL for evaluation of the functional aspects of the instruments as used by the astronauts. Simulations are being conducted to evaluate landmark identification, tracking speeds, tracking conditions, resolution characteristics, etc. The other tests are thermal/vacuum and mechanical integrity vibration evaluations. Kollsman Instrument Corp. has a dual cavity vacuum chamber. Both sides may be pumped to 10^{-9} mm vacuum (approximately 10^{-8} mm with present instrumentation). This chamber enables simulation of the space vacuum on one side and 5 psi cabin pressure on the other, with the instrument between. On the space side there are three viewing positions (ports), one each at viewing axis of 0°, at 12-1/2° off axis, and at 45° off axis. These ports are made of optically flat glass. The sun is simulated by a Genarco source. This instrument may be moved to check scatter conditions. One side of the chamber will be charged with helium-oxygen mixture. The other will contain a mass spectrometer to analyze the leakage characteristics of the seals. The chamber has cryogenic coldwalls capable of about -300°F. The Genarco unit has the equivalent of about three times the power of the sun. It is currently estimated that the temperature during flight on the optical shrouds will be about 125°F on the sun side and about -50°F on the deep space side.

The thermal vacuum tests will evaluate thermal sensitivity of the equipment with respect to accuracy. Instrumentation is available to determine thermal gradients, time constants and transients. This evaluation will begin shortly at Kollsman on AGE-1 optics.

AGE-2 optics will be tested for its response to acoustics, vibration, acceleration and shock. Acceleration tests will be performed on a centrifuge along one axis. Vibration is 3-axis sinusoidal for design evaluation and 3-axis random for qualification tests. These will be at 50%, 75% and 150% of rated design stress levels. These tests will evaluate mechanical integrity of the equipment at launch and flight levels. Re-entry and high Q (abort) constitute survival levels of stress. The instruments need not operate following exposure to these latter levels.

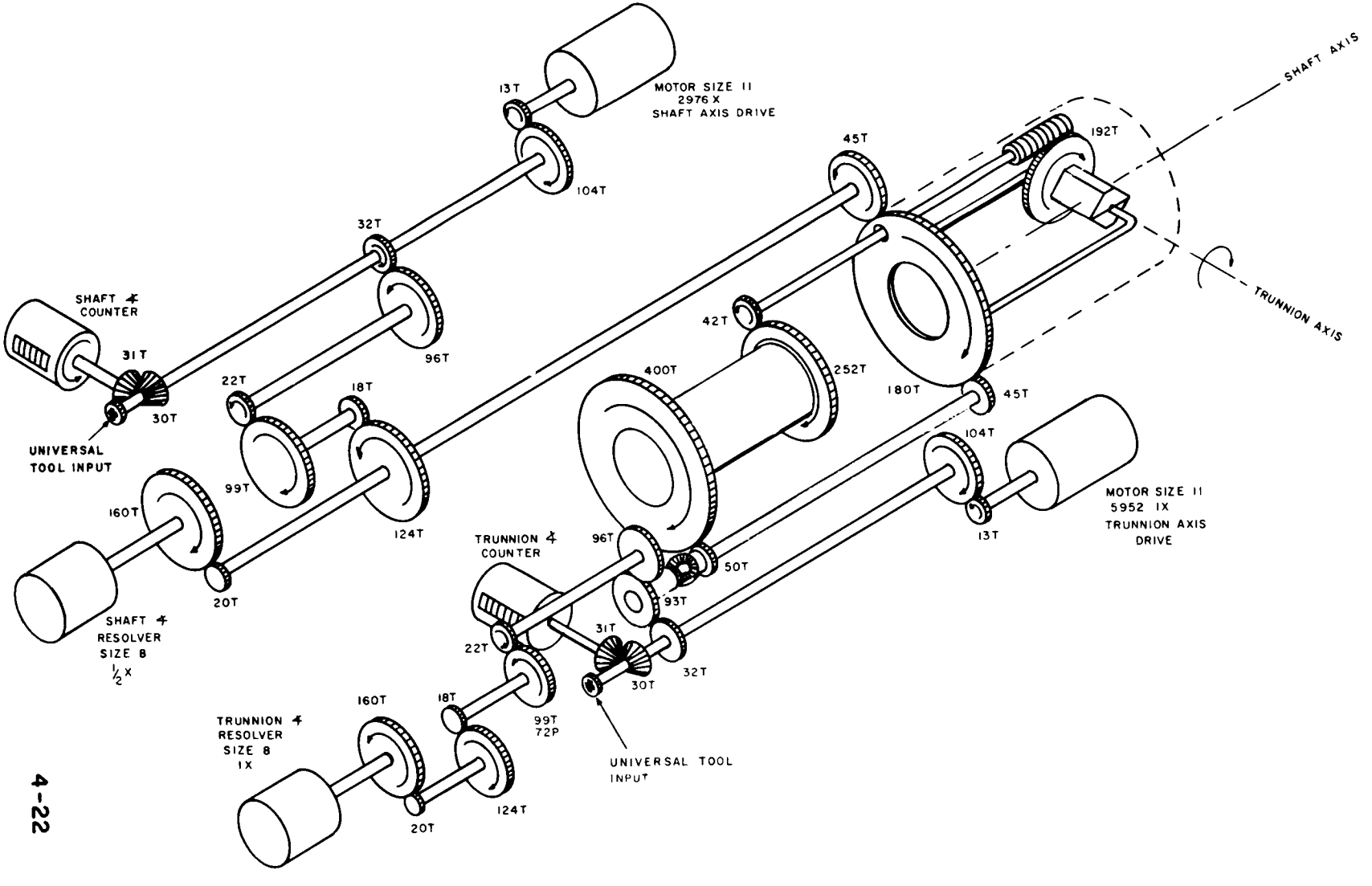

Fig. 11-11 SCT gearing diagram.

Section 12

OPTICS OPERATIONAL MODES AND NAVIGATIONAL PHENOMENA

D. A. Koso

The Optics Subsystem (OSS) is used during the free fall phases of the flight to provide navigational information for the AGC. There are three general categories of measurements which are being considered. One is a bearing measurement (to an earth or lunar landmark), the second a precision angle measurement (between a star and a horizon or landmark), and the third a star occultation measurement.

The landmark bearing measurement provides information about two degrees of freedom for the computer; the remaining two types of measurements provide one degree of freedom.

Figure 12-1 gives a tabulation of these phenomena and when they are used. These will now be described in detail from the viewpoint of the equipment involved and operatinal procedures.

During earth orbit, the vehicle moves with the X axis along the velocity vector. The optical unit (see Fig. 12-2 for the location of the optical unit) is pointed approximately toward the earth. The astronaut uses only the sextant (SXT) to perform the landmark bearing measurement. Using the optics controller (see Fig. 12-3), the astronaut positions the SCT to see the ground ahead of the vehicle. When the landmark becomes discernible, the astronaut positions the center of the SCT reticle on the landmark and commences tracking of the landmark using the optics controller. When the landmark is centered on the SCT reticle, the astronaut pushes the "mark" button on the right-hand side of the panel. About three markings on each landmark are expected. Each "mark" interrupts the computer program and instructs the computer to store the shaft and trunnion angle from the optical unit, the three IMU gimbal angles, and time. The optics mode switch would be placed in the "resolved" mode to make tracking of the landmark easier.

If the landmark appears to be very close to the vehicle ground track (as noted during the initial acquisition), the vehicle has to be rolled to the side (using the minimum impulse controller) to avoid tracking of a landmark too close to the shaft axis of the SCT. The maximum shaft angle rate is 17.2 deg/sec, thus it is impossible to track landmarks too close to the orbital track of the vehicle. The regions where tracking is

EARTH ORBIT

LANDMARK BEARING MEASUREMENT

STAR HORIZON ANGLE MEASUREMENT

MID COURSE

STAR LANDMARK ANGLE MEASUREMENT

STAR HORIZON ANGLE MEASUREMENT

LUNAR ORBIT

LANDMARK BEARING MEASUREMENT

STAR OCCULTATION MEASUREMENT

Fig. 12-1 Navigational phenomena.

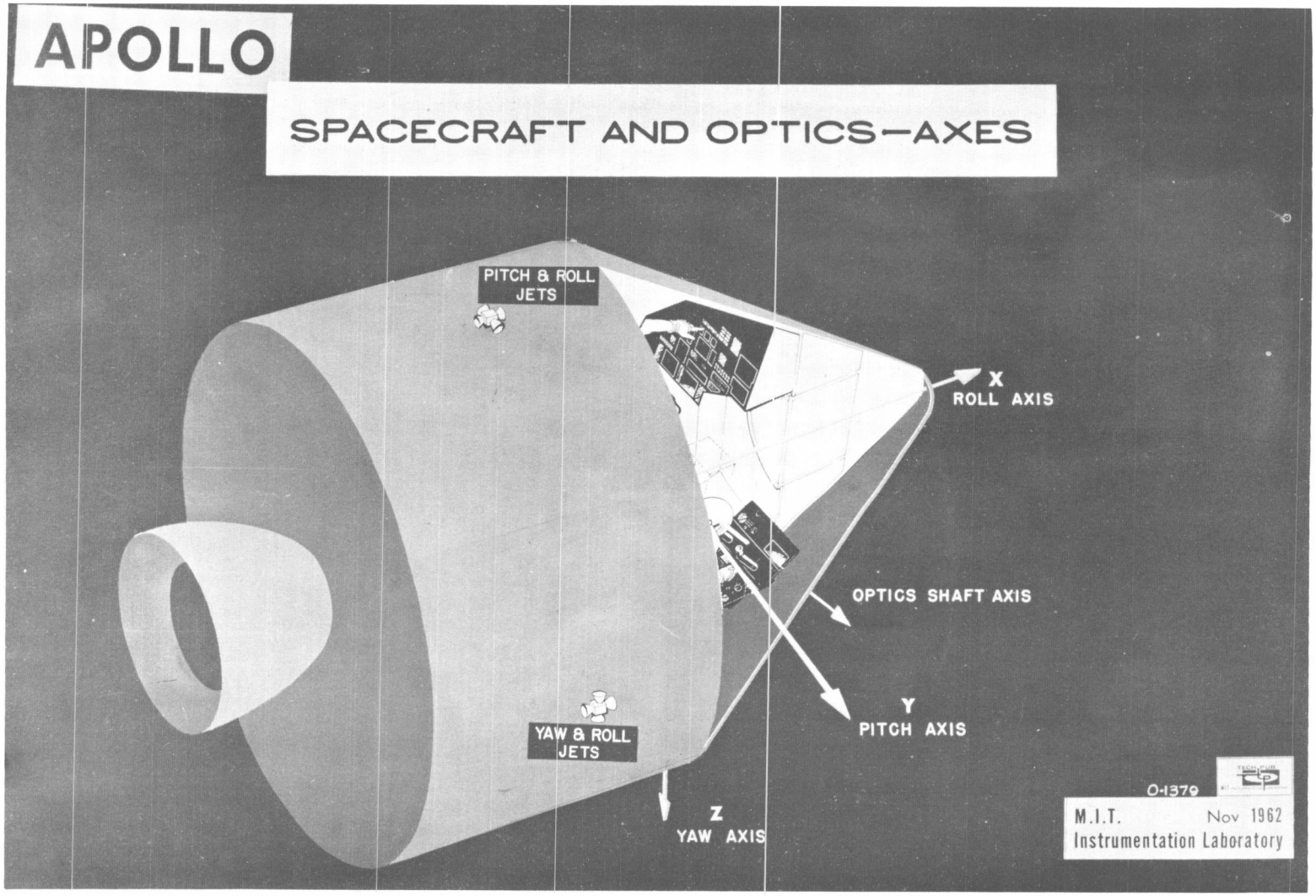
APOLLO
SPACECRAFT AND OPTICS—AXES
PITCH & ROLL JETS
X
ROLL AXIS
OPTICS SHAFT AXIS
Y
PITCH AXIS
YAW & ROLL JETS
Z
YAW AXIS
O-1379
M.I.T.
Nov 1962
Instrumentation Laboratory

Fig. 12-2

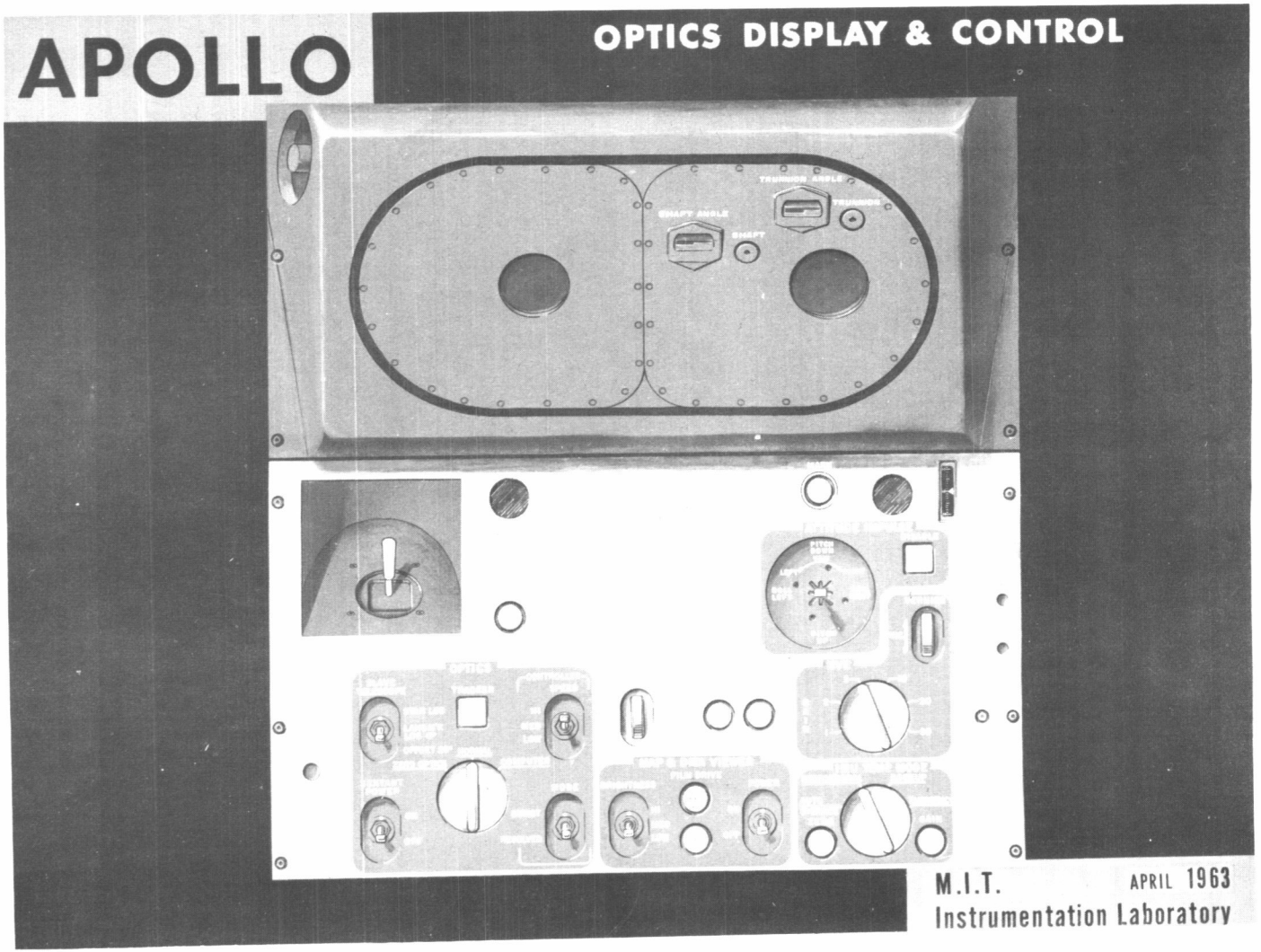
APOLLO
OPTICS DISPLAY & CONTROL
TRUNNION ANGLE
SHAFT ANGLE
SHAFT
M.I.T.
APRIL 1963
Instrumentation Laboratory

Fig. 12-3

impossible are shown in Figs. 12-4 and 12-5 for the earth and moon, respectively. A view of an earth landmark as seen through the SCT is shown in Fig. 12-6 and an illustration of the measurement geometry is shown in Fig. 12-7. (The latter is shown for the lunar case.)

Star horizon measurements are also used during earth orbit. (The equipment used to perform these measurements and the work being performed on horizon definition is described elsewhere in this section.) The vehicle is rolled so that the shaft line of sight is pointed at the horizon. The astronaut then acquires the desired star and centers the star in the SCT and pushes the tracker on button. The automatic star tracker (AST) now keeps the star centered in the field of view of the SXT. The astronaut now waits until the horizon is level (as seen through the SCT, Fig. 12-8). When the horizon appears level, the astronaut sweeps the shaft axis through the horizon. A "mark" is sent automatically to the computer at the proper horizon illumination level.

During the midcourse phase of the flight, star-landmark measurements are also used. The angle between a star and landmark changes as the vehicle moves along its trajectory (see Fig. 12-9). This angle is measured with the SXT to a high degree of accuracy.

First the astronaut sets the expected star-landmark angle into the trunnion CDU. Then he acquires the landmark in the center of the SCT. (The slave telescope SW is set at 0°.) For coarse acquisition, the hand controller is used. Fine acquisition is completed with the minimum impulse controller on the right-hand side of the panel (Fig. 12-3). The astronaut now sets the slave telescope switch to 25°. In this position, the view is as shown in Fig. 12-10. The circle near 0° represents the field of view of the landmark LOS of the SXT. In this position, the astronaut can see in the SCT field of view everything that is visible in the SXT since the shafts of the two instruments are always slaved together; and the SXT trunnion is limited to a 50° excursion. The astronaut now drives the shaft coupling and display unit (CDU) until the desired star appears on the graduated reticle line of the SCT. If the landmark tends to drift from the circle at 0° on the SCT scale, the minimum impulse controller must be used to return it to the center of the circle. When the desired star is on the graduated SCT reticle line at the angle which was originally set into the trunnion CDU, (if it is not, something has gone drastically wrong and backup procedures or a start from the beginning is in order) the astronaut moves over to the SXT and switches the optics mode switch to resolved. In this mode, the motion of the landmark due to motion of the minimum impulse controller, and motion of the star due to optics hand controller displacement will be identical. The view through the SXT is shown in Fig. 12-11. The astronaut now superimposes the star on the landmark and pushes the "mark" button. To make sure that the SXT has held accuracy, the astronaut will (before and after most SXT measurement) first superimpose two stars at zero trunnion and then autocollimate the SXT reticle at 90-deg.

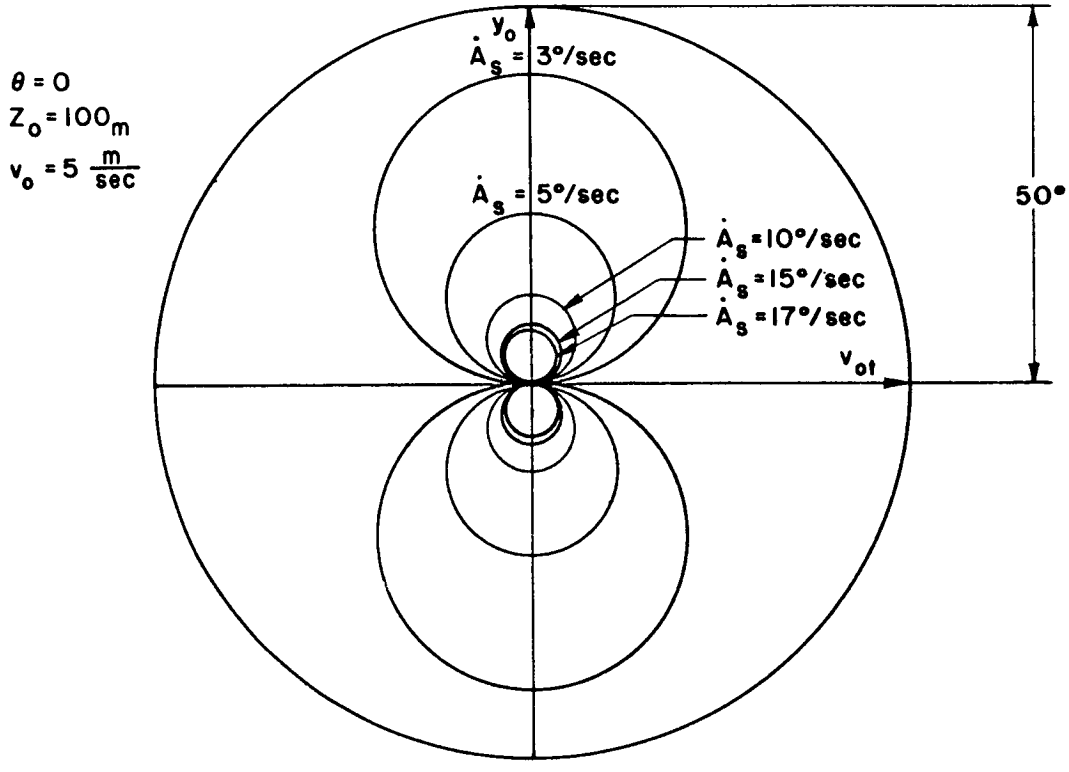

Fig. 12-4 Earth Orbit.

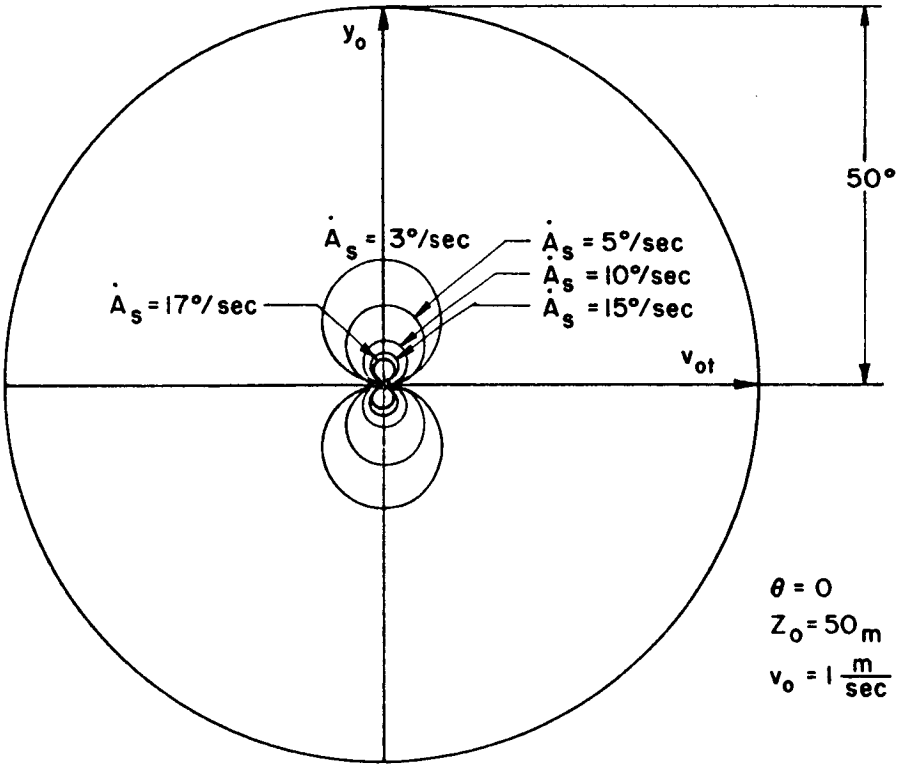

Fig. 12-5 Lunar Orbit

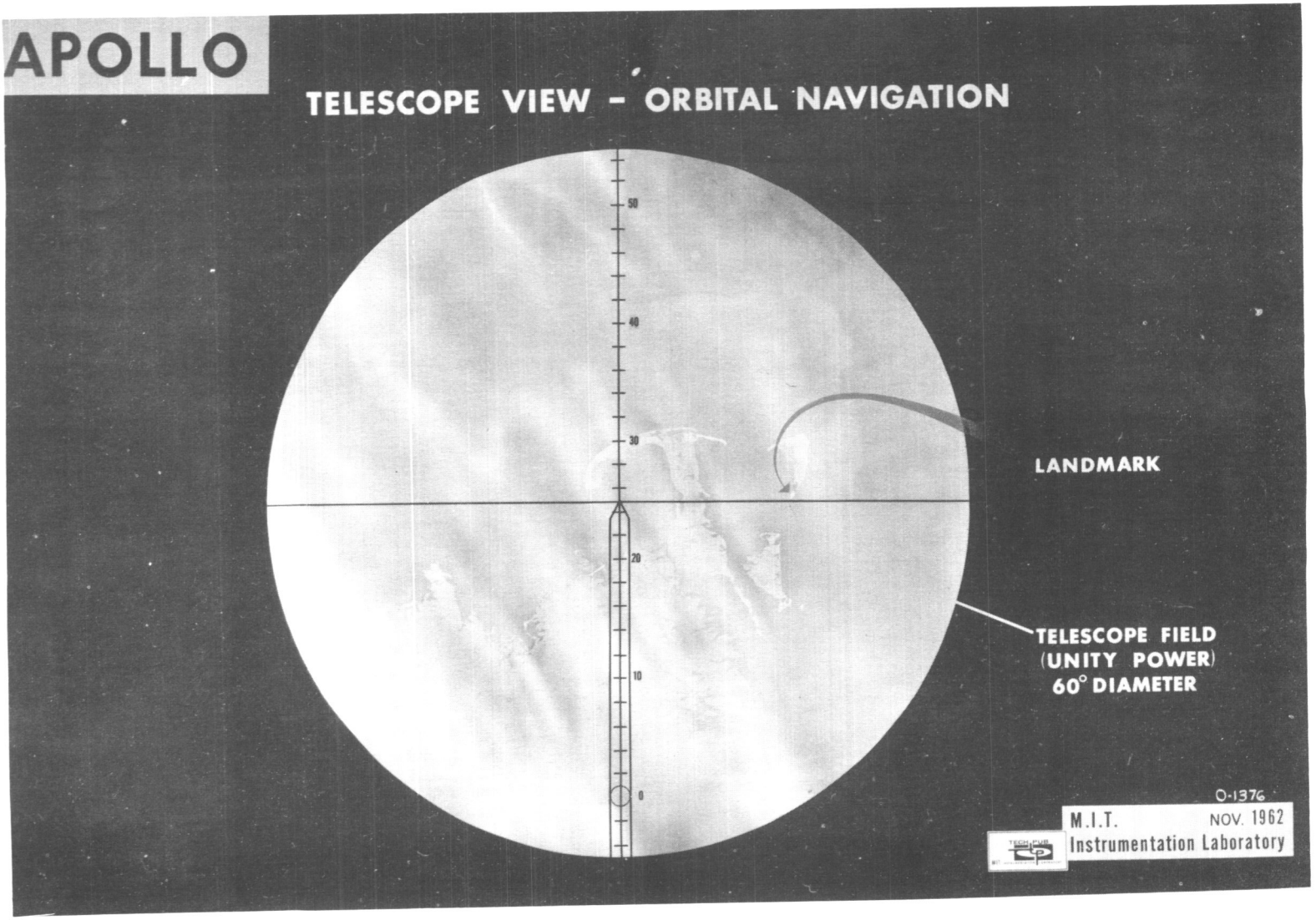
APOLLO
TELESCOPE VIEW - ORBITAL NAVIGATION
50
40
30
20
10
0
LANDMARK
TELESCOPE FIELD
(UNITY POWER)
60° DIAMETER
O-1376
M.I.T.
NOV. 1962
Instrumentation Laboratory

Fig. 12-6

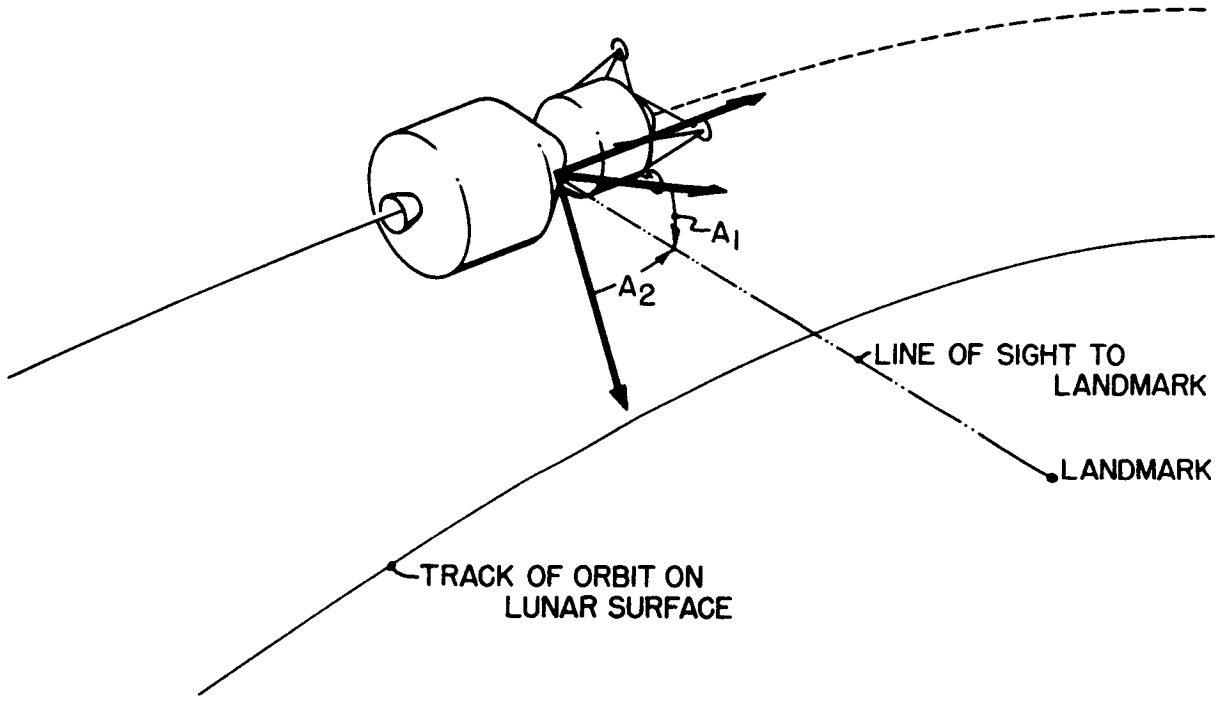

Fig. 12-7 Lunar Orbital determination.

TELESCOPE VIEW
EARTH ILLUMINATED HORIZON LEVELING WITH RESPECT TO STAR

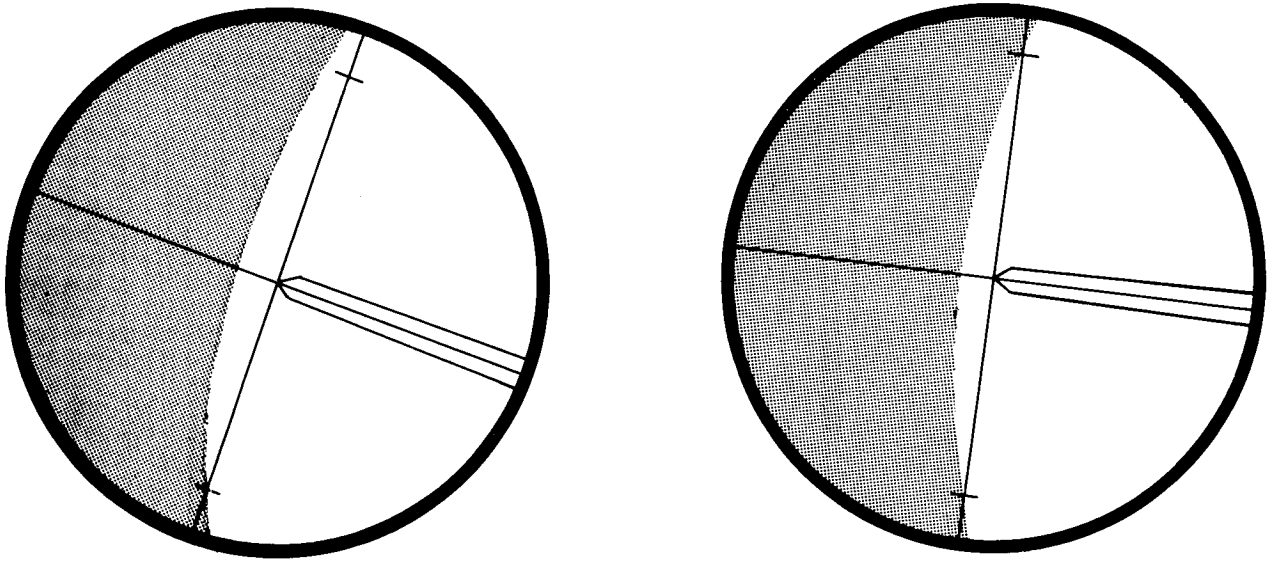

Fig. 12-8

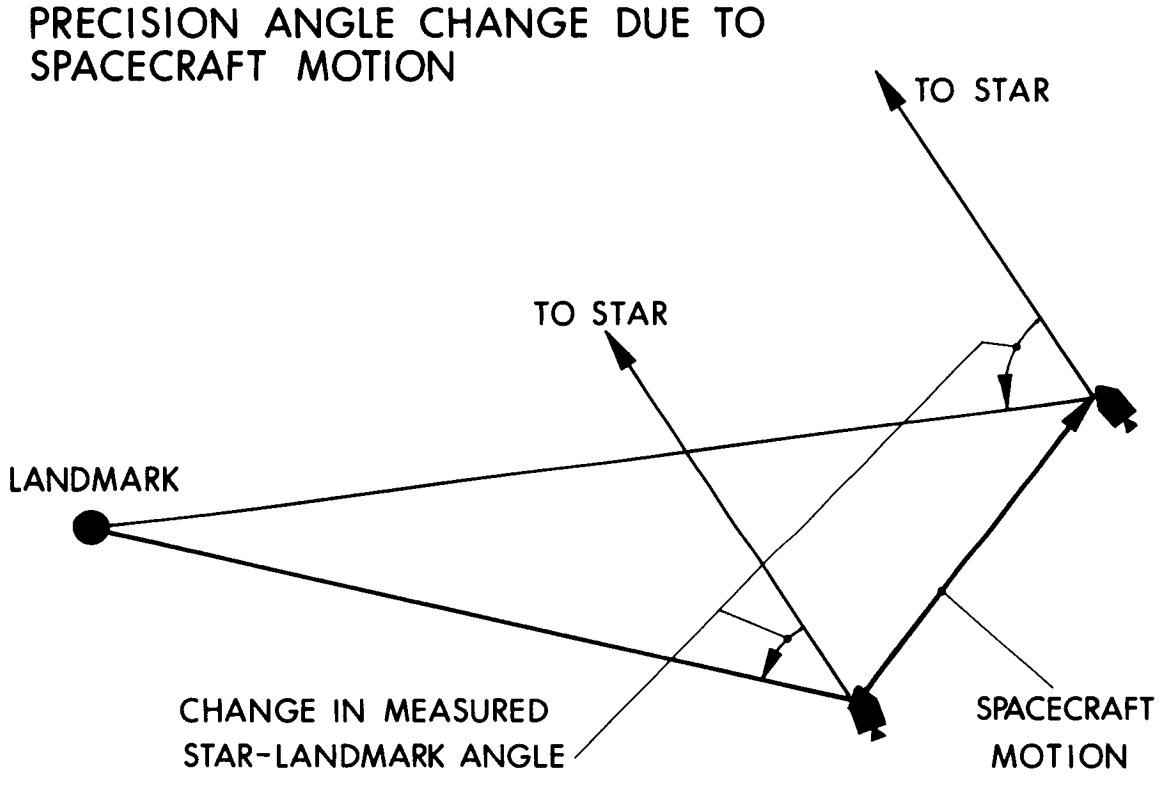
PRECISION ANGLE CHANGE DUE TO
SPACECRAFT MOTION
TO STAR
TO STAR
LANDMARK
CHANGE IN MEASURED
STAR-LANDMARK ANGLE
SPACECRAFT
MOTION

Fig. 12-9

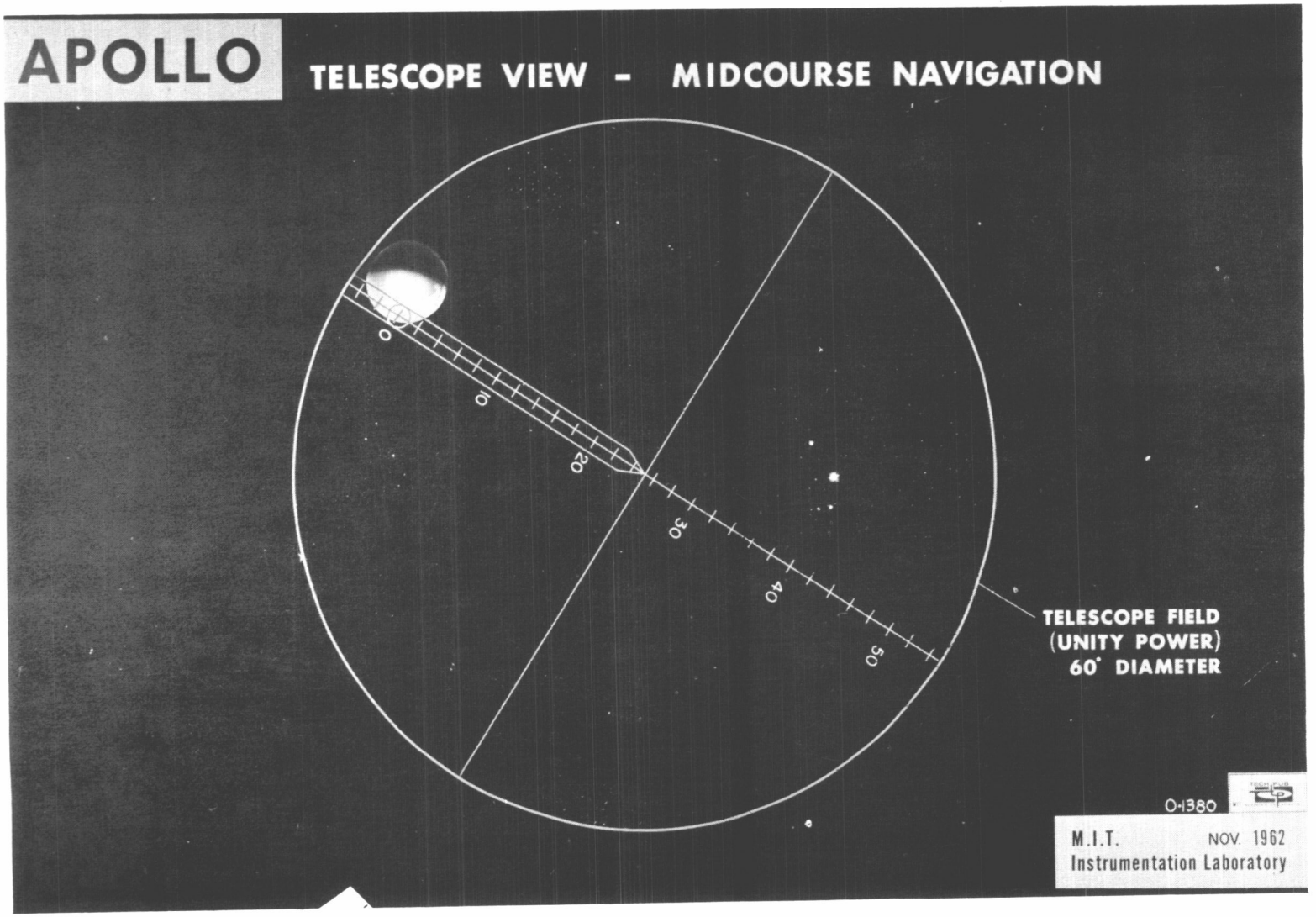
APOLLO
TELESCOPE VIEW - MIDCOURSE NAVIGATION
0
10
20
30
40
50
TELESCOPE FIELD
(UNITY POWER)
60° DIAMETER
0-1380
M.I.T.
NOV. 1962
Instrumentation Laboratory

Fig. 12-10

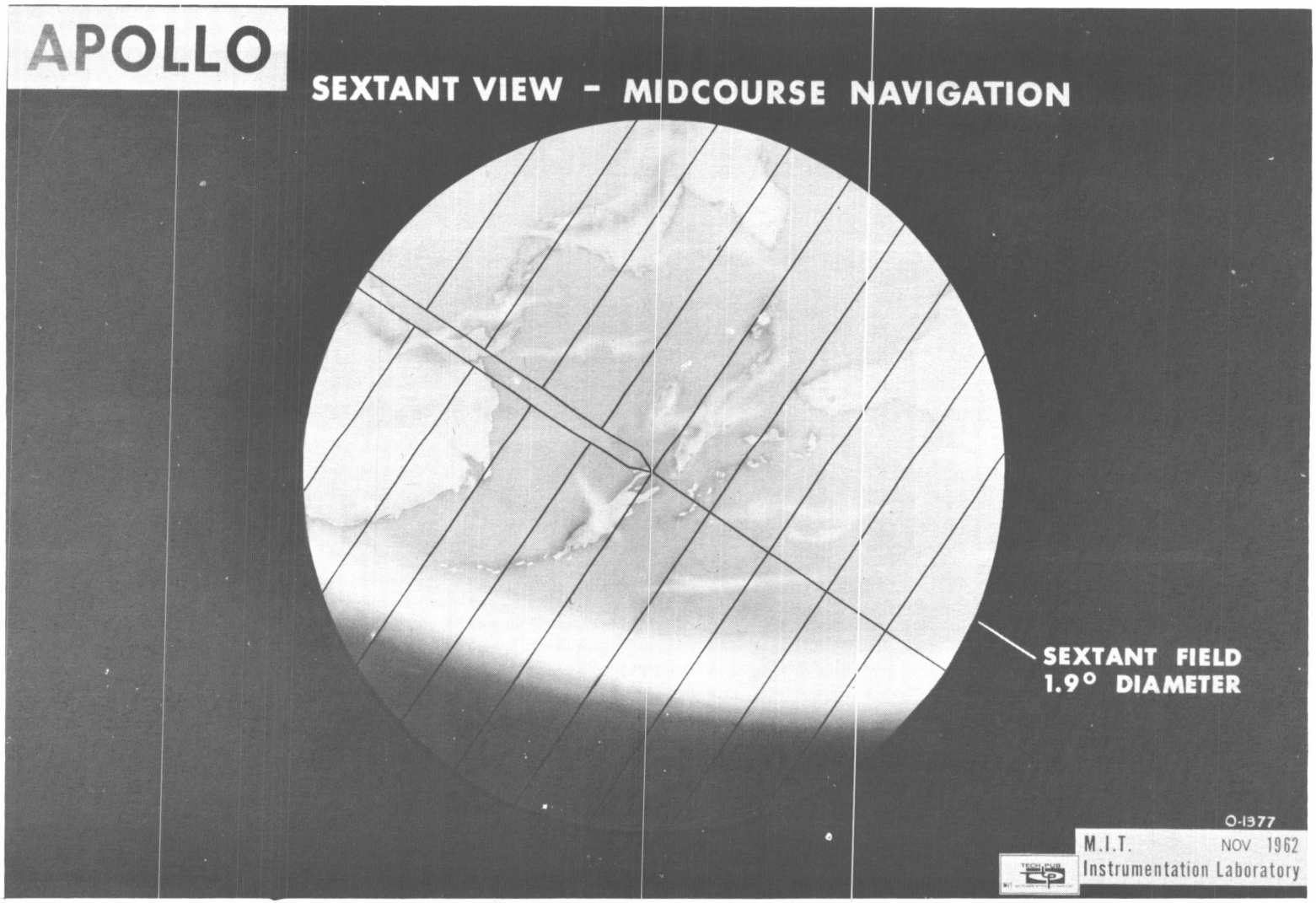
APOLLO
SEXTANT VIEW - MIDCOURSE NAVIGATION
SEXTANT FIELD
1.9° DIAMETER
O-1377
M.I.T.
NOV 1962
Instrumentation Laboratory

Fig. 12-11

trunnion. This procedure is used to make sure that small shifts (which cannot be detected by programming) have not occurred in the optical unit and its associated equipment.

During lunar orbit, star occultations may also be used if sufficient information relating to lunar landmarks is not available. The star occultation measurements are completely manual. The astronaut would track a star and push the "mark" button when the star disappears behind the lunar horizon.

To perform the described measurements, the system was instrumented as shown in Fig. 12-12. The optics hand controller drives the two optics CDU's. These CDU's provide the basic velocity command for the optical unit, and also carry incremental encoders which are used to transmit angular information to the computer. The SXT and SCT are slaved to the CDU with position follow-up servos. A 64-speed resolver is used on the SXT trunnion to provide the basic equipment accuracy; the output from this resolver is fed to a good quality size 11 resolver in the CDU. Thus, any errors in the CDU between this resolver and the incremental encoder are divided by 64. This arrangement makes conventional gear trains feasible and keeps the overall SXT accuracy to 10 arc sec rms.

The motion of the lines of sight in vehicle coordinates is shown in Fig. 12-13. To avoid confusion between the motions in the landmark line-of-sight field and the star line-of-sight field, the resolved mode is used. In this mode, the optics controller commands motion in rectangular coordinates and not shaft and trunnion.

The horizon definition which is being instrumented is based on the following principle. Blue light (350 millimicrons) is scattered in the upper atmosphere as seen from the outside of the earth's atmosphere. The light intensity peaks when the grazing ray altitude reaches about 15 km and decreases for higher altitudes reaching half of the maximum value at about 32 km. Normalization of the profile to the maximum makes the profile relatively independent of sun angle incidence. Horizon definition of this type is expected to provide us with grazing altitude definition of 3,000-3,500 ft. To get a definition of the horizon to this level of accuracy, photographic experimental program has been completed on two Mercury flights and on the X-15. Further experimental equipment for the X-15 is presently under development.

To accomplish the horizon-based measurements, an automatic star tracker and photometer is required. Figure 12-14 shows the major features of the star tracker and photometer. The star tracker uses two crossed tuning forks for the modulation of the incoming star light (Fig. 12-15). This signal is amplified and demodulated to provide the error signal for the SXT servos. The other amplifiers are required to provide an automatic gain control loop to keep the scale factor between star displacement and error signal independent of star magnitude. The photometer (Fig. 12-16) also consists of a

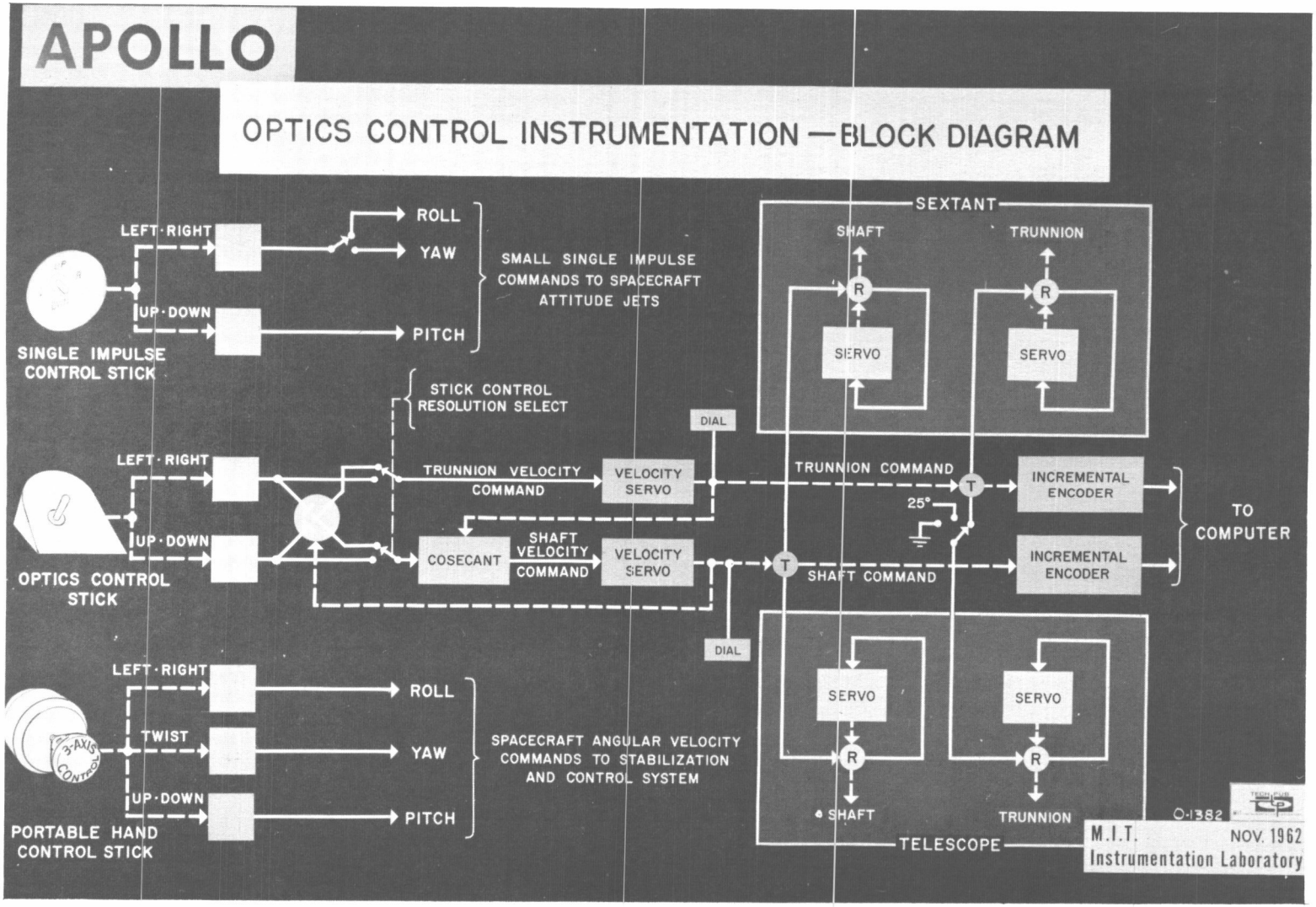
APOLLO
OPTICS CONTROL INSTRUMENTATION — BLOCK DIAGRAM
SINGLE IMPULSE CONTROL STICK
LEFT·RIGHT
UP·DOWN
ROLL
YAW
PITCH
SMALL SINGLE IMPULSE COMMANDS TO SPACECRAFT ATTITUDE JETS
STICK CONTROL RESOLUTION SELECT
OPTICS CONTROL STICK
LEFT·RIGHT
UP·DOWN
TRUNNION VELOCITY COMMAND
VELOCITY SERVO
COSECANT
SHAFT VELOCITY COMMAND
VELOCITY SERVO
DIAL
DIAL
SEXTANT
SHAFT
TRUNNION
R
SERVO
SERVO
TRUNNION COMMAND
T
25°
INCREMENTAL ENCODER
INCREMENTAL ENCODER
TO COMPUTER
SHAFT COMMAND
T
PORTABLE HAND CONTROL STICK
3-AXIS CONTROL
LEFT·RIGHT
TWIST
UP·DOWN
ROLL
YAW
PITCH
SPACECRAFT ANGULAR VELOCITY COMMANDS TO STABILIZATION AND CONTROL SYSTEM
SERVO
SERVO
R
R
SHAFT
TRUNNION
TELESCOPE
O-1382
M.I.T.
Instrumentation Laboratory
NOV. 1962

Fig. 12-12

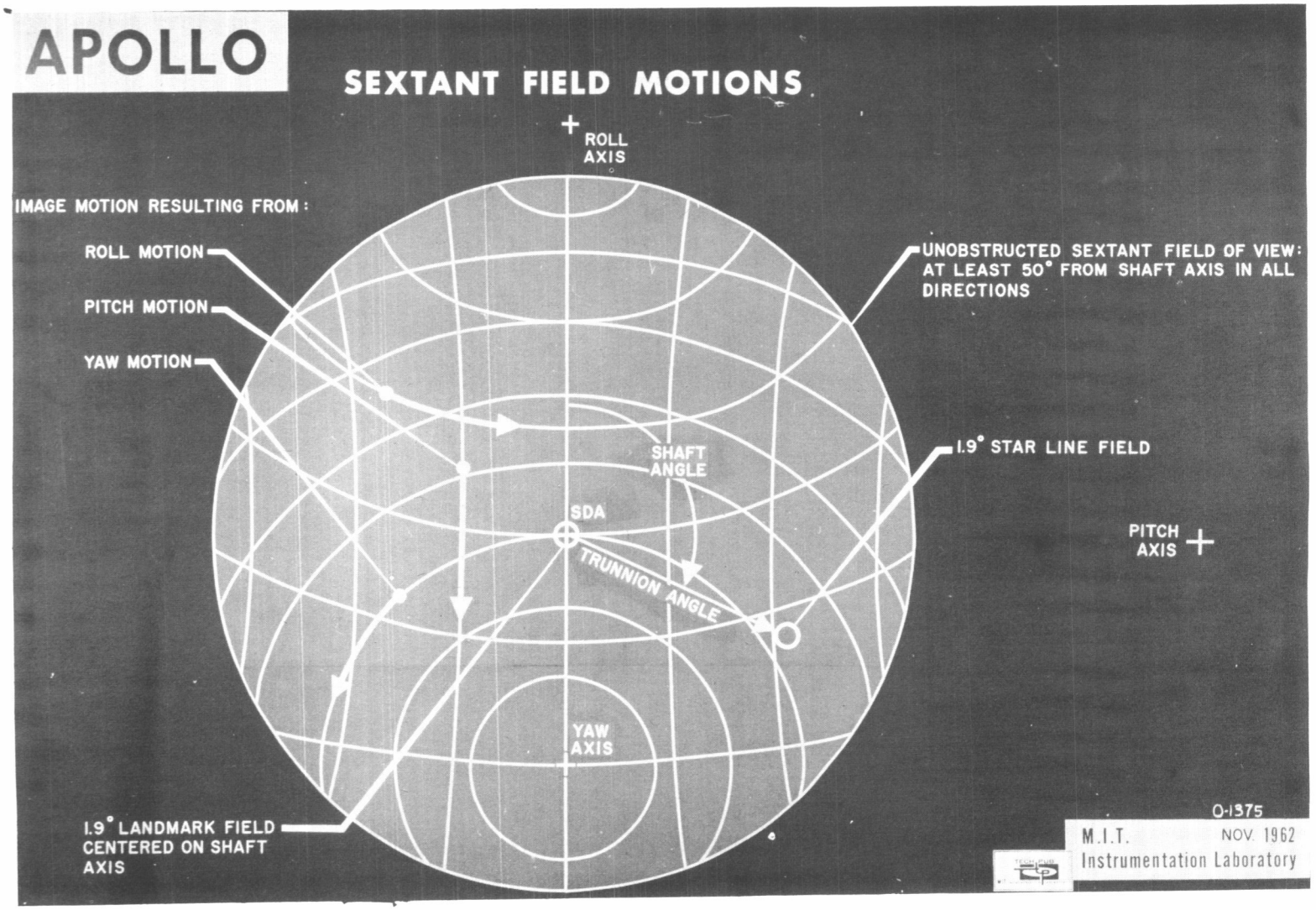
APOLLO
SEXTANT FIELD MOTIONS
ROLL AXIS
IMAGE MOTION RESULTING FROM:
ROLL MOTION
PITCH MOTION
YAW MOTION
UNOBSTRUCTED SEXTANT FIELD OF VIEW: AT LEAST 50° FROM SHAFT AXIS IN ALL DIRECTIONS
1.9° STAR LINE FIELD
SHAFT ANGLE
SDA
TRUNNION ANGLE
PITCH AXIS
YAW AXIS
1.9° LANDMARK FIELD CENTERED ON SHAFT AXIS
O-1375
M.I.T.
NOV. 1962
Instrumentation Laboratory

Fig. 12-13

1.) Star Tracker and Photometer are mounted on the SXT index head.

2.) Star Tracker LOS uses the visual indexing mirror for trunnion motion.

3.) Star Tracker and Photometer rotate with the SXT shaft.

4.) Photometer line of sight is fixed in trunnion at -5.625^{0}.

5.) Photometer line of sight rotates with the shaft.

6.) Star Tracker field coverage $1/2^{0} \times 1/2^{0}$.

Fig. 12-14 Star tracker photometer assembly.

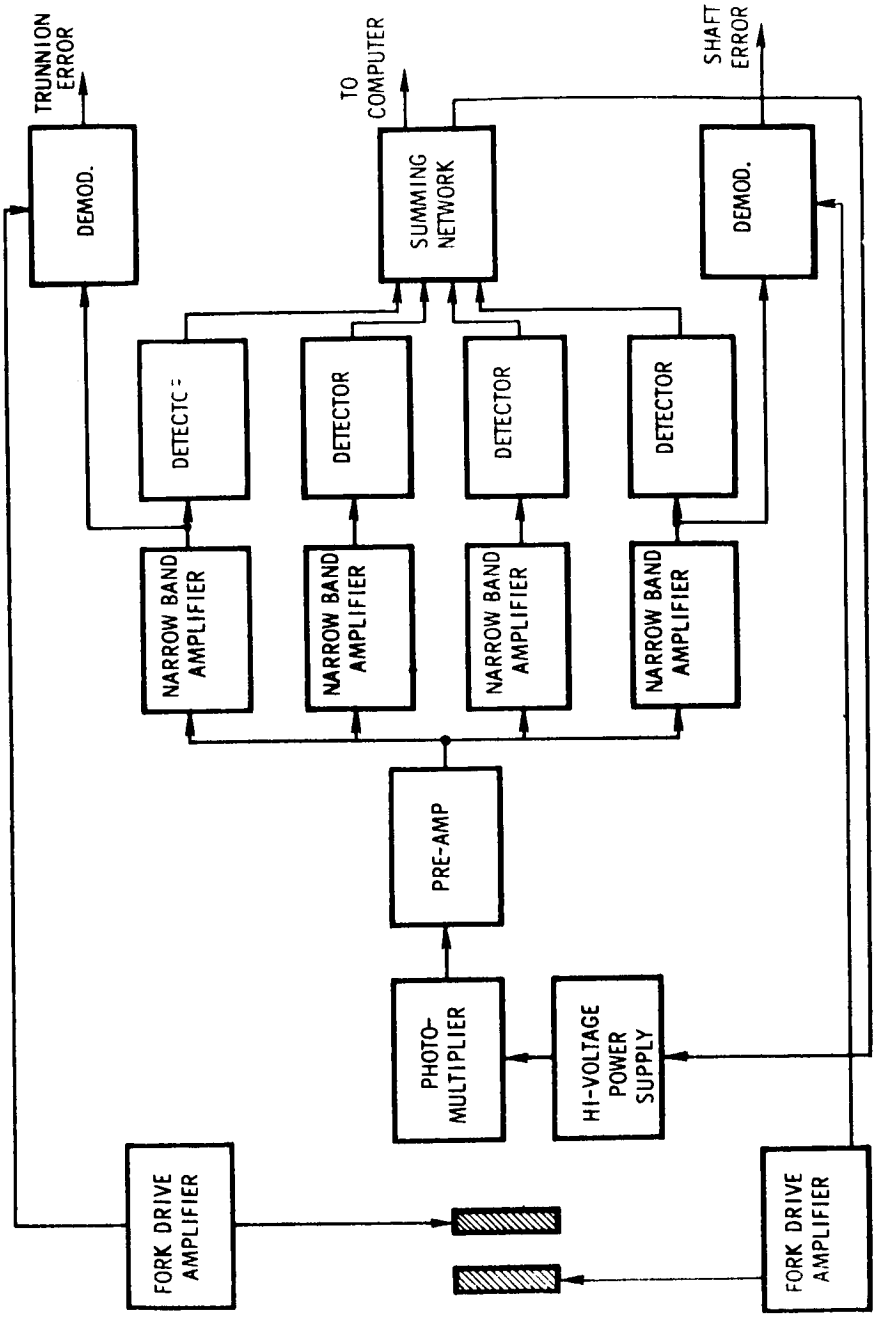

Fig. 12-15 Star tracker.

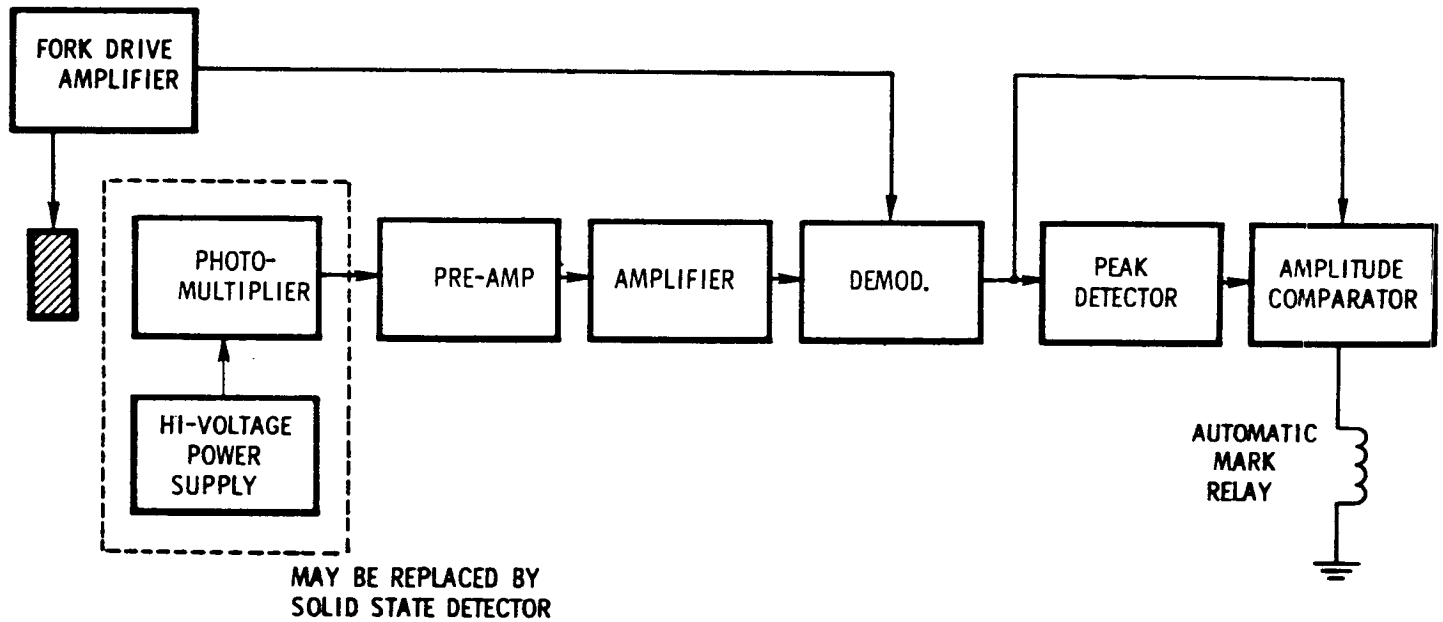

Fig. 12-16 Photometer I.

tuning fork (for light modulation) and signal amplifiers. Since the horizon is determined by the altitude where the scattered light reaches about 1/2 of the maximum, a peak detector and memory circuit is used to provide an automatic mark when the photometer sweeps through the horizon.

Section 13

OPTICAL SIMULATIONS

R. J. Magee

This section deals with optical simulations already completed and those under study by the Optical Section of the Optics and Navigation group.

To insure complete coverage of the optical tasks, as the optical simulation program developed, the simulations were assigned to areas which represented the expected sighting situations. These areas are as follows:

1. Aximuth determination, prior to launch, of the Inertial Guidance System.
2. Earth Orbital Landmark Tracking.
3. Midcourse Navigation sights involving measuring the precision angle between star and landmark.
4. Lunar Orbital Tracking.
5. Lunar descent and landing of the LEM.
6. Lunar launch alignment of the LEM.
7. Rendezvous.
8. Returning to Earth which includes any emergency or backup measures.

Simulation work has been concentrated on items 3 and 6. This was done because the optical system configuration depends largely on the photometric and angular accuracy requirements of these navigational tasks. The areas were then separated into Sextant, Scanning Telescope, and Map and Data Viewer simulations. These simulations were further subdivided into Photometry and Visibility of Targets, Accurate Angular Measurement by means of the instrument, and Specific Techniques for isolated problem areas. Simulation and engineering analysis merge somewhere in the area. Simulation is defined here as use of mathematical or physical model to duplicate real system functions.

Sextant - Photometry and Visibility of Targets Simulation. The first experiment was visibility of point sources against a field of high luminance by the unaided eye. This was to verify the accuracy of laboratory simulation by comparison to data of proven exactness. (Hardy Tiffany Data). The results were within a fraction of a stellar magnitude of the Tiffany Data.

The next experiment was visibility of stars in the daylight sky. The purpose was to acquire and discern stars against a background of luminance comparable to that of the sunlit earth or moon. This experiment used a telescope optically similar to the sextant. Results showed the ability to discern the star Polaris against the noon daylight sky with a 28X T-2 Theodolite. Other results were that instrument focus was sensitive to temperature, and that a reticule pattern is desirable to help the observer properly focus his eye.

The third experiment involved point source visibility against a field of high luminance by telescope in the laboratory. A star collimator was used along with a collimated source of high luminance. The purpose was to determine if the calculated value of the sextant beam splitter was satisfactory. Results showed ability to see a third magnitude star against a sunlit moon.

The next experiment determined the visibility of a star superimposed on the moon in different phases. This was an outdoor field test with Theodolite and beam splitter. Results showed a 3.2 magnitude star could be seen against the sunlit moon. The beam-splitter value was then changed to allow a 4.3-magnitude star to be seen against the sunlit moon, and a 2.5-magnitude star against the sunlit earth.

The next simulation involved blinking the star or moon when both are superimposed in the sextant. The purpose was to determine the usefulness of blinking either star or landmark line of sight. Results showed star blinking did not aid, but moon blinking helped to acquire the star when both were in the field.

The next experiment determined the angular accuracy of sextant alignment on targets. The purpose was to determine the statistical distribution of alignment settings of sextant on target by various observers. The results showed a Gaussian distribution of settings for observations on a symmetrical target. The one-sigma limit was found to be 1.4 seconds of arc.

The next experiment involved the accuracy of superposition of a star on a lunar crater, using the breadboard sextant at night looking at the star Capella and the moon. The two target features Plato and Plinius are shown in Fig. 13-1, the results are shown in Fig. 13-2. The ordinate is the sextant trunnion angle, the abscissa is eastern standard time in 10-min. intervals. The first angle measurement used star Capella and crater Plato; trunnion angle was about 24°. Each triangle or circle is an observation. The data

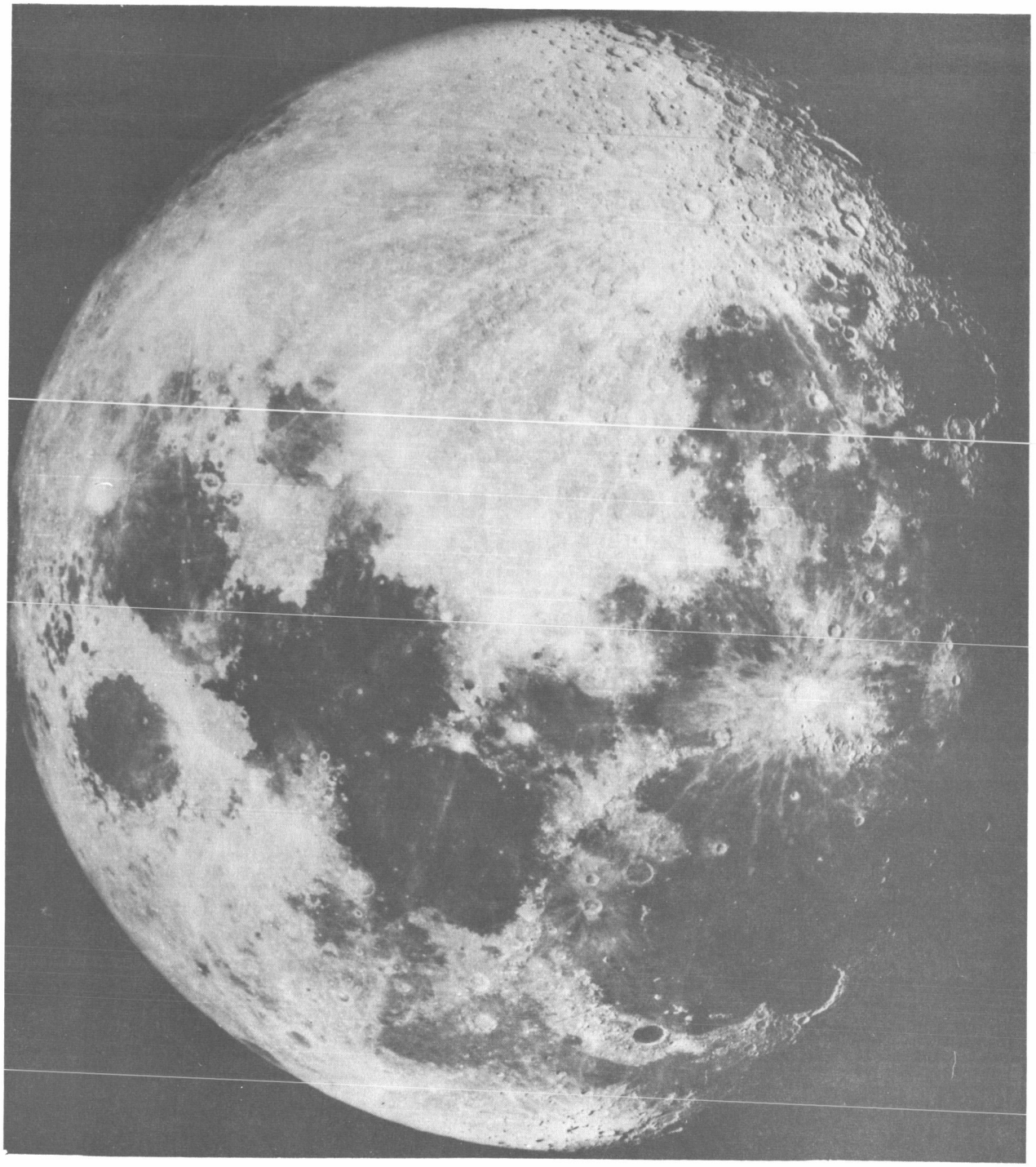

Fig. 13-1 Two target features of Pluto & Plinius

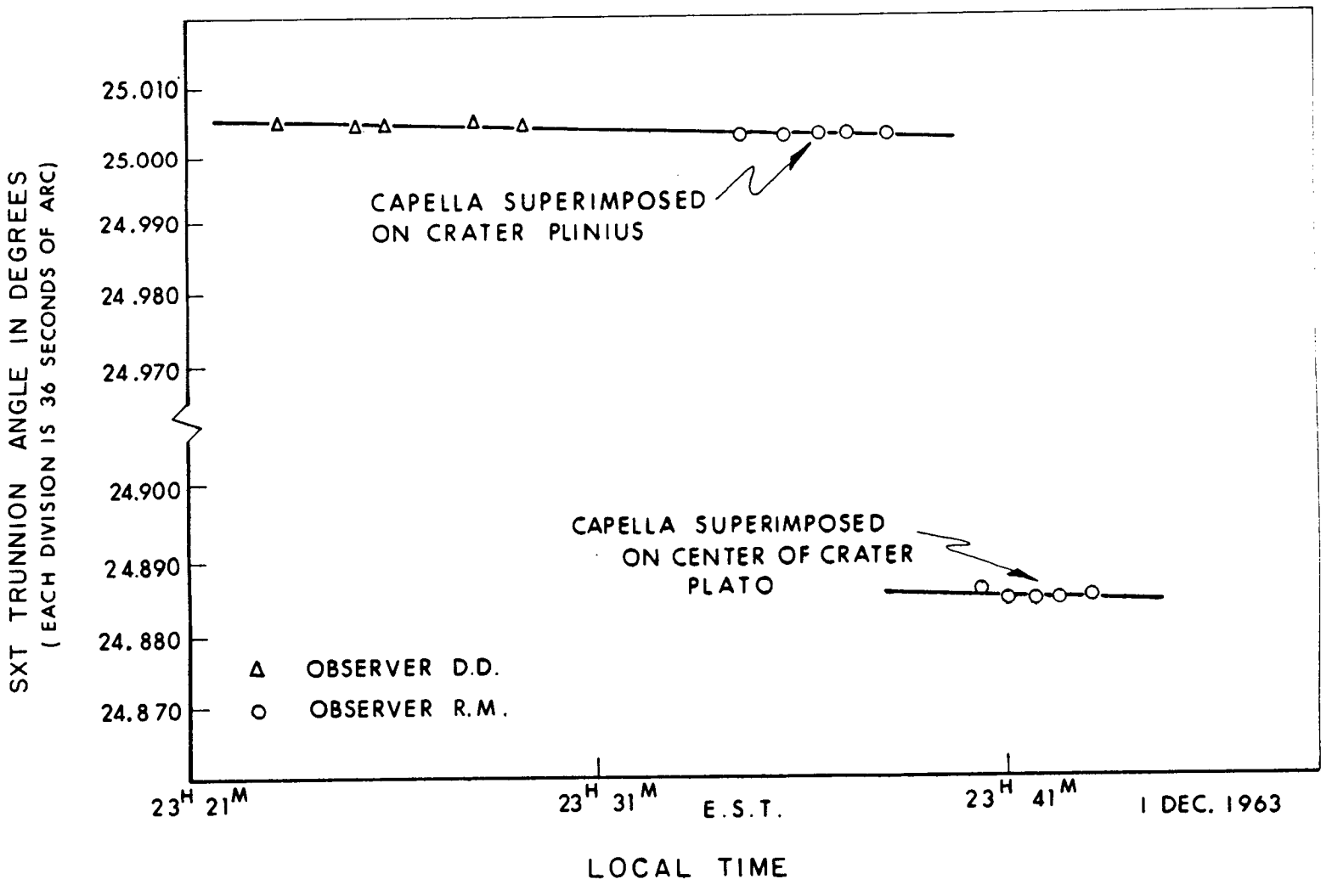

Fig. 13-2 SXT breadboard measuring angle between star capella and lunar features.

was compared with calculations and a 12-sec-of-arc bias was found. Refraction correction was suspected; as temperature and barometric pressure were not accounted for in the correction. A significant feature was that the spread of the data deviates from the straight line by not more than 5 or 6 sec. of arc for both targets.

The next experiment was the accuracy of alignment of the sextant with various magnifications. The purpose was to determine accuracy on a target of low contrast. The results showed an optimum magnification of about 28 - 30X for the aperture size used. Range of magnifications tried was 24X to 40X.

The next experiment tested color filtering to increase landmark contrast. The purpose was to verify calculations which showed color filtering would enhance the contrast of targets of the land-sea boundary type. Scanning such a landmark with a photometer might produce a graph such as shown in Fig. 13-3. The ordinate is luminance, the abscissa is the scanning position. The proper color filter reduces the apparent luminance of the sea by a certain amount, while reducing the luminance of the land by a lesser amount. This improves the contrast, where contrast is represented by the ratio of the difference of the indicated values divided by the lesser value. Work is continuing with several constraints. The filter must be in the landmark line of sight; thus it must be ahead of, or incorporated in, the beam splitter. Only one filter is to be used for all landmarks.

The next experiment tested the accuracy of 1X scanning telescope alignment. The three-sigma value using 49 data points for the distribution of alignment of the reticle on a star is 36 sec. of arc. This is greater accuracy than the resolution of the eye. It has been found that an instrument may be more accurately aligned on a target than the resolution of the system would indicate. However, good image quality and symmetry of target are quite important in obtaining this precision.

The next experiment concerned the visibility of stars in the scanning telescope when the earth was also in the field. The purpose was to verify calculations made on ghost flux in the instrument due to the sunlit earth being in the field. Calculation predicted the ability to see a 4.5-magnitude star; experiment showed ability to see a star of approximately 4th magnitude when no earth is in scanning telescope field. This was without scattering shielding in the instrument, and it is felt the predicted results can be achieved.

The next experiment was to determine the stellar magnitude visible in the field of the sextant when the earth is also in the field. Preliminary data on the unshielded instrument is shown in Fig. 13-4. The ordinate is stellar magnitude, abscissa is separation angle between the star and the earth in the field. The angular diameter of the earth (a bright circle) was 2 degrees; its luminance matched to that of the sunlit earth; the star

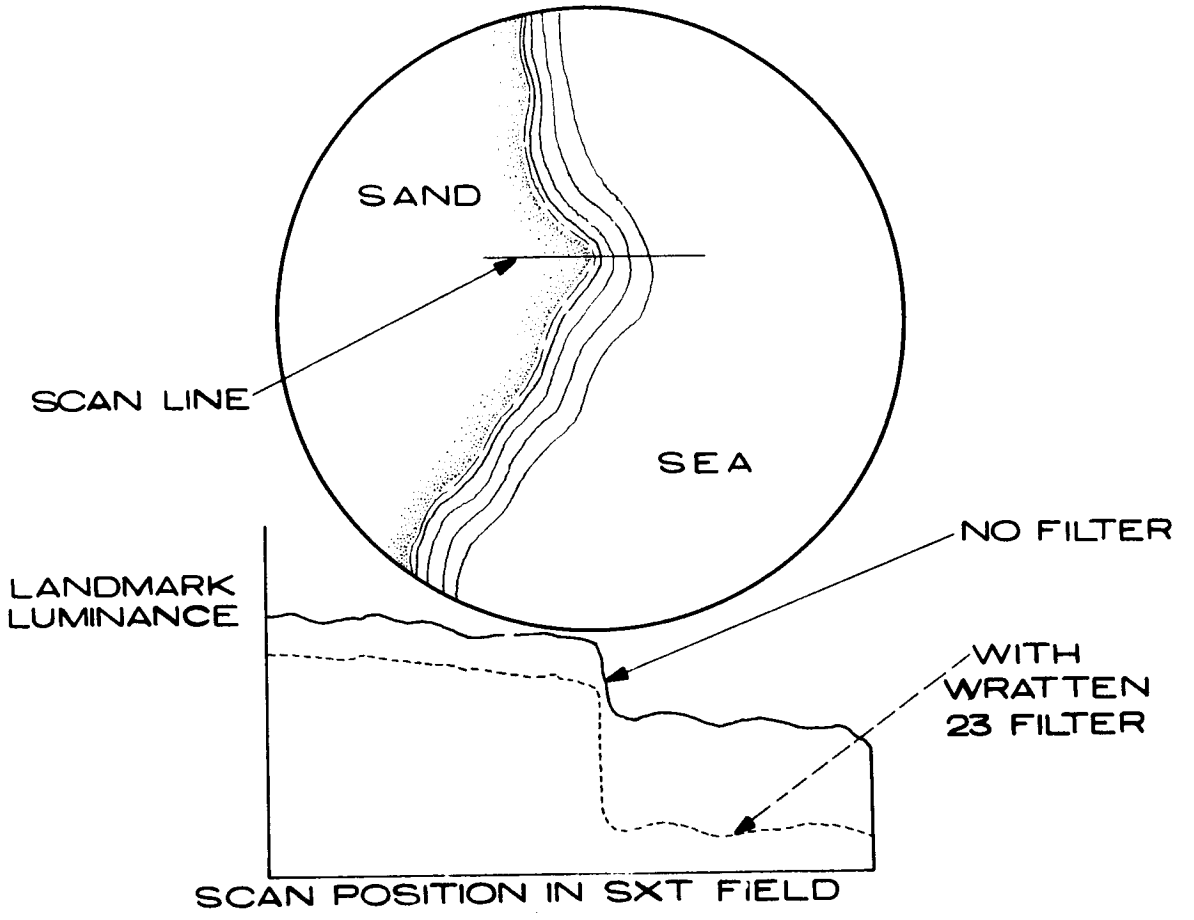

Fig. 13-3 Landmark viewed through sextant.

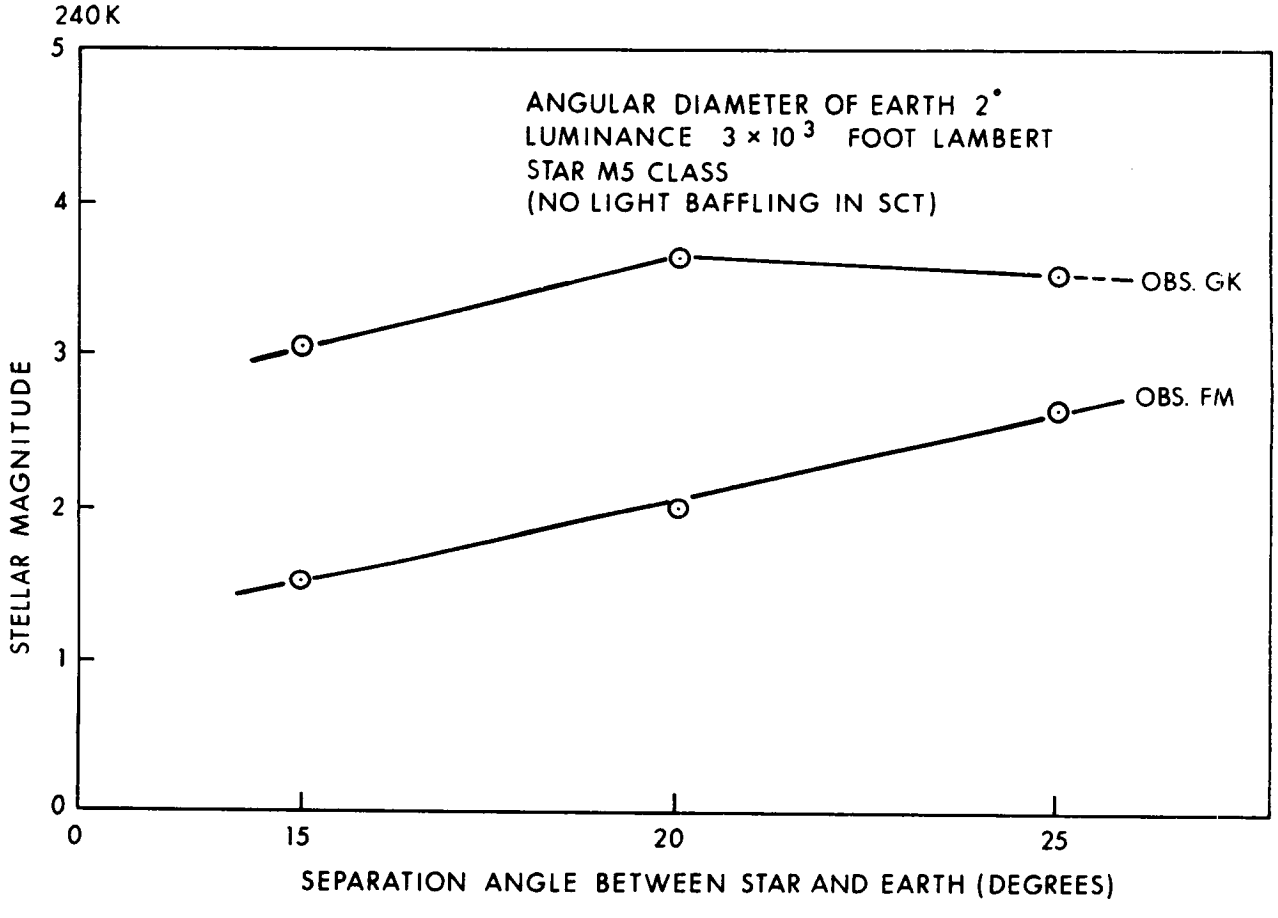

Fig. 13-4 Threshold star when both earth and star are in SCT field.

was approximately the color temperature of Betelgeuse. Results showed a 1.5-to third-magnitude star can be seen at 15 degrees from the earth with brighter stars visible at greater angles.

The spread of data is partially due to the difference of visibility criteria of the two observers, and partially due to the observers themselves. Observer FM wears glasses. A difference of a stellar magnitude between thresholds of two observers can be considered typical if they differ somewhat in age and condition of eyes.

Section 14

SYSTEM CHECKOUT AND FIELD OPERATIONS

L. S. Wilk

This section describes some aspects of System Checkout and Field Operations as outlined in Fig. 14-1.

Figure 14-2 shows that MIT/IL will maintain responsibility for the Guidance and Navigation (G&N) throughout its operation. There will be laboratories and facilities at North American Aviation (NAA), at Grumman (GAEC), at the Manned Spacecraft Center (MSC) and at the Atlantic Missile Range (AMR). In addition, at NAA and at Houston there will be support systems for simulation studies. At AMR, as at all sites, MIT/IL will provide operators for the ACE system. In toto, G&N checkout personnel will have five seats at the ACE system; 1 NASA, 1 NAA or GAEC and 3 MIT/IL or P. C. 's. There will be some G&N support at the IMCC. Field personnel will be rotated in an attempt to get some field experience into any redesign.

The same kinds of tests are used in factory selloff tests, tests in laboratories and tests in the spacecraft. Formal documentation is used. Critical parameters are checked, including the following; zero, 90°, and one intermediate angle are measured accurately on the trunnion axis of the optics. The scale factor and bias of the accelerometers are checked; the drift coefficients of the gyros are also checked. The alignment between optical lines of sight and accelerometer axes is checked. The gyro compass mode is accurately checked in the laboratory. The final system laboratory test is performed in the spacecraft configuration.

The flow of the equipment from contractor to post-flight analysis is described in Figs. 14-3 through 14-8. The Computer, Display and Keyboards and the computer test set are each tested separately; and then jointly as the computer subsystem. The tests are performed according to a Final Test Method (FTM) and Acceptance Test Procedures (ATP). At this point the government buys from Raytheon Mfg. Co. on a DD-250. At Kollsman Instrument Corp. the Optics Assembly and Map & Data Viewer are tested and sold off. The items are then shipped to AC Spark Plug.

AC Spark Plug manufactures and tests the IMU, the IMU control panel, the CDU's, the PSA, the D&C electronics, G&N indicator panel, and the inertial subsystem test equipment. Each is separately tested and then assembled into the inertial subsystem which is tested in accordance with a Class A document, the Inertial Subsystem ATP.

- Field Operation and Checkout Philosophy
- Equipment Flow
- Test Procedure Generation and Documentation
- Lab and Spacecraft Test Outline
- Field Functions
- AGE 4 Test Results

Fig. 14-1 System checkout and field operations

- Responsible for G&N Throughout Operation
  - NAA/GAEC
  - MSC
  - AMR
  - ACE Operation
  - IMCC Support
- Rotate Design Engineers Through Field Assignments
- Mothers
- Design Specialists On Call
- Maintain Test Equipment / Procedure Continuity
- All Test Operations by Class A Documents
- Test Critical Parameters of Mission Requirements
- System Test in Spacecraft Configuration
- Test All Spacecraft Interfaces

Fig. 14-2 Field operation and checkout philosophy.

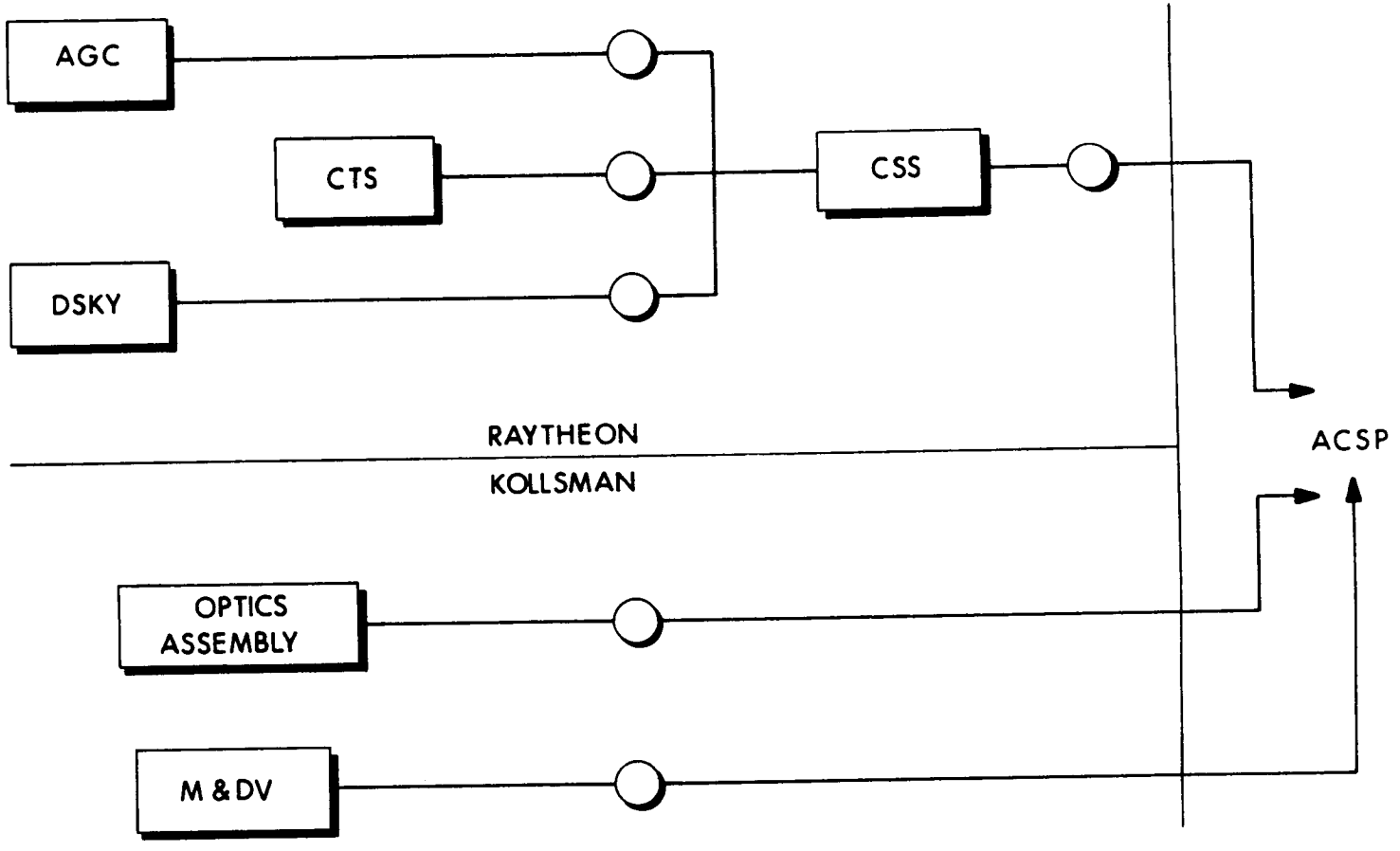

Fig. 14-3 Equipment flow (1).

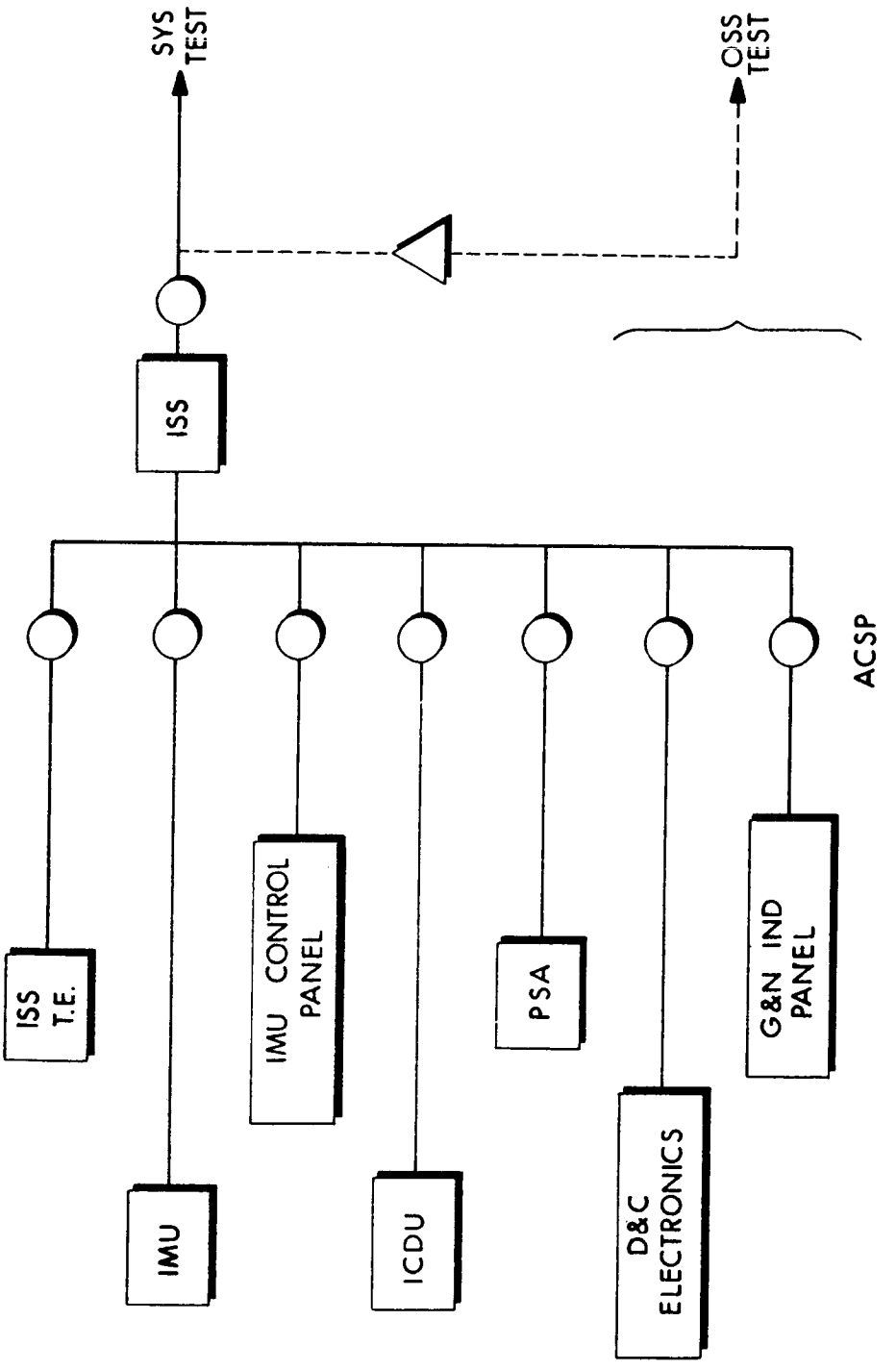

Fig. 14-4 Equipment flow (2).

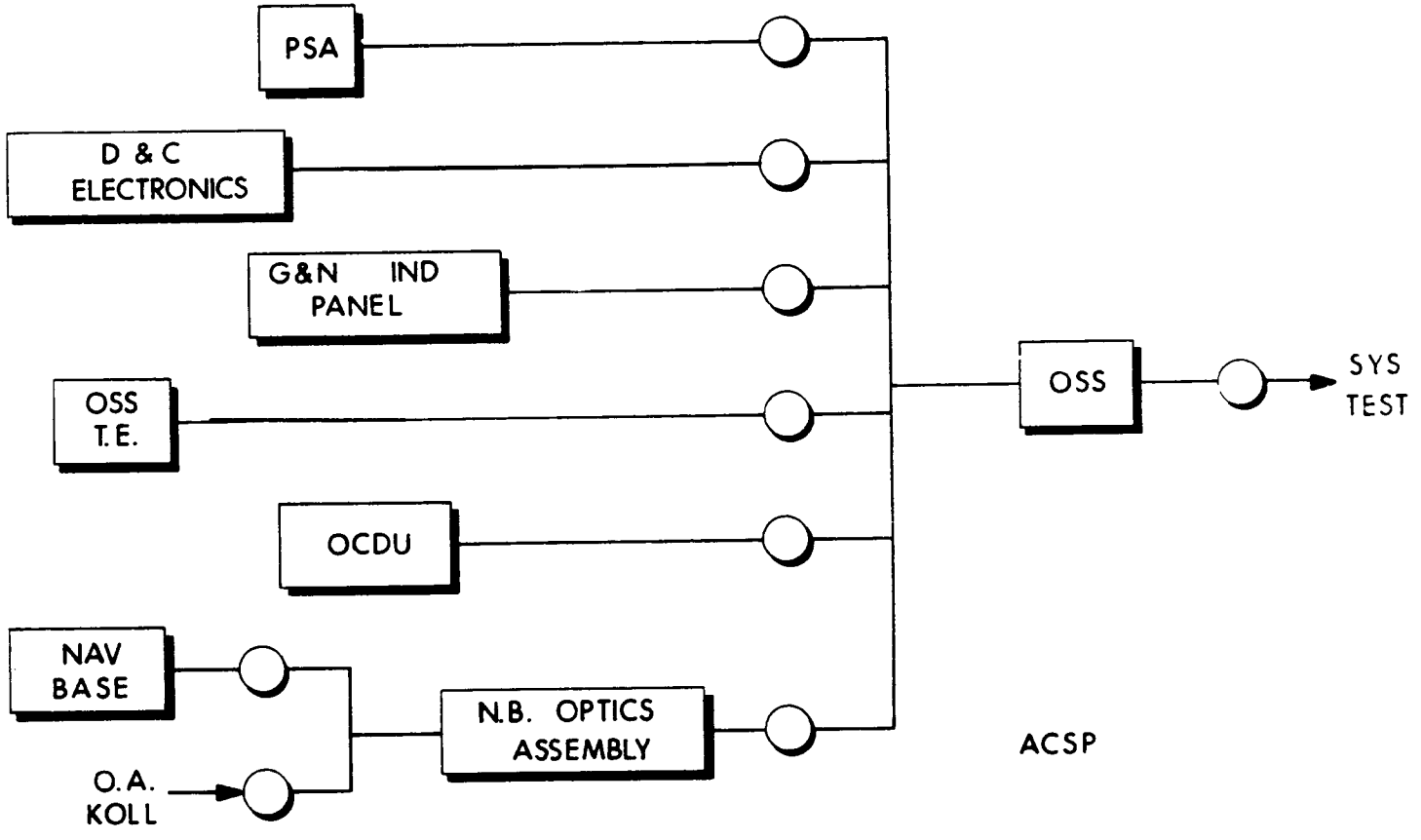

Fig. 14-5 Equipment flow (3).

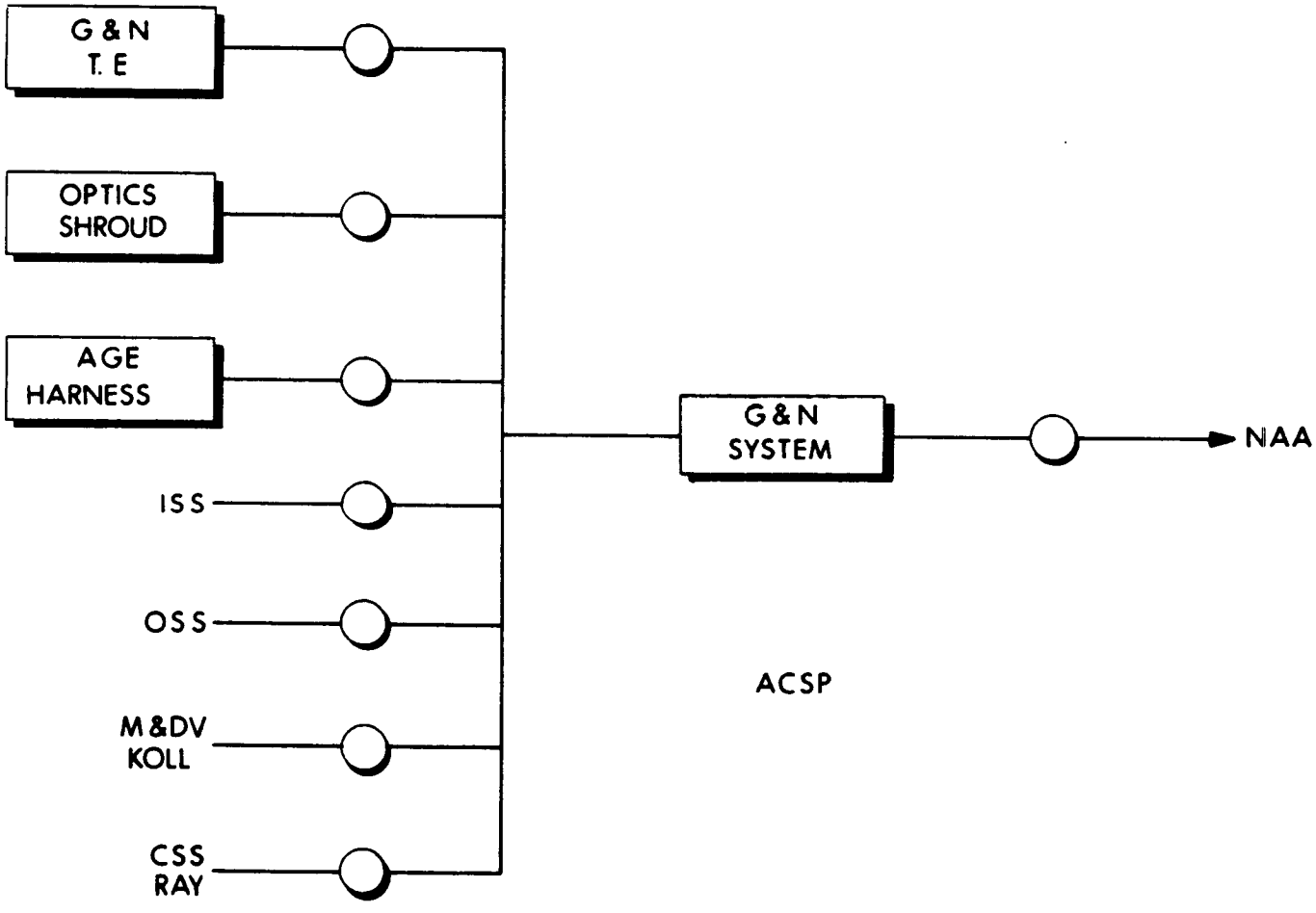

Fig. 14-6 Equipment flow (4).

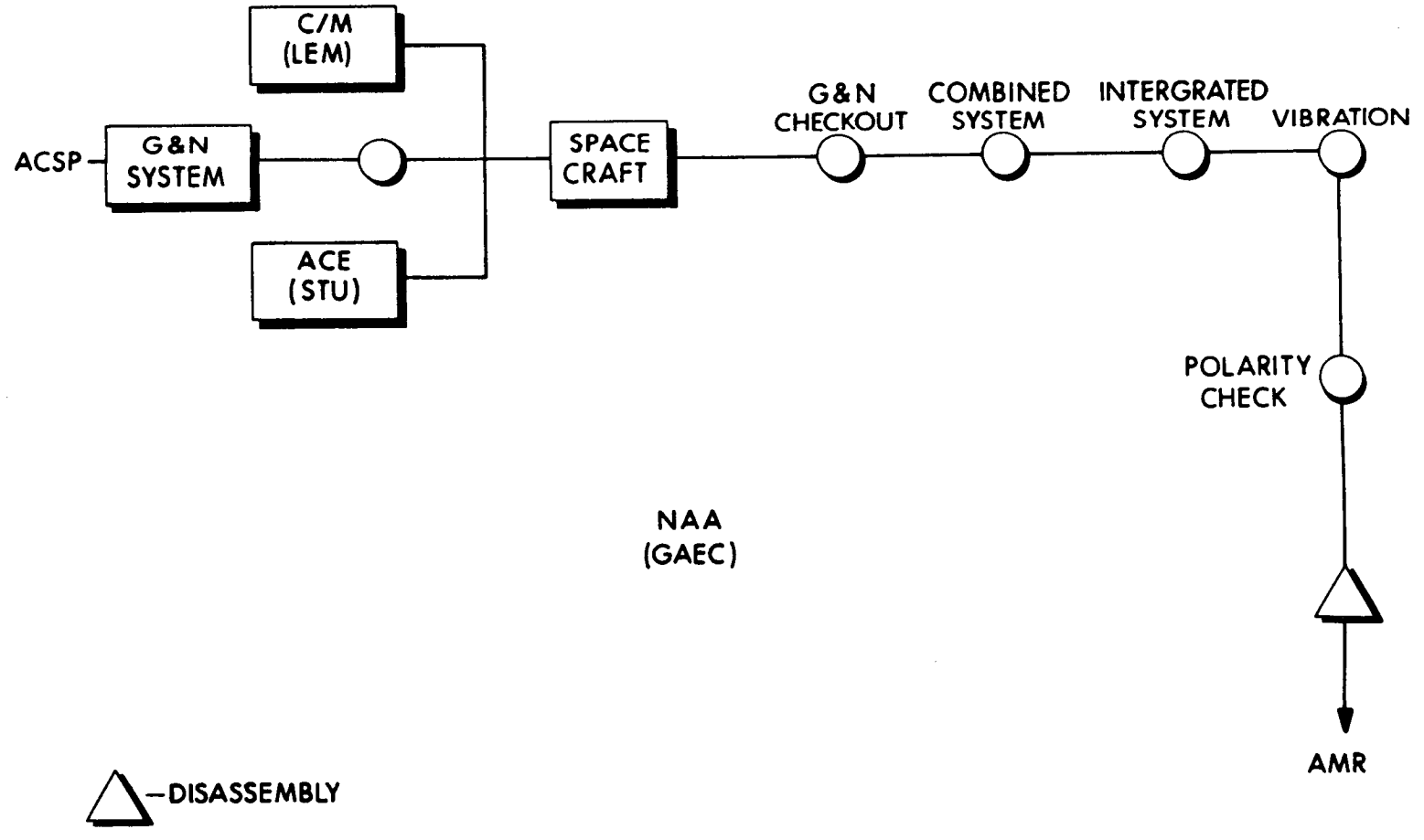

Fig. 14-7 Equipment flow (5).

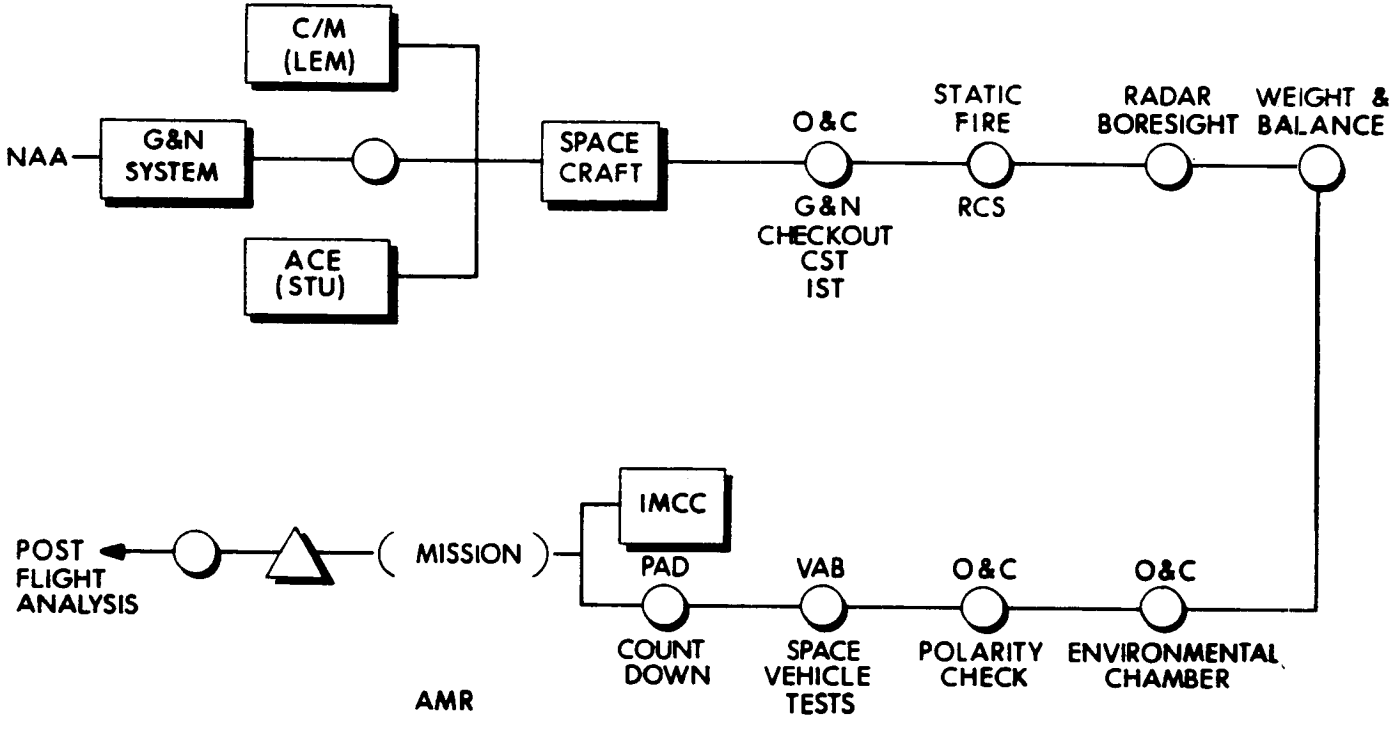

Fig. 14-8 Equipment flow (6).

Parts of the PSA, CDU, D&C electronics and G&N indicator panel are also used for further tests on the Optical Subsystem in the following manner. As the optical subsystem comes in from Kollsman and after receiving an incoming inspection, it is assembled on the Nav. Base and tested again at that level. Then it is assembled with the rest of the equipment for the Optical Subsystem tests.

The M&DV and Computer are inspected when received; the Harness and Shroud are individually tested; and then all equipment is assembled into a complete system and the G&N ATP and FTM are performed.

Systems are shipped to NAA or GAEC, reassembled and tested with the same G&N ATP. After installation, spacecraft tests are performed. The first tests are primarily on the G&N itself, supplied by spacecraft power and coolant, without particular attention to any other spacecraft interfaces. Then combined system tests are performed where all the interfaces are considered. Vibration tests are performed at NAA and at GAEC (with the G&N operating) and finally Polarity and Phasing checks are made. The various subsystems are then removed from the spacecraft and shipped separately to AMR where each is again tested in the MIT facility, reinstalled into the spacecraft and partially retested with the checkout procedures that were previously used. The system will have static firing, radar boresight, weight and balance, environmental, polarity and phasing tests, then proceed to the Vertical Assembly Building for space vehicle tests, and then countdown. After the mission the G&N is removed from the spacecraft and a post-flight analysis is performed.

Figure 14-9 shows how Test Procedures are generated and documented. Starting with the upper left, the figure shows that test requirements are documented from various sources. A measurements list evolves; and hardware configuration and laboratory tests are devised. Spacecraft tests reflect a number of information sources; documents that come from Cape Kennedy, NAA, GAEC, and various meetings. From these MIT/IL writes a detailed Process Specification which is transmitted to NAA. NAA then writes the Operating Test Procedures for use by ACE operators.

Various tests are performed in the laboratories and in the spacecraft. These system tests are outlined in Figs. 14-10 and 14-11.

At the field sites there will be an MIT site manager (now called a Test Operations Director), administrator, a chief engineer, contractor engineers, and support people (Fig. 14-12).

AGE-4 is now assembled and under test. It is the first complete G&N system; at the present time, it has a breadboard harness and a few other interim components. The initial phase of testing will be completed and the system will be ready for shipment to the MIT test facility at NAA in about a month. Some of the results of this operation are listed in Fig. 14-13: the design has been verified, test procedures have been improved using

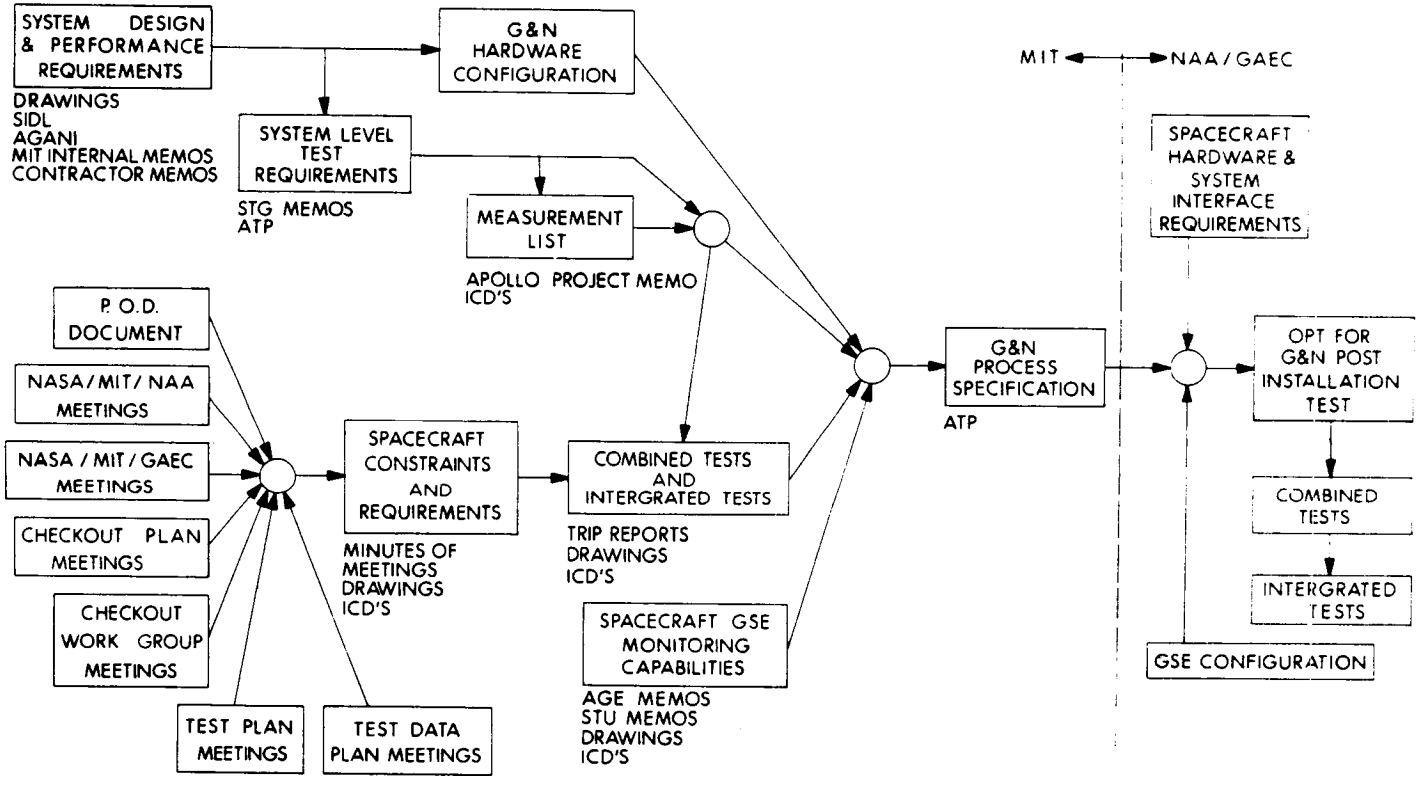

Fig. 14-9 Test procedure generation and documentation.

- Check Power Supplies
- Check Temperature Control
- Check Operation Of
  - Map and Data Viewer
  - Condition Lights
  - Panel Brightness and Lamp Controls
- Check AGC and DSKY's
- Check Optics - CDU Operation
- Check IMU - CDU Operation
- Check CDU - IMU - Optics Servo Characteristics
- Check Gimbal Response and Torque Level
- Measure IRIG Torquing Scale Factor

Fig. 14-10 Lab and spacecraft test outline.

- Measure IRIG Drift Coefficients
- Measure PIPA Scale Factor and BIAS
- Check Optics - AGC Angle Measurement
- Perform Optics - AGC - IMU Alignment
- Perform Gyro Compass Mode
- Check Spacecraft Interface

Fig. 14-11 Lab and spacecraft test outline (cont'd.)

	POSITION OR AREA	ACTIVITY
1.	Test Operations Director (MIT/IL)	Provides overall technical direction at the site, host contractor coordination, long range planning, special testing.
2.	Chief Engineer (MIT/IL)	Assists T. O. D. in technical direction, resolution of problems including failures, direction of special tests, acting as single point of technical contact.
3.	Site Manager (ACSP)	Responsibility for routine administration, test, coordination and management of the site.
4.	Lead Engineer (Raytheon & Kollsman)	Senior representative of their respective companies; under direction of Site Manager.
5.	Bench Maintenance	Area in the laboratory facility reserved for authorized field maintenance.
6.	Test Station Checkout	To certify that the equipment is operating within specified limits.
7.	ACE (Post Installation Checkout)	Support G&N tests conducted after installation in the spacecraft and other G&N interface activities.
8.	Quality Control	Assure safe handling and integrity of the G&N system during all phases of site activities.
9.	Logistics	Satisfy support requirements of each site with facility, manpower, and material assistance to accomplish the necessary operations.

Fig. 14-12 Site functions.

Status

1. Full Operation Except:
    - Breadboard Harness
    - Breadboard Computer
    - Breadboard D&C Control Electronics
    - Breadboard Support Fixture
    - No MDV
    - Interim Optics
2. First Phase Complete

    25 April 1964

Results

- Design Functionally Verified
- GSE Functionally Verified
- Lab Test Procedures Verified
- AGC Programs Proofed
- 390 Operating Hours
- 4 Failures
- 15 Design or Operation Problems Identified

Fig. 14-13 G&N 4 Test results. 25 March 1964.

the system, and programs have been proofed with the breadboard computer. Operating hours have reached 390 during which 4 failures have occurred while 15 prime problems have been identified. The failures and problems are listed in Figs. 14-14 and 14-15.

Failures:

a. Broken Solder Joint
   (connection redesigned)
b. Diode Failure
   (improper installation in breadboard item)
c. Transformer Failure
   (poor test procedures - rewritten)
d. AGC - 4 Transformer Failure
   (no direct course identified)

Problems:

1. AGC Display Inconsistency
2. AGC Interface 102.4 kc Noise
3. AGC - PIPA Interface
4. AGC - Optics CDU Interface
5. PSA Servo Transient During Mode Switching
6. Ducosyn Excitation Voltage Amplitude

Fig. 14-14 G&N 4 Test results. 25 March 1964.

7. PSA 102.4 kc Noise Coupling
8. Optics Zero Mode Ambiguity
9. Optics Reticle Lighting Inadequate
10. Optics Phasing
11. D&C Brightness Control
12. D&C Magnetic Amplifier +28 VDC Source
13. D&C Switch Reliability
14. CDU Manual Mode Operation
15. 6.4 kc Noise on Servo Error Signals and SCS Interface

Fig. 14-15 G&N 4 Test results. 25 March 1964 (cont'd.).

Section 15

G&N FLIGHT DEVELOPMENT PROGRAM

J. M. Dahlen

This section concerns the flight development program. (A more complete description is given in R-434, G&N Development Test Plan.) Figure 15-1 shows the basic framework of objectives which can only be attained in flight. The ground support operation requires a similar verification.

Figure 15-2 shows the test objectives for the early unmanned flights. The primary concern here is crew safety (it is now agreed that Guidance and Navigation (G&N) does influence safety). Objectives not critical to crew safety but to G&N development are also shown. Ground tracking data will be used in place of optics data for navigation. The automatic star tracker will periodically re-align the IMU.

Automatic control of the spacecraft, which is designed to be manned, is shown in Fig. 15-3 and described here. Details are subject to change, but the basic concept is illustrated. Control in unmanned modes will be performed by the Apollo Guidance Computer (AGC) through peripheral equipment required to interface with the spacecraft (S/C) systems. The AGC is responsive to ground commands and data via the Digital Command System and the up-link; data go down via the down-link and PCM telemetry. Control of the S/C will be performed by relay closures in the Display & Keyboard (DSKY) as directed by the AGC. A S/C relay box will probably be required because the power requirements are too high for the DSKY.

It appears there will be about 56 output functions from the computer. Three are required for the reaction control system (RCS) to turn it on after separation from the booster, dumping fuel tanks, and purging fuel tanks after entry. Stabilization Control System (SCS) mode switching for various exercises, including direct control of the jets, requires 14 signals. The electrical power supply (EPS) requires signals to purge fuel cells, to switch to backup batteries, etc. The AGC backs up sequences performed by the Earth Landing System and the Mission Sequencer. Inputs to the service propulsion system (SPS) activate the gimbal motors, restart in case of rough combustion cutoff, etc. The Environmental Control System (ECS) and the Telecommunication System (T/C) will also be activated. Five inputs to the AGC are required. One input from the Earth Landing System is altitude for the sequence start. It monitors two battery voltages. From the SCS it requires indication of failure of the Electronics Control Assembly to switch to

VERIFY GUIDANCE & NAVIGATION SYSTEM

1. STABILITY OF G&N/SPACECRAFT DYNAMIC LOOPS
2. IMU STABILIZATION AND ACCURACY IN FLIGHT ENVIRONMENT
3. OPTICS ACCURACY AND FUNCTIONAL OPERATION
4. PROGRAMS, PROCEDURES AND G&N/SPACECRAFT INTEGRATED OPERATION IN COMPLEX MODES
5. ESTABLISH CONFIDENCE IN GROUND SIMULATIONS TO PERMIT THEIR EXTRAPOLATION TO SUBSEQUENT MISSIONS

VERIFY GROUND OPERATIONAL SUPPORT

1. TELEMETRY CONFIRMATION OF SYSTEM STATUS INDICATED BY ON-BOARD DISPLAYS
2. MSFN TRACKING AND COMPUTATION CAPABILITY FOR:

   TRAJECTORY DETERMINATION

   SUPPLEMENTING OPTICS DATA

   BACK-UP NAVIGATION
3. IMCC GUIDANCE MONITOR CAPABILITY

Fig. 15-1 Flight development program objectives.

GUIDANCE AND CONTROL MODES CRITICAL FOR CREW SAFETY

1. G&N AND SCS THRUST VECTOR CONTROL MODES
2. G&N AND SCS ORBITAL ATTITUDE CONTROL LOOPS
3. G&N ENTRY MODE

OTHER G&N PRIMARY OBJECTIVES

1. MONITOR OF BOOST TRAJECTORY
2. ORBIT NAVIGATION PROGRAM USING RAW NAVIGATION DATA (R, R), VIA UP-LINK
3. AUTOMATIC IMU ALIGNMENT USING STAR TRACKER

GROUND OPERATIONAL SUPPORT

1. TELEMETRY OF SYSTEM DATA
2. BOOST MONITOR AND INJECTION CONFIRMATION
3. MSFN DETERMINATION OF ORBIT AND RETRO PARAMETERS
4. IMCC GUIDANCE MONITOR CAPABILITY FOR EARTH ORBIT MISSIONS

Fig. 15-2 Unmanned C-1B missions - test objectives (201, 202, 203).

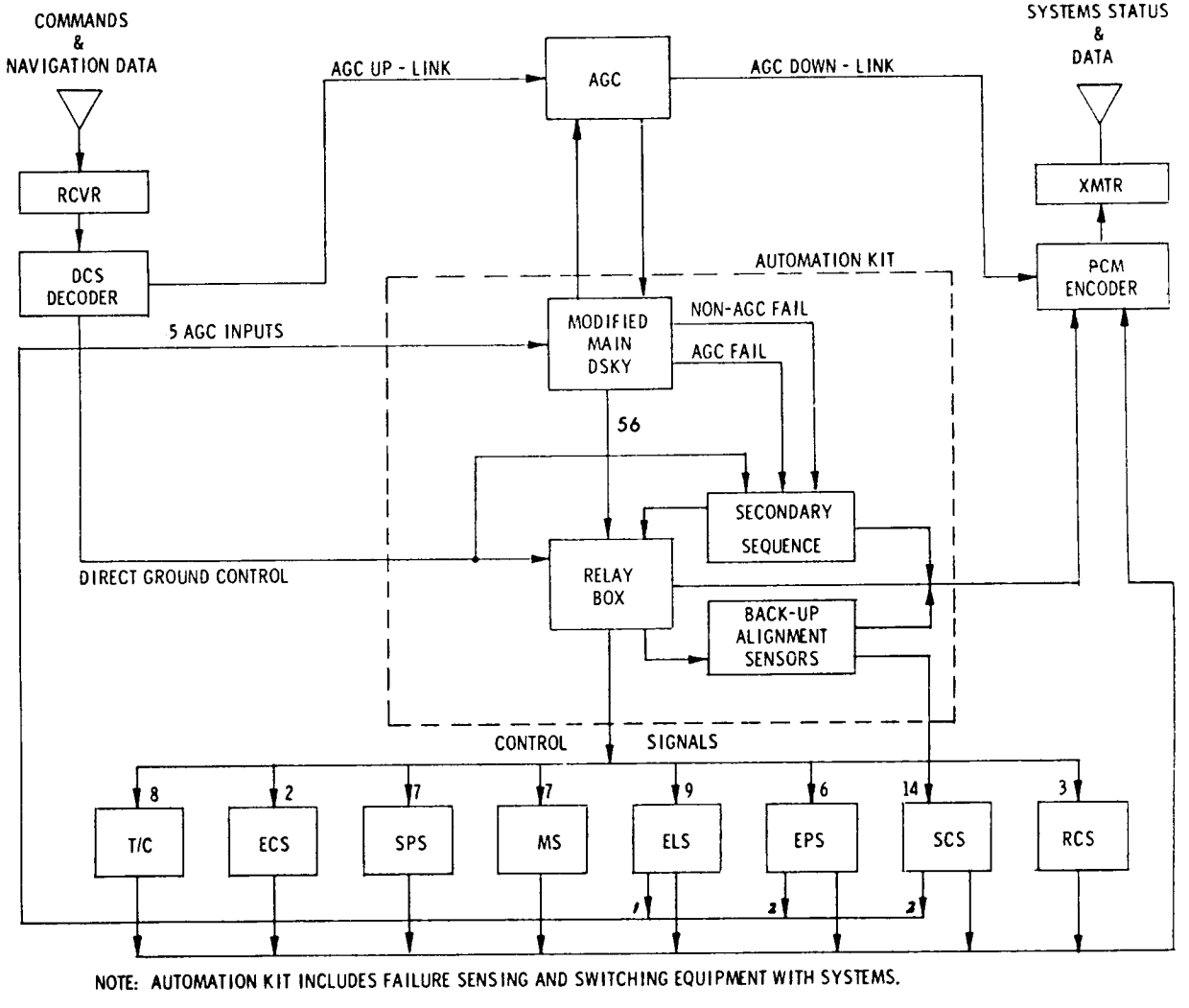

Fig. 15-3 Unmanned spacecraft control.

direct mode; and it requires a zero crossing signal from the ΔV counter to permit loading this counter in the SCS ΔV mode.

North American Aviation wishes to get the command module back in case of failure. This requires a secondary sequencer and backup alignment sensors. This sequencer would be activated in the event of AGC failure to perform the functions which the ground control link cannot perform. In case of non-AGC failure, it would control certain dynamic functions, but the AGC would still be used. The backup alignment sensors will probably be horizon sensors and sun-seekers to establish alignment. This automation kit would be designed for 4-day maximum capability.

Figure 15-4 shows guidance error data for an unmanned circular orbit mission. Error is expressed as a function of N orbits, that is, the number of orbits after 3. If the mission is flown without any updating the error is 42 + 14 N n. m. With up-link navigation data, the error is reduced to 7 + 2. 3 N n. m. This error is primarily due to misalignment of the IMU. The IMU is drifting, and every orbit beyond 3 adds about 2. 3 n. m. of error. If automatic IMU alignment is used the error can be reduced to one n. m. This is equivalent to performance of the manned system.

Figure 15-5 shows the proposed elliptical orbit mission errors. This mission would stress the heat shield more and may constrain the manned elliptical missions. A parking orbit is assumed before going into an elliptical orbit of 3000 n. m. apogee. The entry angle error is of interest to the heat shield people.

Figures 15-6 and 15-7 show test objectives for the C-1B manned missions. All optical modes except the star-earth landmark mode may be performed in circular earth orbit. The star-earth landmark sightings cannot be made in circular orbit, so elliptical orbit missions are proposed to do this. In the elliptical orbit mission, the transearth injection mode can be evaluated since it is similar to the elliptical orbit injection.

About a 3000 n. m. apogee is required for testing the SXT; at lower altitudes the angle rate between star and landmark exceeds one milliradian/sec which is the maximum permissible for proper manual operation of the sextant. Also, the earth subtends a large field of view at low altitudes making star acquisition difficult.

Figure 15-7 also shows Lunar Excusion Module (LEM) test objectives, assuming the LEM is available for rendezvous. Retrieval of the LEM by the Command Service Module (CSM) would be the first objective. Afterwards, LEM rendezvous could be done using the LEM G&N system. Fuel is marginal in these C-1B missions and this hinders the test program.

Figure 15-8 shows the profile for an elliptical orbit mission. The star-landmark angle rate of 0. 65 milliradian/sec corresponds to an apogee of 3700 n. m. , so the apogee could be lower.

UNMANNED CIRCULAR EARTH ORBITAL MISSIONS

SPLASH POSITION ERROR

ASSUMPTIONS:

1. 100 n mi ORBIT
2. COAST FOR 3 + N ORBITS
3. ENTRY RANGE = 1000 n mi (FROM h = 400,000 ft.)

	SPLASH ERROR (1σ) n mi
ALL - INERTIAL GUIDANCE	42 +14N
NAVIGATION DATA VIA UP-LINK	7 + 2.3N
NAVIGATION DATA VIA UP-LINK, PLUS AUTOMATIC IMU ALIGNMENT BEFORE RETRO	1

Fig. 15-4.

ASSUMPTIONS:

1. 100 n mi PARKING ORBIT
2. COAST FOR 3 + N PARKING ORBITS
3. INJECT TO 3000 n mi APOGEE ELLIPTICAL ORBIT
4. ENTRY AT END OF FIRST ELLIPTICAL ORBIT (29,000 fps)
5. ENTRY RANGE = 2000 n mi (FROM h = 400,000 ft.)

	ENTRY ANGLE ERROR, $\sigma(\gamma)$	SPLASH ERROR (1σ) n mi
ALL - INERTIAL GUIDANCE	1 1/4 °	215 + 65N
NAVIGATION DATA VIA UP-LINK	1/4 °	18 + 4N
NAVIGATION DATA VIA UP-LINK PLUS AUTOMATIC IMU ALIGNMENT BEFORE RETRO	NEGLIGIBLE	2

Fig. 15-5 Unmanned elliptical orbit missions splash position error.

FIRST MANNED FLIGHT (204)

1. CREW OPERATION OF SYSTEM IN SPACE ENVIRONMENT
2. OPTICS ACCURACY & FUNCTIONAL EVALUATION:

   IMU ALIGNMENT IN FLIGHT

   LOW ORBIT LANDMARK TRACKING

   SEXTANT STAR-LUNAR LANDMARK ANGLE MEAS.

   STAR EVALUATION ABOVE BRIGHT HORIZON (STAR TRACKER - HORIZON PHOTOMETER MODE)
3. ORBIT NAVIGATION PROGRAM USING OPTICS ANGLE DATA
4. ATTITUDE CONTROL OF S-IVb + SPACECRAFT

ELLIPTIC ORBIT MISSIONS (205, 206)

1. EVALUATION OF TRANSEARTH INJECTION MODE
2. EVALUATION OF SEXTANT IN STAR-EARTH LANDMARK ANGLE MEAS. MODE. REQUIRES ~3000 MILE APOGEE:

   ANGLE RATE EXCEEDS 1 MILLIRADIAN PER SECOND FOR LOWER APOGEES

   ACQUISITION OF NAVIGATIONAL STAR WITHIN 50^{0} (SXT LIMITATION) OF LANDMARK IS UNCERTAIN BELOW 3000 MILES

Fig. 15-6 Manned C-1B missions - test objectives.

GROUND DETERMINATION OF "TRUE" ANGLE IS NOT SUFFICIENTLY ACCURATE FOR ALTITUDES LESS THAN 2000 MILES

3. EVALUATION OF MIDCOURSE NAVIGATION INCL. VELOCITY CORRECTIONS

RENDEZVOUS DEVELOPMENT MISSIONS (207, ...)

1. DEMONSTRATION OF CSM RETRIEVAL OF UNMANNED LEM USING CM G&N SYSTEM
2. DEMONSTRATION OF LEM RENDEZVOUS WITH CSM USING LEM G&N SYSTEM
3. LIMITED EVALUATION OF LEM THRUST VECTOR CONTROL AND ORBITAL ATTITUDE CONTROL MODES

ALL MISSIONS: DEVELOPMENT OF IMCC/MSFN CAPABILITY TO MONITOR CSM - LEM OPERATIONS

Fig. 15-7 Manned C-IB missions - test objectives (cont).

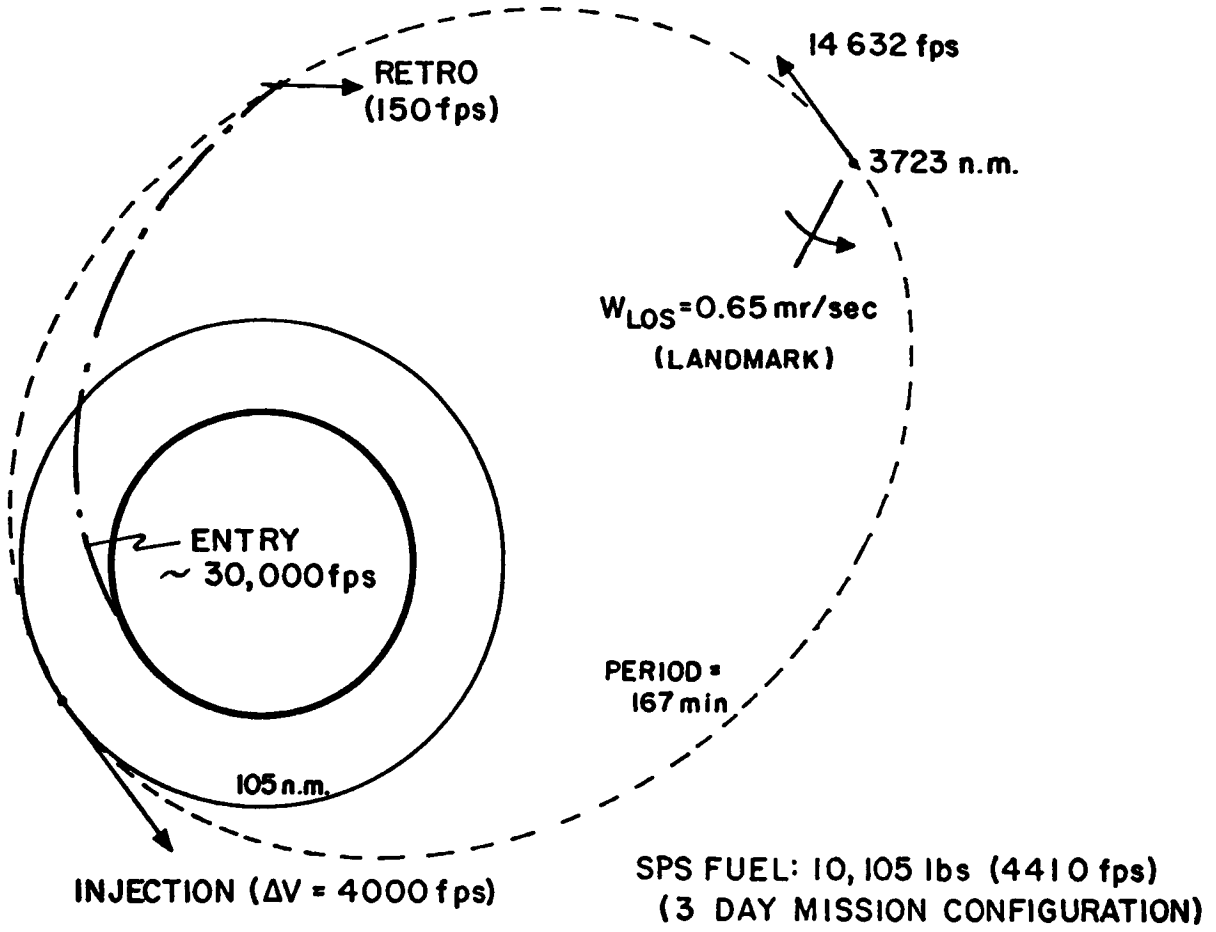

Fig. 15-8 Maximum elliptic orbit -- verification of mid-course guidance.

Figure 15-9 shows the profile of a typical rendezvous mission. The assumed weights and fuel amounts are shown. The first step would be CSM retrieval, and would not require a LEM descent propulsion system. This mission could be done in synchronous orbit fashion.

Figure 15-10 shows a mission assuming complete systems on the LEM, thus reducing its available fuel. The total fuel shown is for both craft and is very marginal.

Figure 15-11 shows test objectives for the unmanned C-V missions. The booster would effectively carry the spacecraft through translunar injection after which the CSM would separate and return to earth. According to present schedules a full LEM will be carried on flights 502 and 503. It is proposed to get the LEM out of the adapter, and exercise the propulsion system and the thrust vector control loops.

Unmanned C-V missions are shown in Fig. 15-12. The proposed mission plan provides for a full mission sequence including insertion by the S-IVB, separation, retromaneuver by the SPS simulating an abort and finally a posigrade thrust to normal lunar return velocity. The total flight time is about 8-1/2 hours.

Entry errors for the mission just described are shown in Fig. 15-13. For the all-inertial case, the errors are intolerable. Position and velocity updating pulls the errors down considerably; addition of automatic IMU alignment reduces the errors to a minimum.

Figure 15-14 illustrates the guidance monitor capability which must be developed concurrently with the G&N system. The guidance monitor capability (or system) is in its embryonic stage right now. Both ground and in-flight monitor hardware and procedures must be defined and verified. It now appears that gross malfunctions will be indicated to the crew by direct displays, inoperable equipment or visual cues. Telemetry will permit the ground to confirm indications that the crew receives. Degradation in performance poses a more difficult problem because it can only be detected after some time delay. The sextant and ground radars, for example, supplement each other in confirming powered maneuvers.

Figure 15-15 is a logic diagram of the objectives in the C-1B and unmanned C-V programs. The unmanned flights demonstrate modes which constrain subsequent manned flights. Manned flights demonstrate the balance of the G&N modes to qualify the system for lunar operations. Each test involving a manned vehicle is constrained by a prior demonstration of required abort modes.

Figure 15-16 shows the test objectives of the manned C-V missions. Because transposition and docking is a manual operation, the spacecraft must be manned in order to test the thrust vector control and attitude control loops for the full CSM and LEM configuration. Landing evaluation requires an actual landing. One can attempt an unmanned

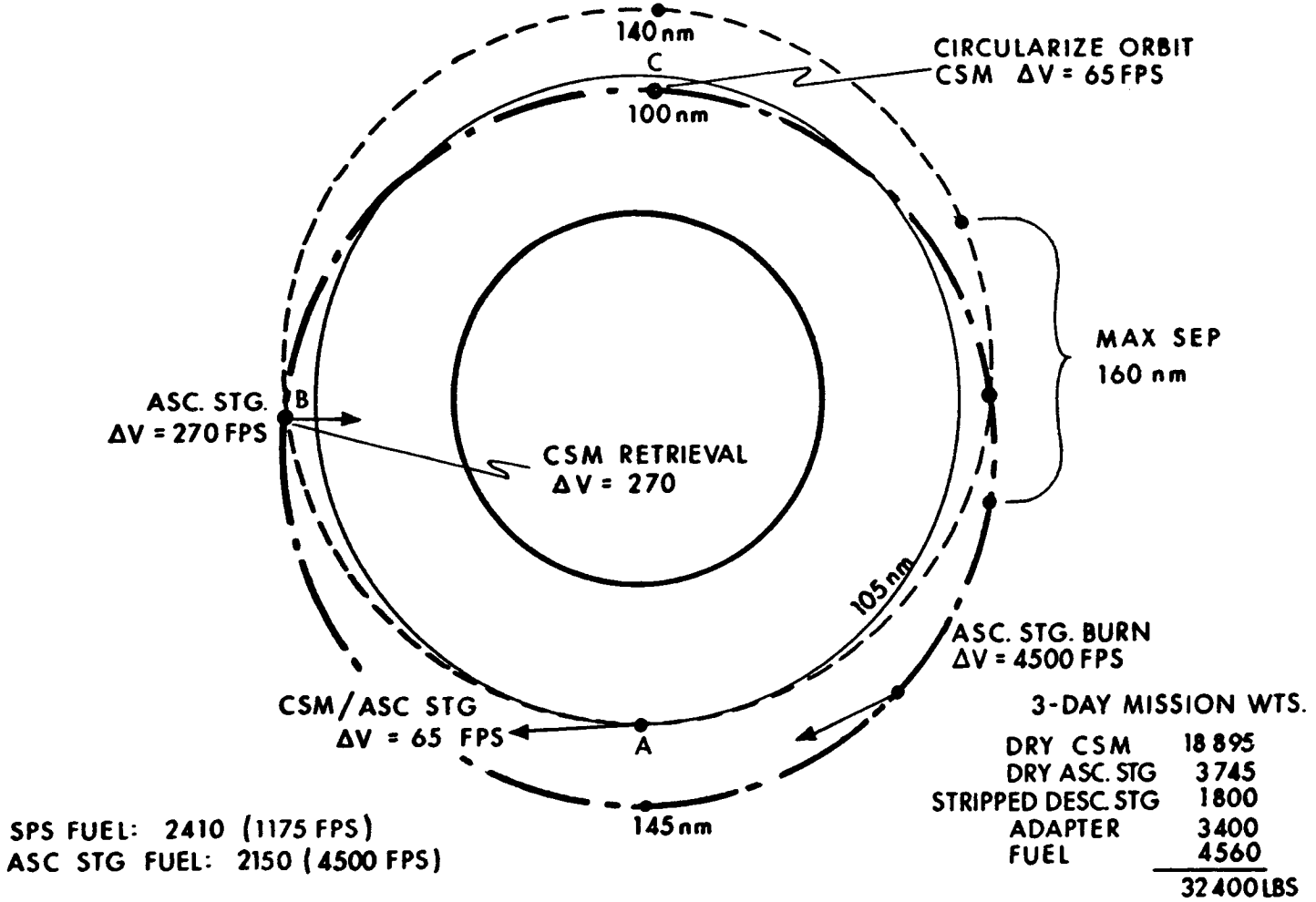

Fig. 15-9 CSM retrieval of unmanned ascent stage

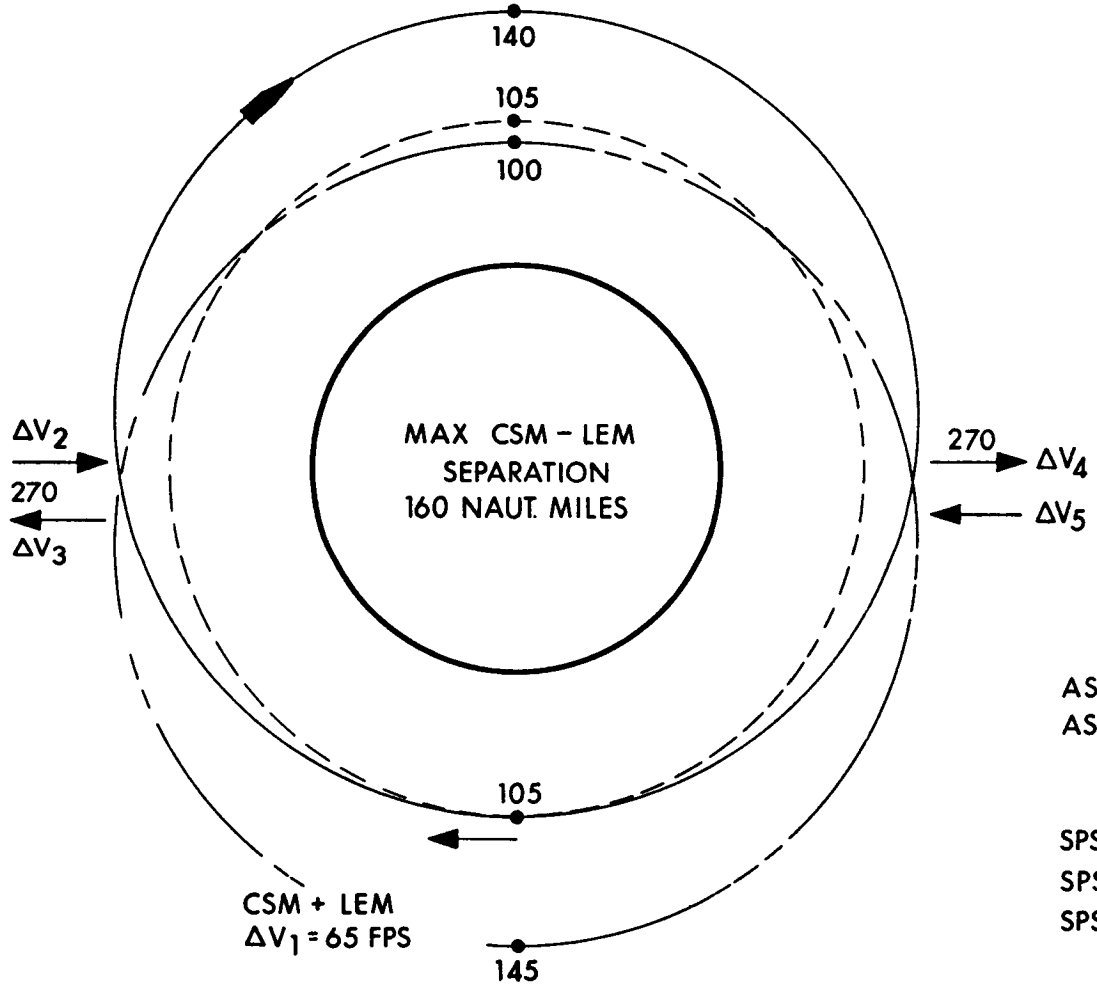

WEIGHTS (3 DAY)

DRY CSM	18,895
DRY ASC	3,745
DRY DSC	3,277
ADAPTER	3,400
FUEL	3,083
TOTAL	32,400

FUEL BUDGET

SPS ΔV_1	(65)	183
ASC + DSC ΔV_2	(270)	208
ASC + DSC ΔV_3	(270)	202
ASC ΔV_4	(270)	108
ASC ΔV_5	(270)	105
SPS CIRCULARIZE	(65)	733
SPS RETRIEVAL	(300)	
SPS RETRO	(750)	1500
TOTAL		3039

Fig. 15-10 Rendezvous demonstration complete S/C.

CM G&N OBJECTIVES (501, 502, 503)

1. MONITOR TRANSLUNAR INJECTION
2. THRUST VECTOR CONTROL OF FULL CSM, SIMULATING ABORT FROM TRANSLUNAR ORBIT
3. DEMONSTRATE ENTRY GUIDANCE AT LUNAR RETURN VELOCITY
4. FURTHER EVALUATION OF MIDCOURSE GUIDANCE

LEM G&N OBJECTIVES (502, 503)

1. DEMONSTRATE THRUST VECTOR CONTROL OF LEM IN LANDING CONFIGURATION - FULL BURN OF DESCENT ENGINE INCLUDING VARIOUS THROTTLE SETTINGS AT HOVER CONDITION
2. DEMONSTRATE THRUST VECTOR CONTROL OF ASCENT STAGE FULL BURN SIMULATING LAUNCH OR ABORT

GROUND OPERATIONAL SUPPORT

1. DEMONSTRATE MSFN CAPABILITY TO CONFIRM INJECTION, DETERMINE MIDCOURSE TRAJECTORY AND PROVIDE BACK-UP MIDCOURSE GUIDANCE INCL. ENTRY INITIAL CONDITIONS
2. CONFIRM IMCC CAPABILITY TO MONITOR GUIDANCE

Fig. 15-11 Unmanned C-V missions - test objectives.

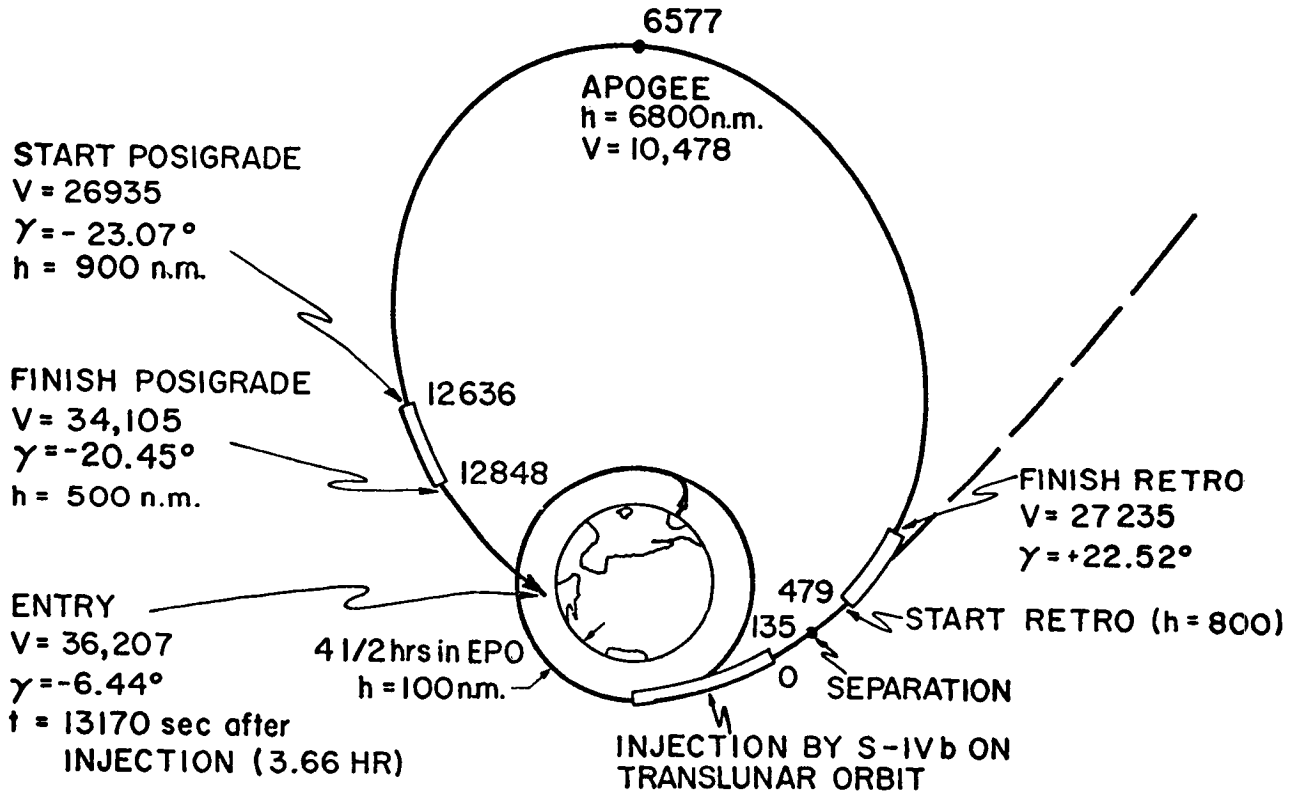

Fig. 15-12 Unmanned translunar abort and super-orbital entry mission (501 or 502).

1. INJECT INTO 100 NM ORBIT
2. COAST FOR 3 ORBITS
3. TRANSLUNAR INJECTION
4. ABORT AT h = 800 NM
5. COAST TO NEAR REENTRY
   (APOGEE ALTITUDE = 6800 NM)
6. INCREASE VELOCITY TO ESCAPE SPEED
7. REENTRY RANGE = 5000 NM

	FINAL ERROR (σ)		
	ENTRY ANGLE	RANGE	TRACK
CASE A INERTIAL NAVIGATION FROM LAUNCH TO LANDING	7°	3500 NM	62 NM
CASE B POSITION AND VELOCITY UPDATE BEFORE FINAL SM FIRING	1/4°	51 NM	46 NM
CASE C POSITION AND VELOCITY UPDATE AND AUTOMATIC IMU ALIGNMENT	~0	7 NM	2 NM

Fig. 15-13 Unmanned translunar abort and super-orbital entry mission errors (501 or 502 or 503).

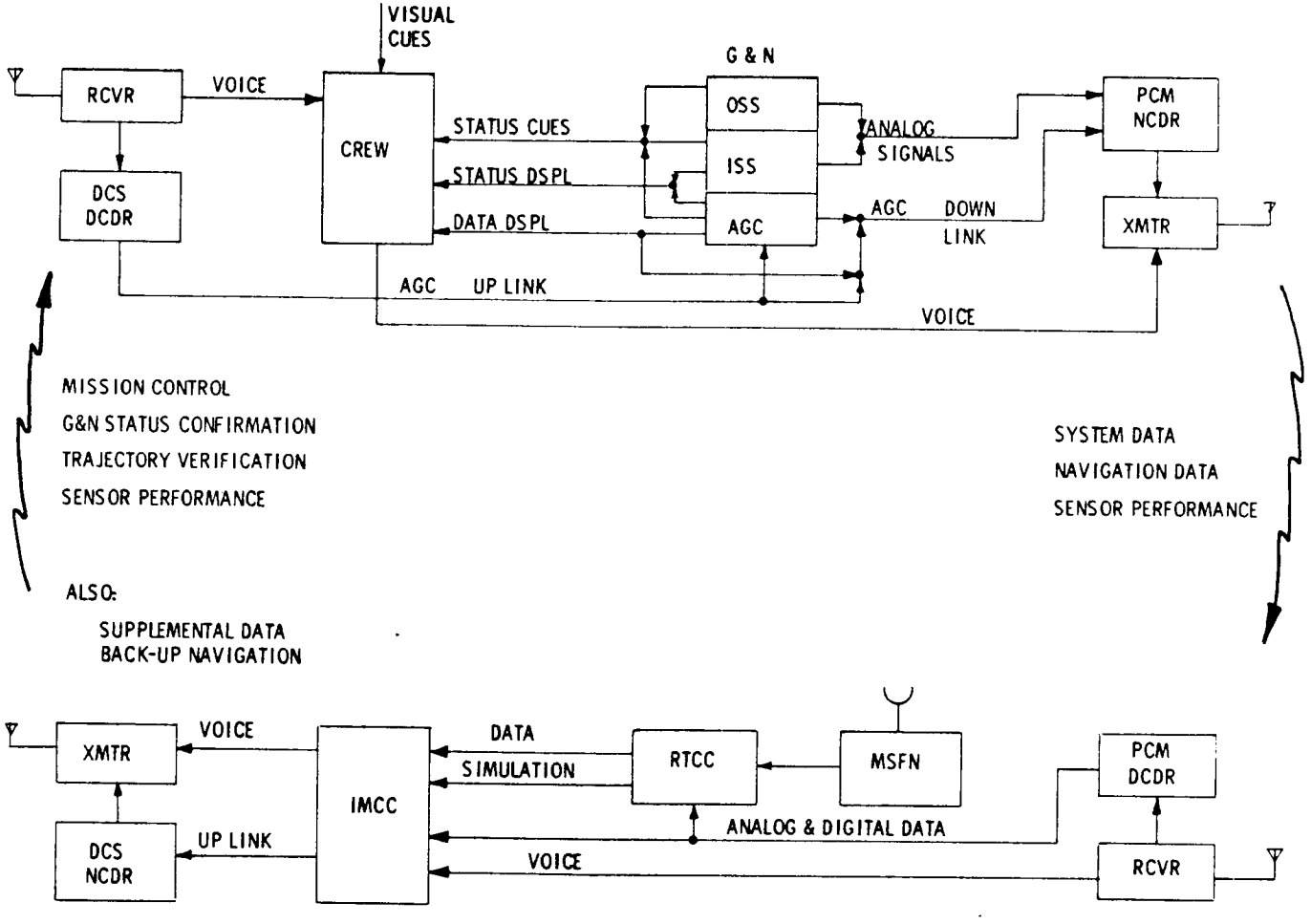

Fig. 15-14 Guidance monitor system (simplified).

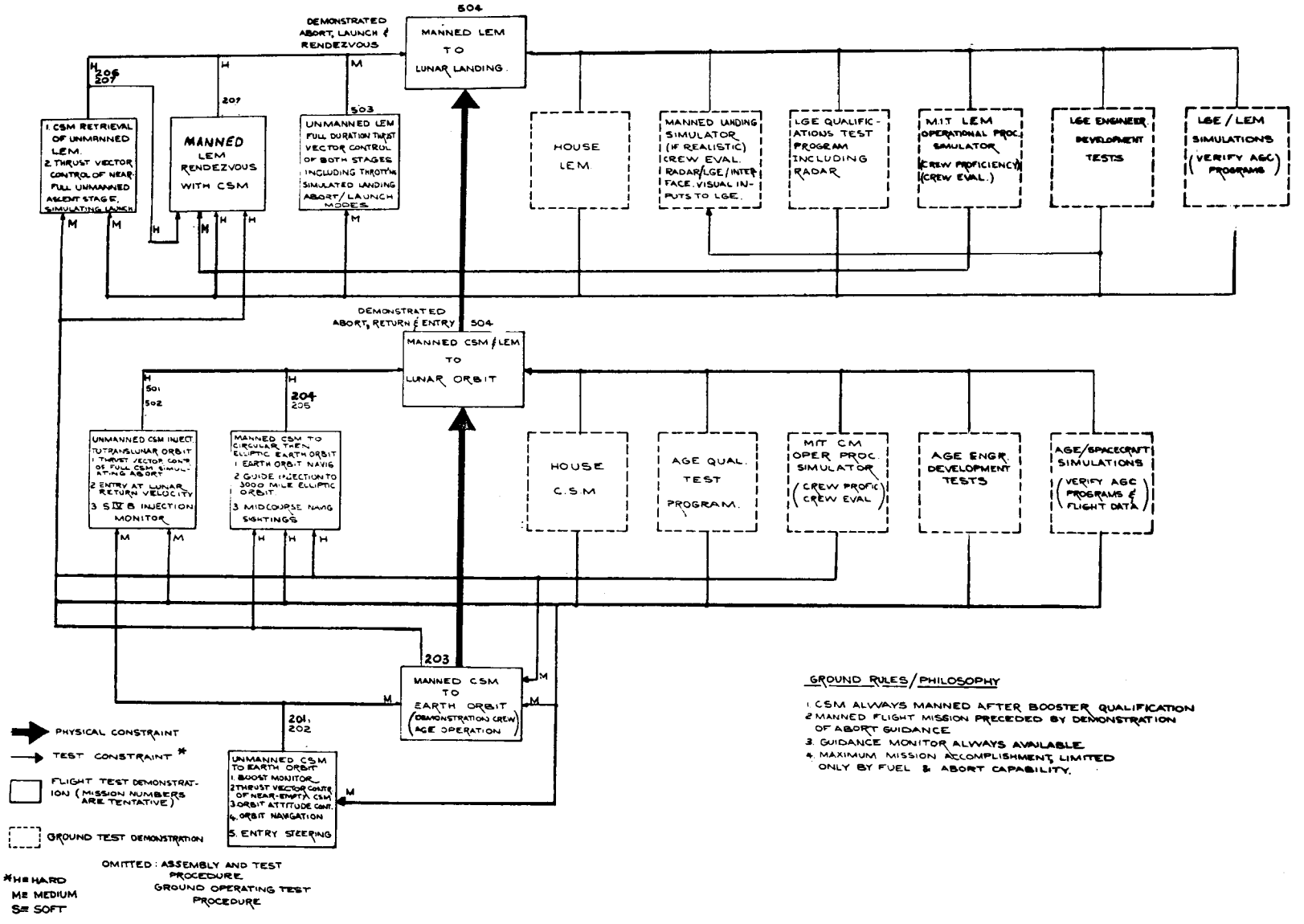

Fig. 15-15 Guidance flight tests -- objectives and constraints.

DYNAMIC LOOPS NOT PREVIOUSLY DEMONSTRATED

- THRUST VECTOR CONTROL OF FULL CSM + LEM
- ORBITAL ATTITUDE CONTROL OF FULL CSM + LEM
  1. UNAVOIDABLE RISK (SPACECRAFT MUST BE MANNED)
  2. MAXIMUM RELIANCE ON GROUND DYNAMIC SIMULATION
- LEM TERMINAL LANDING RADAR/INERTIAL/VISUAL MODE
  1. COMPLETE EVALUATION REQUIRES ACTUAL LUNAR LANDING
  2. UNMANNED LUNAR LANDING WOULD PROVIDE PARTIAL EVALUATION AND THEREFORE REDUCE CREW RISK (LANDING RELIABILITY LESS THAN FOR MANNED LANDING)
  3. UNRESOLVED QUESTION: CAN GUIDANCE PHENOMENA BE SIMULATED USEFULLY ON LANDING TEST VEHICLE?

Fig. 15-16 Manned C-V missions - test objectives.

landing first which, if successful, would reduce the risk in subsequent manned landings; however, a successful landing is much more probable with a full crew. Hence we do not recommend the unmanned landing as a required first step before manned landing.

Programs and procedures (software) not demonstrated prior to the C-V flights are listed in Fig. 15-17. These will not have been done in the actual lunar environment, but they will have been done in earlier simulated missions. Equipment operation will have been demonstrated, but the software for lunar operations is qualified by checking it out on simulators which have been validated by comparison with actual results on earlier missions.

The system would then be ready for a lunar landing attempt as described in Fig. 15-18. The remaining unproven guidance dynamic loops can only be proven with a man in the system and might just as well be tried on the lunar mission so far as G&N is concerned.

Figure 15-19 summarizes the G&N viewpoint on manned C-V objectives. The G&N would be ready for a lunar landing attempt on the first manned C-V mission. Other considerations as indicated will be instrumental in defining the actual objectives, however.

PROGRAMS / PROCEDURES (SOFTWARE) NOT PREVIOUSLY DEMONSTRATED

- MIDCOURSE GUIDANCE TO MOON & RETURN
- LUNAR ORBIT INSERTION
- LUNAR ORBIT NAVIGATION & LANDING SITE SELECTION
- LEM POWERED DESCENT & LANDING
- LEM LAUNCH/ABORT POWERED ASCENT
- RENDEZVOUS IN LUNAR ORBIT
    1. SYSTEM ACCURACY & OPERABILITY WITH SPACECRAFT (HARDWARE) IN ABOVE MODES HAS PREVIOUSLY BEEN DEMONSTRATED
    2. PROGRAM & PROCEDURE SIMULATORS HAVE BEEN VALIDATED BY PREVIOUS MISSIONS AND CAN THEREFORE BE EXTRAPOLATED TO CHECKOUT THE LUNAR MISSION SOFTWARE

Fig. 15-17 Manned C-V missions - test objectives (cont).

G&N READY FOR LUNAR LANDING ATTEMPT ON FIRST MANNED C-V MISSION

- RETURN GUIDANCE PREVIOUSLY DEMONSTRATED
  1. ABORT FROM TRANSLUNAR COAST
  2. TRANSEARTH INJECTION
  3. TRANSEARTH MIDCOURSE GUIDANCE
  4. ENTRY
  5. LEM LAUNCH/ABORT
  6. LEM RENDEZVOUS/CSM RETRIEVAL
- GUIDANCE MONITOR CAPABILITY ASSUMED ADEQUATE
- UNPROVEN GUIDANCE DYNAMIC LOOPS CAN BE TRIED ON THE LUNAR
- MISSION (IMPLIES ON-BOARD MONITOR OF LUNAR ORBIT INSERTION.)
- CONFIDENCE IN HARDWARE BASED UPON PREVIOUS DEMONSTRATIONS
- CONFIDENCE IN SOFTWARE BASED UPON CHECKOUT IN VALIDATED SIMULATIONS

Fig. 15-18 Manned C-V missions - test objectives (cont).

G&N READY FOR LANDING ATTEMPT ON FIRST MISSION

DEFINITION OF G&N OBJECTIVES HINGE UPON:

1. NASA POLICY WITH RESPECT TO URGENCY & ACCEPTABLE RISK

   READINESS OF GROUND OPERATIONAL SUPPORT*

   EVALUATION OF CSM + LEM DYNAMICS*

   UNMANNED LANDING (LESS RELIABLE THAN MANNED LANDING, BUT, IF SUCCESSFUL, WOULD REDUCE HAZARD TO CREW)

2. ALLOWABLE LANDING ERROR

   RECONNAISANCE MISSION REQUIREMENT

   JOINT OPERATIONS WITH LOGISTIC VEHICLE OR PENETROMETER PROBE

*MAY DICTATE INTERMEDIATE HIGH ALTITUDE ELLIPTIC ORBIT MISSION

Fig. 15-19 Manned C-V mission test objectives summary of G&N viewpoint.

Section 16

POWERED FLIGHT GUIDANCE

This Section is in two parts. The first section constitutes a review to date of the main development of powered flight procedures for the command and service module. The second section covers, in more detail, the item of central interest; the development of AGC powered flight programs.

PART 1

E. M. Copps, Jr.

Figure 16-1 is an outline of the analytical procedures used in developing the powered flight portion of the Apollo Guidance Computer (AGC). The present status, as indicated in the figure, is now in AGC program design. The development starts with the synthesis of steering equations which meet the requirements of the Apollo mission.

Figure 16-2 lists three requirements that the steer law computation must meet. A fourth requirement concerns computational economy, in order to meet speed and storage budgets. Steering equations used for the Apollo vehicle meet these requirements. The testing of the steer laws is first done in point-mass simulation, where vehicle dynamics are neglected, and the concentration is on definition of steering algorithms and boundary values. Translunar Injection, Deboost into Lunar Orbit, Transearth Injection, S-IVB Backup into Earth Orbit, and Abort from Midcourse, all use the same steer law, with redefinition of appropriate boundary values for each maneuver.

Figure 16-3 describes the steer law. The $\overline{V}_G$ and $\dot{\overline{V}}_G$ vector are aligned with the appropriate sign sense to shrink the velocity-to-be-gained vector to zero. Cut-off occurs when the $\overline{V}_G$ vector is zero. The $\overline{V}_G$ vector is obtained as the difference between $\overline{V}_R$ and $\overline{V}$ as described in Fig. 16-4. Note that the $\overline{V}_R$ vector is defined in terms of the present state of the vehicle, involving no prediction of future events. It is obtained by a solution of the appropriate boundary value problem for an inverse squared central force field. The $\overline{V}_G$ vector, the time rate of change of the velocity to be gained, is formed by the equation $\dot{\overline{V}}_G = \overline{b} - \overline{a}_T$. The $\overline{b}$ vector is analytically calculated along with the $\overline{V}_R$ vector. The $\overline{a}_T$ vector is obtained by reading the inputs to the AGC from the Pulsed Integrating Pendulum Accelerometers (PIPA's). The calculation of the vectors takes place in an inertial coordinate system instrumented by the Inertial Measurement Unit.

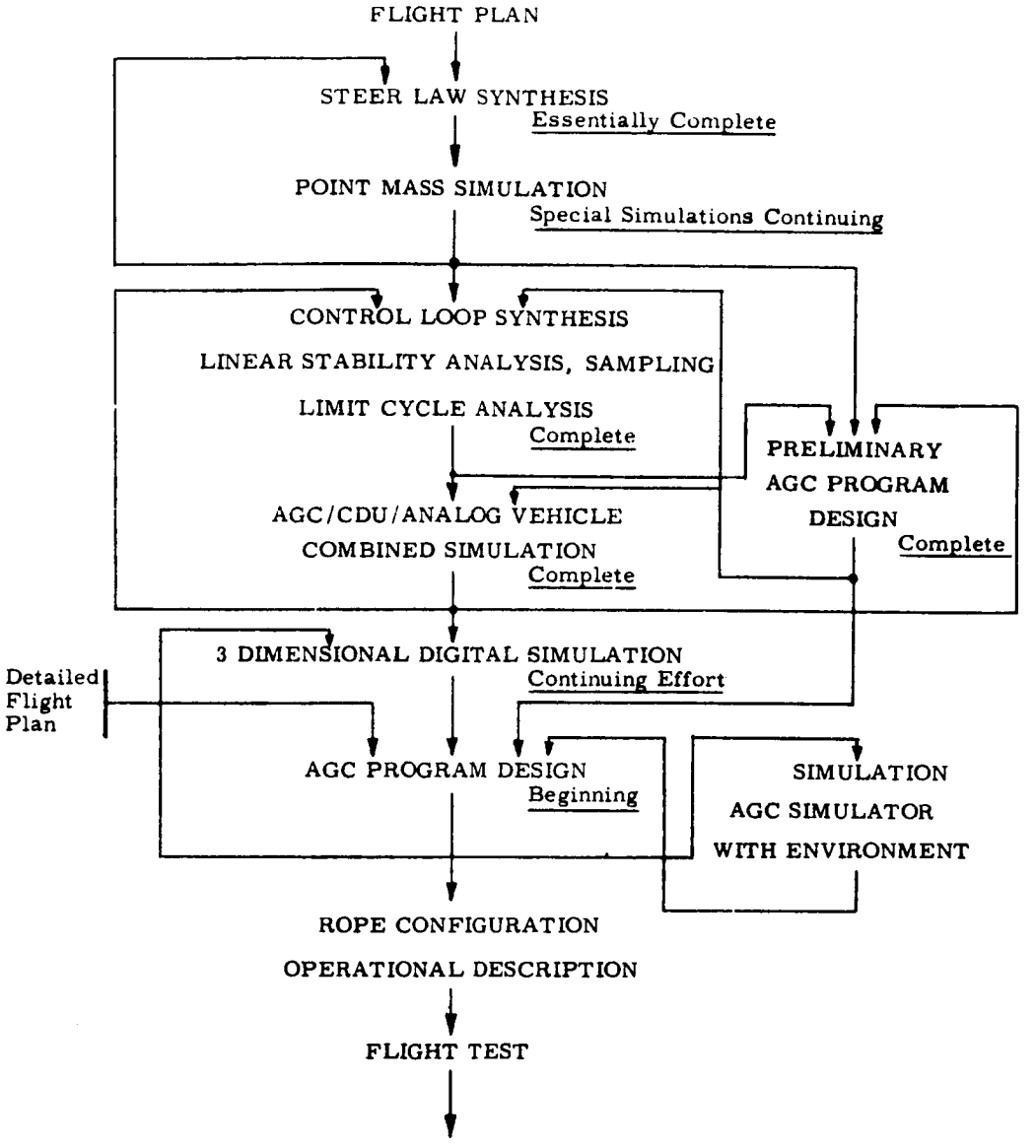
FLIGHT PLAN
STEER LAW SYNTHESIS
Essentially Complete
POINT MASS SIMULATION
Special Simulations Continuing
CONTROL LOOP SYNTHESIS
LINEAR STABILITY ANALYSIS, SAMPLING
LIMIT CYCLE ANALYSIS
Complete
PRELIMINARY
AGC PROGRAM
DESIGN
Complete
AGC/CDU/ANALOG VEHICLE
COMBINED SIMULATION
Complete
3 DIMENSIONAL DIGITAL SIMULATION
Continuing Effort
Detailed
Flight
Plan
AGC PROGRAM DESIGN
Beginning
SIMULATION
AGC SIMULATOR
WITH ENVIRONMENT
ROPE CONFIGURATION
OPERATIONAL DESCRIPTION
FLIGHT TEST

Fig. 16-1

COMPUTATIONS MUST

1) BE ACCURATE, CONSISTENT WITH ERROR CONTRIBUTIONS FROM
   - GUIDANCE HARDWARE
   - NAVIGATION UNCERTAINTIES

2) APPROACH CALCULUS OF VARIATIONS FUEL CONSUMPTION STANDARDS

3) BE SELF CONTAINED (Explicit)

Fig. 16-2 Criteria.

ANALYTIC SOLUTION TO THE APPROPRIATE TWO POINT BOUNDARY VALUE SOLUTION YIELDS TWO VECTORS

$$\bar{V}_G \quad \& \quad \bar{b}$$

where $$\dot{\bar{V}}_G = - \frac{\Delta \bar{V}}{\Delta T} + \bar{b}$$

STEER TO ALIGN $\bar{V}_G$ & $-\dot{\bar{V}}_G$

Fig. 16-3 Basic steer law, CSM.

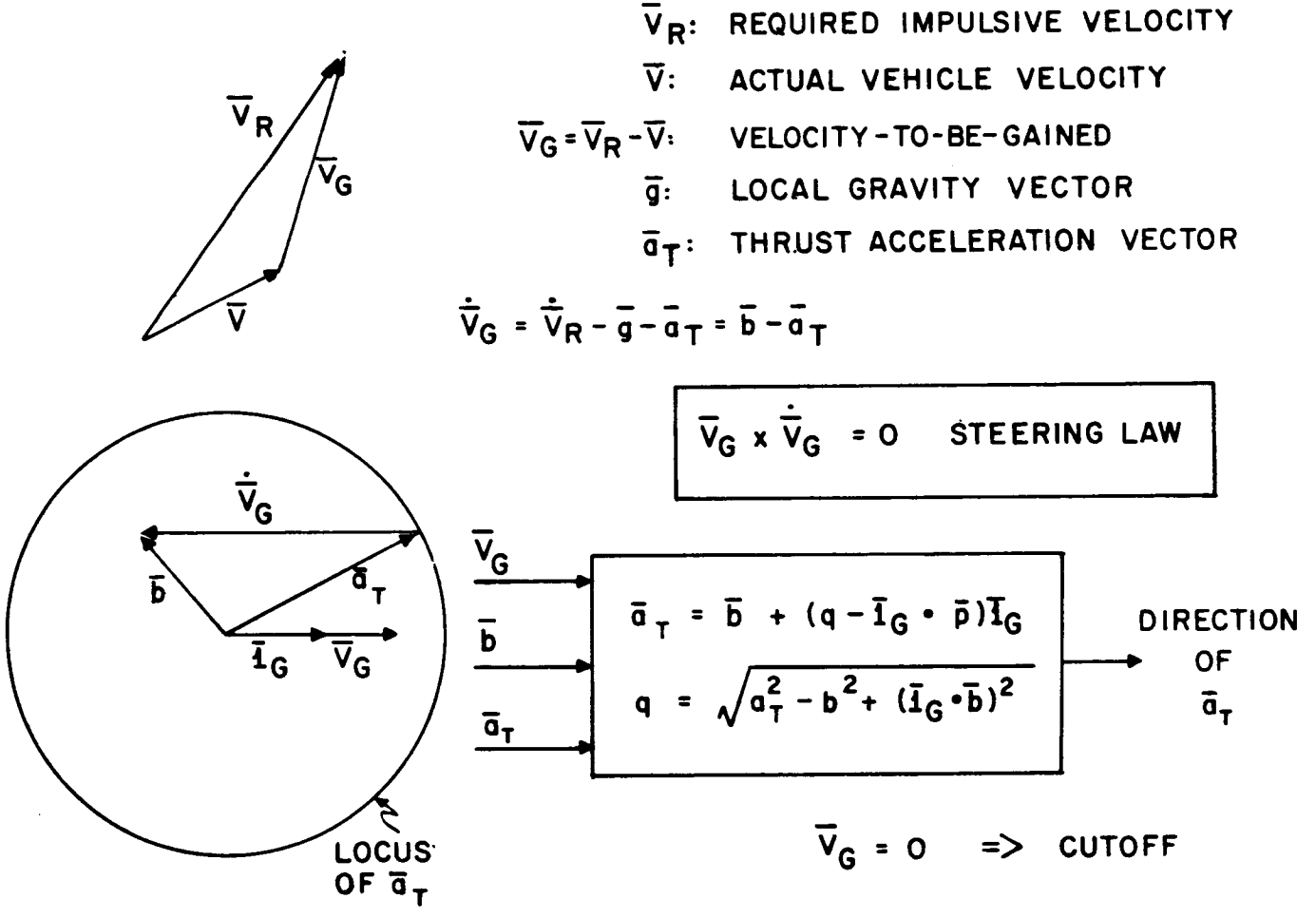

Fig. 16-4 Powered flight steering.

Before engine ignition, the direction that the acceleration vector of the vehicle should assume is calculated by the equations indicated at the bottom of Fig. 16-4. The estimated magnitude of vehicle acceleration is an input to this calculation. After engine ignition the direction of $\overline{a}_T$ is unnecessary. Rather, the cross product of $\overline{V}_G$ and $\dot{\overline{V}}_G$ yields an output which, when properly scaled, represents the magnitude and direction of vehicle rotation required to realign the vectors.

Figure 16-5 shows the information flow from PIPA inputs to Coupling and Display Unit (CDU) incremental rotations. Summarizing the process, incremental velocity information from the PIPA's are summed and sampled at the beginning of the process. This information is used to integrate the average G equations to obtain present position and velocity of the vehicle: $\overline{R}$ & $\overline{V}$.

$\overline{R}$ and $\overline{V}$ are inputs to the boundary value problem appropriate to the particular maneuver, yielding the $\overline{V}_G$ and $\overline{b}$ vector. The PIPA information is differenced over the sampling interval to obtain $\frac{\Delta \overline{V}}{\Delta T}$, an approximation to the $\overline{a}_T$ vector described in Fig. 16-4. The $\dot{\overline{V}}_G$ vector is formed and the cross product is taken. The output of this operation is an incremental rotation vector in stable member coordinates, $\Delta\theta_{sm}$. This vector is transformed to obtain incremental rotation commands to the coupling data units. The process is repeated once per second.

Figure 16-6 lists boundary values appropriate to the various maneuvers. Changing boundary values changes the box in Fig. 16-5 called $\overline{V}_G$, $\overline{b}$ equations. The rest of the calculation is common to all flight phases.

Figures 16-7, 16-8 and 16-9 are typical results of point-mass simulation analyses. Two quantities measured are the fuel used in the powered flight maneuver, and the fuel used in later velocity maneuvers because of inaccuracies in the completion of the present manuever. Several optimum programs based on calculus of variations have been written to test the performance of these equations. In all cases, the performance approaches the optimum solution within levels that make it difficult to detect differences between the planned solution and the optimum.

The next step in program development involves development of dynamical models and the synthesis of stable well-behaved closed-loop systems. Figure 16-10 shows a linear model for the AGC-controlled Apollo vehicle. Extensive linear analysis was performed using Z transform techniques, with linear approximations to the steering equations, and to the vehicle. This analysis permitted the setting of basic stability parameters such as sampling interval, loop gains, and compensation. Variations in performance of particular components were systematically studied for their effect on stability. Figure 16-11 illustrates a locus of Z-transform poles over loop gain for two values of CDU response time constant. Nonlinear techniques were used to identify limit cycle magnitudes and frequencies.

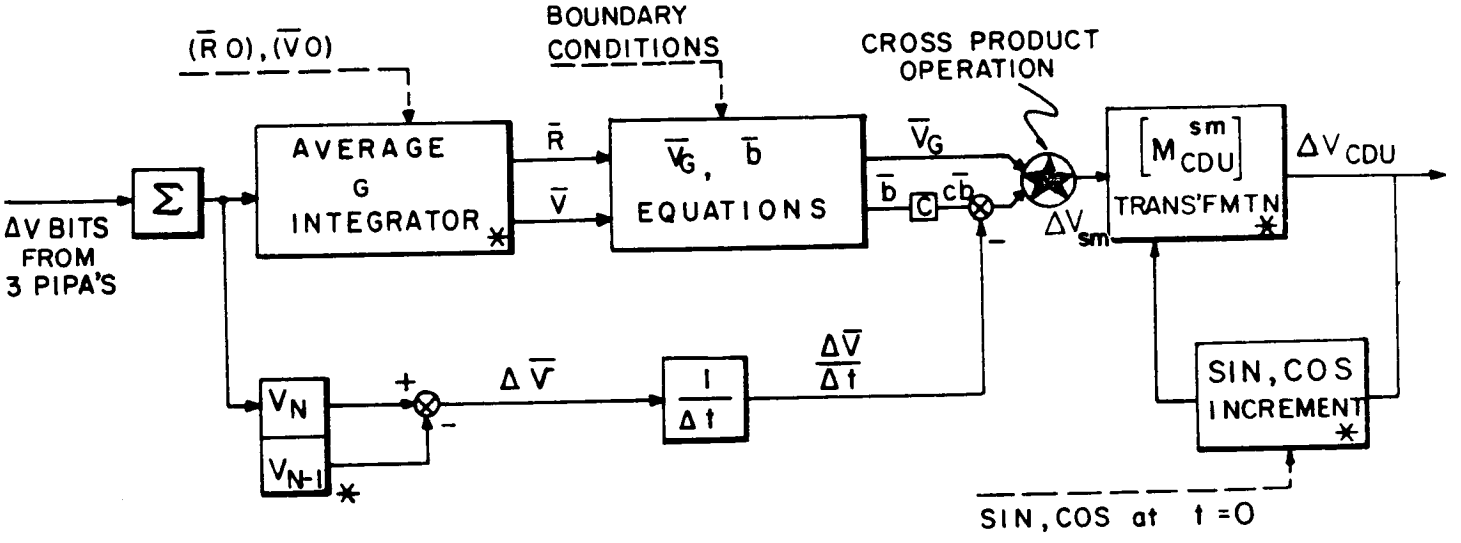

NOTE COMPUTATIONS MARKED WITH * ARE COMMON TO ALL POWERED MANEUVERS

BOUNDARY VALUES

1. TRANSLUNAR INJECTION — AIM POINT VECTOR
2. LUNAR DE-BOOST — CIRCULAR ORBIT
3. TRANSEARTH INJECTION — EXCESS HYPERBOLIC VELOCITY VECTOR
4. ABORT FROM MIDCOURSE — PERIGEE ALTITUDE, ECCENTRICITIES

Fig. 16-5 Thrust vector control, Apollo CSM AGC information flow.

SATURN S IVB BACKUP	LEAST FUEL CIRCULAR ORBIT
TRANSLUNAR INJECTION	CONIC AIM POINT (FIXED SEMI MAJOR AXIS)
MID-COURSE ABORT	FIXED ELLIPSE
LUNAR DE BOOST	LEAST FUEL CIRCULAR ORBIT
TRANS EARTH INJECTIONS	EXCESS HYPERBOLIC VELOCITY VECTOR

Fig. 16-6 Boundary values.

TRANSLUNAR INJECTION, $\overline{VG} \times \dot{\overline{VG}}$ STEERING (C = I)

PERTURBATION	EXTRA VELOCITY REQ'D FROM S-IVB	VELOCITY CORRECTION 1st MIDCOURSE
1. NONE	10,398.4 * ft/sec	.61 * ft/sec
2. THRUST 10% HIGH, I_{Sp} NOMINAL	-6.4	1.65
3. THRUST 5% LOW, I_{Sp} NOMINAL	8.8	2.15
4. THRUST 10% LOW, I_{Sp} NOMINAL	21.1	1.7
5. TRACK VEL. ERROR OF 10 ft/sec AT END OF BOOST INTO ORBIT	1.19	1.45
6. TRACK VEL. ERROR OF 30 ft/sec	1.81	2.38
7. RANGE VEL. ERROR OF 10 ft/sec AT END OF BOOST INTO ORBIT.	5.69	1.09
8. RANGE VEL. ERROR OF 30 ft/sec.	-12.1	3.00
9. 10 SECONDS LATE IGNITION	6.60	.82
10. 30 SECONDS LATE IGNITION	27.07	.51
11. 30 SECONDS EARLY IGNITION	27.81	.63
12. I_{Sp} 1% LOW	105.5	1.85

This is the total velocity used in the nominal case

note: Perturbations 5, 6, 7, and 8 are functions of the angle between boost and translunar injection. The worst value is quoted.

NOMINAL: Initial Wgt. = 276568 lbs Specific Impulse = 424 sec Thr. = 200,000 lbs

Fig. 16-7.

LUNAR DEBOOST -- NO Plane change

NOMINAL

Initial weight = 86,000 lbs

Specific impulse = 320 sec

Thrust = 21,935 lbs

Perturbation	Burn Time sec.	Fuel Used lbs.	Difference In Planes deg.	ΔV ft/sec	Altitude Miles
1. None	326.9	22411.2	0.00	3108.37	97.19
2. Ignition 5 sec. early	327.0	22411.9	0.00	3108.48	96.80
3. Ignition 5 sec. late	327.0	22411.9	0.00	3108.48	97.57
4. Initial Weight 1% high	330.2	22636.3	0.00	3108.52	97.39
5. Initial Weight 1% low	323.7	22186.4	0.00	3108.25	96.98
6. Fuel Flow 3% low	337.1	22414.6	0.00	3108.92	97.82
7. Fuel Flow 6% low	347.9	22419.8	0.00	3109.75	98.50
8. Ignition 15 sec. late, wt. 2% high, fuel flow 6% low	355.3	22890.9	0.00	3113.36	100.10

Fig. 16-8

LUNAR DEBOOST -- 6° Plane change

NOMINAL

Initial weight = 86,000 lbs

Specific impulse = 320 sec

Thrust = 21,935 lbs

Perturbation	Burn Time sec.	Fuel Used lbs.	Difference In Planes deg.	ΔV ft/sec	Altitude Miles
1. None	333.88	22886.3	0.022	3185.58	97.68
2. Ignition 5 sec. early	333.88	22886.8	0.064	3185.66	97.29
3. Ignition 5 sec. late	333.89	22887.2	0.019	3185.73	98.06
4. Initial Weight 1% high	337.24	23116.4	0.009	3185.78	97.89
5. Initial Weight 1% low	330.53	22656.7	0.036	3185.45	97.47
6. Fuel Flow 3% low	344.27	22890.4	0.019	3186.25	98.33
7. Fuel Flow 6% low	355.34	22896.3	0.064	3187.20	99.03
8. Ignition 15 sec. late, wt. 2% high, fuel flow 6% low	362.80	23376.5	0.217	3190.77	100.64

Fig. 16-9

BASIC CROSS-PRODUCT VELOCITY STEERING LOOP

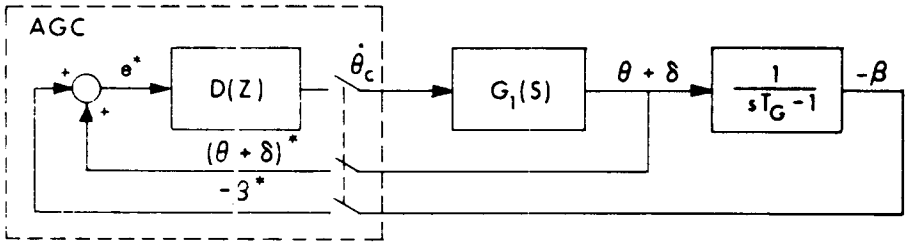

REVISED CROSS-PRODUCT VELOCITY STEERING LOOP

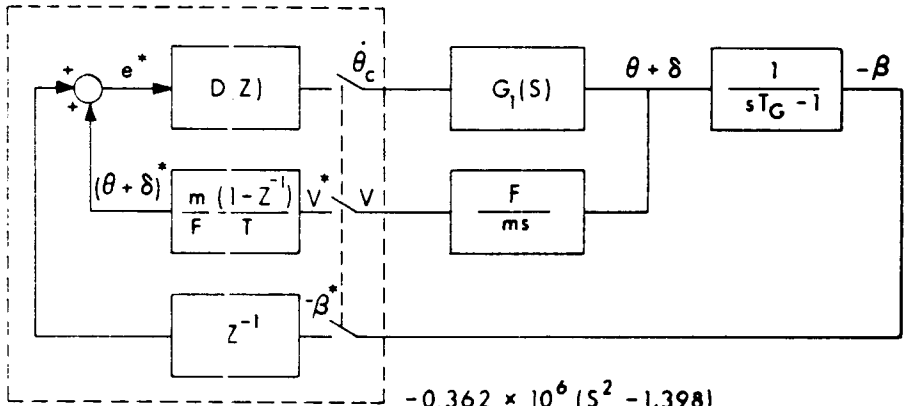

$$G_1(S) = \frac{-0.362 \times 10^6 (S^2 - 1.398)}{S(S+1)(S+5)(S+4.8)(S^2 + 22.2S + 141)(S^2 + 8.3S + 148)}$$

Fig. 16-10.

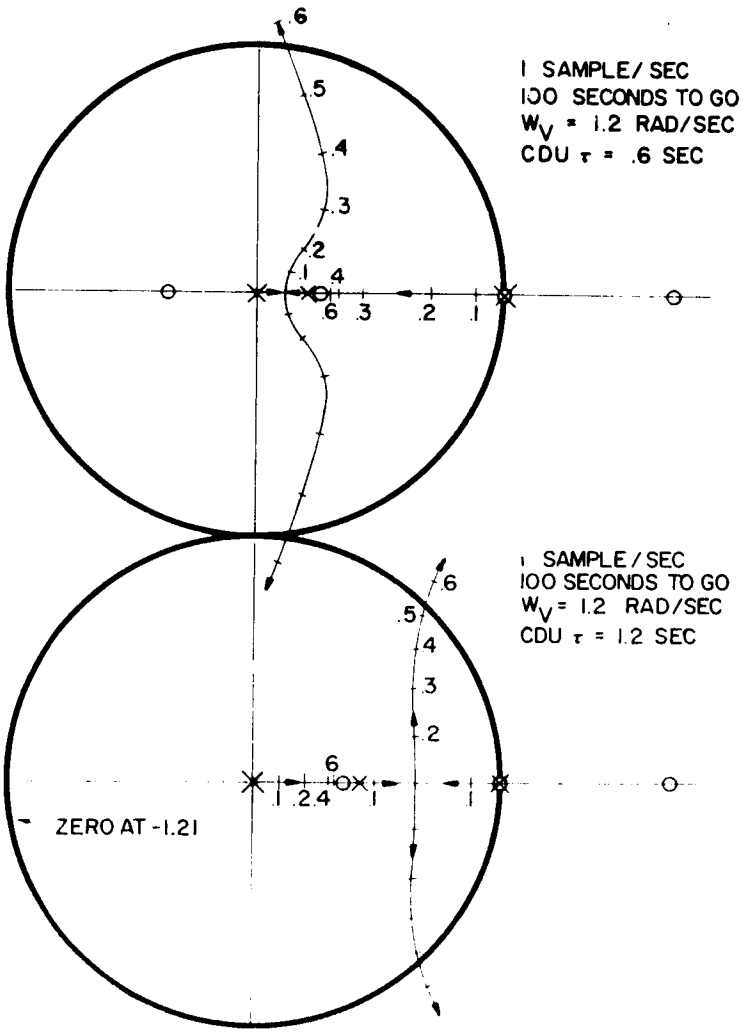

Fig. 16-11 Z Plane Root Loci - Cross Product Steering

Following this paper and pencil analysis, a single-degree-of-freedom combined-analog/digital analysis was used to test the design. Figure 16-12 illustrates the analog portion of this simulation, representing vehicle and kinematics.

Figure 16-13 illustrates the digital portion of the simulation. Note that an actual AGC and CDU are used. The equations solved in the AGC are approximations to the actual flight equations, but are dynamically indistinguishable from the planned equations. Figure 16-14 is a plot of data obtained from this effort.

The next step in the development consisted of a three-dimensional digital simulation, representing the complete control problem with all significant nonlinearities. This was written in floating point "MAC" 800 language and does not require detailed AGC programming since it is not an instruction-by-instruction simulation.

The results of work on this program confirm the previous single-degree-of-freedom results.

PART 2

A. Kosmala

This section describes the programming of the powered flight equations. Figure 16-15 illustrates in block form the problem to be mechanized by the AGC. Velocity increments from the PIPA's form the input data, and commanded CDU angles are the output. The average G integration provides present position and velocity by updating PIPA information, (although shown as part of the Powered Flight program, it is common to other programs). The $\overline{v}_G$ and $\dot{\overline{v}}_G$ calculations provide inputs to the cross-product operation, which is the fundamental steering mechanism. Outputs from this operation are transformed into CDU coordinates by a routine which also keeps track of inertial attitude for use with Block I CDU's.

Figure 16-16 is a summary of the equations mechanized by the Powered Flight program. The time interval has been chosen small enough to allow differential equations to be written in algebraic form. Terms with bars represent vectors with three components.

Figure 16-17 lists the main factors taken into account in writing the program. The AGC operates in fixed-point arithmetic so that it is necessary to compromise the dynamic range and resolution of the variables in order to prevent overflow. Timing is controlled by a central waitlist program, and concerns real-time integration, critical phases such as $\overline{V}_G$ countdown, and scheduling of subroutines such as the CDU angle updating. Programming is carried out in either Basic (machine) or Interpretive language. The Interpreter is a collection of subroutines which provides vector, matrix, double and triple precision operations not available in the 11 basic operation codes. Finally, the affixing of priorities to routines, and mode control for the various mission phases must be determined in order

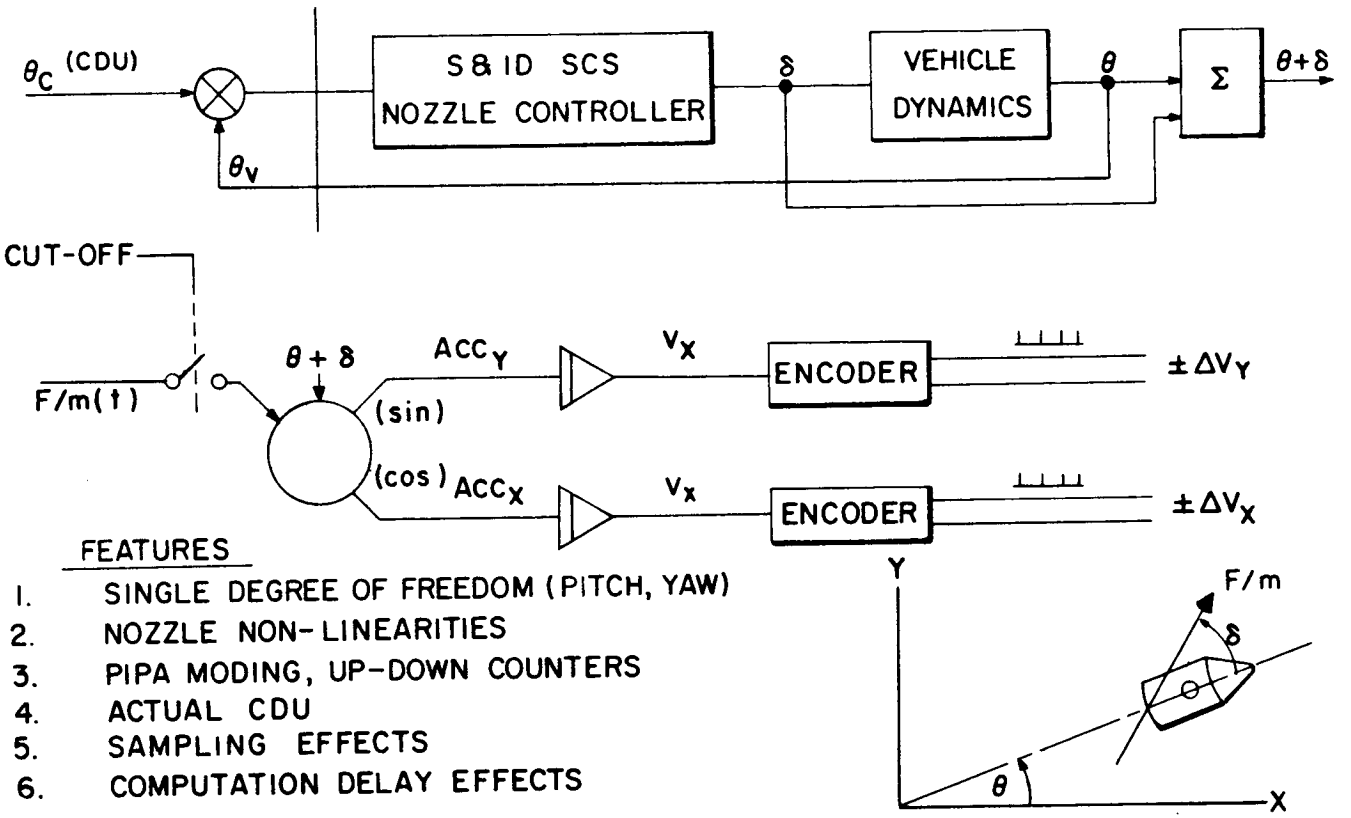

Fig. 16-12 Beckman analog simulator.

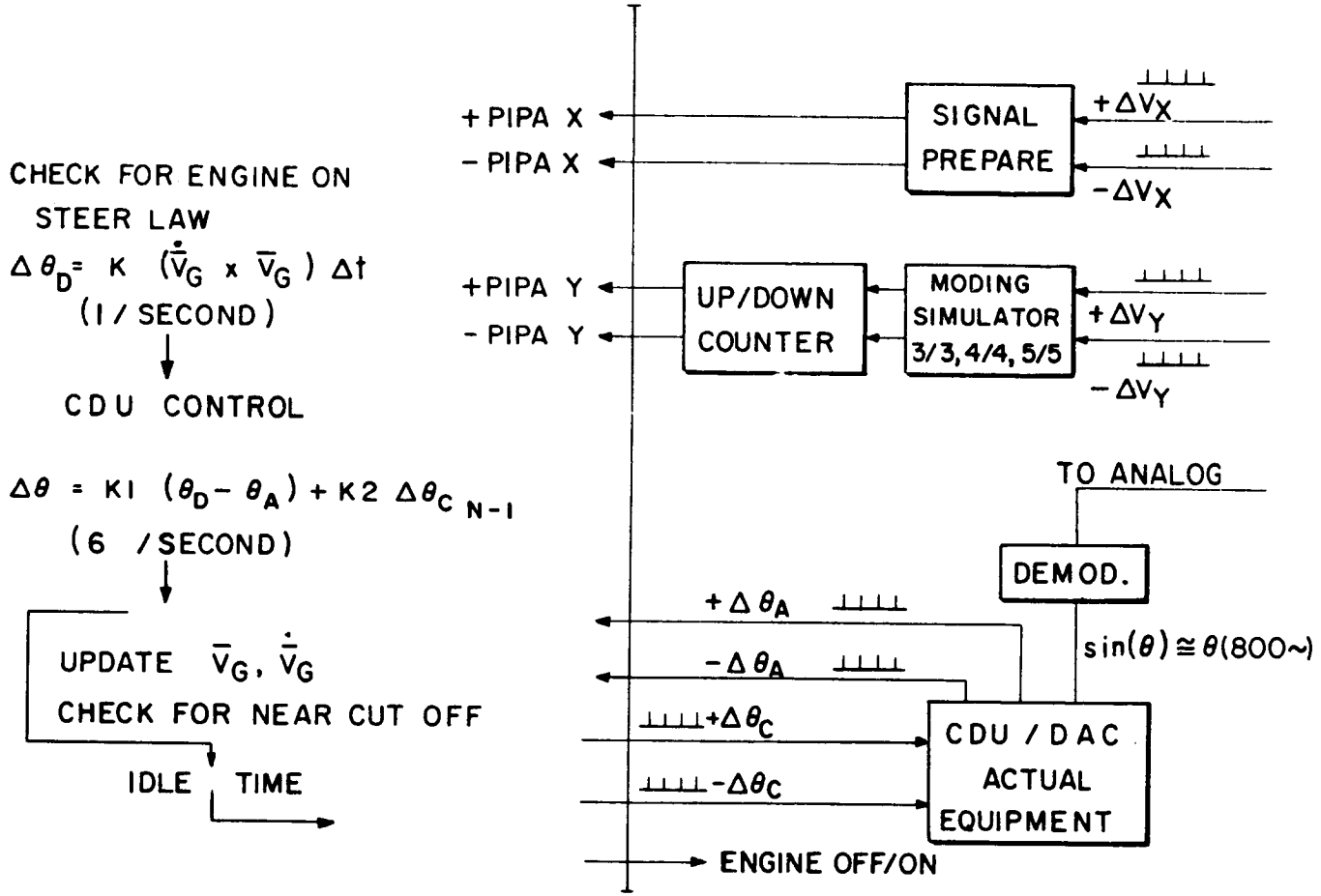

Fig. 16-13 AGC-3.

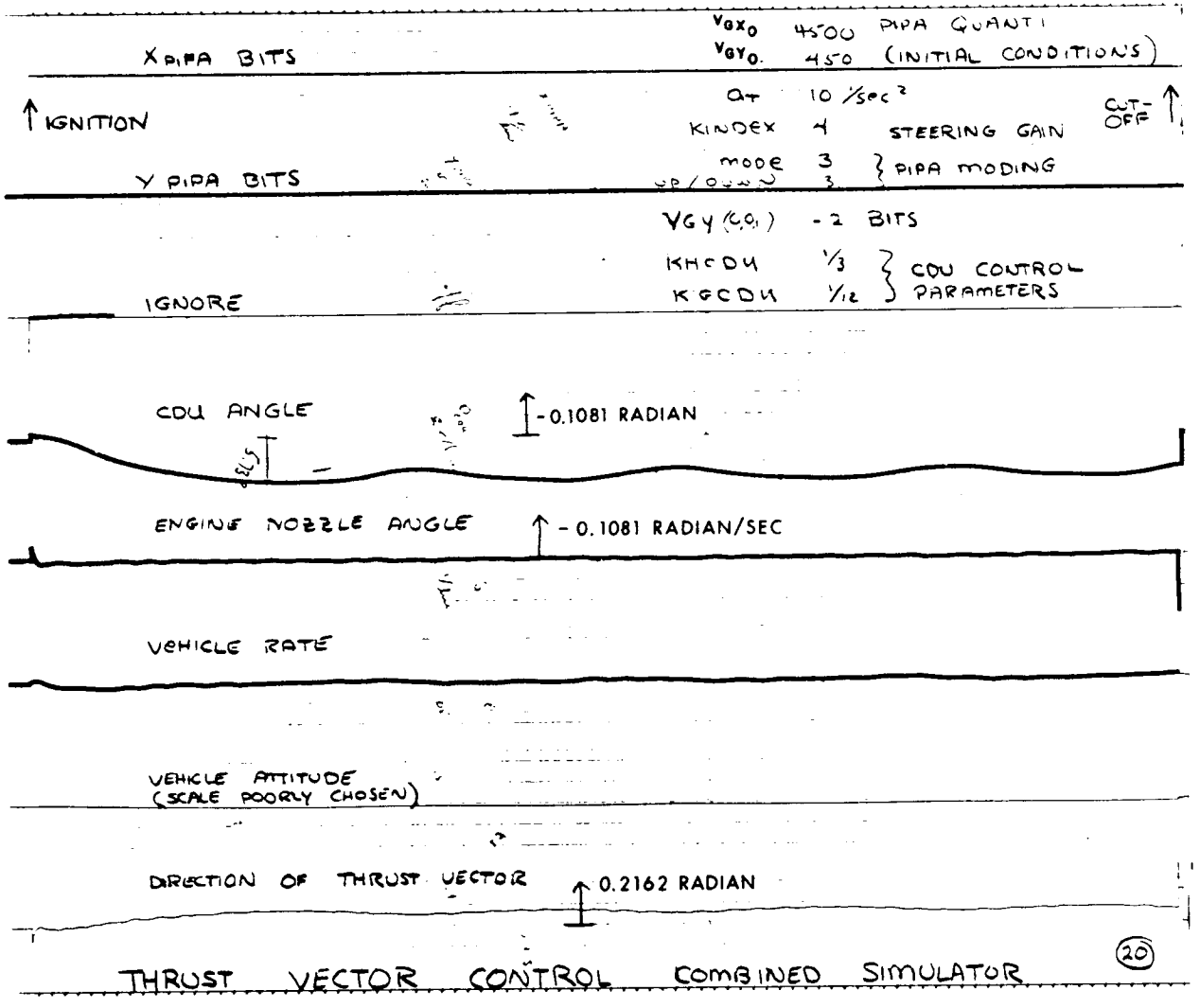
V_{GX_0} 4500 PIPA QUANTI
V_{GY_0} 450 (INITIAL CONDITIONS)
X PIPA BITS
IGNITION
a_T 10 ft/sec²
KINDEX 4 STEERING GAIN
CUT-OFF
mode 3 3 PIPA MODING
Y PIPA BITS
V_{GY} (0,1) - 2 BITS
KHCDU 1/3
KGCDU 1/12 CDU CONTROL PARAMETERS
IGNORE
CDU ANGLE
- 0.1081 RADIAN
ENGINE NOZZLE ANGLE
- 0.1081 RADIAN/SEC
VEHICLE RATE
VEHICLE ATTITUDE (SCALE POORLY CHOSEN)
DIRECTION OF THRUST VECTOR
0.2162 RADIAN
THRUST VECTOR CONTROL COMBINED SIMULATOR
20

Fig. 16-14

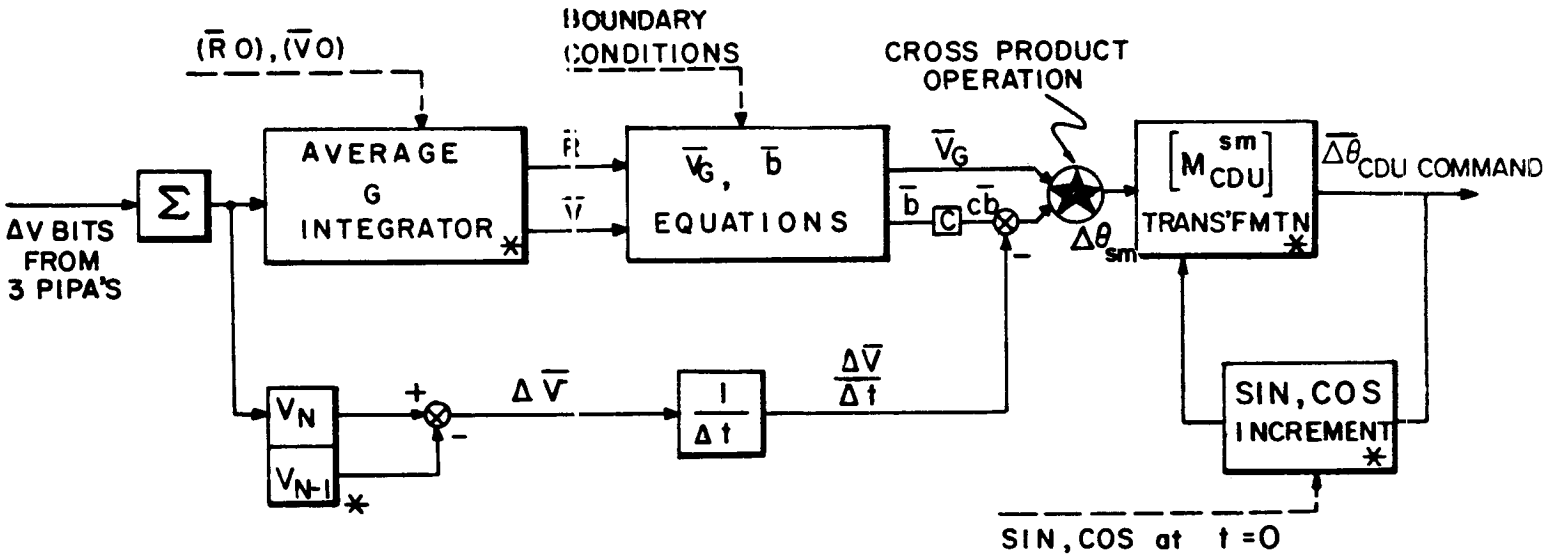

NOTE COMPUTATIONS MARKED WITH * ARE COMMON TO ALL POWERED MANEUVERS

BOUNDARY VALUES

1. TRANSLUNAR INJECTION — AIM POINT VECTOR
2. LUNAR DE-BOOST — CIRCULAR ORBIT
3. TRANSEARTH INJECTION — EXCESS HYPERBOLIC VELOCITY VECTOR
4. ABORT FROM MIDCOURSE — PERIGEE ALTITUDE, ECCENTRICITIES

Fig. 16-15 Thrust vector control, Apollo CSM AGC information flow.

AVE $\bar{G}$

$$\bar{R}_1 = \bar{R}_0 + \bar{V}_0 \Delta T + \bar{G}_0 \Delta T^2/2 + \overline{PIPA}\, \Delta T/2$$

$$\bar{G}_1 = -\mu \bar{1}_R / |\bar{R}_1|^2$$

$$\bar{V}_1 = \bar{V}_0 + (\bar{G}_0 + \bar{G}_1)\Delta T/2 + \overline{PIPA}$$

$\bar{V}_G$, $\bar{G}$

$$\bar{V}_G = \sqrt{\mu / |\bar{R}|}\ (\bar{1}_N \times \bar{1}_R) - \bar{V}$$

$$\bar{G} = (\mu / |\bar{R}|^2)(\bar{1}_R \cdot \bar{1}_N)\bar{1}_N - \sqrt{\mu/|\bar{R}|^3}\ (\bar{V}_G - 3/2\,(\bar{1}_R \cdot \bar{V}_G)\bar{1}_R) \times \bar{1}_N$$

$V_G \times \bar{V}_G$

$$\Delta \bar{V}_G = \bar{G}\Delta T - \overline{PIPA} \qquad \overline{\Delta\theta} = K_{STEER}\,(\Delta \bar{V}_G \times \bar{V}_G)\,\Delta T / |\Delta \bar{V}_G|\ |\bar{V}_G|$$

Transf.

$$\Delta OG = (\Delta\theta_x \cos IG - \Delta\theta_y \sin IG) / \cos MG$$

$$\Delta MG = \Delta\theta_x \sin IG + \Delta\theta y \cos IG$$

$$\Delta IG = \Delta\theta_y - \Delta OG \sin MG$$

sin/cos

$$\sin_1 IG = \sin_0 IG + \cos_0 IG\, \Delta IG - \sin_0 IG\, (\Delta IG)^2 / 2$$

$$\cos_1 IG = \cos_0 IG - \sin_1 IG\ \Delta IG - \cos_0 IG\, (\Delta IG)^2 / 2$$

etc for MG, OG

Fig. 16-16 Powered flight steering equations (lunar deboost).

Scaling	Dynamic Range of Variables	
	Accuracy	
Timing	Integration w. r. t. time	Waitlist
	Time-Critical Phases	
	Scheduling	
Programming	Interpretive	
	Basic	
Organization	Priorities - Executive	
	Mode Control	

Fig. 16-17 Important programming factors.

to integrate all routines into the complete AGC program. This stage of complexity has not yet been reached, so no such definitions have been incorporated into the first powered flight program.

Scaling is a major hurdle in programming the AGC, and Fig. 16-18 illustrates one, but not the only, method of scaling the powered flight equations. The maximum values of the variable were determined by the requirement that operation near the moon or the earth should not involve scale changes. The basic unit was arbitrarily chosen to be one PIPA increment of velocity. The maximum expected velocity was less than 2^{18} ΔV (about 1.5×10^4 meters/sec). This fixed the maximum value of the velocity register, and the scaling of velocity. The basic unit of length became the ΔV sec. The maximum distance was not expected to exceed 2^{33} ΔV sec, (about 5×10^5 kilometers). Since a double precision register is 28 bits in length, the resolution of length was thus 2^5 ΔV (1.872 meters), which appears adequate for all phases of the mission.

The method of translating the problem equations (Fig. 16-16) into machine variable equations is shown in the lower part of Fig. 16-18. The machine variable is treated as a number less than one, i.e., a fraction. Any problem variable is then expressible as a fraction of its maximum value (e.g., the expressions for V, PIPA and G). The method of scaling is shown as applied to the R equation of the average G integration. Note that when adjusting scale factors within an equation it is always desirable to shift to the right, or away from the binary point, to prevent overflow of the most significant bits.

Figure 16-19 is the flow chart for the powered flight program. The first action is an initialization, e.g., of the variables V_0, R_0, T_0, of the control flags, and of the Waitlist. The Waitlist acts as an alarm clock to call for the execution of certain routines at specified times. When a routine is called, it must reset the Waitlist for its next call. The powered flight program consists of the average G routine and the steering computations, performed once each second, and a CDU servicing routine (common to other programs) which updates each CDU about twice per second. As the Powered Flight phase proceeds the velocity to be gained, $\overline{V}_G$, gradually decreases in magnitude. $|V_G|$ is monitored every second and tested (an abortive condition is indicated in case of $|V_G|$ increasing). At 3 secs to cut-off normal steering is stopped and the remaining $|V_G|$ is "counted down" by checking it every 20 ms. (allowance is made for a finite thrust tail-off). When zero (or negative) V_G remains, the cutoff signal is sent to the engine and the flags are reset. The program then returns to an idling average G.

Figure 16-20 is the breakdown of the powered flight program in terms of storage space and operation times. (The figures are for Lunar Deboost steering only.) Those sections written in Interpretive language have the longest operation times. During pre-countdown steering computer usage is about 63% of full time, while during the trial 3 secs usage is about 11% of full time. When the program has assumed its final form, many of the erasable locations will be shared, and the number of fixed locations and total computer usage will have been reduced by optimization.

VELOCITY	BASIC UNIT	=	1 PIPA INCREMENT (ΔV) = 0.0585 METERS / SEC
	MAX VALUE	=	2^{18} ΔV = 15,335·424 METERS / SEC
LENGTH	BASIC UNIT	=	1 ΔV SEC = 0.0585 METER
	MAX VALUE	=	2^{33} ΔV = 502, 511, 173.6 METERS
ΔTIME	BASIC UNIT	=	1 SEC
	MAX VALUE	=	2^3 SECS = 8 SEC

SCALING METHOD

Problem variable = Machine variable x scale factor

e.g. $V = \tilde{V}\, 2^{18}$

$PIPA = \tilde{PIPA}\, 2^{14}$

$G = \tilde{G}\, 2^{6}$

e.g. $R_1 = R_0 + \Delta T \left[V_0 + G_0 \Delta T / 2 + PIPA / 2 \right]$

$\tilde{R}_1 2^{33} = \tilde{R}_0 2^{33} + \tilde{\Delta T} 2^3 \left[\tilde{V}_0 2^{18} + \tilde{G}_0 2^{16} \tilde{\Delta T} 2^3 / 2 + \tilde{PIPA} 2^{14} / 2 \right]$

$\tilde{R}_1 = \tilde{R}_0 + \tilde{\Delta T} \left[\tilde{V}_0 + \tilde{G}_0 \tilde{\Delta T} + 2^{-5} PIPA \right] 2^{-12}$

Fig. 16-18 Example of scaling for powered flight AGC program.

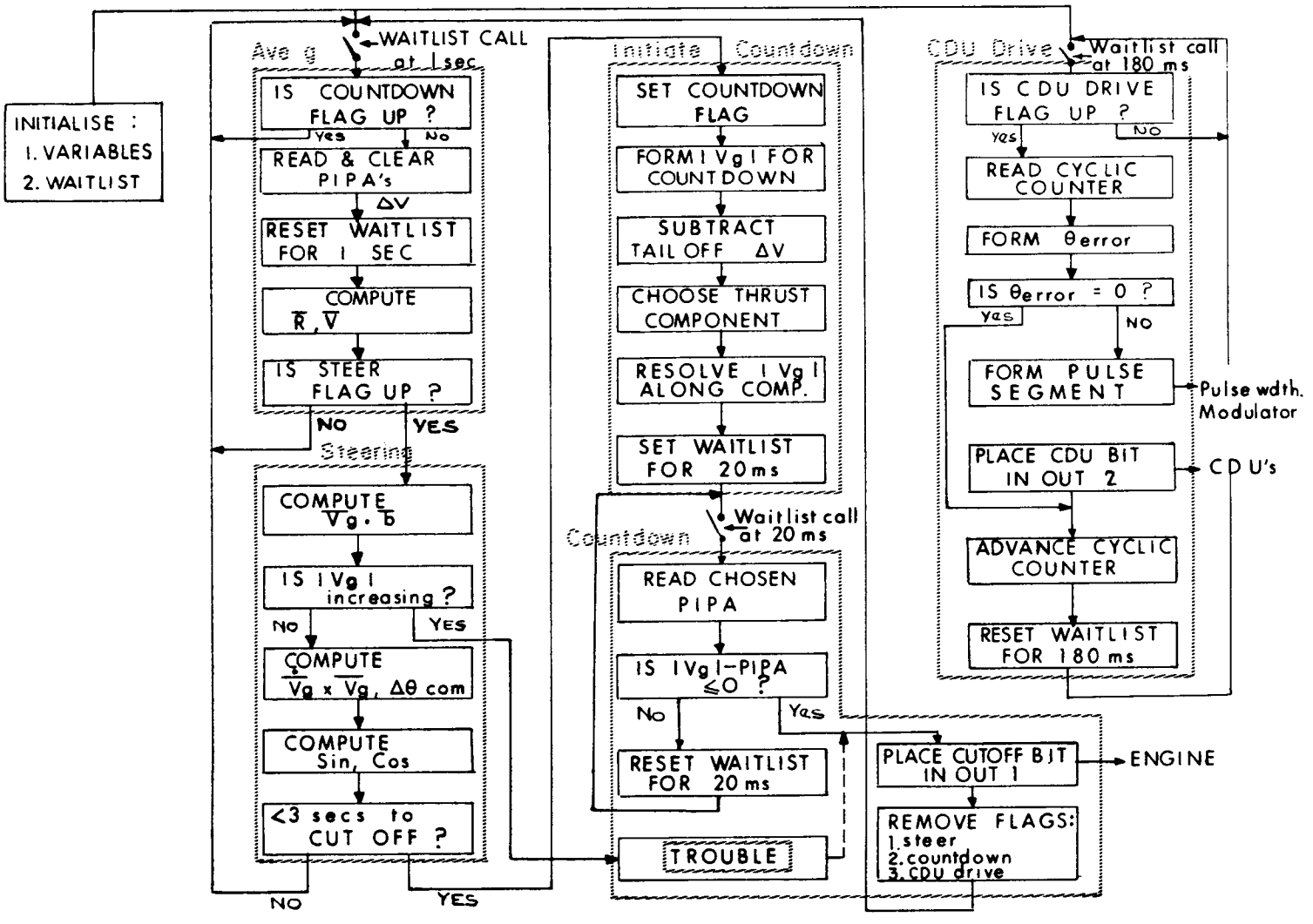

Fig. 16-19 Powered flight AGC program flow chart.

ROUTINE	No. STORAGE LOCATIONS		EXECUTION TIME ⑤
	FIXED	ERASABLE	ms
READ PIPA's ④	18	6	2.5
AVERAGE G ④	54	35	168.0
$\bar{V}_G$, $\bar{b}$ ②	38	8	154.1
$(\dot{\bar{V}}_G \times \bar{V}_G)$ & Transform'tn	37	14	107.0
sin/cos, & INIT. COUNTDN	107	25	183.8
COUNTDOWN	38	5	2.2
③ CDU (DRIVE) ④ (no drive)	59	6	3.3 1.0
TOTALS	351	99①	627 AVERAGE

① THIS FIGURE WILL BE IMPROVED BY LOCATION SHARING
② FIGURES FOR LUNAR DEBOOST ONLY
③ THIS IS NOT THE OPERATIONAL ROUTINE
④ SHARED BY NON-POWERED FLIGHT ROUTINES
⑤ NOT OPTIMISED

Fig. 16-20 Breakdown of powered flight AGC program.

The instruction-by-instruction simulation of the AGC on the Honeywell 1800 was used in conjunction with simulations of the CM/SM, the CDUs, and the IMU to check out the preliminary powered flight program. The results are summarized in Fig. 16-21. The standard of comparison of performance was a point-mass simulation of the Lunar Deboost problem, in which an inertia-less vehicle was constrained to move so that the cross product $\dot{\overline{V}}_G \times \overline{V}_G$ was zero at all times. The "Actual" column in Fig. 16-21 indicates figures obtained by an exact solution of the simulated motion of the CM/SM, and the "Computer" column indicates values of the same variables as computed by the simulated AGC-4 program. The simulation was made for the last 96 secs of the Lunar Deboost problem, and figures for the 93rd sec are compared. Agreement to within one ΔV (0.0585 m/s) and one R bit (1.872 m) is shown. Comparison of the "Point-Mass" and "Actual" columns indicates the performance of the cross-product steer law when used to steer a "real" vehicle. Comparison of the "Actual" and "Computed" column indicates the errors arising out of truncation and algorithm approximations in the AGC program.

1. DATA AT 93 ① secs

DATA	POINT-MASS ②	ACTUAL ③	COMPUTED ④
RADIUS (m)	1, 921, 688.9	1, 921 619·2	1, 921, 618·0
|VELOCITY| (m/s)	1, 608·000	1, 608·060	1, 608·046

2. DATA AT THRUST TERMINATION

TIME ① (secs)	96·17	96·22	—
|Vg| (m/s)	0		0.625

① T_0 = 230 secs AFTER IGNITION
② DATA FROM POINT-MASS SIMULATION (USED AS STANDARD)
③ DATA FROM EXACT SOLUTION OF EQUATIONS OF MOTION
④ AGC SOLUTION

Fig. 16-21 Simulation of powered flight AGC program.

TABLE I

MEETINGS ATTENDED BY MIT/IL APOLLO PERSONNEL

Period 1 March through 31 March 1964

Date	Location	Subject
2 March	MIT	Status Review
3 March	Raytheon	Status Review
4 March	Sperry	Status Review
5 March	KIC	Status Review
5-6 March	S&ID	AGC/STU Checkout Bay Discussion S&ID/MIT #89B
6 March	ACSP	Status Review
10 March	AMR	G&N Prelaunch Checkout Panel
10 March	MSC	Acceptance Data Package
10 March	MSC	Failure Effects Analysis
10 March	MIT	Test Review Board
10 March	AMR	Checkout Plan Mtg (LEM)
11 March	MIT	Radar/LGC Interface (L35B)
11 March	MIT	Management Review
11-12 March	MSC	Reliability Program Plans
12 March	GAEC	Radar Coordination Mtg between NAA & GAEC
13 March	MIT	Northeast Executives Visit
13 March	AMR	Checkout Work Group #5
17 March	AMR	Checkout Work Group (Special)
18 March	S&ID	Entry Equation Discussion
18 March	MSC	Reliability Assessment
23 March	GAEC	ARA Specs, L37B
23 March	MIT	Block II Change Requirements for GSE
23 March	AMR	Checkout Work Group (Special)
24-25 March	AMR	Checkout Work Panel #9
25 March	NAA	Checkout Work Group Mtg.#6
25 March	GAEC	Dynamic Simulations
25-26 March	MIT	Design Review
26 March	AMR	Signal Conditioning Carry-on, 93B
31 March	MSC	Review of G&N Training & Motivat. Program
31 March	MIT	Analog Flight Telemeter Requirements, L38
31 March, 1 April	S&ID	Mechanical ICD's, Number to be Assigned

BIBLIOGRAPHY

TECHNICAL PROGRESS REPORTS

No.	Type	Period Ended
E-1067	Monthly	August 11 through September 13, 1961 (C)
E-1068	Monthly	September 13 through October 4, 1961 (C)
E-1099	Monthly	October 4 through November 9, 1961 (C)
E-1116	Quarterly	Period ended December 11, 1961 (C)
E-1117	Monthly	December 11, 1961 through January 16, 1962 (C)
E-1139	Monthly	January 16 through February 1962 (C)
E-1140	Quarterly	Period ended March 11, 1962 (C)
E-1157	Monthly	March 11 through April 11, 1962 (C)
E-1177	Monthly	April 11 through May 1, 1962 (C)
E-1199	Quarterly	Period ended June 11, 1962 (C)
E-1236	Monthly	June 11 through July 17, 1962 (C)
E-1237	Monthly	July 17 through August 21, 1962 (C)
E-1238	Quarterly	Period ended September 11, 1962 (C)
E-1302	Monthly	September 11 through October 11, 1962 (C)
E-1303	Monthly	October 11 through November 13, 1962 (C)
E-1304	Quarterly	Period ended December 11, 1962 (C)
E-1305	Monthly	December 11, 1962 through January 11, 1963 (C)
E-1306	Monthly	January 11 through February 11, 1963 (C)
E-1307	Quarterly	Period ended March 1963 (C)
E-1308	Monthly	April 1963 (C)
E-1378	Monthly	May 1963 (C)
E-1389	Quarterly	Period ended June 1963 (C)
E-1410	Monthly	July 1963 (C)
E-1445	Monthly	August 1963 (C)
E-1474	Quarterly	Period ended September 1963 (C)
E 1494	Monthly	October 1963 (U)
E-1495	Monthly	November 1963 (U)
E-1496	Quarterly	Period ended December 1963 (U)
E-1534	Monthly	January 1964 (U)
E-1544	Monthly	February 1964 (U)
E-1573	Quarterly	Period ended March 1964 (U)

BIBLIOGRAPHY (Cont'd)

ENGINEERING REPORTS

E-1054 J. Rocchio, Analysis of the PNP and NPN Latch Circuit, September 1961 (U)

E-1074 D. Shansky, Erasable Ferrite Memory, MOD 3C Computer, October 1961 (U)

E-1077 R. L. Alonso, J.H. Laning, Jr., and H. Blair-Smith, Preliminary MOD 3C Computer Program, November 1961 (U)

E-1078 Development Plan, November 27, 1961 (to be revised) (C)

E-1087 Documentation Handbook, Levy, May 1963 (U)

E-1091 E.J. Hall, Assembly Procedures and Specifications for Apollo 25 IRIG, June 1962 (C)

E-1092 J.H. Flanders, IMU Preliminary Operational Duty Cycle, December 1961 (C)

E-1097 Work Statement for Industrial Support, January 1962 (C), Addendum, February 1962 (C)

E-1100 M. Sappupo, Work Statement for PIP MOD D, December 15, 1961 (C)

E-1101 E.J. Hall, Work Statement for Apollo 25 IRIG, December 15, 1961 (C)

E-1103 E.J. Hall, Assembly Procedures and Specifications for 25 IRIG MARK 45 MOD 2, December 15, 1961 (C)

E-1104 M. Sappupo, Preliminary Assembly and Test Manual 16 PIP MOD D, January 1962 (C)

E-1106 P.G. Felleman, Analysis of Guidance Techniques for Achieving Orbital Rendezvous, January 1962 (U)

E-1113 System Identification Data List, (SIDL), issued August 20, 1962 (to be revised and supplemented monthly)

ENGINEERING REPORTS (Cont'd)

E-1114 J.E. Levy, Glossary of Terms and Symbols, April 1962 (C) (Revised July 1962) (C)

E-1118 R.A. Scholten and P.J. Philliou, Investigations of Midcourse Maneuver Fuel Requirements, March 1962 (C)

E-1124 J.S. Miller and J.J. Deyst, Preliminary Study of Aborts from Circumlunar Trajectories, March 1962 (U)

E-1125 R. L. Alonso, Preliminary Resolver Angle Measurements, February 1962 (U)

E-1126 A. L. Hopkins, Jr., AGC MOD 3C Computer Circuits General, February 1962 (U)

E-1130 J. E. Levy, Maintanance Plan, March 1962 (U)

E-1131 J. S. Miller and R. H. Battin, Preliminary Summary of Data for a Variety of Circumlunar Trajectories, February 1962 (U)

E-1134 A. C. Hardy, Photometric Units in the MKS System, March 1962 (U)

E-1142 J. E. Levy, System Status Report, 15 March 1962, revised July 1962, (to be revised monthly) (C)

E-1144 J. E. Levy, Apollo Guidance and Navigation Interfaces, (to be published) (C)

E-1158 D. Shansky, Erasable Store MOD 3C, July 1962 (U)

E-1161 I. Halzel, Technical Directive Procedures for Apollo G & N System Participating Contractors, May 1962 (U)

E-1164 F. D. Grant, The Relationship between IMU Drift Misalignments and Target Errors, May 1962 (C)

E-1167 Drawing Standards, 15 June 1962 (U)

ENGINEERING REPORTS (Cont'd)

E-1172 A. C. Hardy, The Visibility of Stars, June 1962 (U)

E-1173 R. M. Jansson, The Heat Transfer Properties of Structural Elements for Space Environment, June 1962 (U)

E-1179 R. G. Scott, Rope Core Tester, July 1962 (C)

E-1186 Technical Data Release Procedures, August 1962, (revised December 12, 1962) (U)

E-1195 N. E. Sears, Earth Orbital Rendezvous, May 1962 (C)

E-1196 M. W. Johnston, Analysis of Two Lunar Landing Techniques Providing Direct Landing Site Visibility Prior to Touchdown, July 1962 (U)

E-1203 G. A. Davidson and H. H. Seward, Calibration Techniques for Precision Rotary Components, August 1962 (U)

E-1206 H. H. Seward, The Blue-White Boundary Horizon Senser, September 1962 (U)

E-1212 F. D. Grant, Error Data Summaries for Various Trajectories, (Preliminary), September 1962 (C)

E-1215 T. C. Taylor, Thermal Models for High Density Computer Circuit Structures, September 1962 (U)

E-1230 J. E. Miller and J. H. Flanders, Comprehensive Alignment Tests for IMU, February 1963 (C)

E-1233 T. C. Taylor, Technique of Circuit Fabrication with State-of-the-Art Weldable Multilayer Boards, October 1962 (U)

E-1256 J. W. Hursh, Apollo Midcourse Guidance, November 1962 (C)

E-1257 L. J. Lareau, Jr., Atmospheric Refraction as a Means of Horizon Determination, December 1962 (U)

ENGINEERING REPORTS (Cont'd)

E-1260 P. K. Bryant, Procedures of the Apollo Management, (to be published) (C)

E-1261 G. M. Levine, Application of Midcourse Guidance Techniques to Orbit Determination, December 1962 (U)

E-1278 G. Gilbert, MIT Space Implementation, Interim Report, January 1963 (U)

E-1285 A. C. Hardy, Some Luminance Values for Sun, Earth, and Moon, January 1963 (C)

E-1287 J. M. Dahlen and J. H. Long, Backup Thrust Vector Control, February 1963 (C)

E-1288 F. D. Grant, Alignment Errors of the IMU Stable Member, February 1963 (C)

E-1295 R. Boyd, AGE Field Operations Program Plan, (Preliminary) April 1963 (U)

E-1297 J. H. Flanders, Inertial Subsystem (ISS) Calibration Tests, (Preliminary), June 1963 (U)

E-1313 T. C. Taylor, Thermal Grounding Analysis for Circuit Structures, April 1963 (U)

E-1322 G. W. Mayo, Apollo G & N Failure Reporting and Corrective Action Plan, April 1963 (U)

E-1329 Apollo 16 PIPA Test Console Reference Manual, September 1963 (U)

E-1330 Apollo 16 PIPA Test Console, Job Description Cards for Operation and Maintenance 1963, July 1963 (U)

E-1343 G. Oberbeck, Ternary Pulse Torquing, May 1963 (U)

E-1344 D. G. Hoag, Consideration of Apollo IMU Gimbal Lock, April 1963 (C)

ENGINEERING REPORTS (Cont'd)

E-1350 W. Briggs, Statistical Decision Theory for Logistics Planning, May 1963 (U)

E-1353 E. M. Copps, D. A. Koso, K. Nordtvedt, and M. B. Trageser, The Horizon Photometer and other Earth Parking Orbit G & N Measurements, May 1963 (C)

E-1359 J. Dahlen, T. Heinsheimer, J. Suomala, Flight Test Plan - Apollo G & N System AGE 5, May 1963 (C)

E-1363 T. Heinsheimer, Status of Apollo Flight Safety System Design and Development, June 1963 (U)

E-1381 R. Boyd, Data Analysis and Dissemination Instruction, (to be published) (U)

E-1385 (Prof.) Hardy, Visibility Data and the Use of Optical Aids, July 1963 (U)

E-1386 S. Smith, Report on Clear Resins, August 1963 (U)

E-1388 J. Sciegienny, Summary of Error Propogation in an Inertial System, August 1963 (U)

E-1395 J. McNeil, Date Console Job Description Cards for Operations and Maintenance, (to be published) (U)

E-1396 J. McNeil, Date Console Reference Manual, (to be published) (U)

E-1398 J. Dahlen, J. Suomala, Comments on the Lunar Landing Mission Design Plan of 15 April 1963, August 1963 (C)

E-1413 J. Partridge and Arnold Borofsky, Some Reversible and More Permanent Effects of Moisture on the Electrical Characteristics of Germanium Transistors following Stress, September 1963 (U)

E-1420 J. Partridge, On the Extrapolation of Accelerated Stress Conditions to Normal Stress Conditions of Germanium Transistors, September 1963 (U)

ENGINEERING REPORTS (Cont'd)

E-1425 C. Perez, A Comparison of the Readout Resolution of the Proportional Elastance vs Constant Elastance Torque-to-Balance Systems, September 1963 (U)

E-1429 D. Baker, N. Sears, J. Suomala, R. White, Lunar Orbit Determination by Star Occultations and MSFN Tracking, September 1963 (U)

E-1432 GSE Familiarization Manual, January 1964 (U)

E-1467 E. K. Bender, Sampled-Data Velocity Vector Control of a Spacecraft, March 1964 (U)

E-1473 J. Dahlen, M. Johnston, Analysis of LEM Mission Inertial Uncertainties, December 1963 (C)

E-1482 F. Grant, Inflight Alignment Errors of the IMU Stable Member, December 1963 (C)

E-1492 G. A. Davidson, A. C. Hardy, On the Perception of Flashes of Light at the Limit of Their Perceptibility, January 1964 (U)

E-1522 R. Booth, Assembly Procedures and Specifications for Apollo II IRIG, (to be published) (C)

E-1524 C. S. Smith, Evaluation of Eurethane Foam for Potting, February 1964 (U)

E-1539 T. C. Taylor and T. A. Zulon, Thermal Properties of Some Structural Members for Spaceborne Computer Assemblies, (to be published) (U)

E-1540 K. Nordtvedt, A Preliminary Study of a Backup Manual Navigation Scheme, (to be published) (U)

E-1541 J. Flanders and R. McKern, Test Results on Apollo Inertial Subsystem No. 4, (to be published) (C)

ENGINEERING REPORTS (Cont'd)

E-1543 J. Fresina and E. Spencer, Apollo G & N Field Safety Manual, (to be published) (U)

E-1547 P. Bowditch, A. Koso, J. Mudgett, Optical Equipment Handling Guidelines, March 1964 (U)

E-1548 R. Gras, Brazing of Beryllium, March 1964 (U)

E-1551 A. Klumpp and R. Larson, Function and Mechanization of Apollo G & N System, Vol. 1 Inertial Subsystem, (to be published) (C)

E-1557 W. Nadler, Average Power Profiles for Apollo G & N in the Command Module and Lunar Excursion Module, April 1964 (U)

E-1560 M. Johnston, A Manual LEM Backup Guidance System, (to be published) (U)

E-1564 A. Green and J. Rocchio, Keyboard and Display System Program for AGC Program SUNRISE, (to be published) (U)

BIBLIOGRAPHY (Cont'd)

TECHNICAL REPORTS

R-339 M. B. Trageser, Guidance and Navigation System Information for Apollo Spacecraft Bidders, September 1961 (C)

R-341 R. H. Battin, Statistical Optimization for Space Flight, September 1961, (Revised May 1962) (U)

R-342 C. S. Draper, W. G. Denhard, and M. B. Trageser, Development Criteria for Space Navigation Gyroscopes, October 1961 (U)

R-348 E. J. Hall, J. Miller, and J. Aronson, A. Lattanzi, Specification for Procurement of Apollo IRIG, December 1961, (Revised August 1962) (C)

R-349 G. W. Mayo, Guidance and Navigation System Reliability Program, December 1961 (U)

R-353 R. H. Battin and J. S. Miller, Circumlunar Trajectory Calculations, April 1962 (U)

R-358 R. L. Alonso, A. L. Green, H. E. Maurer, and R. E. Oleksiak, A Digital Control Computer Developmental Model 1B, April 1962 (U)

R-367 P. H. Gillinson, Jr., C. R. Dauwalter, and J. A. Scoppettuolo, Multirange Precision Torque Measuring Devices, July 1962 (U)

R-368 G. W. Mayo and E. T. Driscoll, Reliability Handbook for Electronic Engineers, August 1962 (Revised October 1962) (U)

R-372 J. H. Flanders, Velocity Steering Studies for the Apollo Mission, August 1962 (C)

R-373 J. M. Dahlen, P. G. Felleman, R. D. Goss, N. E. Sears, M. B. Trageser, R. L. White, Guidance and Navigation System for Lunar Excursion Module, July 1962 (Revised August 1962) (C)

R-376 R. E. Curry (NASA), Two Impulse Abort Trajectories from Translunar Flight, October 1962 (U)

TECHNICAL REPORTS (Cont'd)

R-380 Development of High Capacity Heat Storage Materials Phase 1 - Study of Materials, July 1962 (U) by Cyro-Therm, Inc.

R-382 R. H. Battin, Universal Formulae for Conic Trajectory Calculations, September 1962 (U)

R-383 G. W. Mayo, Design Review Procedures, September 1962 (U)

R-385 R. C. Hutchinson, Inertial Orientation of the Moon, October 1962, (U)

R-386 Max Petersen, Earth Limb Definition Photography, MA-7 Mercury Flight, Cmdr. Carpenter, (to be published) (U)

R-387 S. J. Madden, Jr., Orbital Element Variation for a Body in Orbit Around the Moon, July 1963 (U)

R-388 D. G. Hoag, A Progress Report on the Apollo Guidance System, December 1962 (C)

R-389 G. W. Mayo, Requirements of an Index to Design Evaluation Qualification and Reliability Test Program, March 1963 (U)

R-391 D. G. Shepard, The Effect of Retrorocket Exhaust on Visibility during Lunar Touchdown, December 1962 (U)

R-393 R. L. Alonso, A. L. Hopkins, Jr., and H. Blair-Smith, Logic Description for Apollo Guidance Computer AGC 4. March 1963 (C)

R-395 G. W. Mayo and G. Kruszewski, Guidance and Navigation System Reliability Apportionment and Initial Analysis, February 1963 (C)

R-396 E. T. Driscoll, Quality Assurance Plan, April 1963 (U)

R-399 W. S. Crocker and I. G. McWilliams, Design and Checking of Indexing, April 1963 (U)

R-404 Apollo Staff, Radar Requirements for Primary Guidance and Navigation Operation, April 1963 (C)

TECHNICAL REPORTS (Cont'd)

R-405 E. T. Driscoll, Quarterly Reliability and Quality Assurance Status Report, April 1963 (U)

R-408 Eldon Hall, Design Concept of the Apollo Guidance Computer, June 1963 (C)

R-410 Eldon Hall, General Characteristics of the Apollo Guidance and Navigation Computer, May 1963 (C)

R-411 D. G. Hoag, A Problem in Man and Machine Integration, April 1963 (C)

R-415 D. J. Lickly, H. R. Morth, B. S. Crawford, Apollo Reentry Guidance, July 1963 (C)

R-416 R. Alonso, Apollo Guidance Computer, August 1963 (U)

R-417 G. W. Cherry, A Class of Unified Explicit Methods for Steering Throttleable and Fixed-Thrust Rockets, January 1964 (Revised) (U)

R-429 E. Driscoll, Reliability and Quality Assurance Progress Report, December 1963 (C)

R-434 Apollo Staff, Preliminary Guidance Navigation Test Plan, December 1963 (U)

R-437 R. Kerrigan, Specification Procurement of Apollo II Inertial Reference Integrating Gyro, February 1964 (C)

R-438 T. L. Shuck, High Performance, High Reliability via Magnetic Amplifiers in the Apollo Guidance Temperature Control System, (to be published((U)

R-439 G. Kruszewski, Failure, Trouble and Corrective Action Summary Design Phase Report #1, February 1964 (U)

R-440 E. T. Driscoll, Quarterly Reliability and Quarterly Assurance Progress Report, Apollo G&N Program, Period ended 31 December 1963, February 1964 (U)

TECHNICAL REPORTS (Cont'd)

R-445 N. E. Sears, Technical Development Status of Apollo Guidance and Navigation, April 1964 (U)

R-446 N. E. Sears, Preliminary G & N System for Lunar Orbit Operations, (to be published) (U)

THESES

T-351 M. A. Lanman, Analysis of a Position Control Servo Incorporating Quantized Feedback, May 1963 (U)

T-352 R. L. Fortenbaugh, Description and Analysis of the Apollo Space Sextant Simulator, May 1963 (U)

T-353 Gary Stone (EE), The Use of Rate Feedback in Compensation of a Temperature Control System, (to be published) (U)

T-355 Erich Bender (RS), Sampled-Data Velocity Vector Control of a Spacecraft, June 1963 (U)

E-1573

DISTRIBUTION LIST

Internal

R. Alonso
J. Arnow (Lincoln)
R. Battin
W. Bean
E. Berk
P. Bowditch
A. Boyce
R. Boyd
P. Bryant
R. Byers
G. Cherry
E. Copps
R. Crisp
W. Crocker
G. Cushman
J. Dahlen
E. Duggan
J. Dunbar
K. Dunipace (MIT/AMR)
R. Euvrard
P. Felleman
S. Felix (MIT/S & ID)
J. Flanders
J. Fleming
L. Gediman
F. Grant
D. Grief
Eldon Hall
I. Halzel
D. Hanley
W. Heintz
E. Hickey
D. Hoag
A. Hopkins
F. Houston
L.B. Johnson
M. Johnston
B. Katz
A. Koso
M. Kramer
W. Kupfer
A. Laats
D. Ladd
A. LaPointe
J. Lawrence (MIT/GAEC)
T. Lawton
D. Lickly
R. Magee
G. Mayo
J. McNeil
R. McKern
R. Mudgett
James Miller
John Miller
J. Nevins
G. Nielson
J. Nugent
E. Olsson
C. Parker
W. Patterson
K. Samuelian
P. Sarmanian
W. Schmidt
R. Scholten
E. Schwarm
J. Sciegienny
N. Sears
D. Shansky
W. Shotwell (MIT/ACSP)
T. Shuck
J. Sitomer
E. Smith
W. Stameris
J. Suomala
W. Tanner
R. Therrien
W. Toth
M. Trageser
R. Weatherbee
R. White
L. Wilk
R. Woodbury
W. Wrigley
D. Yankovich
Apollo Library (2)
MIT/IL Library (6)

External

(ref. PP1-64; April 8, 1964)

P. Ebersole (NASA/MSC)	(2)
W. Rhine (NASA/RASPO)	(1)
S. Gregorek (NAA S & ID/MIT)	(1)
T. Heuermann(GAEC/MIT)	(1)
AC Spark Plug	(10)
Kollsman	(10)
Raytheon	(10)
WESCO	(2)
Capt. W. Delaney (AFSC/MIT)	(1)

NAA RASPO:	National Aeronautics and Space Administration Resident Apollo Spacecraft Program Office North American Aviation, Inc. Space and Information Systems Division 12214 Lakewood Boulevard Downey, California	(1)
FO:	National Aeronautics and Space Administration, MSC Florida Operations, Box MS Cocoa Beach, Florida 32931 Attn: Mr. B.P. Brown	(3)
HDQ:	NASA Headquarters 600 Independence Ave., SW Washington, D.C. 20546 MAP, E.T. Sullivan	(6)
AMES:	National Aeronautics and Space Administration Ames Research Center Moffett Field, California Attn: Library	(2)
LEWIS:	National Aeronautics and Space Administration Lewis Research Center Cleveland, Ohio Attn: Library	(2)
FRC:	National Aeronautics and Space Administration Flight Research Center Edwards AFB, California Attn: Research Library	(1)

LRC:	National Aeronautics and Space Administration Langley Research Center Langley AFB, Virginia Attn: Mr. A.T. Mattson	(2)
GSFC:	National Aeronautics and Space Administration Goddard Space Flight Center Greenbelt, Maryland Attn: Manned Flight Support Office Code 512	(2)
MSFC:	National Aeronautics and Space Administration George C. Marshall Space Flight Center Huntsville, Alabama Attn: R-SA	(2)
GAEC:	Grumman Aircraft Engineering Corporation Bethpage, Long Island, New York Attn: Mr. A. Whitaker	(1)
NAA:	North American Aviation, Inc. Space and Information Systems Division 12214 Lakewood Boulevard Downey, California Attn: Mr. R. Berry	(1)
GAEC RASPO:	National Aeronautics and Space Administration Resident Apollo Spacecraft Program Officer Grumman Aircraft Engineering Corporation Bethpage, L.I., New York	(1)
ACSP RASPO:	National Aeronautics and Space Administration Resident Apollo Spacecraft Program Officer Dept. 32-31 AC Spark Plug Division of General Motors Milwaukee, Wisconsin Attn: Mr. L.J. Lewandowski	(1)
WSMR:	National Aeronautics and Space Administration Post Office Drawer D White Sands Missile Range White Sands, New Mexico Attn: AW 1	(2)
MSC:	National Aeronautics and Space Administration Manned Spacecraft Center Apollo Document Control Group Houston 1, Texas 77058	(45)